BIOLOGICAL OBJECT REPRESENTATION
FOR
IDENTIFICATION

BY

MAENGSUB CHO

A doctoral thesis

submitted in partial fulfilment of the requirements

for the award of

Doctor of Philosophy of the Loughborough University of Technology

November 1992

ACKNOWLEDGEMENTS

ABSTRACT

This thesis is concerned with the problem of how to represent a biological object for computerised identification. Images of biological objects have been generally characterised by shapes and colour patterns in the biology domain and the pattern recognition domain. Thus, it is necessary to represent the biological object using descriptors for the shape and the colour pattern. The basic requirements which a description method should satisfy are those such as invariance of scale, location and orientation of an object; direct involvement in the identification stage; easy assessment of results. The major task to deal with in this thesis was to develop a shape-description method and a colour-pattern description method which could accommodate all of the basic requirements and could be generally applied in both domains.

In the colour-pattern description stage, an important task was to segment a colour image into meaningful segments. The most efficient method for this task is to apply ´ Cluster Analysis. In the image analysis and pattern recognition domains, the majority of approaches to this method have been constrained by the problem of dealing with inordinate amounts of data, i.e. a large number of pixels of an image. In order to directly apply ´ ~ Cluster Analysis to the colour image segmentation, data structure, the Auxiliary Means is developed in this thesis.

CONTENTS

LIST OF FIGURES

CHAPTER 4.

CHAPTER 5.

LIST OF TABLES

Chapter 1

INTRODUCTION.

1.1 Background.

1.2 Objectives.

1.3 Summary: chapter by chapter.

1.1 BACKGROUND.

There are an enormous number of different kinds of biological objects in the natural world. For each biological object, there are a great number of species. For example, there are about 15,000 species of butterfly known to science (Ehrlich & Raven, 1965). One species is generally discriminated from the other by means of various features such as life style, internal or external structure, shape or colour etc. In the domain of morphology, which is one of the academic branches of biology, the shape is an important feature which is employed in species identification. A great deal of research work on computerised species identification by means of shape, such as chromosome identification and leaf species identification and so on has been conducted in the domain of biology (see, for example West & Noble, 1984, Ferson et. al, 1985). On the other hand, in some domains, such as the domain of the butterfly, no attempt to undertake computerised species identification using wing shapes or colour patterns on the wings has been made. A visual comparison of butterflies is currently done manually and requires great experience and expertise.

Most of the research which has been performed for automatic and semi-automatic species identification in the biology domain has mainly relied on black-and-white images rather than colour, since shape has been regarded as the most important feature in species identification. On the other hand, in butterfly species identification, colour features play an important role because the colour patterns on the wings of butterflies are essential for species identification. There are several reasons for manual, visual comparison in the domain of the butterfly such as:

2

(1) Firstly, sophisticated computer equipment which is essential to colour image analysis was not generally available.

(2) Secondly, existing methods for colour pattern extraction which have been published are generally so complex that they have not been applicable in practice. Another difficulty with the existing methods is that they require enormous computing time in their implementation.

Recent technological developments have made it possible to utilise not only colour image capturing devices, but also high resolution colour image analysis devices. Thus, there is no longer a colour device problem in this domain. An immediate necessity in biological object identification is to develop new methods which can be generally applied to colour pattern extraction utilising these new devices.

In the botany domain, various shape description methods, published in the pattern recognition and image analysis domains, have been widely employed in computer systems to discriminate leaf species. However, White and Prentice (1988) have pointed out that, among biologists, systematists prefer the more traditional manual measurement method, that is, a method relying on measuring lengths, widths and angles, etc. of leaves in order to quantify shape variation patterns. This reveals that existing shape description methods do not satisfy all the requirements of species identification in the botany domain. The detailed investigation, described in this thesis, on the corresponding existing methods for shape description has also revealed exactly the same problems. Thus, the development of a new method for shape description which can be generally and efficiently used in species identification is required.

3

In colour image analysis, it is generally considered that colour comparison for various purposes such as colour pattern extraction and boundary extraction etc. should be undertaken in a three-dimensional uniform colour space (e.g., RGB) to obtain a precise result. However, most colour image digitising systems do not directly create the three-dimensional colour space, and also the spectral sensitivity of a colour image capturing device is usually different from that of another colour image capturing device. Thus, it is impossible to apply a system which has been established for one computer system to another computer system which has a colour image capturing device whose spectral sensitivity is different from that of the first system. However, most colour comparisons for colour image analysis have been performed without seriously considering this sensitivity problem. Thus, it is necessary to calibrate the colour image capturing system to establish a correct three-dimensional uniform colour space. There are several reasons for the lack of attention paid to calibration in the colour image analysis domain, such as lack of equipment or expertise.

1.2 OBJECTIVES.

The main objective of the work described in this thesis was to develop representation methods for biological objects which could be generally applied to a computerised system for object identification. The second objective was to construct a prototype identification system which would be used for the evaluation of the methods developed in this thesis. The shapes of biological objects are characterised into two categories:-
   o two-dimensional shapes,
   o three-dimensional shapes.
The subject of this thesis concerns representation methods for biological objects which have two-dimensional shape such as leaves and butterflies.

The basic design strategies of the representation of each biological object were:
(1) The features of a biological object should be described in order to be independent of the scale, location and orientation of the object in an image. Objects in images taken by camera or image scanner usually vary in size, location and orientation. Since these variations seriously affect the various measurements of an object, a descriptor should be designed to be independent of these variations.
(2) The features of a biological object should be described in order to be directly involved in an identification procedure. A descriptor usually plays an important role in computerised object-identification. Shape descriptors and colour pattern descriptors were designed to be utilised in the object identification stage without any additional modification. In

5

general, the external features of biological objects vary in size, shape and colour pattern within a species (Bookstein et al., 1985). Thus, in this design strategy the variation factor was considered.

(3) Descriptors should be easily interpreted not only by visual assessment, but also by systematic methods. When the result of a computerised object-identification is analysed, if the descriptors are easily interpreted, it will be possible to make a correct decision on the result as a human expert does.

(4) Descriptors should be used as input data to the multivariate statistical analysis procedure for further study in a relevant domain.

In order to accommodate these basic design strategies, shape descriptors were developed based on ratios of segments; and colour pattern descriptors were developed based on important factors such as normalised centre of gravity and ratios for segments which can characterise each colour pattern forming an object.

For colour pattern extraction and boundary extraction, colour comparison was required. The colour comparison should be undertaken in a three-dimensional uniform colour space in order to obtain a precise result. Since the spectral sensitivity of a colour image capturing device is usually different from that of another colour capturing device, it was decided to develop a calibration method for a colour image scanner digitising system in the CIE $L^*a^*b^*$ colour space by utilising the Macbeth colour checker chart which is a widely available colour reference standard.

The success of colour pattern description is dominated by a reasonable and efficient method for extracting colour patterns

6

from colour images. Development of this method was considered as a sub-objective of this thesis. In order to improve a method for colour-pattern extraction, an algorithm which can directly apply Cluster Analysis to the colour image segmentation was developed. In particular, this algorithm was designed to employ Auxiliary Means which was devised in this thesis to make the algorithm directly apply , Cluster Analysis to colour pattern extraction.

The sample objects which were chosen to test the various methods developed in this thesis are leaves and butterflies. As far as image analysis is concerned, leaves are characterised by their shapes (outlines); and butterflies are characterised by wing shapes and the colour patterns. Thus, in the case of leaves the design of the representation concentrated on the shapes; and in the case of butterflies, on the wing shapes and the colour patterns of wings.

1.3 SUMMARY: CHAPTER BY CHAPTER.

Chapter 2. Colour for Colour Image Analysis:

This chapter reviews colour from its basic concepts to its uniform spaces such as the CIE L*A*B* space since colour, as argued earlier, is an important factor in the biological image analysis and pattern recognition. Once a colour image is digitised, each colour composing the image is expressed numerically. The numerical values are utilised in colour comparison enabling a colour image analysis system to extract the boundary of an object; to segment the object into meaningful regions; to discriminate a segmented region from other regions and so on. To perform an accurate colour comparison it is shown that it is necessary to establish a three-dimensional uniform colour space. An algorithm for calibration of a colour image scanner digitising system in this space is illustrated. An important feature of the algorithm is the use of the Macbeth colour checker chart, which is a widely available colour reference standard.

Chapter 3. Boundary Extraction Methods:

This chapter concerns the algorithms for extraction of the boundary of an object in a colour image. Algorithms concerning the boundary extraction are surveyed. The procedure of the boundary extraction algorithm which utilises a three-dimensional uniform colour space is illustrated.

Chapter 4. Colour Pattern Extraction Methods:

This chapter concerns algorithms for splitting a colour image into meaningful segments. Existing algorithms concerning colour image segmentation are surveyed. The three-dimensional

clustering method is known to be the most efficient method for colour image segmentation. However, this method has been avoided in the colour image analysis domain because it requires enormous core memory. A detailed review of Cluster Analysis is undertaken to clarify the basic algorithm of the Cluster Analysis and the reason why it has not been utilised in practice. The major concept of the Auxiliary Means, which was developed to directly apply the colour image segmentation to the Cluster Analysis, is illustrated. An algorithm for colour image segmentation employing the Auxiliary Means to the Cluster Analysis routine in the SPSS-X (a statistical package) is discussed.

Chapter 5. Shape Description Methods:

This chapter reviews the existing shape description methods and proposesa new method to improve some of the deficiency for biological objects which are utilised in a species identification procedure. In particular, a detailed analysis of the existing methods which are closely related to the shape description for biological objects is performed, attempting to extract problems and to resolve them. The new shape description method, based on human colour vision, developed in this thesis is illustrated.

Chapter 6. Colour Pattern Extraction Methods:

This chapter describes important factors for colour pattern descriptions. A colour pattern description method which was developed based on these factors is discussed. The discussion of the colour pattern description method is accomplished utilising wing patterns of butterflies as samples.

Chapter 7. The Structure of the Species Identification System:

This chapter describes the structure of the prototype system for

a species classification for biological objects. The system is an integration of the algorithms developed in the previous chapters. For the system two kinds of biological objects are used as samples: leaf and butterfly.

Chapter 8. Conclusions:

This chapter attempts to draw conclusions about biological object representation.

Chapter 9. References.

Chapter 2

COLOUR FOR COLOUR IMAGE ANALYSIS.

2.1 Introduction.

2.2 The Nature of Colour.

2.3 Uniform Colour Spaces.

2.4 The CIE RGB System and the CIE XYZ System.

2.5 Calibration of a Colour Image Scanner Digitising System in the CIE L*a*b* Colour Space.

2.6 Conclusion.

2.1 INTRODUCTION.

In colour image analysis, colour obviously plays an important role. Once a colour image is digitised using a colour image digitising system, each colour composing the image is represented by tristimulus values of R (red), G (green) and B (blue); and each of these tristimulus values is represented by a numerical value. The numerical values of each colour are utilised in colour comparison enabling a colour image analysis system to extract the boundary of an object in an image plane; to segment the object into meaningful regions; to discriminate a segmented region from other regions and so on. In this chapter, the investigation will concentrate on several aspects of colour from its nature to its representation in three-dimensional space, thus giving the theoretical background of colour pertinent to colour image analysis. In section 2.2, the nature of colour is discussed. In section 2.3, uniform colour spaces, which have been introduced by the CIE (Commission Internationale de l'Eclairage, i.e. International Commission on Illumination), are discussed. A colour comparison is performed in this uniform colour space. In particular, the necessity of the uniform colour spaces and their formulae is discussed in detail. In section 2.4, quite a detailed investigation on a transformation procedure from the CIE RGB system to the CIE XYZ (an alternative colour space) system is undertaken. It is necessary to understand this transformation procedure because the CIE XYZ system is essential to the formulae for the uniform colour spaces, but the XYZ system cannot be obtained directly from any colour digitising system. There are various kinds of colour image digitising systems such as colour video digitising systems, colour image scanning systems and so

on. If each colour composing an image is treated in a uniform colour space, the colour image digitising system should be calibrated. A method for this calibration utilising the Macbeth colour chart is illustrated in section 2.5.

2.2 THE NATURE OF COLOUR.

In this section, the investigation will concentrate on the nature of colour and the basic aspects of human vision which perceive colour. In colour science, colour is defined as perceived colour (Bouma, 1971):

Perceived colour is that aspect of visual perception by which an observer may distinguish differences between two fields of view of the same size, shape and structure, such as may be caused by differences in the spectral composition of the radiation concerned in the observation.

Then, how many different colours can be distinguished by the human visual system? Judd and Wyszecki (1975) estimated that an experienced person with normal colour vision can distinguish about ten million different surface colours under optimum viewing conditions. What an enormous number it is! What are the major factors of the nature of colour? An immediate answer to this question is that there are two important factors that are commonly known in colour science: light and the human visual system.

Firstly, let us consider the importance of light in detail. In 1666, Sir Isaac Newton discovered that white sunlight was composed of a mixture of all the colours of the spectrum. Figure 2.1.(a) is a sketch of his proposed colour diagram, in which seven monochromatic (single-wavelength) spectral colours, i.e. red, orange, yellow, green, blue, indigo and violet, are placed around the periphery of a circle in the order that they appear in the spectrum. He then found that these colours could be recombined into white light with a lens. Newton also demonstrated that the

14

set of perceived colours is but a small subset of all the possible colours obtainable by mixing different combinations of colours (Rodieck, 1973). He mixed red with green and created yellow as shown in Figure 2.1.(b).
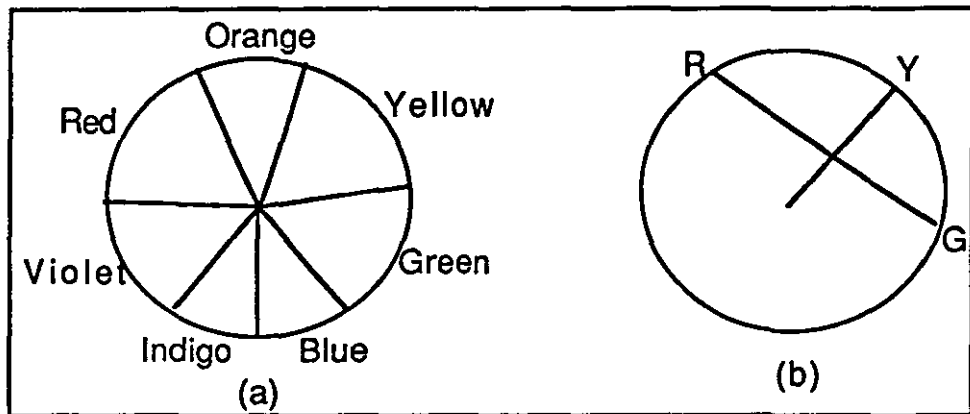
Figure 2.1 Isaac Newton's Colour circles. (a) Newton's colour circle. (b) Mixture of R (red) and G (green) yields Y (yellow).

In physics, light is known to be a form of radiant energy. More precisely, light is electromagnetic energy, a category of radiant energy that includes X-rays, radio waves, etc. In general, light is commonly defined as visible radiant energy. The term visible radiant energy for light implies correctly that the visual system responds to it giving the experience of seeing. Since all light has wave-like properties, and the light in different parts of the spectrum corresponds to waves of a different length, it is convenient to define each spectral colour by the wavelength of its light. The main spectral colours occupy approximately the following wavelength bands: violet 450 nm and less; blue 450 to 480 nm; blue-green 480 to 510 nm; green 510 to 550 nm; yellow-green 550 to 570 nm; yellow 570 to 590 nm; orange 590 to 630 nm; and red 630 nm and greater, where nm is the nanometre

which is one thousand-millionth (10^{-9}) of a metre (Agoston, 1979). These regions are shown in Figure 2.2. This implies that the visible range of radiation extends from 380 to 780 nm. It is generally known that a normal eye is essentially blind to all radiation of wavelengths shorter than 380 nm and longer than 780 nm.
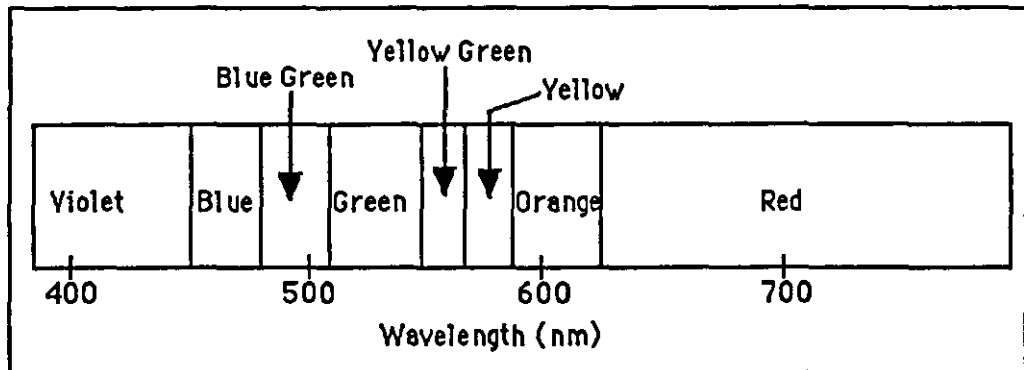
Figure 2.2 The distribution of colours in the spectrum.

Secondly, let us briefly consider the human visual system. How does the normal eye recognise various kinds of colours? To consider an answer to this question let us take a close look at the human visual system. There are two types of light-sensitive receptor cells in the retina, known as rods and cones (Hurvich, 1981). It is known that the rods, which respond only to light and dark, are characterised by high sensitivity; they are capable of responding to light of very low intensity. Thus, the rods enable us to see in dimly lit rooms or in moonlight. At such low levels of illumination we are unable to distinguish hues and we cannot discern detail as well as we can in daylight (Evance, 1974). Evance (ibid.) has noted that at very low light intensities the cones, which are responsible for colour vision, are considered not sensitive enough to respond. He has added that there are three

16

classes of photo-sensitive pigments: one pigment absorbs reddish light, another greenish light, and a third bluish light; and each cone contains only one of the three types of pigments. Electrical signals are generated in the form of nerve impulses and these signals convey colour information to the brain. This is the way the normal eye recognises each of the colours.

2.3 UNIFORM COLOUR SPACES.

In colour-image analysis, a basic task is the comparison of colours. Suppose that there are two colours which are to be compared with each other. An immediate problem for this comparison is how to describe these colours. In practice, this problem corresponds to what kind of attributes should be involved in the description of each colour. The overwhelming empirical evidence is that for an observer with normal colour vision three specific component attributes are sufficient for him to completely describe any colour he perceives, regardless of the observing conditions under which he views the display (Wyszecki, 1981). The three perceptual attributes of colour are lightness, hue, and chroma which are also defined as follows (Wyszecki & Stiles, 1982):

(1) Lightness is that attribute of a visual sensation according to which the area in which the visual stimulus is presented appears to emit more or less light in proportion to that emitted by a similarly illuminated area perceived as a 'white' stimulus. In a sense, lightness may be referred to as relative brightness.

(2) Hue is that attribute of colour perception denoted by blue, green, yellow, red, purple and so on.

(3) Chroma is that attribute of a visual sensation which permits a judgment to be made of the degree to which a chromatic stimulus differs from an achromatic stimulus of the same brightness.

Wyszecki has noted that since any colour perception which is represented by a point P lying within the bounded domain of chromatic perceptions can be varied in only three independent ways P1, P2 and P3, represented by the three perceptual attributes lightness, hue and chroma, these attributes form a

three-dimensional space.

The most prominent example of a three-dimensional colour space composed of these perceptual attributes is the Munsell colour space. The Munsell colour space consists of painted colour chips which are equally spaced in each of the three dimensions. On each constant-hue chart the chips are arranged in rows and columns. It was intended that the chips in any one row should be perceived to have equal lightness under ordinary viewing conditions and that the chips in any one column should be perceived to have colours of equal chroma, where the ordinary viewing condition is defined as average daylight illumination that corresponds to the standard illuminant C. These colour chips were stuck on charts and published as the first colour atlas in 1915 (McLaren, 1983).

The logical representation of this colour space is a three-dimensional Euclidian space expressed in cylindrical coordinates as shown in Figure 2.3, There are five principal hues in the hue circle and each hue is subdivided into finer divisions which are equally spaced scales as shown in Figure 2.3.(a). The vertical axis represents the lightness which is designated on a scale 0 to 10 as shown in Figure 2.3.(b). Each of the concentric cylinders as shown in Figure 2.3.(b) represents constant chroma.

These Munsell colour chips can only be used for visual evaluations. Thus the development of a satisfactory colour-difference formula which can be applied to systematic colour comparison is necessary. In fact, this task obviously corresponds to the development of a three-dimensional uniform colour space.

The uniform colour space would simplify colour specification and the setting of colour tolerances, it would be an important guide to the preparation of reference colour samples as standards, and it would aid the selection of harmonious colour combinations (Judd & Wyszecki, 1975). The development of a uniform colour space has generally been regarded as one of the most challenging projects in the field of colour science.
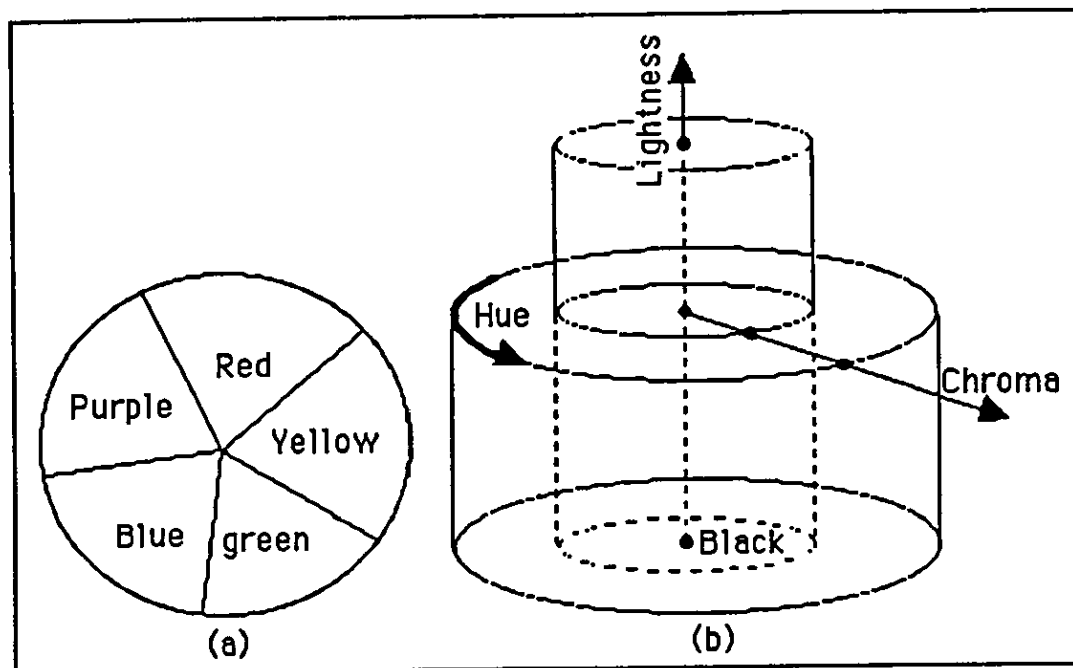
Figure 2.3 Munsell colour specification system. (a) Munsell hue circle. (b) Cylindrical arrangement of lightness, hue and chroma in Munsell colour space.

At the 18th session of the CIE held in London in 1975 the Colorimetry Committee approved the adoption of two new colour spaces and associated colour difference formulae, known as the 1976 $L^*u^*v^*$ colour space (CIELUV space) and the CIE 1976 $L^*a^*b^*$ colour space (CIELAB space) (CIE, 1986). Although these two formulae are only approximately uniform colour spaces, they are considered as the best formulae recommended by the CIE.

20

(1) The CIE 1976 L*u*v* Colour Space and Colour-Difference Formula

The first approximately uniform colour space is produced by plotting in rectangular coordinates, L*, u* and v*, quantities denoted by the following equations (CIE, 1986):

$$L^* = 116(Y/Y_0)^{1/3} - 16 \quad \text{if } Y/Y_0 > 0.008856,$$
$$L^* = 903.3(Y/Y_0) \quad \text{if } Y/Y_0 <= 0.008856,$$
$$u^* = 13L^*(u - u_0),$$
$$v^* = 13L^*(v - v_0), \quad\quad\quad (2.3\text{-}1)$$

where Y, u and v are the colour stimulus and Y_0, u_0 and v_0 are a specified white object colour stimulus. In Equation (2.3-1), the quantities u, v, u_0 and v_0 are calculated from:

$$u = \frac{4X}{X + 15Y + 3Z}, \qquad v = \frac{9Y}{X + 15Y + 3Z},$$

$$u_0 = \frac{4X_0}{X_0 + 15Y_0 + 3Z_0}, \qquad v_0 = \frac{9Y_0}{X_0 + 15Y_0 + 3Z_0}.$$

$$(2.3\text{-}2)$$

The tristimulus values X_0, Y_0 and Z_0 define the colour of the nominally white object-colour stimulus. This stimulus is usually given by the spectral radiant power distribution of one of the CIE standard illuminants, such as A or C, reflected into the observer's eye by the perfect diffuser. Under these conditions, X_0, Y_0 and Z_0 are the stimulus values of the chosen standard illuminant, and Y_0 is equal to 100. The tristimulus values X, Y and Z will be illustrated in detail in section 2.4.

The CIE 1976 L*u*v* colour-difference formula ΔE_{uv}^* that applies to the L*u*v* colour space is given by the Euclidian distance:

$$\Delta E_{uv}{}^* = [\,(\Delta L^*)^2 + (\Delta u^*)^2 + (\Delta v^*)^2\,]^{1/2}.$$ (2.3-3)

where ΔL^*, Δu^* and Δv^* are the differences between two colours in L^*, u^* and v^*, respectively. In fact, $\Delta E_{uv}{}^*$ is equal to the distance between the two points representing colours in the CIELUV space. In the CIELUV colour space, there is a vertical metric lightness L^* (also called the CIE 1976 lightness function) axis passing through evenly spaced horizontal planes that are subdivided into square grids containing coordinates (u^*, v^*). Figure 2.4 shows the vertical axis L^* that passes through the horizontal plane (u^*, v^*), at $L^* = 50$, for example.
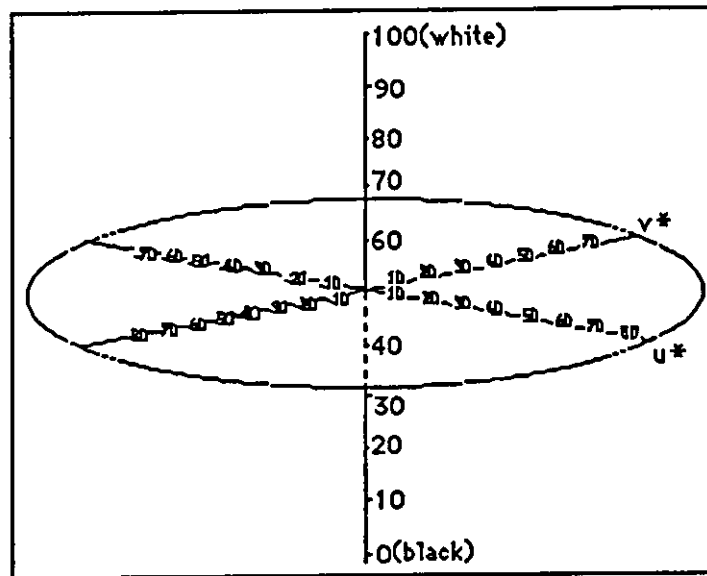
Figure 2.4 The CIELUU colour space.

(2) The CIE 1976 L*a*b* Colour Space and Colour-Difference Formula

The second approximately uniform colour space is produced by plotting in rectangular coordinates, L^*, a^* and b^*, quantities defined by the following equations (CIE, 1986):

$$L^* = 116(Y/Y_o)^{1/3} - 16, \qquad \text{if } Y/Y_o > 0.008856,$$

22

$$L^* = 903.3(Y/Y_0), \qquad \text{if } Y/Y_0 <= 0.008856,$$

$$a^* = 500[(X/X_0)^{1/3} - (Y/Yo)^{1/3}], \qquad \text{if } X/X_0 > 0.008856 \text{ and}$$
$$Y/Y_0 > 0.008856,$$

$$b^* = 200[(Y/Y_0)^{1/3} - (Z/Z_0)^{1/3}], \qquad \text{if } Y/Y_0 > 0.008856 \text{ and}$$
$$Z/Z_0 > 0.008856,$$

$$a^* = 500[f(X/X_0) - f(Y/Y_0)],$$
$$b^* = 200[f(Y/Y_0) - f(Z/Z_0)], \qquad\qquad (2.3\text{-}4)$$

$$\text{where } f(X/X_0) = (X/X_0)^{1/3}, \qquad \text{if } X/X_0 > 0.008856,$$
$$f(X/X_0) = 7.787(X/X_0) + 16/116, \quad \text{if } X/X_0 <= 0.008856,$$
$$f(Y/Y_0) = (Y/Y_0)^{1/3}, \qquad \text{if } Y/Y_0 > 0.008856,$$
$$f(Y/Y_0) = 7.787(Y/Y_0) + 16/116, \quad \text{if } Y/Y_0 <= 0.008856,$$
$$f(Z/Z_0) = (Z/Z_0)^{1/3}, \qquad \text{if } Z/Z_0 > 0.008856,$$
$$f(Z/Z_0 = 7.787(Z/Z_0) + 16/116, \quad \text{if } Z/Z_0 <= 0.008856.$$

The tristimulus values X_0, Y_0 and Z_0 are respectively those of the tristimulus values X, Y and Z, for the appropriately chosen reference white. The tristimulus values X, Y and Z will be illustrated in section 2.4. The CIE 1976 $L^*a^*b^*$ colour-difference formula ΔE_{ab}^* that applies to the $L^*a^*b^*$ colour space is given by the Euclidian distance:

$$\Delta E_{ab}^* = [(\Delta L^*)^2 + (\Delta a^*)^2 + (\Delta b^*)^2]^{1/2}, \qquad\qquad (2.3\text{-}5)$$

where ΔL^*, Δa^* and Δb^* are the differences between two colours in L^*, a^* and b^*, respectively. In fact, ΔE_{ab}^* is equal to the distance between the two points representing colours in the CIELAB space. It should be noted that the CIELUV space or the CIELAB space can be easily linked to the Munsell colour space as follows:

The quantity L^*, given in Equation (2.3-1) or (2.3-4) is directly used as the lightness quantity of the Munsell colour space. The hue-angle, H, of the Munsell colour space is obtained by the CIE

23

1976 u, v hue-angle:

$$H_{uv}{}^* = \arctan[(v - v_o)/(u - u_o)]$$

$$= \arctan(v^*/u^*), \tag{2.3-6}$$

the CIE 1976 a, b hue-angle:

$$H_{ab}{}^* = \arctan(b^*/a^*). \tag{2.3-7}$$

The chroma, C, of the Munsell colour space is obtained by the CIE 1976 u, v chroma:

$$C_{uv}{}^* = (u^{*2} + v^{*2})^{1/2}, \tag{2.3-8}$$

the CIE 1976 a, b chroma:

$$C_{ab}{}^* = (a^{*2} + b^{*2})^{1/2}. \tag{2.3-9}$$

The lightness difference ΔL^* and chroma difference ΔC^* corresponding to the Munsell colour space are simply calculated as follows:

$$\Delta L^* = L1^* - L2^*,$$

$$\Delta C^* = C1^* - C2^*,$$

where $L1^*$ and $L2^*$ are the quantities of lightness of two points in the Munsell colour space, respectively; and $C1^*$ and $C2^*$ are the quantities of chroma of two points in the Munsell colour space, respectively. The hue difference, ΔH^*, however, is obtained using $\Delta E_{uv}{}^*$ or $\Delta E_{ab}{}^*$, $\Delta C_{uv}{}^*$ or $\Delta C_{ab}{}^*$, and ΔL^*, as follows:

the CIE 1976 u, v hue difference $\Delta H_{uv}{}^*$:

$$\Delta H_{uv}{}^* = [(\Delta E_{uv}{}^*)^2 - (\Delta L^*)^2 - (\Delta C_{uv}{}^*)^2]^{1/2},$$

the CIE 1976 a, b hue difference $\Delta H_{ab}{}^*$:

$$\Delta H_{ab}{}^* = [(\Delta E_{ab}{}^*)^2 - (\Delta L^*)^2 - (\Delta C_{ab}{}^*)^2]^{1/2}.$$

Consequently, either the CIELUV space or the CIELAB space can be directly employed in the systematic operation for the colour comparison task. The important feature of each space is that this can be easily transformed to the Munsell colour space as previously shown. Thus, a computerised operation with the

transformed space from the CIELUV or the CIELAB space can replace any task which could be performed by visual evaluations with the colour chips in the traditional Munsell Book of Colour. However, it is unfortunate that in 1976 the CIE could not recommend a single colour space and associated colour difference formula. Since the CIELUV and CIELAB colour spaces were recommended, much research (Robertson, 1977; Kuehni, 1977; Pointer, 1981; McLaren, 1981) has been carried out to compare the two spaces, revealing that there are no significant differences between the CIELUV and CIELAB spaces. On the other hand, Lozano, (1977) showed that the CIELAB was significantly more reliable. Ohta et al. (1980)   have argued that the CIELAB space gives better results than the CIELUV space in segmenting colour pictures. Thus, the CIELAB space will be employed in this thesis.

2.4 THE CIE RGB SYSTEM AND THE CIE XYZ SYSTEM.

In the previous section, the uniform colour systems have been considered. However, none of these systems have clarified the relationship with the RGB system. In order to correctly understand these uniform colour systems, it is necessary to consider the relationship between the CIE RGB system and the CIE XYZ system. This consideration will obviously provide the fundamental background and guide the calibration of a colour image digitising system which is the major subject of the next section. Let us firstly consider the relationship among the three colour coordinate systems, i.e. the CIE RGB system, the CIE XYZ system and the CIE LAB system, each of which is a colour specification system. As already discussed in the foregoing section, a uniform colour space is required to obtain the optimum result of a colour comparison in colour image analysis. Since the CIE RGB system or the CIE XYZ system does not form a uniform colour space as Figure 2.12 shows, the CIE has developed an approximately uniform colour space, that is, the CIELAB colour space. The CIELAB colour coordinate system is transformed from the CIE XYZ system, where it seems that the CIE RGB system is not involved, but, in fact the CIE RGB system is involved in the derivation of the CIE XYZ system. The relationships between these systems can be described using the functional forms as follows:

the CIELAB system = f(X, Y, Z),

the CIE XYZ system = f(R, G, B).

Consequently, the CIELAB system is a function of the CIE RGB system, where the parameters are the red (R), green (G) and blue (B) values. Equation (2.3-4) which defines the CIELAB space only includes the X, Y and Z tristimulus values. It should be noted that

26

an image capturing device usually provides the R, G and B tristimulus values of a colour rather than the X, Y and Z tristimulus values. Thus, the transformation from the CIE RGB system to the CIE XYZ system would precede adopting the CIE system in a practical implementation.
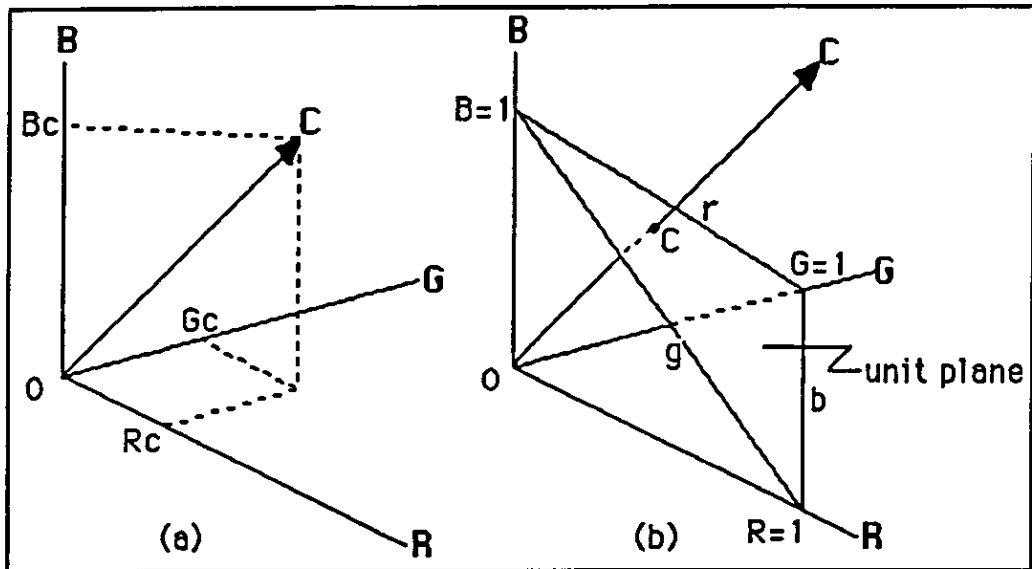
Figure 2.5 A tristimulus colour space.

To clarify the basic concept of the RGB system, let us consider a colour space in which a colour C is represented by the coordinates Rc, Gc and Bc measured along three axis represented by the three primary stimuli R, G and B. If the intensity of this colour is changed, each of the coordinates Rc, Gc and Bc will be changed proportionally. The locus of points corresponding to changes of intensity is a straight line passing through the origin and the point (Rc, Gc, Bc) as shown in Figure 2.5.(a). This colour can be expressed by the simple equation:

$$C = Rc \times R + Gc \times G + Bc \times B. \tag{2.4-1}$$

This equation is usually used to match a given colour C to the additive matrix in suitable amounts of the three fixed primary

27

stimuli **R**, **G** and **B**. Wyszecki and Stiles (1982) have noted that the representation of colour stimuli in the colour space is informative, but usually not convenient in colorimetric practice, thus a two-dimensional representation is commonly preferred. The two-dimensional representation is obtained in the unit plane which is formed by connecting the three points of the three axes, each of which marks the unit length as shown in Figure 2.5.(b). The unit plane is commonly called the chromaticity diagram. The unit plane which is in the shape of an equilateral triangle was used in the early days of colorimetric practice and is sometimes referred to as the Maxwell colour triangle. In practice, the triangle defines chromaticity coordinates (r, g, b). The chromaticity coordinates of a point C which is an intersection of the straight line 0C with the unit plane are related to the tristimulus values R = Rc, G =Gc and B = Bc of **C** by the following equations:

$$r_c = R/(R + G + B),$$
$$g_c = G/(R + G + B),$$
$$b_c = B/(R + G + B). \qquad\qquad (2.4\text{-}2)$$

The coordinates r_c, g_c and b_c are given by the distances of C from the three sides of the triangle, that is, from GB, BR and RG, respectively, as shown in Figure 2.6.(a), where R, G and B are the chromaticty points of the primary stimuli **R**, **G** and **B** which are located at the corners of the triangle. A more convenient version is a right-angled triangle in which the r and g coordinate axes are perpendicular to one another as shown in Figure 2.6.(b) (Bouma, 1971).
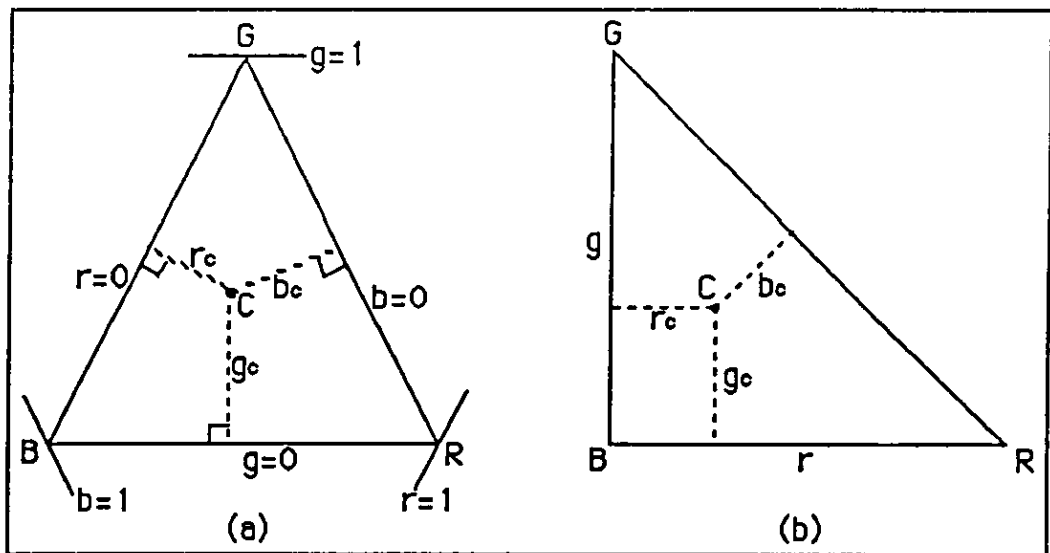
Figure 2.6 Chromaticity diagrams. (a) Chromaticity diagram (equilateral triangles). (b) Chromaticity diagram (right-angled triangle).

So far some basic concepts of the RGB system have been discussed, let us briefly consider the colour-matching function and the corresponding chromaticity diagram of the RGB system which were both introduced by the CIE, since they dominate the properties of the RGB system. The CIE derived the colour-matching function in Figure 2.10.(a) from the data in Table 2.1 obtained by Guild (1931) and Wright (1928). To understand this function it is necessary to review the theoretical background of obtaining the data and a way of using this function. Imagine a visible spectrum ranging from λ_a = 380 nm to λ_b = 780 nm as shown in Figure 2.7, where λ is wavelength and nm is nano (10^{-9}) metre. The spectrum is subdivided into n intervals, each interval has a wavelength band $\Delta\lambda$. Within each interval, a wavelength λi is chosen at which the spectral connection is $P_{\lambda i}$. The radiant power in the wavelength interval of width d_λ centred at the wavelength λi which is represented by $P_{\lambda i} \times d_\lambda$, the area of

29

the shaded rectangle in Figure 2.7, is a monochromatic stimulus C_λ of wavelength λ.
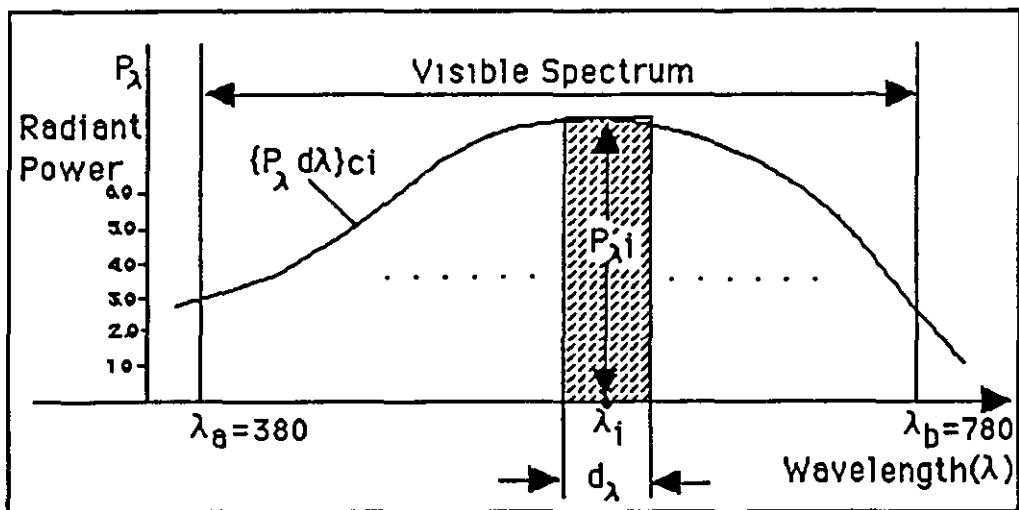
Figure 2.7 A monochromatic stimulus of wavelength λ (Wyszecki & Stiles, 1982).

Each monochromatic stimulus C_λ is expressed by applying Equation (2.4-1) as follows:

$$C_\lambda = R_\lambda \times R + G_\lambda \times G + B_\lambda \times B, \qquad (2.4\text{-}3)$$

where R_λ, G_λ and B_λ are the tristimulus values of C_λ. The tristimulus values of a colour stimulus are generally defined as the amounts of the three primary colour stimuli required to give by additive mixture a colour match with the colour stimulus considered (Wyszecki & Stiles, 1982). All the monochromatic stimuli C_λ which have unit radiant power, i.e. P_λ is equal to 1, at every wavelength λ within the visible spectrum, as shown in Figure 2.8, are equal-energy stimuli denoted by E_λ. The equation for a colour match involving a monochromatic constituent E_λ of the equal-energy stimulus E is:

$$E_\lambda = \bar{r}(\lambda)R + \bar{g}(\lambda)G + \bar{b}(\lambda)B, \qquad (2.4\text{-}4)$$

where $\bar{r}(\lambda)$, $\bar{g}(\lambda)$ and $\bar{b}(\lambda)$ are spectrum tristimulus values of E_λ.

30

In the colour matching experiment by Guild and Wright, four monochromators were used as shown in Figure 2.9, three to produce primary stimuli; and one to produce the test stimulus E_λ. The monochromator is an optical device which disperses the radiant flux from an incandescent lamp into its spectrum, from which any desired narrow band of wavelengths can be isolated with a slit aperture (Wyszecki & stiles, 1982). The primary stimuli were set at $\lambda_R = 700$ nm for red (R), at $\lambda_G = 546.1$ nm for
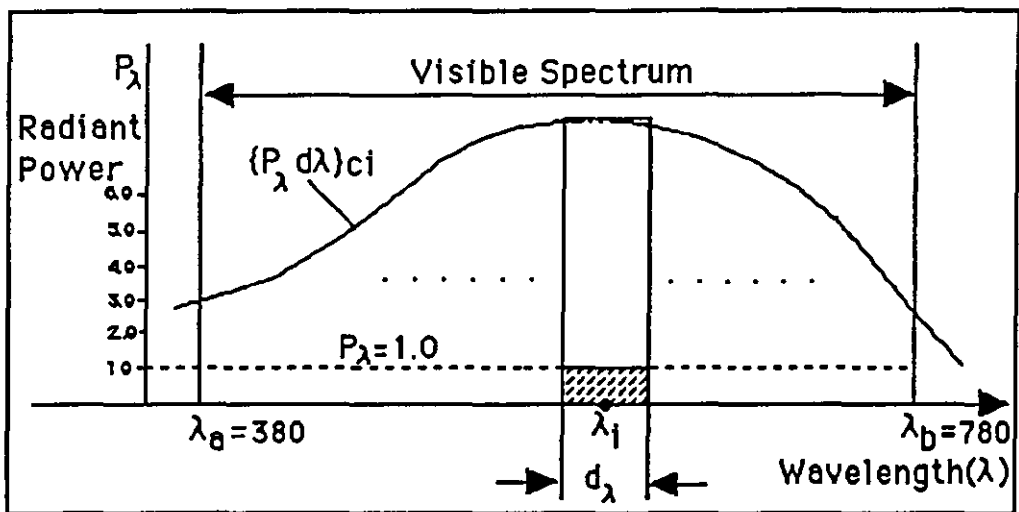
Figure 2.8 An equal-energy stimulus.

green (G) and $\lambda_B = 435.8$ nm for blue (B). The unit values of these primaries were chosen so that the colour of a mixture of unit amounts of the primaries might match the colour of an equal-energy stimulus. As Figure 2.9 shows, whenever each test stimulus E_λ of wavelength λ, from $\lambda = 380$ nm to 780 nm at intervals of $\Delta\lambda$ nm, was produced by the monochromator located in the lower part of Figure 2.9, the mixture of the primary stimuli which matched the test stimulus was produced by the three monochromators, where the amount of each primary stimulus involved in the match was obtained. The amounts of primary

31

stimuli matched at wavelength λ are $\bar{r}(\lambda)$, $\bar{g}(\lambda)$ and $\bar{b}(\lambda)$, respectively, as shown in Table 2.1, where in many cases, one of the tristimulus values is negative, in other cases, one or two tristimulus values are zero. The set of spectral tristimulus values $\bar{r}(\lambda)$, $\bar{g}(\lambda)$ and $\bar{b}(\lambda)$ of the monochromatic stimuli E_λ of unit radiant power are called colour-matching functions. Figure 2.10 illustrates these functions as drawn from the set of data. The chromaticity diagram in Figure 2.10.(c) was drawn by applying the spectral tristimulus values $\bar{r}(\lambda)$, $\bar{g}(\lambda)$ and $\bar{b}(\lambda)$ to Equation (2.4-2). An important fact to note is how to use these functions. To illustrate the use of these colour-matching functions consider
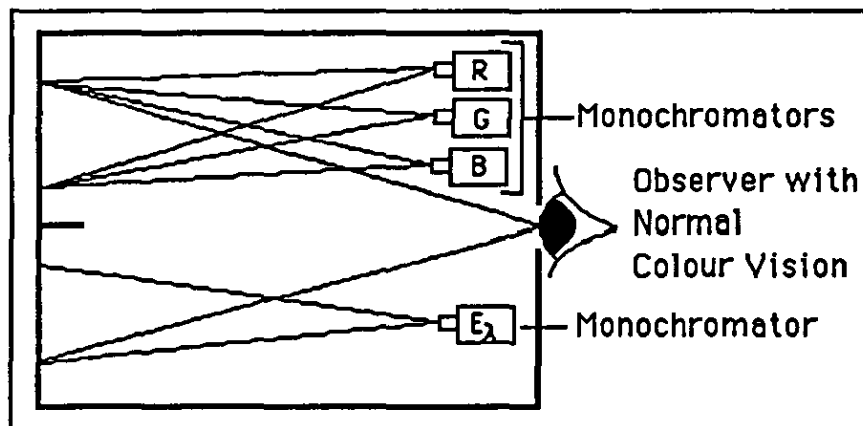
Figure 2.9 Diagram of an arrangement of monochromators for colour-matching experiment.

how to determine the tristimulus values of a colour stimulus C which is defined by a spectral radiant power distribution $\{P_\lambda d\lambda\}_c$ in Figure 2.7. In order to apply Equation (2.4-4) to a colour stimulus C of the various sizes of bands of wavelength, multiply radiant power, $P_\lambda \times d\lambda$, both sides of Equation (2.4-4), then the following equation is obtained:

32

$(P_\lambda \times d\lambda)E_\lambda$

$$= (P\lambda \times d\lambda)\bar{r}(\lambda)\mathbf{R} + (P\lambda \times d\lambda)\bar{g}(\lambda)\mathbf{G} + (P\lambda \times d\lambda)\bar{b}(\lambda)\mathbf{B}, \qquad (2.4\text{-}5)$$

where $(P_\lambda \times d\lambda)E_\lambda$ is equal to C_λ, because E_λ has unit radiant power in Figure 2.8. Since P_λ in Figure 2.7 is assumed to be a continuous function, Equation (2.4-5) is integrable. . Thus, the tristimulus values Rc, Gc and Bc of the stimulus **C** are respectively,

$$Rc = \int_{\lambda a}^{\lambda b} P\lambda\,\bar{r}(\lambda)\,d\lambda,$$

$$Gc = \int_{\lambda a}^{\lambda b} P\lambda\,\bar{g}(\lambda)\,d\lambda,$$

$$Bc = \int_{\lambda a}^{\lambda b} P\lambda\,\bar{b}(\lambda)\,d\lambda, \qquad (2.4\text{-}6)$$

where λa and λb are respectively the lower and upper limits of the band of wavelength of the stimulus **C**. If there are two colour stimuli **C1** and **C2** which are respectively defined by spectral radiant power distributions $\{P_{1\lambda}d\lambda\}$ and $\{P_{2\lambda}d\lambda\}$, the two sets of tristimulus values of the colours are:

$$Rc_1 = \int_{\lambda a}^{\lambda b} P_1\lambda\,\bar{r}(\lambda)\,d\lambda,$$

$$Gc_1 = \int_{\lambda a}^{\lambda b} P_1\lambda\,\bar{g}(\lambda)\,d\lambda,$$

$$Bc_1 = \int_{\lambda a}^{\lambda b} P_1\lambda\,\bar{b}(\lambda)\,d\lambda,$$

$$Rc_2 = \int_{\lambda a}^{\lambda b} P_2\lambda\,\bar{r}(\lambda)\,d\lambda,$$

$$Gc_2 = \int_{\lambda a}^{\lambda b} P_2\lambda\,\bar{g}(\lambda)\,d\lambda,$$

$$Bc_2 = \int_{\lambda a}^{\lambda b} P_2\lambda\,\bar{b}(\lambda)\,d\lambda. \qquad (2.4\text{-}7)$$

If Rc1 = Rc2, Gc1 = Gc2 and Bc1 = Rc2, the colour stimulus **C1** matches the colour stimulus **C2**. Consequently, the colour-matching functions are used for a colour match. As previously

33

illustrated, the colour-matching functions and the corresponding chromaticity coordinates include negative values. When Equation (2.4-6) is applied to evaluate tristimulus values of a test colour, the calculation with positive or zero values is simple, but the calculation with negative and positive values is complex. This is inconvenient. It is known that there are many cases in which negative values are used in spite of this inconvenience. However, since these cases are not related to the subject in this thesis, it is not necessary to consider them. Due to such reasons, the CIE has developed the spectral values $\bar{x}(\lambda)$, $\bar{y}(\lambda)$ and $\bar{z}(\lambda)$ which are also called the colour-matching functions in which negative values are not included as shown in Figure 2.10.(b). The colour-matching functions $\bar{x}(\lambda)$, $\bar{y}(\lambda)$ and $\bar{z}(\lambda)$ were transformed by the CIE from the colour-matching functions $\bar{r}(\lambda)$, $\bar{g}(\lambda)$ and $\bar{b}(\lambda)$ using the following equations:

$$\bar{x}(\lambda) = 0.49 \, \bar{r}(\lambda) + 0.31 \bar{g}(\lambda) + 0.26 \bar{b}(\lambda) ,$$

$$\bar{y}(\lambda) = 0.17697 \bar{r}(\lambda) + 0.8124 \bar{g}(\lambda) + 0.01063 \bar{b}(\lambda) ,$$

$$\bar{z}(\lambda) = 0.0 \, \bar{r}(\lambda) + 0.01 \bar{g}(\lambda) + 0.99 \bar{b}(\lambda) . \qquad (2.4-8)$$

These colour-matching functions are used in calculations to provide the CIE tristimulus values X, Y and Z. The X, Y and Z are obtained from the following equations:

$$X = \int_{\lambda a}^{\lambda b} P\lambda \, \bar{x}(\lambda) \, d\lambda,$$

$$Y = \int_{\lambda a}^{\lambda b} P\lambda \, \bar{y}(\lambda) \, d\lambda,$$

$$Z = \int_{\lambda a}^{\lambda b} P\lambda \, \bar{z}(\lambda) \, d\lambda. \qquad (2.4-9)$$

Although colours can be specified by the CIE tristimulus values X, Y and Z, this is rarely done (Agoston, 1979). It is more meaningful

to employ the chromaticity coordinates $x(\lambda)$, $y(\lambda)$ and $z(\lambda)$ of the spectral stimuli than to use the spectral stimulus values X, Y and Z. The chromaticity coordinates $x(\lambda)$, $y(\lambda)$ and $z(\lambda)$ of the spectral stimuli are derived from the spectral tristimulus values $\bar{x}(\lambda)$, $\bar{y}(\lambda)$ and $\bar{z}(\lambda)$, by forming ratios (CIE, 1986):

$$x(\lambda) = \frac{\bar{x}(\lambda)}{\bar{x}(\lambda) + \bar{y}(\lambda) + \bar{z}(\lambda)}$$

$$y(\lambda) = \frac{\bar{y}(\lambda)}{\bar{x}(\lambda) + \bar{y}(\lambda) + \bar{z}(\lambda)}$$

$$z(\lambda) = \frac{\bar{z}(\lambda)}{\bar{x}(\lambda) + \bar{y}(\lambda) + \bar{z}(\lambda)} \,.$$

$$(2.4\text{-}10)$$

The CIE 1931 (x, y)-chromaticity diagram which is drawn using the chromaticity coordinates is shown in Figure 2.10.(d). The chromaticity coordinates x(l), y(l) and z(l) are converted to the tristimulus values X, Y and Z as follows (the CIE, 1986):

$$X = (\frac{x}{y})\,Y \qquad \text{and} \qquad Z = (\frac{z}{y})\,Y.$$

$$(2.4\text{-}11)$$

Wave-length λ (nm)	Tristimulus Values					
	$\bar{r}(\lambda)$	$\bar{g}(\lambda)$	$\bar{b}(\lambda)$	$\bar{x}(\lambda)$	$\bar{y}(\lambda)$	$\bar{z}(\lambda)$
380	0.00003	-0.00001	0.00117	0.0014	0.0000	0.0065
400	0.00030	-0.00014	0.01214	0.0143	0.0004	0.0679
420	0.00211	-0.00110	0.11541	0.1344	0.0040	0.6456
440	-0.00261	0.00149	0.31228	0.3483	0.0230	1.7471
460	-0.02608	0.01485	0.29821	0.2908	0.0600	1.6692
480	-0.04939	0.03914	0.14494	0.0956	0.1390	0.8130
. . . . . .	.	.	. .	.	.	. .
760	0.00006	0.00000	0.00000	0.0002	0.0001	0.0000

Table 2.1 Average colour-matching functions $\bar{r}(\lambda)$, $\bar{g}(\lambda)$ and $\bar{b}(\lambda)$, and $\bar{x}(\lambda)$, $\bar{y}(\lambda)$ and $\bar{z}(\lambda)$ (Judd & Wyszecki, 1975).

It is important to note that the chromaticity diagram of either the CIE RGB system or the CIE XYZ system has no uniform colour space. Colours within each ellipse in Figure 2.11 have the same chromaticity. Since the CIE 1931 (x, y)-chromaticity coordinate system has a multiform colour space, the CIE has developed the CIELAB system and the CIELUV system.
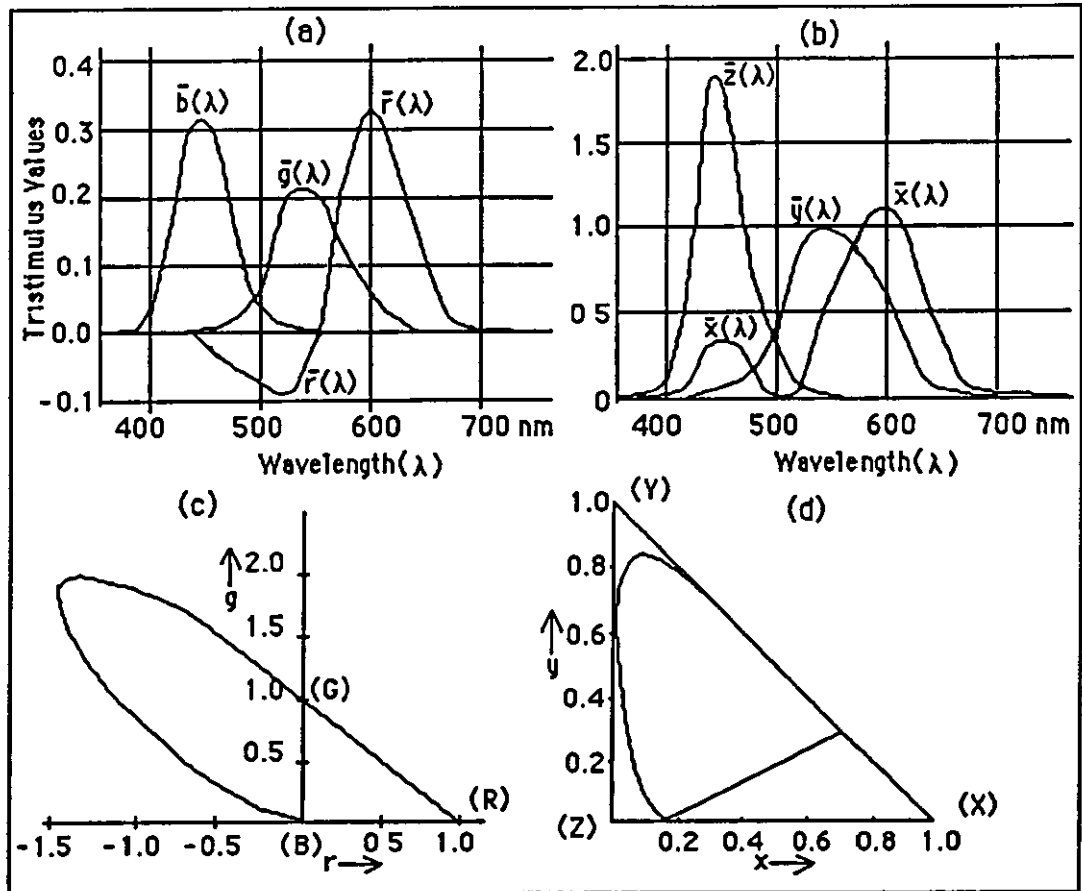
Figure 2.10 Colour-matching functions. (a) $\bar{r}(\lambda)$, $\bar{g}(\lambda)$, $\bar{b}(\lambda)$ **colour-matching function. (b)** $\bar{x}(\lambda)$, $\bar{y}(\lambda)$ **and** $\bar{z}(\lambda)$ **colour-matching function. (c) The CIE 1931 (r, g) chromaticity diagram. (d) The CIE 1931 (x, y) chromaticity diagram (Wyszecki & Stiles, 1982).**

36

The concepts of the CIE RGB system and the CIE XYZ system and the backgrounds and motivation of the development of the CIE 1931 XYZ system have been previously considered to allow the understanding of the relationship between these two systems.
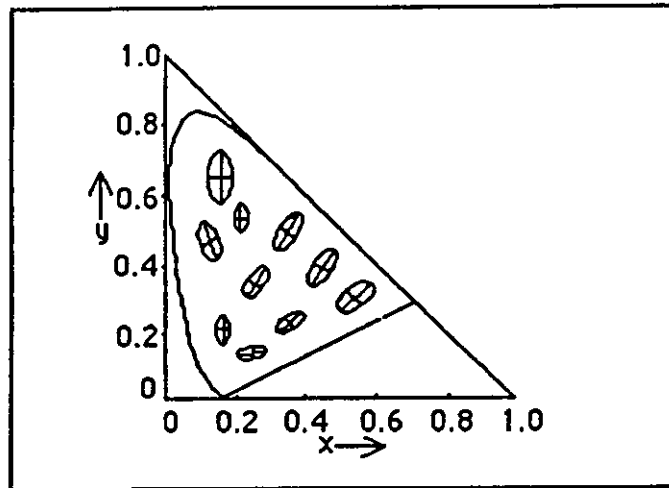
Figure 2.11 A multiform colour space of the CIE 1931 (x, y)-chromaticity diagram (Judd & Wyszecki, 1975).

2.5 CALIBRATION OF A COLOUR IMAGE SCANNER DIGITISING SYSTEM IN THE CIE L*A*B* COLOUR SPACE.

There are many kinds of measuring devices which measure weight, distance, length, volume, electrical resistance, speed, etc. Some of them need calibration before use because of changes of environmental factors which can affect the result of measurement. In the colour image analysis field, colour images are usually captured using colour video cameras or colour image scanners, etc. If the captured images are analysed utilising colour comparison applying the uniform colour space such as the CIE L*a*b* colour space, calibration of the colour image capturing system is required because a digitising system's spectral sensitivities are not always the same as the human colour-matching functions illustrated in the previous section. In much research undertaken in the image analysis field, colour has been used to segment images into sets of uniform colour regions. However, little attention has been paid to calibration. Ito and Fukushima (1976) have noted that the filter characteristics of their colour film reader and digital colour TV scanner are different from the CIE standards, so they have developed two new transformation-coefficient matrices for their devices, where each matrix is used for transforming the RGB values into the XYZ values. However, the detailed procedure for obtaining these matrices has not been illustrated. Strachan et al. (1990) published a paper describing the calibration of a video digitising system with a detailed procedural illustration and assessment of the result obtained. However, no paper describing a method of calibrating a colour image scanner digitising system has been published. One of the

38

main reasons for the small amount of attention paid to calibration in the colour image analysis field is that special equipment which is dominately required to obtain the most relevant information for colour analysis and the relevant expertise is not available. In the colour science domain, the spectral irradiance of the illuminant and the spectral reflectance of the colour samples are used as the basic data for colour analysis, where this information can only be obtained using spectroradiometers and sophisticated illumination standards. However, if a digitising system's spectral

No.	Name	CIE (1931)		
		x	y	Y
1.	dark skin	0.4002	0.3504	10.05
2.	light skin	0.3773	0.3446	35.82
3.	blue sky	0.2470	0.2514	19.33
4.	foliage	0.3372	0.4220	13.29
5.	blue flower	0.2651	0.2400	24.27
6.	bluish green	0.2608	0.3430	43.06
7.	orange	0.5060	0.4070	30.05
8.	purplish blue	0.2110	0.1750	12.00
9.	moderate red	0.4533	0.3058	19.77
10.	purple	0.2845	0.2020	6.56
11.	yellow green	0.3800	0.4887	44.29
12.	orange yellow	0.4729	0.4375	43.06
13.	Blue	0.1866	0.1285	6.11
14	Green	0.3046	0.4782	23.39
15.	Red	0.5385	0.3129	12.00
16.	Yellow	0.4480	0.4703	59.10
17.	Magenta	0.3635	0.2325	19.77
18.	Cyan	0.1958	0.2519	19.77
19.	white	0.3101	0.3163	90.01
20.	*neutral 8	0.3101	0.3163	59.10
21.	*neutral 6.5	0.3101	0.3163	36.20
22.	*neutral 5	0.3101	0.3163	19.77
23.	*neutral 3.5	0.3101	0.3163	9.00
24.	black	0.3101	0.3163	3.13

Table 2.2 Colour names and specifications (McCamy et al., 1976). The chromaticity coordinates are based on the CIE illuminant C. (*): The neutral greys are named as the Munsell notations are usually spoken.

sensitivities are different from the human visual system and spectral devices which can be used for measuring the spectral sensitivities of the digitising system are not available, how can the three-dimensional uniform colour space be obtained? In order to give a reasonable answer to this question, a simple method of calibrating a colour image scanner digitising system using the Macbeth colour chart in the CIE L*a*b* colour space will be described. The Macbeth colour chart which is a subset of the Munsell colour standards has been developed to facilitate quantitative or visual evaluation of colour reproduction processes employed in photography, television, and colour printing. The chart consists of the 4 x 6 array of patches, each about 50 mm square, which includes a well-spaced series of six neutral patches ranging from white to black, and a wide gamut of chromatic colours, additive and subtractive primaries. Each patch is characterised by an assigned name and the CIE 1931 x, y and Y as shown in Table 2.2 (McCamy et al., 1976), where the chromaticity coordinates of each colour have been obtained under the CIE illuminant C (average daylight). The chromaticity coordinates x, y and Y are transformed into the tristimulus values X, Y and Z, using Equation (2.4-11). The tristimulus values X, Y and Z are also transformed into the CIE L*, a* and b* coordinates by simply applying Equation (2.3-4), where the coordinates Xo, Yo and Zo for the illuminant C reference white are:

Xo = 98.07, Yo =100.0 and Z = 118.23 (Hunt, 1989).

The X, Y and Z values calculated using the x, y and Y values in Table 2.2 and the L*, a* and b* values calculated using these X, Y and Z values are in Table 2.3. Thus, the calibration of a colour image scanner can be performed using the Macbeth colour chart and the tristimulus values X, Y and Z derived from the

40

chromaticity coordinates of each patch created by McCamy et al. If the tristimulus values R, G and B of each patch of the Macbeth colour chart are obtained by scanning the chart using a colour image scanner, the problem of this calibration can be abstracted to a modelling problem, where these R, G and B values are independent variables and the corresponding X, Y and Z values are dependent variables. Let us consider the modelling procedure in detail. Firstly, the 24 colours in the Macbeth colour chart were measured using the colour image scanner (JX600) which was connected to a Macintosh IIx system. As Table 2.6 shows, the red, green and blue levels of the black patch (No. 24) in the chart were

No.	X	Y	Z	L*	a*	b*
1.	11.48	10.05	7.15	37.93	12.12	14.48
2.	39.22	35.82	28.91	66.38	13.28	16.97
3.	18.99	19.33	38.57	51.07	.17	-22.04
4.	10.62	13.29	7.58	43.20	-16.84	22.02
5.	26.81	24.27	50.05	56.36	12.62	-25.42
6.	32.74	43.06	49.74	71.60	-30.71	1.17
7.	37.36	30.05	6.42	61.70	27.56	58.23
8.	14.47	12.00	42.10	41.22	17.59	-43.11
9.	29.31	19.77	15.57	51.58	43.02	14.76
10.	9.24	6.56	16.68	30.78	25.86	-23.46
11.	34.44	44.29	11.90	72.42	-28.37	59.42
12.	46.54	43.06	8.82	71.60	12.43	66.83
13.	8.87	6.11	32.57	29.69	27.51	-51.36
14	14.90	23.39	10.62	55.47	-41.27	33.66
15.	20.65	12.00	5.70	41.22	50.84	25.86
16.	56.30	59.10	10.27	81.35	-4.04	79.26
17.	30.91	19.77	34.35	51.58	48.99	-15.95
18.	15.37	19.77	43.35	51.58	-21.70	-26.64
19.	88.25	90.01	106.32	96.00	-.04	.06
20.	57.94	59.10	69.81	81.35	-.05	.05
21.	35.49	36.20	42.76	66.67	-.04	.04
22.	19.38	19.77	23.35	51.58	-.04	.04
23.	8.82	9.00	10.63	35.98	-.05	.03
24.	3.07	3.13	3.70	20.56	.01	.00

Table 2.3 The X, Y, Z, L*, a*, and b* values calculated using the x, y and Y values in Table 2.2.

41

too high to be used in a normalisation procedure. Thus, a nearly perfect reflecting diffuser which had a black colour was additionally scanned. Although each patch had a uniform colour, the captured image of each patch contained a number of slightly different colours because of minor surface-irregularity. Thus, 3600 red, green and blue values for each patch were selected in order to calculate an average value. In this measuring procedure, the 25 sets of red, green and blue values for each patch were obtained, which are given in Table 2.6. The red, green and blue values of each of the 24 colours were then normalised according to the black and white levels as follows:

$$Rn = \frac{R(i) - R(b)}{R(w) - R(b)} \times 100,$$

$$Gn = \frac{G(i) - G(b)}{G(w) - G(b)} \times 100,$$

$$Bn = \frac{B(i) - B(b)}{B(w) - B(b)} \times 100,$$

(2.5-1)

where n and i = 1, 2, 3, ..., 24, respectively; R(i), G(i) and B(i) represent the red, green and blue values of each of 24 colours; R(b), G(b) and B(b) represent the red, green and blue values of black; and R(w), G(w) and B(w) represent the red, green and blue values of white. The reason for this normalisation is that the red, green and blue values of each of the 24 colours are to be corrected according to the values of black and white. The normalised Rn, Gn Bn values are given in Table 2.6. In the colour science domain, it is well known that the Y tristimulus value has a linear relationship with the intensity of each of the tristimulus values red, green and blue of each colour (Judd & Wyszecki, 1975). However, the Y tristimulus values did not have a linear relationship with the corresponding Rn, Gn and Bn values of the 24

42

colours. Figures 2.12.(a) through to (c) show a non-linear relationship between the Y tristimulus values and each of their corresponding Rn, Gn and Bn values. In the particular case of the
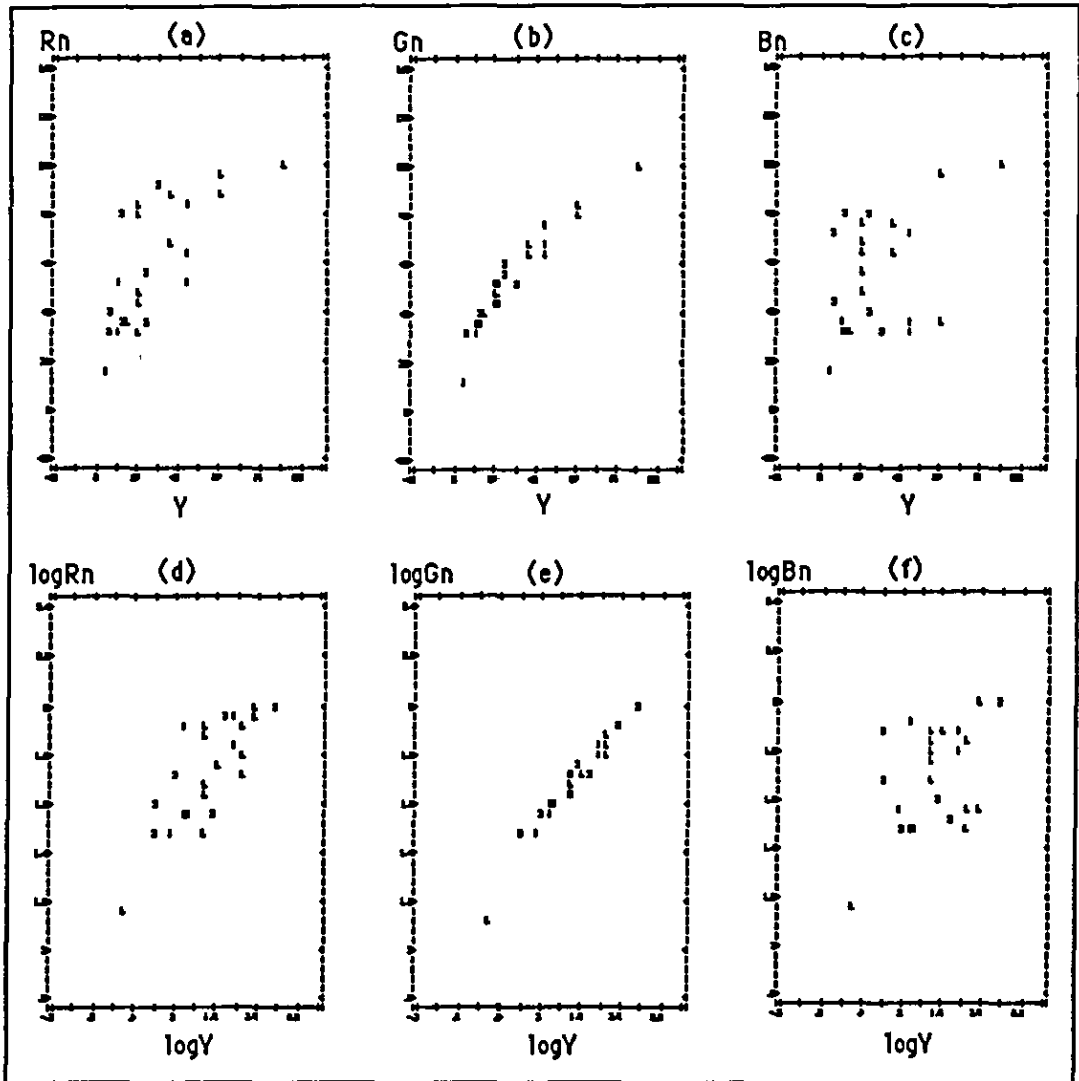
Figure 2.12 Scatter diagrams. (a) A scatter diagram of the Rn values against the Y values. (b) A scatter diagram of the Gn values against the Y values. (c) A scatter diagram of the Bn values against the Y values. (d) A scatter diagram of the $\log_{10}Rn$ against the $\log_{10}Y$ values. (e) A scatter diagram of the $\log_{10}Gn$ against the $\log_{10}Y$ values. (f) A scatter diagram of the $\log_{10}Bn$ against the $\log_{10}Y$ values.

43

non-linear relationship, the non-linear relationship can be reduced to a linear relationship by an appropriate transformation of variables. Thus, transform the Y tristimulus values into the Common logarithm of Y, $\log_{10}y$; and the Rn, Gn and Bn into $\log_{10}Rn$, $\log_{10}Gn$ and $\log_{10}Bn$, respectively. Then, the $\log_{10}Y$ values have a linear relationship with the $\log_{10}Rn$, $\log_{10}Gn$ or $\text{Log}_{10}Bn$ values. Figures 2.12.(d) through to (f) show a linear relationship between the $\log_{10}Y$ values and the $\log_{10}Rn$, $\log_{10}Gn$ or $\log_{10}Bn$ values.

Finally, obtaining the linear relationship becomes a problem of calculating a regression coefficient using the transformed variables $\log_{10}Y$ and each of $\log_{10}Rn$, $\log_{10}Gn$ and $\log_{10}Bn$ as follows:

$$\log_{10}Rn = \gamma_R \log_{10}Y,$$
$$\log_{10}Gn = \gamma_G \log_{10}Y, \text{ and}$$
$$\log_{10}Bn = \gamma_B \log_{10}Y, \tag{2.5-2}$$

where γ_R, γ_G and γ_B are respectively the regression coefficients of the regression equations. These regression coefficients, obtained by applying the regression analysis routine of the SPSS-X, are γ_R = 1.26094, γ_G = 1.23629 and γ_B = 1.22524, respectively, as Table 2.4 shows. It can be concluded that each regression equation accurately represents the sample data, which have been involved

Dependent Variable	Independent Variable	Regression Coefficient	Standard Error	T Value (Ta)	Prob. (T>Ta)	R square
log₁₀Rn	log₁₀Y	1.26094	0.05	26.30	0 0	0.97
log₁₀Gn	log₁₀Y	1.23629	0.04	30.57	0.0	0.98
log₁₀Bn	log₁₀Y	1.22524	0.06	20.66	0.0	0.95

Table 2.4 The results of regression analyses.

44

in the regression analysis, since each R-square is nearly 1.0 and each significant value (probability of T > Ta) is 0.0. Each of the equations in Equation (2.5-2) is transformed into the following equations which have no logarithms:

$$Y = Rn^{(1/\gamma_R)},$$

$$Y = Gn^{(1/\gamma_G)}, \text{ and}$$

$$Y = Bn^{(1/\gamma_B)}. \tag{2.5-3}$$

Since the Y values have a linear relationship with their corresponding $Rn^{(1/\gamma_R)}$, $Gn^{(1/\gamma_G)}$ or $Bn^{(1/\gamma_B)}$ values, these latter values can be involved in the following modelling procedures. Let $Rn^{(1/\gamma_R)}$, $Gn^{(1/\gamma_G)}$ and $Bn^{(1/\gamma_B)}$ be Rr, Gr and Br, respectively.

The conventional model which has been used to transform the Rr, Gr and Br values into the X, Y and Z tristimulus values in the colour science field is defined as follows (Hunt, 1989):

$$\begin{bmatrix} X \\ Y \\ Z \end{bmatrix} = \begin{bmatrix} C11 & C12 & C13 \\ C21 & C22 & C23 \\ C31 & C32 & C33 \end{bmatrix} \begin{bmatrix} Rr \\ Gr \\ Br \end{bmatrix}, \tag{2.5-4}$$

where the 3 x 3 matrix represents the transformation coefficients. In this model, since the variables X, Y and Z are independent of each other, this model can be broken down into three different submodels as follows:

$$X = C11Rr + C12Gr + C13Br, \tag{2.5-5.a}$$
$$Y = C21Rr + C22Gr + C23Br \text{ and} \tag{2.5-5.b}$$
$$Z = C31Rr + C32Gr + C33Br. \tag{2.5-5.c}$$

To obtain each coefficient, a multiple regression analysis has been performed using the regression analysis routine of the SPSS-X, where the Rr, Gr and Br values and the tristimulus X, Y and Z

45

Dependent Variable	Independent Variable	Regression Coefficient	Standard Error	T Value (Ta)	Prob. (T>Ta)	R square
X	Rr	0.5184	0 38	1.36	0 19	0.89
	Gr	1.1304	0.52	2.16	0.04	
	Br	-0.4065	0 30	-1.35	0.19	
Y	Rr	-0.2616	0.38	-0.70	0.49	0.89
	Gr	2.1879	0.52	4 22	0.0	
	Br	-0 6730	0.29	-2.27	0.03	
Z	Rr	-0.7748	0.47	-1.66	0.11	0.86
	Gr	0.3829	0.64	0.59	0.55	
	Br	1.5719	0.37	4.25	0.0	

Table 2.5 The results of multiple regression analyses.

values of each of the 24 colours in the Macbeth colour chart have been used as the sample data. The results obtained by the regression analysis as shown in Table 2.5 are as follows:

$$X = 0.5184Rr + 1.1304Gr - 0.4065Br, \qquad (2.5\text{-}6.a)$$
$$Y = -0.2616Rr + 2.1879Gr - 0.6730Br, \qquad (2.5\text{-}6.b)$$
$$Z = -0.7748Rr + 0.3829Gr + 1.5719Br. \qquad (2.5\text{-}6.c)$$

The results of the multiple regression analysis can be evaluated by the following procedure. Firstly, calculate the L^*, a^* and b^* values using the X, Y and Z tristimulus values, measured by McCamy et al., by applying Equation (2.3-4), where the X_o, Y_o and Z_o for the illuminant C reference white are 98.07, 100.0 and 118.23, respectively. Secondly, calculate the L^*, a^* and b^* values using the X, Y and Z values which are calculated from the models in Equation (2.5-6) by applying Equation (2.3-5). Let the L^*, a^* and

46

b* values obtained in the first step be L^*_{Mc}, a^*_{Mc} and b^*_{Mc}, respectively; and those obtained in the second step be respectively L^*_{cal}, a^*_{cal} and b^*_{cal}. Applying the colour difference formula in Equation (2.3-5) results in:

$$\Delta E_{ab}^*$$

$$= [(L^*_{Mc} - L^*_{cal})^2 + (a^*_{Mc} - a^*_{cal})^2 + (b^*_{Mc} - b^*_{cal})^2]^{1/2}. \qquad (2.5-7)$$

After calculating the colour difference ΔE_{ab}^* for each of the 24 colours, the average value of ΔE_{abi}^*, where i = 1 to 24, which has been calculated is 11.93. No criterion for evaluating the average value of ΔE_{abi}^* has been introduced. However, the basic principle of the evaluation obviously is that the lower the average value of ΔE_{abi}^*, the better. To reduce the average value, several experiments with the different types of models were performed, where the three variables Rr, Gr and Br were basically used with various combinations, making sure all variables undergo similar operations, since they are the primary stimuli of ⌐ human vision. Among the models, the following model could provide the least average value of ΔE_{abi}^*:

$$\begin{bmatrix} \log_{10}X \\ \log_{10}Y \\ \log_{10}Z \end{bmatrix} = \begin{bmatrix} C11 & C12 & C13 & C14 & C15 & C16 & C17 & C18 & C19 \\ C21 & C22 & C23 & C24 & C25 & C26 & C27 & C28 & C29 \\ C31 & C32 & C33 & C34 & C35 & C36 & C37 & C38 & C39 \end{bmatrix} \begin{bmatrix} Rr \\ Gr \\ Br \\ Rr^2 \\ Gr^2 \\ Br^2 \\ RrGr \\ GrBr \\ BrRr \end{bmatrix}.$$

$$(2.5-7)$$

This model can be broken down into three different submodels as follows:

47

$$\log_{10}X = C11Rr + C12Gr + C13Br + C14Rr^2 + C15Gr^2 + C16Br^2 + C17RrGr$$
$$+ C18GrBr + C19BrRr, \qquad\qquad (2.5\text{-}8.a)$$

$$\log_{10}Y = C21Rr + C22Gr + C23Br + C24Rr^2 + C25Gr^2 + C26Br^2 + C27RrGr$$
$$+ C28GrBr + C29BrRr, \qquad\qquad (2.5\text{-}8.b)$$

$$\log_{10}Z = C31Rr + C32Gr + C33Br + C34Rr^2 + C35Gr^2 + C36Br^2 + C37RrGr$$
$$+ C38GrBr + C39BrRr. \qquad\qquad (2.5\text{-}8.c)$$

The result of the multiple regression analyses are as follows:

$$
\begin{aligned}
\log_{10}X = \quad & 0.022514Rr \\
& + 0.046143Gr \\
& - 0.005592Br \\
& + (9.04773E\text{-}05)Rr^2 \\
& - (3.28888E\text{-}04)Gr^2 \\
& + (2.93842E\text{-}04)Br^2 \\
& - (1.66215E\text{-}04)RrGr \\
& - (1.62771E\text{-}04)GrBr \\
& - (9.93195E\text{-}05)BrRr, \qquad\qquad (2.5\text{-}9.a)
\end{aligned}
$$

$$
\begin{aligned}
\log_{10}Y = \quad & - 0.016447Rr \\
& + 0.100839Gr \\
& - 0.020879Br \\
& + (3.60334E\text{-}04)Rr^2 \\
& - 0.001285Gr^2 \\
& + (1.98717E\text{-}04)Br^2 \\
& + (5.43750E\text{-}05)RrGr \\
& + (1.87177E\text{-}04)GrBr \\
& + (1.10345E\text{-}04)BrRr, \qquad\qquad (2.5\text{-}9.b)
\end{aligned}
$$

$$
\begin{aligned}
\log_{10}Z = \quad & - 0.003715Rr \\
& - 0.024801Gr \\
& + 0.088003Br \\
& - (1.63468E\text{-}04)Rr^2 \\
& + (3.08820E\text{-}04)Gr^2 \\
& - 0.001085Br^2 \\
& + (2.96476E\text{-}04)RrGr \\
& + (3.22757E\text{-}04)GrBr \\
& + (3.64685E\text{-}05)BrRr. \qquad\qquad (2.5\text{-}9.c)
\end{aligned}
$$

48

The R-square for each multiple regression analysis is greater than 0.99. In a practical calculation, equations (2.5-9.a) through to (2.5-9.c) are respectively transformed into the following equations:

$$
\begin{aligned}
X = 10^{**}(& \ 0.022514Rr \\
& + 0.046143Gr \\
& - 0.005592Br \\
& + (9.04773E-05)Rr^2 \\
& - (3.28888E-04)Gr^2 \\
& + (2.93842E-04)Br^2 \\
& - (1.66215E-04)RrGr \\
& - (1.62771E-04)GrBr \\
& - (9.93195E-05)BrRr),
\end{aligned}
\tag{2.5-10.a}
$$

$$
\begin{aligned}
Y = 10^{**}(& - 0.016447Rr \\
& + 0.100839Gr \\
& - 0.020879Br \\
& + (3.60334E-04)Rr^2 \\
& - 0.001285Gr^2 \\
& + (1.98717E-04)Br^2 \\
& + (5.43750E-05)RrGr \\
& + (1.87177E-04)GrBr \\
& + (1.10345E-04)BrRr),
\end{aligned}
\tag{2.5-10.b}
$$

$$
\begin{aligned}
Z = 10^{**}(& - 0.003715Rr \\
& - 0.024801Gr \\
& + 0.088003Br \\
& - (1.63468E-04)Rr^2 \\
& + (3.08820E-04)Gr^2 \\
& - 0.001085Br^2 \\
& + (2.96476E-04)RrGr \\
& + (3.22757E-04)GrBr \\
& + (3.64685E-05)BrRr).
\end{aligned}
\tag{2.5-10.c}
$$

These X, Y and Z values calculated by equations (2.5-10.a) through to (2.5-10.c) are in Table 2.6. The L^*, a^* and b^* values calculated using the X, Y and Z values and Xo, Yo and Zo values for the illuminant C reference white by applying Equation (2.3-4) are shown in Table 2.6. The ΔE_{abi}^* values in the right-most column of Table 2.6 are calculated by Equation (2.5-7). The average value of ΔE_{abi}^* obtained applying 'equations (2.5-10.a) through to (2.5-10.c) is 4.54 and the standard deviation of ΔE_{abi}^* is 2.07. This average value compares very well with a value of 9.11 obtained by Strachan et al. (1990). They measured the red, green and blue values of the 24 colours in the Macbeth colour chart with a colour video camera under illuminant A. They obtained the conventional style 3 x 3 matrix as shown in Equation (2.5-4) by minimising the average value of ΔE_{uvi}^*, where the $L^*u^*v^*$ values of the Macbeth chart under illuminant A which were measured using a colorimeter by a Hunter Lab Colour QUEST Spectrophotometer were used as reference data.

Table 2.6 Macbeth colours measured by colour image digitising system.

No.	R1	Gi	Bi	Rn	Gn	Bn	Rr	Gr	Br	X_p	Y_p	Z_p	L^*_p	a^*_p	b^*_p	ΔEab^*
1.	33041	23901	20571	50.24	36.28	31.14	22.34	18.26	16.55	13.04	11.32	7.53	40.11	13.33	16.88	3.46
2.	57224	42586	42629	87.27	64.88	64.92	34.61	29.23	30.14	43.51	39.64	31.89	69 21	14.04	17 69	3.02
3.	29554	33924	49149	44.90	51.62	74.90	20.43	24.29	33.88	19.37	19.22	40.71	50.95	2.64	-24.75	3 67
4.	23901	26986	20561	36.25	41.01	31.12	17.24	20.16	16.54	11.46	14.23	7.81	44.70	-17.16	23.79	2.34
5.	26771	25980	51943	55.95	54.77	79.18	24.33	25.48	35.45	25.05	22.69	44.09	54.76	12.27	-21.97	3.82
6.	33713	48583	47254	51.27	74.06	72.16	22.70	32.53	32.86	29.74	38.25	46.00	68.28	-27.35	-.70	5.08
7.	59168	34352	21043	90.25	52.28	31.86	35.55	24.54	16.06	36.04	29.31	6.73	61.05	29.65	55.90	2 65
8.	23952	26985	52133	36.32	41.00	79.47	17.27	20.16	35.55	14.11	11.59	42.35	40.55	10.25	-44.54	1.71
9.	54723	29199	31875	69.44	44.39	49.45	33.40	21.50	23.74	27.64	18.41	15.39	49.99	44.15	12.41	3 05
10.	26984	20561	30195	40.97	31.17	45.09	19.00	16.15	22.71	9.79	7.45	16 30	32.02	21.54	-19.32	6.32
11.	41111	45745	23901	62.60	69.71	36.24	26.59	30.97	18.73	31.10	39.35	10.74	69.01	-25.13	56.66	5.46
12.	54452	41119	20719	69.03	62.69	31.96	33.27	28.40	16.63	39.23	38.69	7.20	68.53	4.11	67.03	8.87
13.	20560	20631	47641	31.13	31.28	72.59	15.28	16.28	33.02	9.63	6.69	37.29	31.10	27.70	-34.95	3.86
14	23901	38968	26648	36.25	59.34	40.44	17.24	27.19	20.48	17.03	27.53	13.19	59.46	-46.20	33.81	6.35
15.	53372	23901	20560	81.38	36.28	31.12	32.75	18.26	16.54	22.33	13.14	6.40	42.98	32.03	26.01	2.12
16.	63314	53521	23909	96.60	81.61	36.25	37.51	35.18	18.74	61.69	62.89	10.91	83.37	.01	80.97	4.85
17.	51707	29555	42610	78.83	44.94	64.89	31.93	21.72	30.13	27.48	17.52	27.56	48.91	47.38	-11.16	5.71
18.	20560	34431	44299	31.13	52.40	67.48	15.28	24.59	31.11	15.04	19.69	35.10	51.48	-23.26	-17 07	9.70
19.	65535	65535	65535	100.00	100.00	100.00	38.56	41.47	42.89	85.45	88.28	100.76	95.28	-2.09	2 24	3.07
20.	57269	56370	64165	87.34	85.97	97.90	34.63	36.70	42.1	65.62	66.89	77.98	85.45	.05	.81	4.17
21.	44282	44186	50948	67.46	67.33	77.66	28.22	30.11	34.89	35.58	36.24	47.30	66.70	.15	-4.78	4.82
22.	31868	31868	37581	48.45	48.48	57.19	21.70	23.09	27.18	17.47	17.58	24.97	48.99	1.23	-7.06	7 66
23.	20632	20619	23903	31.24	31.26	36.24	15.32	16.19	18.73	8.06	8.11	10.81	34.21	.98	-3.53	4.11
24.	9991	9119	9836	14.95	13.66	14.69	8.54	8.29	8.96	3.17	3.08	3.32	20.35	2.54	1.88	3.16
25.	229	193	241	0.00	0.00	0.00										

2.6 CONCLUSION.

Since the three-dimensional uniform colour spaces such as the CIELAB and the CIELUV spaces were introduced by the CIE in 1976, these uniform colour spaces have been commonly used for colour image analysis. Thus, in this chapter, the detailed aspects which are pertinent to transforming the RGB values into one of these three-dimensional colour spaces have been investigated. In the transformation procedure, it was necessary to understand several fundamental concepts of colour, from its nature to various colour systems such as the CIE RGB system and the CIE XYZ system. It has become apparent during the investigation that the spectral sensitivity of a colour digitising system is not always the same as that of another system. Therefore, the tristimulus R, G and B values of an image measured by one colour digitising system are not always the same as those measured by another system. An important fact to note is that a three-dimensional uniform colour space cannot be obtained without the calibration of a colour image digitising system. To cope with the variation of the spectral sensitivity of a colour image scanner digitising system and to obtain a three-dimensional uniform colour space with minimum errors, a calibration method for the space has been developed applying regression analysis. An important feature of this method is that neither expensive devices such as spectroradiometers nor sophisticated illumination standards are required, only the Macbeth colour checker chart. Since the Macbeth colour chart can be easily obtained, the method developed in this thesis can be widely adopted in the calibration of a colour image scanner digitising system. Thus, colour comparison for various purposes in colour image analysis can be more accurately

performed in a three-dimensional uniform colour space with minimum errors.

Chapter 3

BOUNDARY EXTRACTION METHODS.

3.1 Introduction.

3.2 Characteristics of Edges.

3.3 Edge Detection.

3.3.1 Differentiation Methods.

3.3.2 Mask Matching Methods.

3.4 Boundary Extraction From Colour Image.

3.4 Conclusion.

3.1 INTRODUCTION.

In object identification, extracting the boundary of an object from a scanned image is a very important stage. The boundary is defined as a border line lying between a background and an object. The boundary data extracted from an image plays an important role in describing a shape of a two- or three-dimensional object. The current concern of boundary extraction methodologies seems to be how to extract the boundary of an object from a natural image using computers to mimic human beings and animals.

The majority of research pertaining to boundary extraction that had been performed by the early 1980's was mainly concerned with black-and-white images. The main reason for this was due to the fact that image handling devices were available only for black-and-white image handling. Most of the methodologies for black-and-white images have usually relied on one-dimensional information. In fact, the criteria for decision making obtained from one-dimensional information are theoretically limited to the one-dimensional domain. As far as colour image handling is concerned, proper methods to deal with three-dimensional colour features such as lightness, hue and chroma are inevitably required. The algorithm developed in this thesis has been designed to extract the boundary of an object applying three-dimensional colour features, that is, the CIE L^*, a^* and b^* colour features.

For boundary extraction, an investigation has been carried out not only to understand the theoretical concepts and backgrounds

of closely related methodologies, but also to devise feasible methods. A number of methods for boundary extraction have been developed using region segmentation techniques. In general, most of the methods were designed mainly for region extraction. Of course, these methods can be applied to boundary extraction which is the main subject of this chapter. However, the pertinent point is that after the region of an object is extracted from an image, the creation of boundary data, which will be used in shape analysis, should be undertaken. This seems a duplication of effort to extract a region and create a set of boundary data using the extracted region. Thus, in this chapter, the illustration of boundary extraction will focus on differentiation methods, mask matching methods, and a method combining the two above methods.

3.2 CHARACTERISTICS OF EDGES.

Before boundary extraction is considered, it is worth taking a detailed look at features of edges and their detection methodologies. An edge, defined as the boundary between two regions with relatively distinct grey levels or colour properties has its profile, which has one of the features in Figure 3.1. The features are represented by an abrupt change in grey level of a black-and-white image or values of colour feature the CIE L^*, a^* and b^* of a colour image when a cross section across the boundary between regions is viewed.

The idealised edge models (Levine, 1985) in Figure 3.1 are:
(1) An ideal step, as shown in Figure 3.1.(a), is usually considered as an edge feature with an assumption that an image consists of an object with a constant colour feature; and a background with a uniform colour feature or another object, adjacent to the first, which has also another different uniform colour feature. In this case the point e1 in Figure 3.1.(a) is an edge point.

(2) An ideal roof edge, as shown in Figure 3.1.(b), which is made up of two ramp singularities is explained as an edge feature when an image consists of an object with various colour features and another object with various colour features different from the features of the former. The point e2 in Figure 3.1.(b) is an edge point.

(3) An edge combining the unit step with the unit ramp, as shown in Figure 3.1.(c), is explained as an edge feature when an image consists of an object with a uniform colour feature and another

57

object, adjacent to the first, which has various colour features. The point e3 in Figure 3.1.(c) is an edge point.

(4) A spike edge, as shown in Figure 3.1.(d), which has two unit steps is for an image containing a line which is highly contrasted to the background in colour features. An edge in this case is either point e4 or point e5 in Figure 3.1.(d).
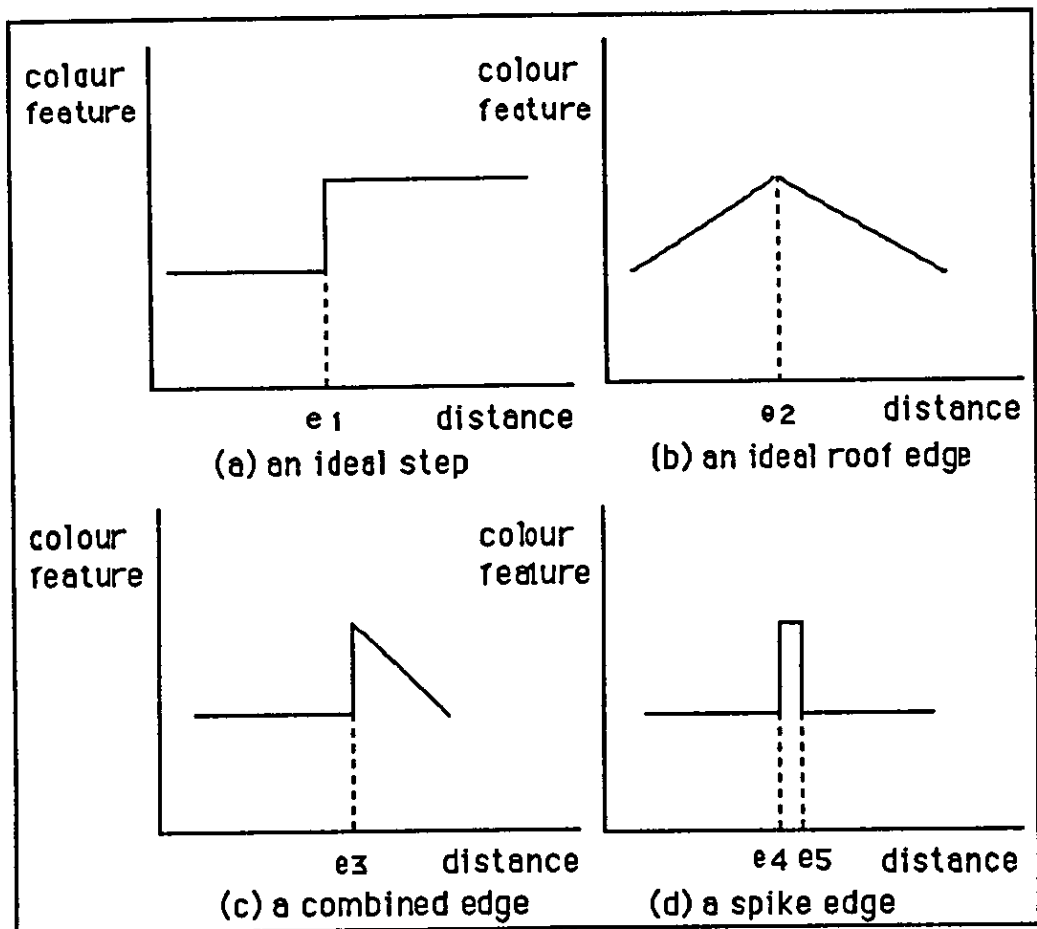
Figure 3.1 The idealised edge models.

3.3 EDGE DETECTION.

In the previous section, the characteristics of edges have been illustrated with their local features. In this section, the principal concepts of edge detection methods will be discussed.

Chow and Kaneko (1972) have divided edge detection algorithms into two categories based on one of the two basic properties of colour features or grey levels of pixels:

(1) discontinuity, and

(2) similarity.

In the first category, an edge is detected when colour features or grey levels of pixels change abruptly at a border point lying between two neighbouring regions. The methods in this category are usually called 'differentiation methods'.

In the second category, an edge is determined based on whether a local feature of colours or grey levels of pixels is similar to a predefined pattern or not. The methods in this category are usually called 'mask' or 'template' matching methods.

3.3.1 Differentiation Methods.

The basic paradigm of the edge detection method that is illustrated in this section is the computation of a local derivative operator. The main reason why the derivative operator has been used in edge detection will become clear after the geometrical features of a derivative are considered.

Suppose that one of the rows is extracted from an image array, the row is the x-axis and the grey level of each pixel is the

y-axis, then a function y = f(x) can be imagined, as in Figure 3 2, connecting the top mid point of every value of colour feature or grey level along the x-axis.
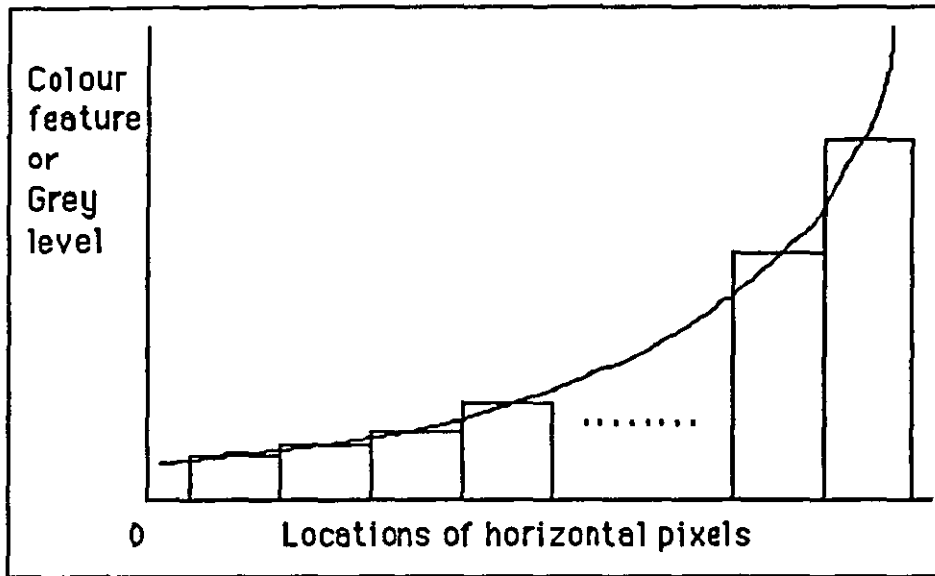
Figure 3.2 Function formulation.

Where the function y = f(x) obtained above is given in Figure 3.3, $\triangle x$ denotes a change from an arbitrary point b of x and $\triangle y$ denotes a change of y; if $\triangle x$ approaches zero ($\triangle x \rightarrow 0$), the derivative of the function at the point b is defined as follows:

$$\frac{\partial f(x)}{\partial x} = \lim_{\triangle x \to 0} \frac{\triangle y}{\triangle x} = \lim_{\triangle x \to 0} \frac{f(b + \triangle x) - f(b)}{\triangle x} \quad (3.3.1-1)$$

The derivative $\partial f(x)/\partial x$ in Equation (3.3.1-1) is usually considered as the gradient of the line segment joining the two points P and Q because in geometry a gradient of the line segment PQ is represented by change in y divided by the change in x:

gradient of a line segment PQ = (change in y)/(change in x)

$$= (\triangle y / \triangle x).$$

60
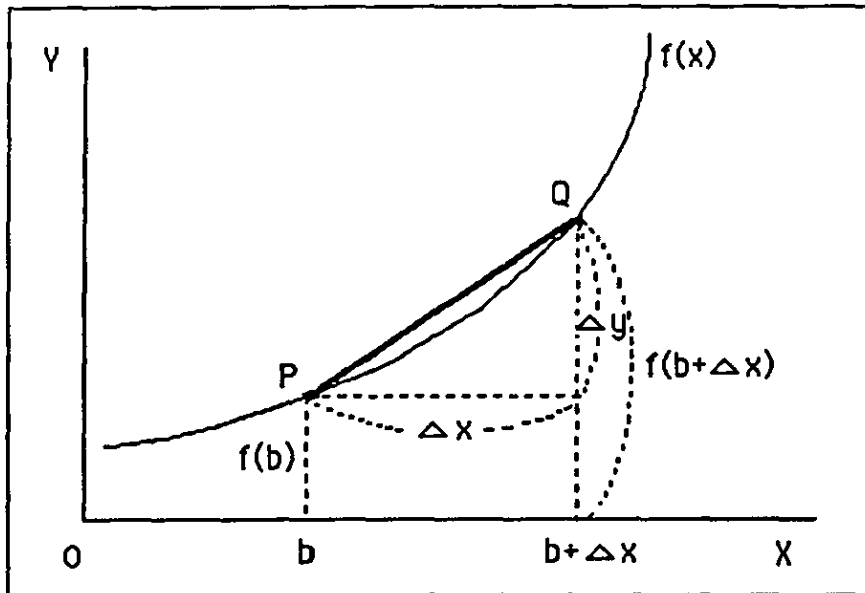
Figure 3.3 Geometrical feature of a derivative.

Fu, Gonzalez and Lee (1987) illustrated this concept with the aid of Figure 3.4. The image of a light object with a constant grey level on a dark background has a grey-level profile along a horizontal scan line. The dotted parts of both sides of the object denote slightly blurred areas, where the level of the blurring is reducing as the location moves further from the background along the horizontal line. Below the grey-level profile the first and second derivatives of the profile are depicted. The locations a, b, c, d, e and f of the image correspond to the locations a', b', c', d', e' and f' of the profile respectively along the horizontal line. Take a close look at the profile along the horizontal line, and it may be found that since segment lines, a'b', c'd' and e'f', have constant grey levels respectively, their first derivatives are all 0's (zeros). However, the segment line b'c' has a positive slope with respect to the horizontal line, therefore the first derivative of any location in this segment line has a positive value +h, on the other hand, the segment line d'e'

61

has a negative slope with respect to the horizontal line, thus the first derivative of any location in this segment line has a negative value -h. It is clear that at the location b' the first derivative value has been changed abruptly from 0 (zero) to +h and at the location e' the first derivative value has also changed abruptly from -h to 0. Since both the locations, b' and e', are physically boundary locations, it can be concluded that the first derivative values can be used efficiently to detect an edge lying between neighbouring regions.
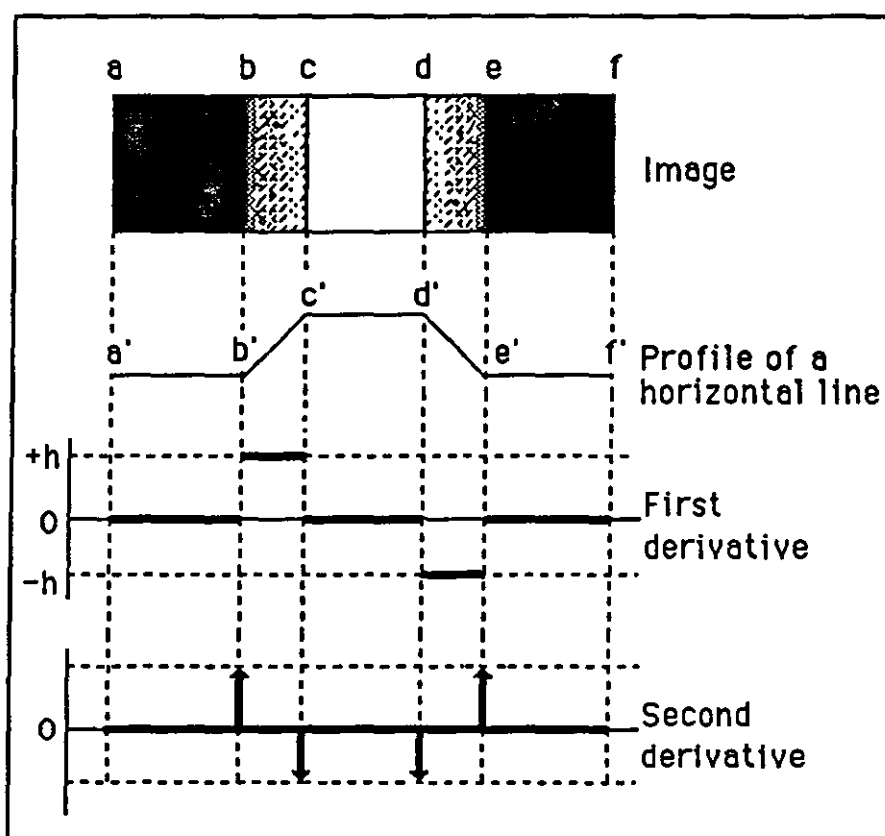
Figure 3.4 Elements of edge detection by derivative operators.

The second derivatives are usually obtained through a calculation using the first derivative values. The second derivatives at the locations, b' and e', are +h's and -h's at the locations, c' and d'. On

62

the other hand, the second derivatives of the other locations except these points are all 0's. An important fact to be noted is that the positive values of the second derivative are located at both the boundary locations, b' and e', while, the negative values of the second derivative are located inside the object, the locations, c' and d'. Based on the previous findings, it can be concluded that the sign of the second derivative is able to be used to determine whether an edge pixel lies on the dark or light side of an edge.

The previous discussion has been limited to a one-dimensional horizontal profile, however, since an actual image has a two-dimensional profile, the previous concepts should be applied to the horizontal profile and the vertical profile simultaneously. Assume that a function $z = f(x, y)$ representing the two-dimensional profile is given, the gradient of the horizontal profile, i.e. the partial derivative of $f(x, y)$ with respect to x, at a point (a, b) is

$$\text{gradient of } x = \frac{\partial f}{\partial x}$$

$$= \lim_{\triangle x \to 0} \frac{f(a + \triangle x, y) - f(a, b)}{\triangle x} , \quad (3.3.1\text{-}2)$$

the gradient of the vertical profile, i.e. the partial derivative with respect to y, at the point (a, b) is

$$\text{gradient of } y = \frac{\partial f}{\partial y}$$

$$= \lim_{\triangle y \to 0} \frac{f(a, b + \triangle y) - f(a, b)}{\triangle y} . \quad (3.3.1\text{-}3)$$

The partial derivatives of $f(x, y)$ with respect to x and y at the point (a, b) can be geometrically interpreted as the gradients of

63

the curves of the intersection of the surface z = f(x, y) with the planes, y=b and x=a, respectively. Figure 3.5 shows geometrically
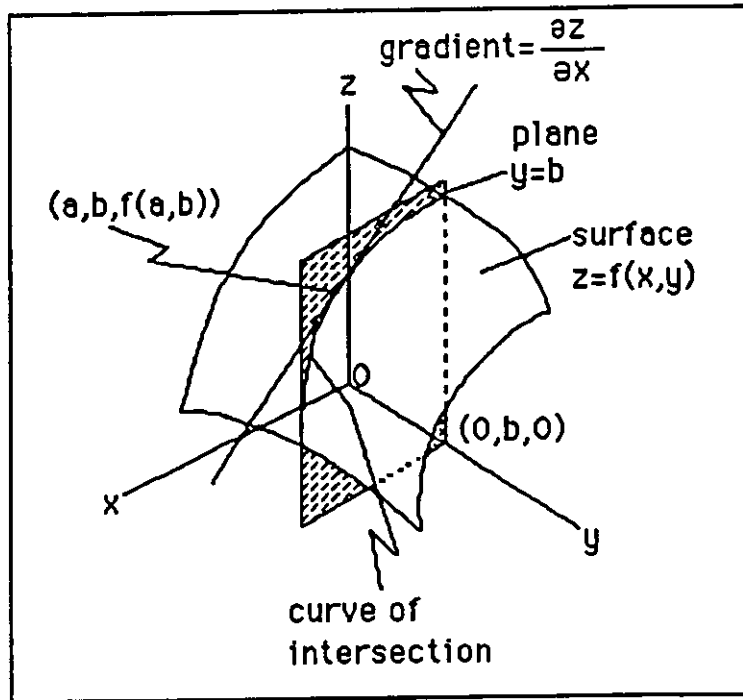
Figure 3.5 Geometrical illustration of the partial derivative.

the partial derivative, $\partial f/\partial x$, with respect to x, where the shaded plane is a plane, y = b, and is parallel to the plane xoz; and the slope of the tilted straight line touching, at the point (a, b, f(a, b)), the curve of the intersection of the surface z = f(x, y) with the shaded plane is the gradient, $\partial z/\partial x$.

The previous discussion can be arranged as follows, if a function f(x, y) is given, the gradient of f(x, y) at coordinates (x, y) is defined as the vector,

$$Gr[f(x, y)] = \begin{bmatrix} Gr_x \\ Gr_y \end{bmatrix} = \begin{bmatrix} \dfrac{\partial f}{\partial x} \\ \dfrac{\partial f}{\partial y} \end{bmatrix} \qquad (3.3.1-4)$$

64

where Gr_x is a partial derivative of $f(x, y)$ with respect to x,

Gr_y is a partial derivative of $f(x, y)$ with respect to y,

$x=1, 2, 3, \ldots\ldots, n-1$, ($n$: the number of pixels in a row)

$y=1, 2, 3, \ldots\ldots, l-1$, ($l$: the number of pixels in a column).

In practice, there are two important properties (Goldmark & Hollywood, 1951) of the gradient:

(1) the vector $Gr[f(x, y)]$ represents the direction of the maximum rate of increase of the function $f(x, y)$, and

(2) the magnitude of $Gr[f(x, y)]$ denoted by $Mag\_Gr[f(x, y)]$ is given by

$$Mag\_Gr[f(x, y)] = magnitude[Gr]$$
$$= (Gr_x{}^2 + Gr_y{}^2)^{1/2}$$
$$= \sqrt{\left[\frac{\partial f}{\partial x}\right]^2 + \left[\frac{\partial f}{\partial y}\right]^2}$$
$$\cong |Gr_x| + |Gr_y|. \qquad\qquad (3.3.1\text{-}5)$$

This equals the maximum rate of increase of $f(x, y)$ per unit distance in the direction Gr. In image differentiation methods, the magnitude of the gradient in the equation (3.3.1-5) has been considered as the basis for a number of algorithms. As a matter of fact, modelling the function $f(x, y)$ using digital image data usually not only needs laborious effort, but also is considered a meaningless procedure in the image domain. Therefore it is necessary to approximate the partial derivatives in the equation (3.3.1-5). Thus, other methods that can be used to calculate the magnitude of the gradient approximately have been developed, based on the theoretical background as discussed above, by Goldmark and Hollywood (1951) and Roberts (1965).

One of the methods in which the partial derivatives in Equation (3.3.1-5) are approximated by differences is given by the relation (Goldmark & Hollywood, 1951),

Mag_Gr[f(x, y)]

$$\cong \{ [f(x, y) - f(x+1, y)]^2 + [f(x, y) - f(x, y+1)]^2 \}^{1/2}. \quad (3.3.1-6)$$

Using absolute values produces similar results,

Mag_Gr[f(x, y)]

$$\cong |f(x, y) - f(x+1, y)| + |f(x, y) - f(x, y+1)|. \quad (3.3.1-7)$$

This approximation reflects not only the theoretical basis of calculating the partial derivatives but also the efficiency and adaptability of a computer implementation. The basic principle behind the relationship between pixels in equations (3.3.1-6) and (3.3.1-7) is clearly shown in Figure 3.6.

(a)

(b)
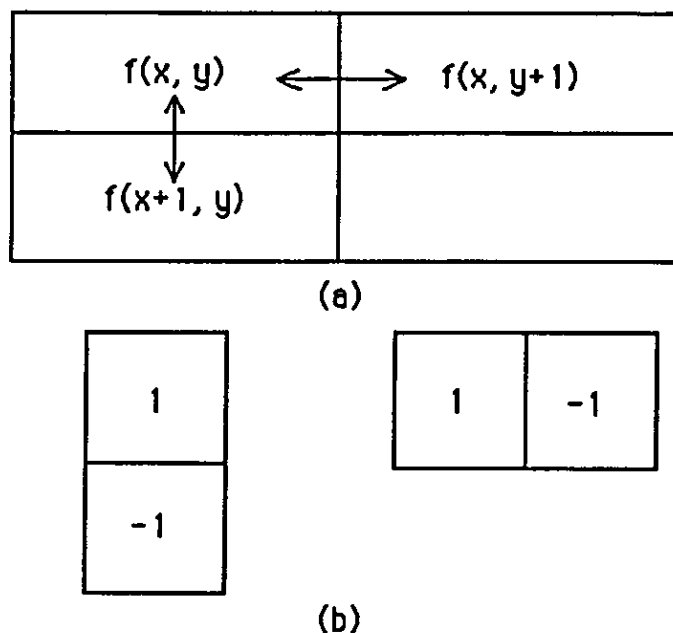
Figure 3.6 Goldmark operator. (a) A procedure for computing a two-dimensional, discrete gradient. (b) The masks for the operator.

The values of f(x, y) - f(x+1, y) and f(x, y) - f(x, y+1) in Figure 3.6 approximate those of $\partial f / \partial x$ and $\partial f / \partial y$ in the equation (3.3.1-

5), respectively. This approach is very efficient in computing terms, but, on the other hand, there has been some criticism about its sensitivity to noise.

Another method in which the partial derivatives, Gr_x and Gr_y, in the equation (3.3.1-5) are approximated by differences is given by the following relation, the so-called Roberts cross operator (Roberts, 1965):

Mag_Gr[f(x, y)] =

$$\{ [f(x, y) - f(x+1, y+1)]^2 + [f(x+1, y) - f(x, y+1)]^2 \}^{1/2} \quad (3.3.1-8)$$

or using absolute value,

Mag_Gr[f(x, y)] $\cong$

$$|f(x, y) - f(x+1, y+1)| + |f(x+1, y) - f(x, y+1)|. \quad (3.3.1-9)$$

The relationship between pixels and masks for this operator are shown in Figure 3.7.

(a)
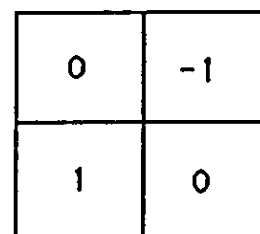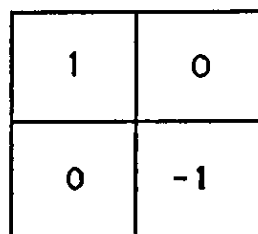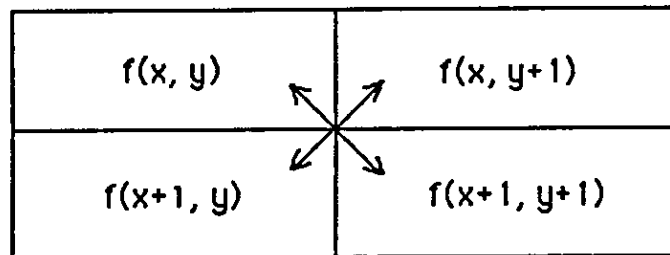
(b)

Figure 3.7 Roberts cross operator. (a) A procedure for computing a two-dimensional discrete gradient. (b) The masks for the Roberts cross operator.

It is commonly known that the Roberts cross operator can be efficiently used to detect both horizontal and vertical edges, while it is also sensitive to noise and object surface irregularities. However, this approach and the previous one have been used in computerised tomography to detect edges in three-dimensional object space and for colour edge detection in the three-dimensional colour space (Liu, 1977; Sankar, 1978).

Prewitt (1970) and Sobel (Robinson, 1977) devised other slightly more complicated methods using a 3 x 3 operator to approximate the partial derivatives at an arbitrary point (x, y). Their intention was to make the derivative operations less sensitive to noise. First, consider the Prewitt operator in Figure 3.8. The mask in Figure 3.8.(b) is used to approximate the partial derivative Gr_x, and another mask in Figure 3.8.(c) is used to approximate the partial derivative Gr_y. The gradient in the x-direction at a point (x, y) is obtained by employing the former mask as follows:

$$Gr_x = f(x+1, y-1) + f(x+1, y) + f(x+1, y+1) - f(x-1, y-1) - f(x-1, y)$$
$$-f(x-1, y+1). \qquad (3.3.1-10)$$

The gradient in the y-direction at a point (x, y) is obtained by employing the latter mask as follows:

$$Gr_y = f(x-1, y-1) + f(x, y-1) + f(x+1, y-1) - f(x-1, y+1) - f(x, y+1)$$
$$-f(x+1, y+1). \qquad (3.3.1-11)$$

(a)

$f(x-1, y-1)$	$f(x-1, y)$	$f(x-1, y+1)$
$f(x, y-1)$	$f(x, y)$	$f(x, y+1)$
$f(x+1, y-1)$	$f(x+1, y)$	$f(x+1, y+1)$

Figure 3.8 Prewitt operator. (a) A 3 x 3 local image. (b) Mask for Gr_x at (x, y). (c) Mask for Gr_y at (x, y) (continued).

68

(b)

-1	-1	-1
0	0	0
1	1	1

(c)

1	0	-1
1	0	-1
1	0	-1

Figure 3.8 Prewitt operator. (a) A 3 x 3 local image. (b) Mask for Gr_x at (x, y). (c) Mask for Gr_y at (x, y) (continued).

The magnitudes of these gradients are obtained by convolving the two masks.

Second, the Sobel operator gives greater weight to points lying closer to (x, y) as shown in Figure 3.9. Apart from this weighting, it is similar to the Prewitt operator. It is known that the result obtained using the Sobel operator is superior to that of the Prewitt operator in diagonal edge detection.

-1	-2	-1
0	0	0
1	2	1

(a)

1	0	-1
2	0	-2
1	0	-1

(b)

Figure 3.9 Sobel operator. (a) Mask for Gr_x at (x, y). (b) Mask for Gr_y at (x, y).

3.3.2 Mask Matching Methods.

In the previous section, boundary detection methods using the approximated magnitudes of the gradients were discussed. These approaches, ideally, yield only pixels lying on the boundary

69

between an object and the background, however, if there is severe noise in the image, the result obtained applying these approaches will be different from the real boundary. Thus, in order to cover such situations mask matching methods have been used in the image analysis domain. In this section, edge detection methods in which local patterns or masks (templates) are involved will be discussed.

There are a few masks that have been used to detect an abrupt change in colour features or grey levels and the edge orientation at that point. Let us consider four different kinds of operators, which have commonly been used in the image analysis domain, each of which has eight parallel masks as shown in Figure 3.11, where each mask is just the rotated version of a standard operator. The standard operator is a mask which is considered as a basis and is composed of nine components, i.e. a 3 x 3 array. At the centre of the mask, a current point (x, y) is located. The first and third columns in Figure 3.11 are the Prewitt operator and the second column is the Kirsch operator. It is known that the Kirsch operator is quite sensitive to small changes in gradient. The right-most column in Figure 3.11 is the Sobel operator in which greater weight is assigned to the points lying closer to the location of a current point (x, y). In the application of these operators, a contrast function and the edge orientation play an important role in boundary detection. The contrast function, denoted by **Contr**(x, y), which is corresponds to the first differences in eight directions at each location (x, y) is defined by

Contr(x, y)

$$= \max\{\ |Gr_0(x,\ y)|,\ |Gr_1(x,\ y)|,\ |Gr_2(x,\ y)|,\ \ldots\ldots,\ |Gr_7(x,\ y)|\ \}\qquad (3.3.2\text{-}1)$$

70

where $Gr_i = \sum_{j=1}^{9}(w_j * f_j),$ (3 3 2-2)

$i = 0, 1, 2, \ldots\ldots, 7$ (the location of each of eight neighbours as shown in Figure 3.10.(c);

$j = 1, 2, 3, \ldots\ldots, 9$ (the location of each point in Figure 3.10.(a) or (b));

w_j = each component of a mask as shown in Figure 3.10.(b);

f_j = each grey level of a local image of a 3x3 array in Figure 3.10.(a).

The edge orientation $\theta(x, y)$ is defined as

$\theta(x, y)$ = compass direction of largest Gr_i,   (3.3.2-3)

where 8 compass directions are shown in Figure 3.10.(c).
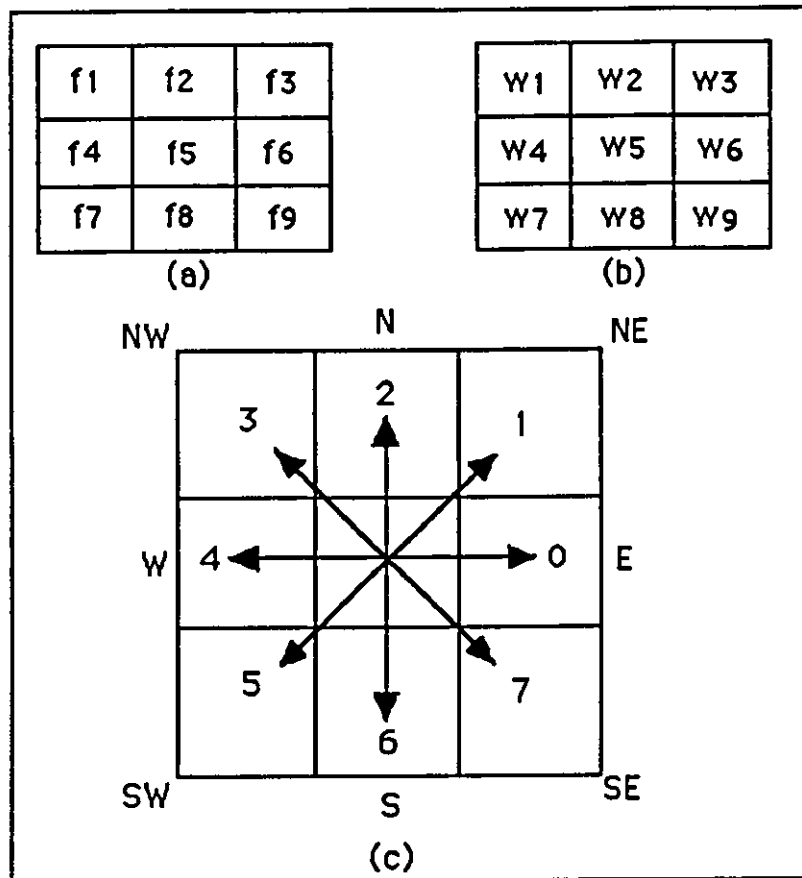
Figure 3.10 Major factors for the edge detecting operation. (a) Grey levels of a local image. (b) Components of a mask. (c) The compass directions.

71

Direction of edge	Direction of gradient	Prewitt operator	Kirsch operator	Prewitt operator	Sobel operator
0	N	1 1 1 1 -2 1 -1 -1 -1	5 5 5 -3 0 -3 -3 -3 -3	1 1 1 0 0 0 -1 -1 -1	1 2 1 0 0 0 -1 -2 -1
1	NW	1 1 1 1 -2 -1 1 -1 -1	5 5 -3 5 0 -3 -3 -3 -3	1 1 0 1 0 -1 0 -1 -1	2 1 0 1 0 -1 0 -1 -2
2	W	1 1 -1 1 -2 -1 1 1 -1	5 -3 -3 5 0 -3 5 -3 -3	1 0 -1 1 0 -1 1 0 -1	1 0 -1 2 0 -2 1 0 -1
3	SW	1 -1 -1 1 -2 -1 1 1 1	-3 -3 -3 5 0 -3 5 5 -3	0 -1 -1 1 0 -1 1 1 0	0 -1 -2 1 0 -1 2 1 0
4	S	-1 -1 -1 1 -2 1 1 1 1	-3 -3 -3 -3 0 -3 5 5 5	-1 -1 -1 0 0 0 1 1 1	-1 -2 -1 0 0 0 1 2 1
5	SE	-1 -1 1 -1 -2 1 1 1 1	-3 -3 -3 -3 0 5 -3 5 5	-1 -1 0 -1 0 1 0 1 1	-2 -1 0 -1 0 1 0 1 2
6	E	-1 1 1 -1 -2 1 -1 1 1	-3 -3 5 -3 0 5 -3 -3 5	-1 0 1 -1 0 1 -1 0 1	-1 0 1 -2 0 2 -1 0 1
7	NE	1 1 1 -1 -2 1 -1 -1 1	-3 5 5 -3 0 5 -3 -3 -3	0 1 1 -1 0 1 -1 -1 0	0 1 2 -1 0 1 -2 -1 0

Table 3.1 Four sets of mask for computing the gradient and orientation (Robinson, 1977).

In the edge detection operation, an edge detector moves from the current location (x, y) to one of eight neighbouring points

72

according to the edge orientation. It is important to note that, in a boundary extraction process, in order to detect a maximum gradient and its direction, each of eight parallel masks´ in Table 3.1 should be involved in this calculation. Note that in Table 3.1 the direction of the edge is perpendicular to that of the gradient. This information and the previous location are used in deciding the direction of movement of an edge detector. In order to clarify and to examine the efficiency of these methods consider the procedure for finding the maximum gradient and the orientation of ´the gradient at an arbitrary point (x, y) with the following example by applying the Sobel operator. Suppose a local image represented by a 3 x 3 array in Figure 3.11. Apply the Sobel operator in Table 3.1 to the image to detect a maximum gradient and the orientation of the gradient at the

0	0	0.9
0	0.2	0
0	0.5	0

Figure 3.11 A sample local image.

location (the centre of the array) whose intensity level is 0.2, where the previous location is assumed to be the location whose intensity is 0.5. The result of the application of Equation (3.3.2-2) is as follows:

Gr_0 = (1x0 + 2x0 + 1x0.9 + 0x0 + 0x0.2+ 0x0 -1x0 -2x0.5 -1x0) = -0.1

Gr_1 = (2x0 + 1x0 + 0x0.9 + 1x0 + 0x0.2 -1x0 + 0x0 -1x0.5 -2x0) = -0.5

Gr_2 = (1x0 + 0x0 -1x0.9 + 2x0 + 0x0.2 -2x0 + 1x0 + 0x0.5 -1x0) = -0.9

$Gr_3 = (0x0 -1x0 -2x0.9 + 1x0 + 0x0 \ 2 -1x0 + 2x0 + 1x0.5 + 0x0) = -1.3$

$Gr_4 = (-1x0 -2x0-1x0.9 + 0x0 + 0x0.2 + 0x0 + 1x0 +2x0.5 + 1x0) = 0.9$

$Gr_5 = (-2x0 -1x0 + 0x0.9 -1x0 + 0x0.2 + 1x0 + 0x0 + 1x0.5 + 2x0) = 0.5$

$Gr_6 = (-1x0 + 0x0 + 1x0.9 -2x0 + 0x0.2 + 2x0 -1x0 + 0x0.5 + 1x0) = 0.9$

$Gr_7 = (0x0 + 1x0 + 2x0.9 -1x0 + 0x0.2 + 1x0 -2x0 -1x0.5 + 0x0) = 1.3$

Since values, $|Gr_3| = |Gr_7| = 1.3$, are maximum, the directions of the edge are 3 and 7; and the directions of the gradients are SW and NE. Considering the result and the previous location, an edge detector would move from the location of grey level 0.2 to the upper right corner in Figure 3.11. In fact, the edge detecting operation should be carried out at each pixel point with a similar procedure. There is no doubt that these approaches are inefficient because they require a considerable amount of time. When one of these approaches is employed to detect the boundary of an object in a colour image, this operation should be carried out on a gradient image rather than on separated images of the lightness, hue and chroma. This is another aspect that makes these approaches worse in terms of system efficiency.

3.4 BOUNDARY EXTRACTION FROM COLOUR IMAGES.

In this section, the design of the boundary extraction system which has been developed in this thesis is discussed in detail. It was considered in the design stage that the system should be flexible enough to be used to extract a boundary not only from colour images but also from black-and-white images. This flexibility may be undoubtedly regarded as an attractive and strong feature of this system. Another important feature of this system is the extraction of a boundary without creating a binary edge map which consists of 0's and 1's. However, most approaches published commonly rely on the binary edge map, which the contour-following or border-following procedure utilises. The procedure mainly consists of three steps. The first step is to transform an input image into the gradient image. The second step is to create a binary edge map using a thresholding operation. The third step is to perform a contour- or border-following procedure. On the other hand, even though the mask matching method is adopted for the edge detection, the binary edge map is also created and then a contour- or border-following procedure is followed.

Note that in a system, for instance, a robot vision system, where the execution time is an important factor, the previous approaches employing the edge-detecting procedure and the contour- or border-following procedure separately cause error in an urgent situation. The procedure developed in this thesis was designed to extract a boundary accurately. Apart from the previous features such as flexibility and efficiency, the accuracy of the boundary extraction procedure has been emphasised since

75

not only the shape description stage, but also the colour pattern description stage depend entirely upon the result of the procedure. This principle is not exclusive to this problem. Consider one of many practical approaches in this domain, the so-called Papert's turtle (Papert, 1973). It has been assumed that a turtle crosses a binary edge map until it reaches a boundary point, then passes through the boundary, and immediately turns to the left and crosses the neighbouring boundary point and then turns to the right as in Figure 3.12.(a). Repeating this process, the turtle will follow the boundary in a clockwise direction until it returns to the starting point of the boundary. The set of points passed by the turtle eventually forms a boundary data set. This idea, from the behaviour of a turtle, is brilliant enough. However, as Figure 3.12.(b) shows, the turtle failed to pass the sharp curve on the upper right corner. In practice, this approach cannot be used to extract the boundaries of objects such as maple leaves that have sharp curves.

(a)   (b)

Figure 3.12 Boundary extraction procedure.

From now on the boundary extraction procedure developed by this thesis will be illustrated step by step. The procedure

76

consists of two steps: the first step is to create a gradient array using the CIELAB colour difference formula and the second step is to extract a boundary directly from the gradient array without creating any binary edge map.

In the first step, before creating the gradient array it was necessary to choose a colour difference calculation formula, which could be used to calculate a colour difference between two colour points, among the many formulae published so far in the colour science domain. According to McLaren's survey (McLaren, 1983), over twenty colour difference formulae were developed between 1936 and 1976. Fortunately, the CIE (International Commission on Illumination) has recommended a colour difference calculation formula called the CIELAB, because uniformity of practice allows for the exchange of information on a common basis.

As already illustrated in section 2.3, the (L^*, a^*, b^*) coordinates of the CIELAB space can be obtained by merely applying simpler functions to X/X_o, Y/Y_o and Z/Z_o. Suppose the (L^*, a^*, b^*) coordinates of two points, $P1(i, j)$ and $P2(i, j+1)$, in the CIELAB space obtained are (L_{ij}, a_{ij}, b_{ij}) and $(L_{i(j+1)}, a_{i(j+1)}, b_{i(j+1)})$, respectively, and

$$| L_{ij} - L_{i(j+1)} | > 0,$$
$$| a_{ij} - a_{i(j+1)} | > 0,$$
$$\text{and } | b_{ij} - b_{i(j+1)} | > 0.$$

Thus,
$$\Delta L_{ij,i(j+1)} = L_{ij} - L_{i(j+1)},$$
$$\Delta a_{ij,i(j+1)} = a_{ij} - a_{i(j+1)},$$
and
$$\Delta b_{ij,i(j+1)} = b_{ij} - b_{i(j+1)},$$

where Δ signifies 'difference'. The colour difference between the two points can be represented by:

77

$$\Delta E_{ij,i(j+1)} = [\ (\Delta L_{ij,i(j+1)})^2 + (\Delta a_{ij,i(j+1)})^2 + (\Delta b_{ij,i(j+1)})^2\ ]^{1/2}. \qquad (3.4\text{-}1)$$

In fact, the $\Delta E_{ij,i(j+1)}$ is the Euclidian distance between two points in the CIELAB space. The gradient of an arbitrary point (i, j) is calculated employing Equation (3.3.1-5) as follows:

$$G[i, j] = \Delta E_{ij,\ (i+1)j} + \Delta E_{ij,\ i(j+1)}$$

$$= [\ (\Delta L_{ij,\ (i+1)j})^2 + (\Delta a_{ij,\ (i+1)j})^2 + (\Delta b_{ij,\ (i+1)j})^2\ ]^{1/2}$$

$$+ [\ (\Delta L_{ij,\ i(j+1)})^2 + (\Delta a_{ij,\ i(j+1)})^2 + (\Delta b_{ij,\ i(j+1)})^2\ ]^{1/2}$$

$$= [\ (L_{ij} - L_{(i+1)j})^2 + (a_{ij} - a_{(i+1)j})^2 + (b_{ij} - b_{(i+1)j})^2\ ]^{1/2}$$

$$+ [\ (L_{ij} - L_{i(j+1)})^2 + (a_{ij} - a_{i(j+1)})^2 + (b_{ij} - b_{i(j+1)})^2\ ]^{1/2}. \qquad (3.4\text{-}2)$$

Hence, the gradient array G for each point (i, j), i=1, 2, 3, ..., m-1, j=1,2, 3, ..., n-1, is created, where m is the number of rows and n is the number of columns, in the array G.

(a)   (b)
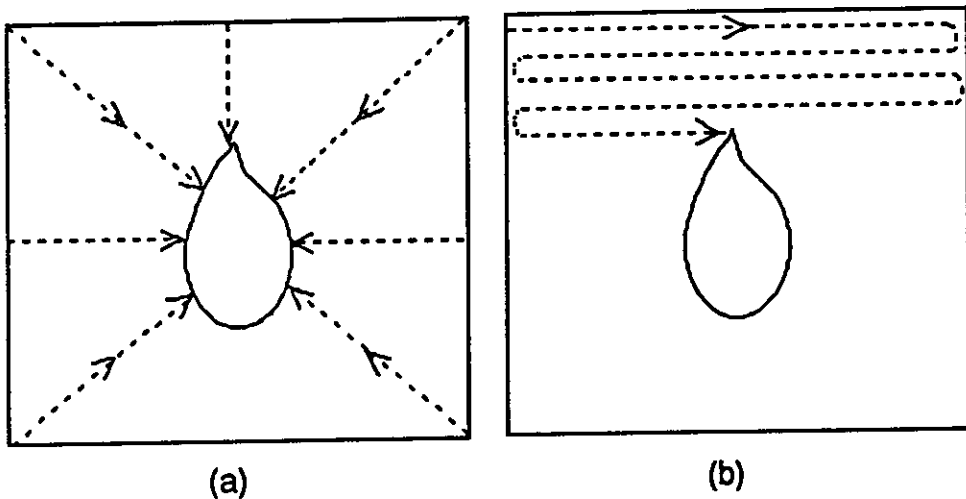
Figure 3.13 The scanning methods for boundary detection.

The second step begins with an operation for detecting a larger value of the gradient than a predetermined threshold from the upper left corner of the gradient array G. The starting point of the operation is not restricted to the corner, but could be one of the points on the outskirts of the array G in Figure 3.13.(a). The direction of the operation is straightforward to the centre of the array G as Figure 3.13.(a) shows. This strategy, under the

78

assumption that an object forming a boundary lies in the middle of an image plane, has two effects:

(1) it quickly reaches one of boundary points,

(2) the probability of avoiding spot-like noise will be increased.

However, most of the existing boundary detection operations have been designed to scan line by line, as Figure 3.13.(b) shows. If the size of an image plane is quite large and that of an object is relatively small, this scanning operation will be inefficient.

Determination of a Threshold

Although the original background has a uniform colour, tiny bubble-like spots have been scattered because of the surface irregularity. However, there is little difference between the colour of the spots and that of the other part of the background. This fact becomes clear when we examine the histogram in Figure 3.14. The vertical axis represents the locations of array components of the array G along the diagonal line and the horizontal axis represents the gradient level of each location. Both the extreme upper and lower parts of the horizontal axis correspond to the background. Very little fluctuation of the gradient levels in the two extremes reveals that there are colour differences among the pixels in the background, but these are extremely small. After analysing the histogram or the frequency of the gradient levels in the background a threshold value was determined. The threshold value is critical because it is used to decide whether an arbitrary point belongs to the background or is one of the boundary points. The process of the decision making can be represented by:

if $G[i, j] \leq T$, the point $(i, j) \, \varepsilon$ the background,

79

if G[i, j] > T, the point (i, j) ε the boundary,   (3.4-3)

where T is a threshold value determined above.
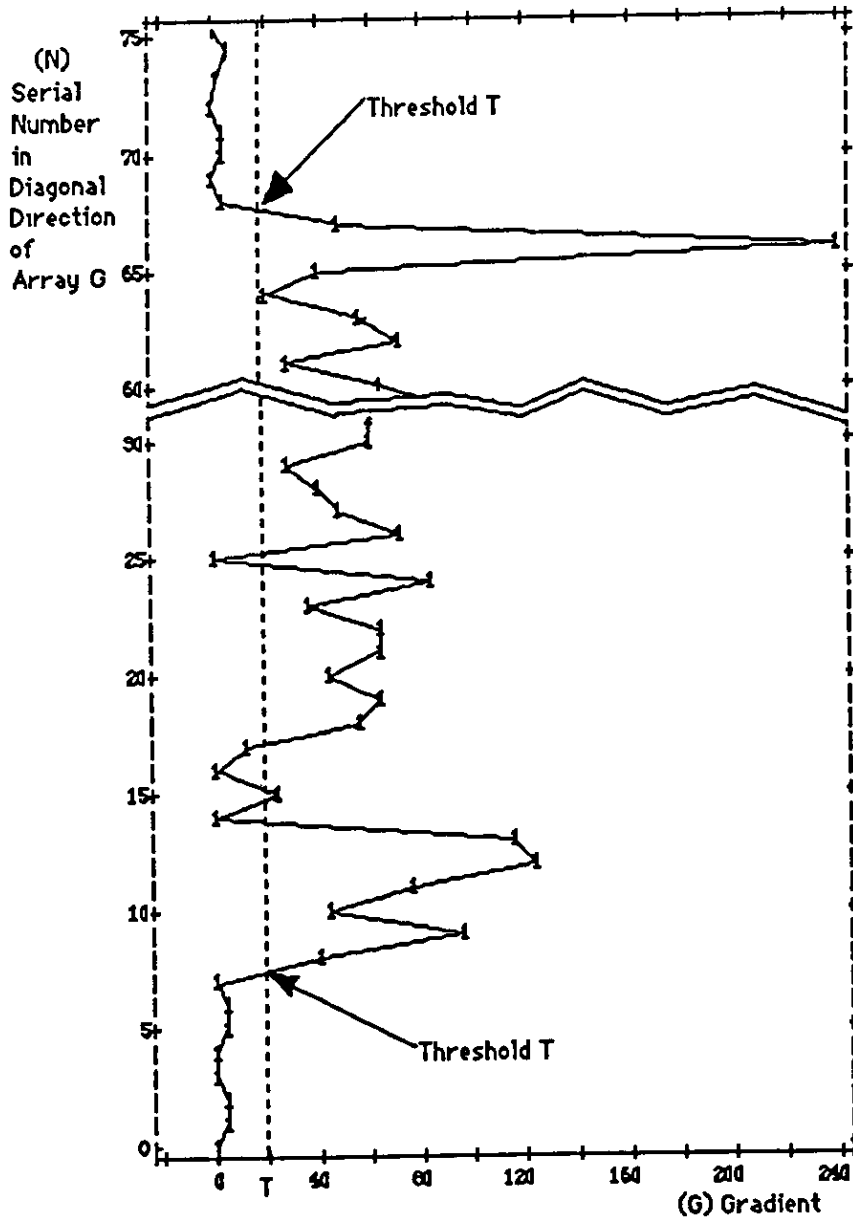
Figure 3.14 The histogram along the diagonal line of the gradient array G.

As soon as one of ᵗʰᵉ boundary points is detected, the immediate process is as follows:

Initially, assign the gradient values of the eight neighbours of the

80

point (i, j) into a ring-shaped 1 x 8 array Et, respectively, as Figure 3.15.(b) shows:

$Et[1] = G[i-1, j-1]$,

$Et[2] = G[i-1, j]$,

$Et[3] = G[i-1, j+1]$,

$Et[4] = G[i, j+1]$,

$Et[5] = G[i+1, j+1]$,

$Et[6] = G[i+1, j]$,

$Et[7] = G[i+1, j-1]$,

$Et[8] = G[i, j-1]$,

where the 3 x 3 array in Figure 3.15.(a) represents the local gradient image and the ring-shaped 1 x 8 array Et stores the gradient values of the eight neighbours of the current point (i, j). Note that the ring shaped one-dimensional array Et in Figure 3.15.(b) is involved in the circling operation of boundary detection. Then, assign the x- and y-coordinates of the eight neighbours into 1 x 8 arrays X and Y, respectively, as in Figures 3.15.(c) and 3.15.(d) show,

$X[1] = i-1$, $Y[1] = j-1$,

$X[2] = i-1$, $Y[2] = j$,

$X[3] = i-1$, $Y[3] = j+1$,

$X[4] = i$, $Y[4] = j+1$,

$X[5] = i+1$, $Y[5] = j+1$,

$X[6] = i+1$, $Y[6] = j$,

$X[7] = i+1$, $Y[7] = j-1$,

$X[8] = i$, $Y[8] = j-1$,

where the arrays X and Y temporarily store the (x, y) coordinates of the eight neighbours of the current point (i, j). At the same time, assign a number, which can be used as an identifier (i.d.) of the boundary point in the boundary extraction and the colour

81

pattern extraction procedures, and is larger than the maximum gradient values, to the G[i, j] where a boundary point was detected. In fact, the gradient values will always be less than 1,000, hence this value is assigned to the first i.d. assigned would be 1,000. Later on, whenever a new boundary point is detected, the i.d is incremented and assigned to the G[i, j].
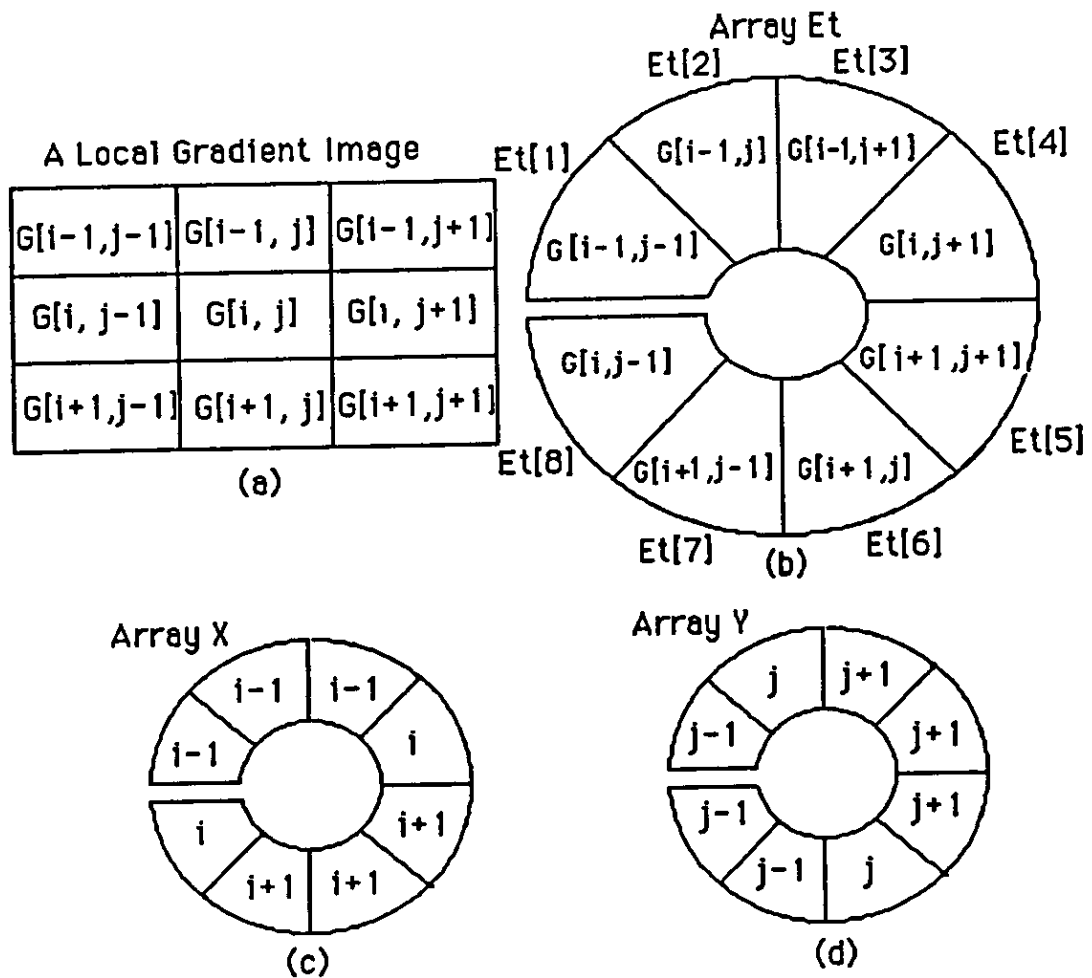
Figure 3.15 A local gradient image and arrays assigned with gradients and the x-and y-coordinates of the point (i, j). (a) A local gradient image. (b) Gradient values of eight neighbours which are assigned to the array Et. (c) The x-coordinates of the eight neighbours of the point (i, j) which are assigned to the array X. (d) The y-coordinates of the eight neighbours which are assigned to the array Y.

82

This boundary point becomes the current boundary point. In the second step, the principal focus of the boundary detecting process is detecting the location of the next boundary point among the eight neighbours of the current boundary point (i, j). Firstly, detect the largest value from the eight neighbouring gradient values since the location of the previous boundary point found has an i.d. value greater or equal to 1,000. Figure 3.16 represents the details of this process. Secondly, the next boundary point is determined by thresholding (refer to Equation (3.4-3)) clockwise each eight neighbouring points, starting from the previous boundary point, where the threshold value, T=20, is used. This process is represented in detail in Figure 3.16. The value n, at the end of the second process in Figure 3.16, represents the location of the next boundary point in the array Et. Hence, the corresponding (x, y) coordinates are X[n] and Y[n], respectively. Finally, the process will stop when the starting boundary point is detected.

The algorithm developed in this thesis is similar in principle to Ledley's (Ledley, 1964). The main difference is that his algorithm is mainly for black-and-white images, however, the algorithm developed in this thesis is for colour images as well as black-and-white images. The so-called border-following algorithm published by Rosenfeld (1969) is originated from Ledley's algorithm. The border-following algorithm is also similar to the algorithm in this thesis. Rosenfeld's algorithm is for the binary images which consists of 0's and 1's.
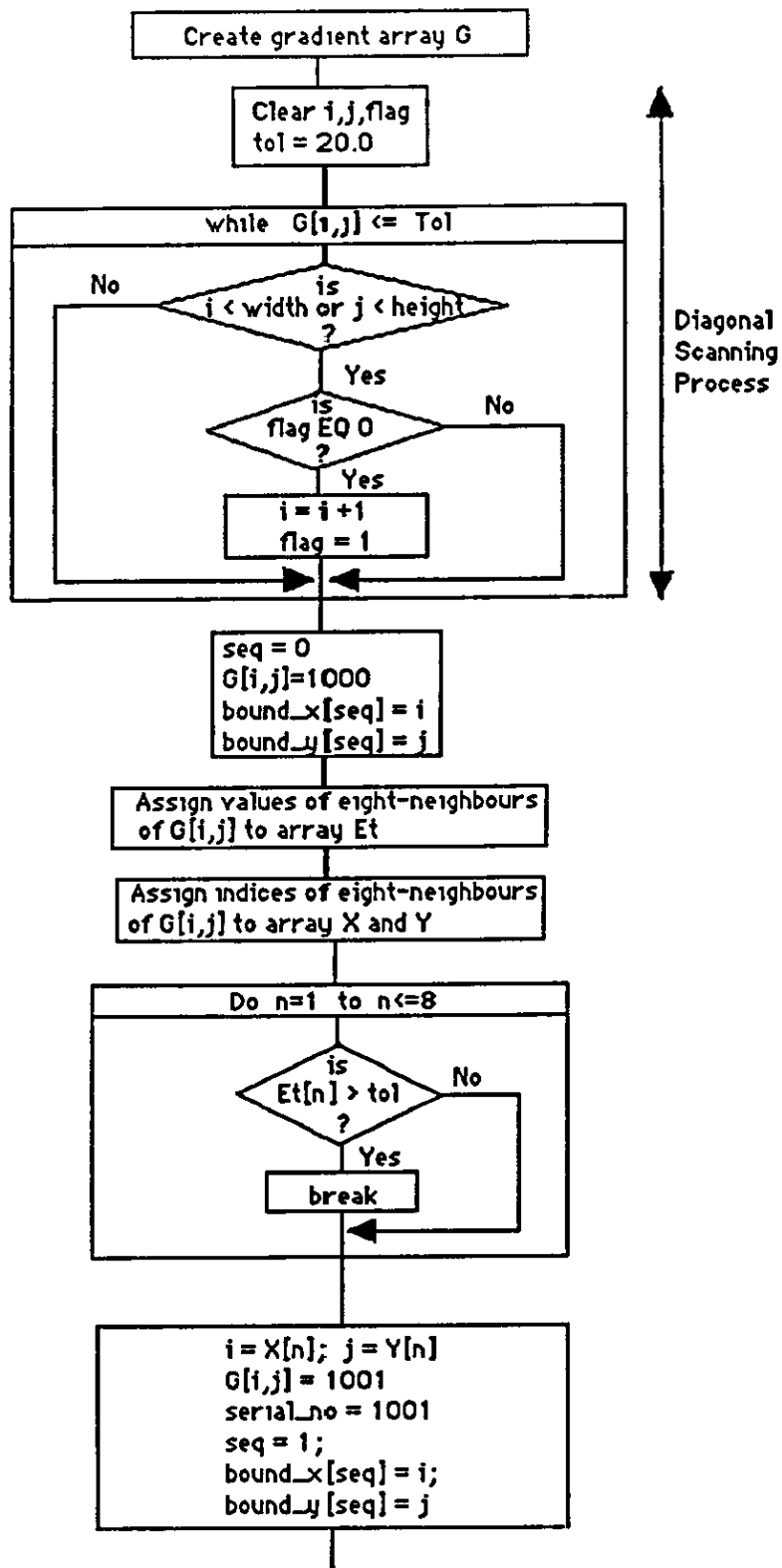
Figure 3.16 Boundary point detecting operation (continued).

84

```
┌─────────────────────────────────────────────────────────┐
│              while  G[i,j]  NE 1000                      │
├─────────────────────────────────────────────────────────┤
│                                                         │
│          ┌─────────────────────────────────┐           │
│          │ Assign values of eight-neighbours│          │
│          │    of G[i,j] to array Et        │           │
│          └─────────────────────────────────┘           │
│          ┌─────────────────────────────────┐           │
│          │ Assign indices of eight-neighbours│         │
│          │   of G[i,j] to array X and Y    │           │
│          └─────────────────────────────────┘           │
│               ┌─────────────────┐                       │
│               │   max = Et[1]   │                       │
│               │   pnt = 1       │                       │
│               └─────────────────┘                       │
│       ┌─────────────────────────────────┐               │
│       │        Do  k=2  to  8           │   ▲           │
│       ├─────────────────────────────────┤   │  (the 1st process)
│       │           ╱is╲          No       │   │  ============│
│       │         ╱max < Et[k]╲─────────┐  │   │  Detect       │
│       │          ╲    ?    ╱         │  │   │  the maximum  │
│       │            ╲ Yes ╱           │  │   │  value        │
│       │          ┌─────────┐         │  │   │  (the previous│
│       │          │max = Et[k]│       │  │   │  point)       │
│       │          │pnt = k   │        │  │   │               │
│       │          └─────────┘         │  │   │               │
│       │            ◄─────────────────┘  │   ▼           │
│       └─────────────────────────────────┘               │
│                                                         │
│       ┌─────────────────────────────────┐               │
│       │     Do  k=pnt+1  to  pnt+8      │   ▲           │
│       ├─────────────────────────────────┤   │  (the 2nd process)
│       │          ┌─────────┐            │   │  ===========│
│       │          │  n = k  │            │   │  Detect the next│
│       │          └─────────┘            │   │  boundary point│
│       │           ╱is╲         No        │   │               │
│       │         ╱Et[n] > tol╲──────────┐ │   │               │
│       │          ╲   ?   ╱            │ │   │               │
│       │            ╲Yes╱              │ │   │               │
│       │          ┌────────┐           │ │   │               │
│       │          │ break  │           │ │   │               │
│       │          └────────┘           │ │   ▼           │
│       │            ◄──────────────────┘ │               │
│       └─────────────────────────────────┘               │
│  Yes              ╱─────────────╲                        │
│  ┌────────────────  Et[n] Eq 1000 ╲                      │
│  │                 ╲─────────────╱                       │
│  │                       │ No                            │
│  │          ┌──────────────────────────────┐            │
│  ┌────────┐ │ i = X[n] ;  j = Y[n]          │            │
│  │i = X[n]│ │ seq = seq + 1                │            │
│  │j = Y[n]│ │ bound_x[seq] = i             │            │
│  └────────┘ │ bound_y[seq] = j             │            │
│             │ serial_no = serial_no + 1    │            │
│             │ G[i,j] = serial_no + 1       │            │
│             └──────────────────────────────┘            │
│                          ────►                          │
└─────────────────────────────────────────────────────────┘
```

Figure 3.16 Boundary point detecting operation (continued).

85
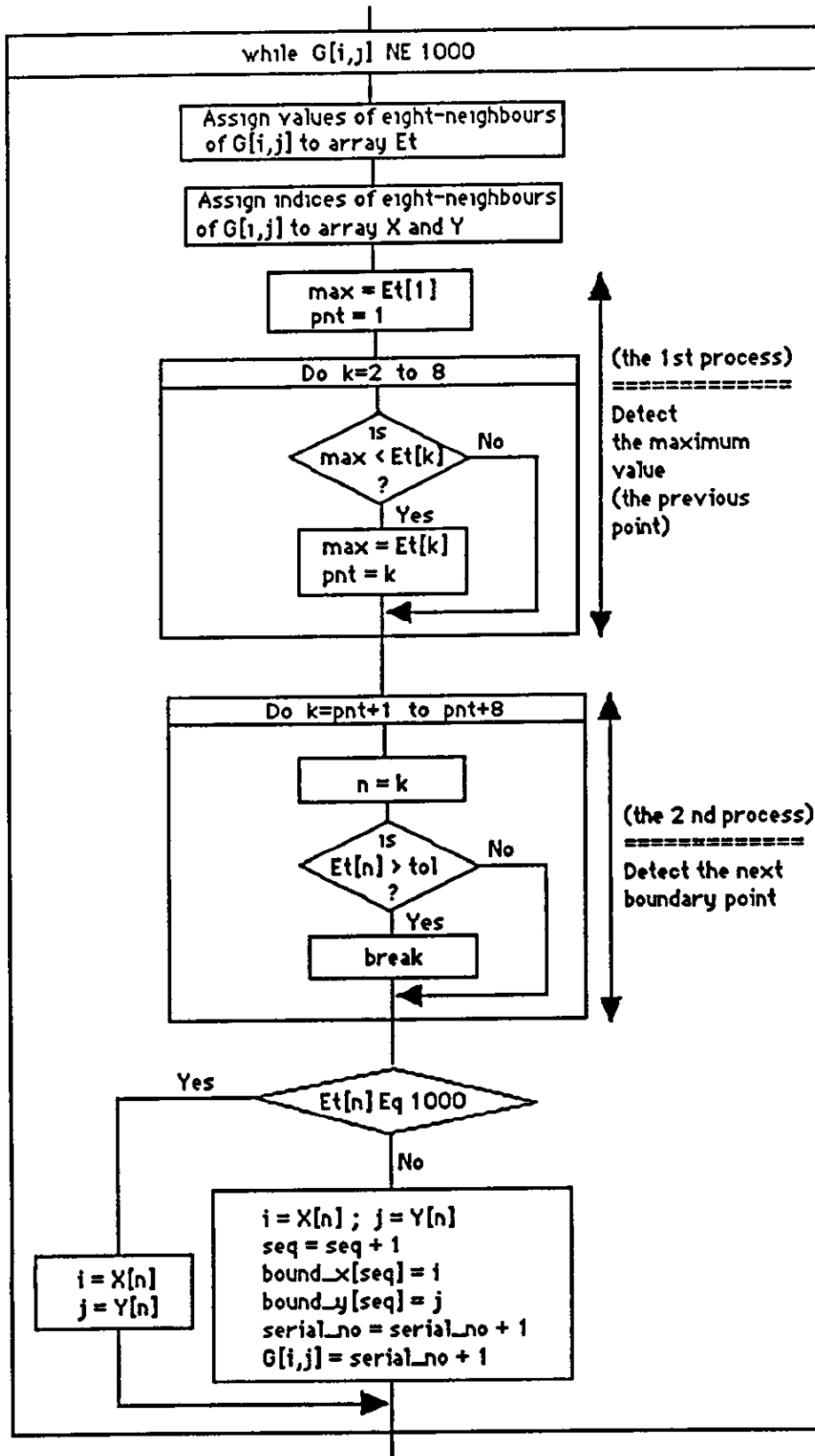
In order to clarify the concepts of the two previous processes, consider the following examples as shown in Figures 3.17 through 3.19. These examples are just a small portion of all the possible cases in the practical situation. In the examples, P stands for a previous boundary point, C for a present boundary point, and Q for a next boundary point. A value larger than 1,000 assigned to a previous boundary point represents an arbitrary point already traversed. The shaded regions on the left-hand side of Figures 3.17 through 3.19 are a part of the actual boundary shape, and the ring-shaped one-dimensional arrays on the right-hand side of Figures 3.17 through 3.19 represent the gradient values g1, g2, ..., g8 of the eight neighbours of the present boundary point which are assigned to an 1 x 8 array Et.

(1) When a boundary forms a straight line segment:
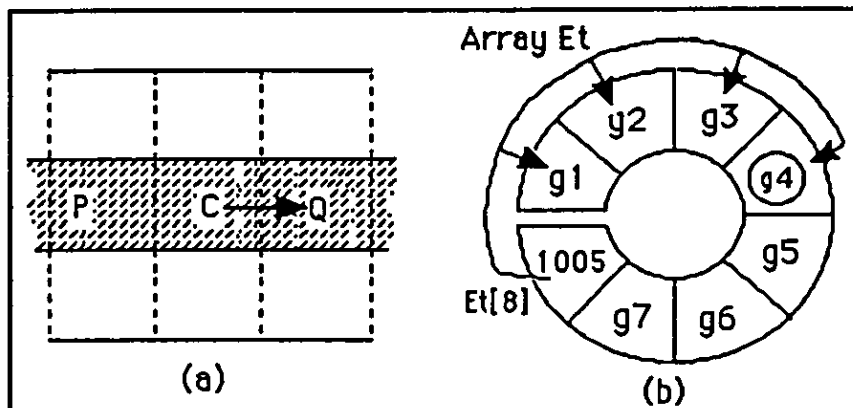
Figure 3.17 Boundary detecting process. (a) Actual boundary shape. (b) Ring-shaped 1 x 8 array Et.

Let the gradients, g1, g2, g3, g5, g6 and g7 be less than a threshold T and g4 be larger than T; and 1,005 be an i.d. assigned to the previous boundary point. In the first process in Figure 3.16, the location of the 8th component of the array Et whose value is maximum (1,005) can be detected. In the second process in Figure

86

3.16, a series of thresholdings is performed clockwise, as Figure 3.17.(b) shows, from the first component of the array Et, because the largest value was detected at the eighth component of the array Et, as follows:

since Et[1] = g1 < T, the boundary detector moves to Et[2],

since Et[2] = g2 < T, the boundary detector moves to Et[3],

since Et[3] = g3 < T, the boundary detector moves to Et[4],

since Et[4] = g4 > T, the point Et[4] is regarded as a next boundary point. Thus, the boundary detector moves from the point C to the point Q as Figure 3.17.(a) shows.

(2) When a boundary point forms a sharp curve :.

(a) When a boundary forms a sharp convex curve: ;

(a)   (b)
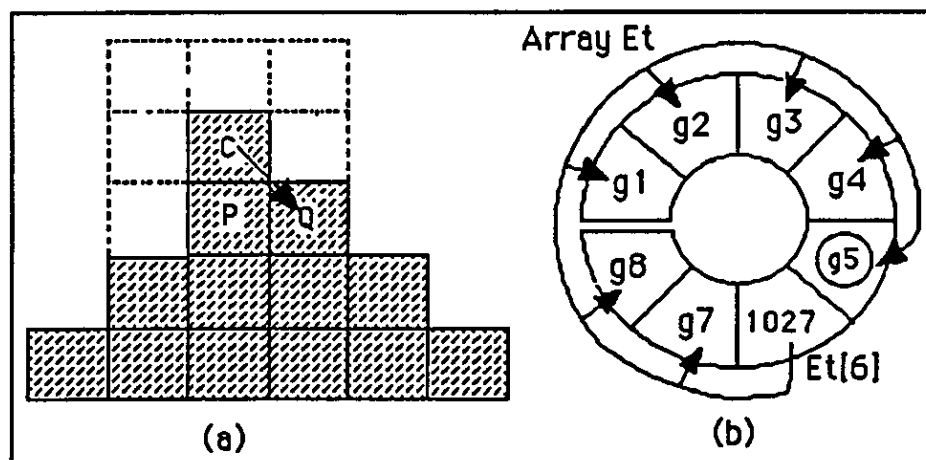
Figure 3.18 Boundary detecting process. (a) Actual boundary shape. (b) A ring-shaped 1 x 8 array Et.

Let the gradients, g1, g2, g3, g4, g7 and g8 be less than a threshold T and g5 be larger than T; and 1,027 be an i.d. assigned to the previous boundary point. In the first process, the location of the 6th component of the array Et whose value is the largest (1,027) can be detected. In the second process in Figure 3.16, a

series of thresholdings is performed clockwise, as Figure 3.18.(b) shows, from the seventh component of the array Et, because the largest value was detected at the sixth component of the array Et, as follows:

since Et[7] = g7 < T, the boundary detector moves to Et[8],

since Et[8] = g8 < T, the boundary detector moves to Et[1],

since Et[1] = g1 < T, the boundary detector moves to Et[2],

since Et[2] = g2 < T, the boundary detector moves to Et[3],

since Et[3] = g3 < T, the boundary detector moves to Et[4],

since Et[4] = g4 < T, the boundary detector moves to Et[5],

since Et[5] = g5 > T, the point Et[5]   is regarded a next boundary point. Thus, the boundary detector moves from the point C to the point Q as Figure 3.18.(a) shows.

(b) When a boundary forms a sharp concave curve:

(a)   (b)
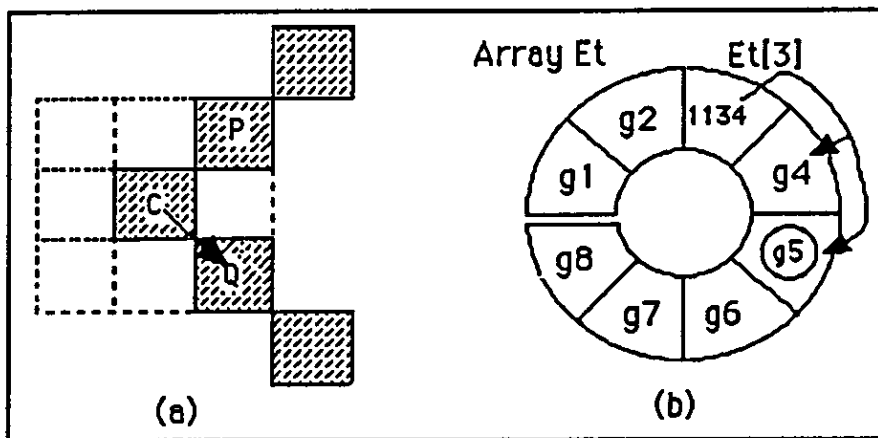
Figure 3.19 Boundary detecting process. (a) Actual boundary shape. (b) A ring-shaped 1 x 8 array Et.

Let the gradients g1, g2, g4, g6, g7 and g8 be less than a threshold T and g5 be larger than T; and 1,134 be an i.d. assigned to the previous boundary point. In the first process, the location of the third component of the array Et whose value is maximum (1,134)

88

is. detected. In the second process, a series of thresholdings is performed clockwise, as Figure 3.19.(b) shows, from the fifth component of the array Et, because the largest value was detected at the third component of the array Et, as follows:

since Et[4] = g4 < T, the boundary detector moves to Et[5],

since Et[5] = g5 > T, the point Et[5] is regarded as a next boundary point. Thus, the boundary detector moves from the point C to the point Q as Figure 3.19.(a) shows.

As the above examples show, the algorithm can be easily used to extract any boundary that has even quite sharp curves or has a more complicated shape. The examples of the application of the algorithm are shown in Figure 3.20. As the figure shows, the boundary of a maple leaf which had a complicated shape was successfully extracted.
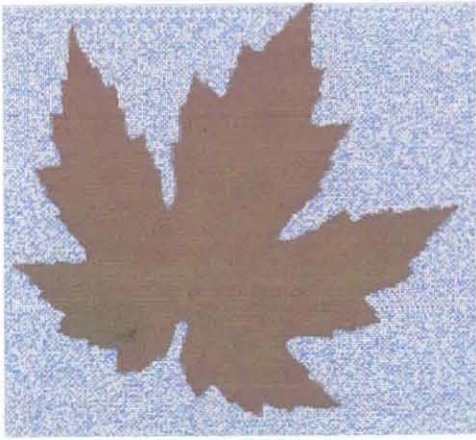
(a)
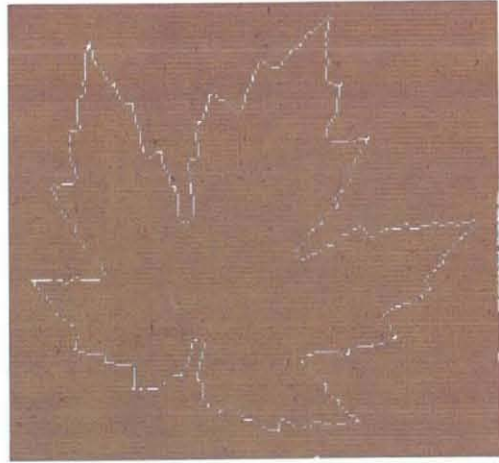
(b)

(c)
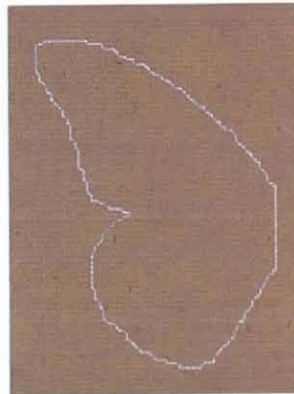
(d)

Figure 3.20 The images and their boundaries.

3.5 CONCLUSION.

A boundary extracted from an image plays an important role in image analysis, since it is usually used for shape-description and also for region-extraction procedures. As rapid progress has recently been made in the development of colour-image capturing devices, the demand for colour-image analysis is increasing dramatically. However, most of the boundary extracting algorithms so far developed have been restricted only to black-and-white images. Thus, it was necessary to develop a new algorithm which could extract a boundary not only from a black-and-white image, but also from a colour image and could be generally used in this domain. The CIELAB colour difference formula has been adopted to calculate the colour difference between pixels in this algorithm. In fact, the colour difference has been determined in the CIELAB space which is a three-dimensional space of L^*, a^* and b^*. In the calculation of gradients of each point of the image, partial derivatives have been approximated by the relation published by Goldmark and Hollywood (1951). The boundary extracting processor in this thesis has been designed to be implemented on the gradient plane using a threshold.

Chapter 4

COLOUR PATTERN EXTRACTION METHODS.

4.1 Introduction.

4.2 Image Segmentation.

4.3 Cluster Analysis.

4.4 Colour Pattern Extraction.

4.4.1 Auxiliary Means for Colour Image Segmentation.

4.4.2 A Procedure for Colour Pattern Extraction.

4.5 Conclusion.

4.1 INTRODUCTION.

In the image analysis domain, it has been regarded as a very important task to split an image into meaningful segments. The reason is that each of the segments is essentially used in the procedure of identifying the whole image. For example, suppose that two different species of butterfly have exactly the same shape of wings as well as other organs, but different colour patterns. The discrimination of the two species by a computer system using only a shape interpretation function will soon show its limitations by producing a wrong result, e.g. they appear to be exactly the same species. The main aim of this chapter is to explain how to extract the patterns with distinctly different colour features from the colour image of an object. In terms of the whole system for the identification of biological objects, the procedure of extracting patterns is a preliminary stage for the description of patterns in the next procedure. Since the description of each pattern absolutely depends upon the result of the extraction procedure, this procedure is usually regarded as a very important task.

So many approaches have been performed attempting to achieve the same goal of splitting a colour image into meaningful segments that a vast range of papers has been produced. The majority of the approaches mainly rely on one- or two-dimensional histograms. An investigation of some of the approaches which are closely related to the subject of this thesis has been carried out. The important fact to be noted is that most of the approaches are regarded as just alternatives to a three-dimensional clustering method. The investigation will concentrate

on clarifying the major reason why the direct application of the three-dimensional Cluster Analysis to the colour image segmentation has been avoided. In order to clarify the reason, the theoretical aspect of the Cluster Analysis which is one of multivariate analyses in statistics will be reviewed in detail.

The concept of the Auxiliary Means which has been devised in this thesis will be introduced from the motivation for its development and the necessity to its actual application to Cluster Analysis. The method for applying the Cluster Analysis procedure to colour image segmentation employing the Auxiliary Means will be discussed. At the same time, a sub-algorithm to remove noise will be introduced; noise being a problem with this approach. This approach has been successfully implemented to extract patterns of distinctly different colour features from an image containing the left-side wings of a butterfly.

4.2 IMAGE SEGMENTATION.

In this section, existing methods for segmenting an image into regions which contain pixels with similar features are investigated. There are two approaches to the image segmentation: the region-merging method and the region-splitting method. In the region-merging method, the pixels are firstly grouped into regions based on the similarities of some attribute such as grey level or colour feature, and then these regions are checked for merging with the neighbouring regions based on their average properties and spatial relationships. In the region-splitting method, large regions are successively split into smaller regions based on differences between the properties of the pixels in the regions. Another method is the split-and-merging method, combining the two previous methods.

The dynamic threshold method developed by Chow and Kaneko (1972), which is an example of a region-splitting method, was used to extract the shape of the left ventricle from a cardiac cineangiogram, an x-ray motion picture of a heart image. It is important to note that the fundamental assumption in their method is that the probability distribution of the intensity for any small region of the image consisting solely of the object or the background is unimodal. This is because the intensity seldom remains constant over any region in the image. Thus, in a small region of the image which contains a boundary, there are two unimodal distributions, one for the object and one for the background as in Figures 4.1.(a) and (b), respectively. These two distributions generally overlap. Chow and Kaneko have contended that the overall distribution of the small region is consequently a

95

mixture of two unimodal distributions and is generally bimodal as Figure 4.1.(c) shows. They divided the entire area into 7 x 7 regions with 50 % overlap. Each region contains 64 x 64 picture elements.
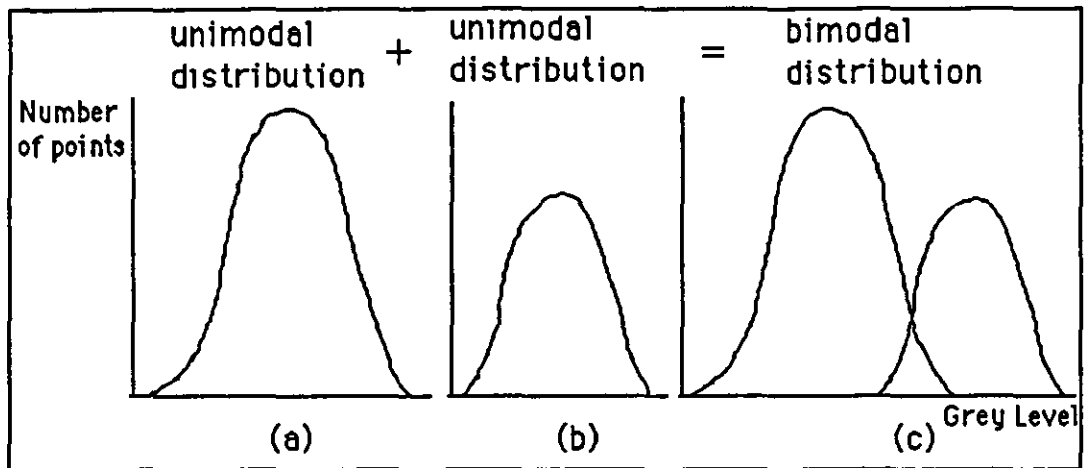
Figure 4.1 Unimodal distribution and bimodal distribution. (a) The histogram of a background region. (b) The histogram of an object. (c) The histogram of a region containing a boundary.

An intensity histogram wascomputed over each region. Since it is quite difficult to find the right valley point from a raw histogram, the histogram is smoothed. The right valley point can be used to divide the image into an object and a background. This procedure is illustrated in Figure 4.2. In this method, the valley point is considered as an important threshold. Ballard and Brown (1982) have pointed out that problems can occur with this kind of method using a single threshold when an image has a background of varying grey levels, or when regions vary smoothly in grey levels by more than the threshold. However, in this method the threshold varies depending upon the location of the region. Thus, the difficulty with the single threshold is increased. However, the main critical problem in this method is

that a sub-image can fail to have a threshold if the grey-level histogram is not bimodal, that is, if the histogram has more than two peaks. Another problem is that if the two distributions heavily overlap, using the threshold obtained from the histogram can produce quite different sub-images. A histogram obtained from a colour image containing a biological object, for instance, a butterfly (which is pertinent to this thesis), will in general consist of more than two peaks. Therefore, if this method is applied to the extraction of patterns with various colours, the above problems, undoubtedly, could arise immediately.
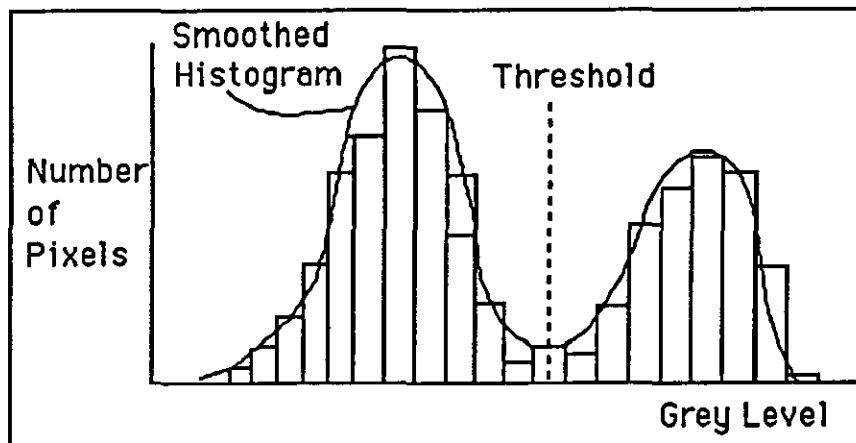
Figure 4.2 A smoothed histogram and valley point.

Another approach is a recursive region splitting method, developed by Ohlander et al. (Ohlander, Price, & Reddy, 1978), which has been commonly used even for colour images. The principle of the segmentation operation is based on some generalisation of the Chow and Kaneko's ideas, that is, histogram analysis. They have computed nine histograms of the red, blue and green colour components, the intensity, hue and saturation components and Y, I and Q components which are parameters used in the N.T.S.C. colour television. Since this method was published, a number of similar studies have been undertaken in the colour

97

analysis domain. Most of the approaches have adopted the principal philosophy of peak-finding from a histogram. Thus, it will be worth considering the detailed procedure of the method. The process of Ohlander et al.'s method is as follows:

(1) Take an entire region of the image.

(2) Compute histograms for the nine components of the portion of the image which is contained in the region. At the same time, smooth the histograms to eliminate small peaks.

(3) Apply a peak-finding test to each histogram. If at least one component passes the test, pick the component. On the other hand, if all the histograms fail the test then this region is considered to be segmented.

(4) Determine two thresholds, one either side of the peak and divide the region into subregions using these thresholds.

(5) Eliminate small holes in regions, small regions, or thin connections between regions by smoothing.

(6) Continue the segmentation process on the remainder of the region which had been segmented. Terminate the segmentation of the remaining region when there are too few pixels left.

Obviously, this approach applied to a high-resolution image is computationally expensive because the nine histograms must be calculated in every repeating process and the smoothing operation must be performed in each process. Nevatia (1982) has stated that small regions in a large image may not produce a distinct histogram peak, even if they are distinct from their surroundings. Ohta et al (1982) conducted experiments to derive a set of effective colour features using this algorithm. Tomina (1988) has further explored this approach using colour features of lightness, hue and chroma, where each of the features is projected. Similar research has

98

been performed by Celenk (1988). The primary principle of the foregoing approaches based on peak finding and valley finding is called a one-dimensional histogram method. A more improved technique, a two-dimensional approach described by Underwood and Aggarwal (1977) and Ali and Aggarwal (1977) is based on the projections of the (X, Y, I) normalised colour space onto the X-Y, X-I and Y-I planes. In this interactive method, rectangular-type broad and refined colour bandpass filters are used to detect a specific region from an image. Ali et al. (1977) further explored this approach for colour aerial photographs, where the segmentation was accomplished by rather simple decision surfaces in the (X, Y, I) normalised colour feature space. They have developed a system which allows the user to specify,
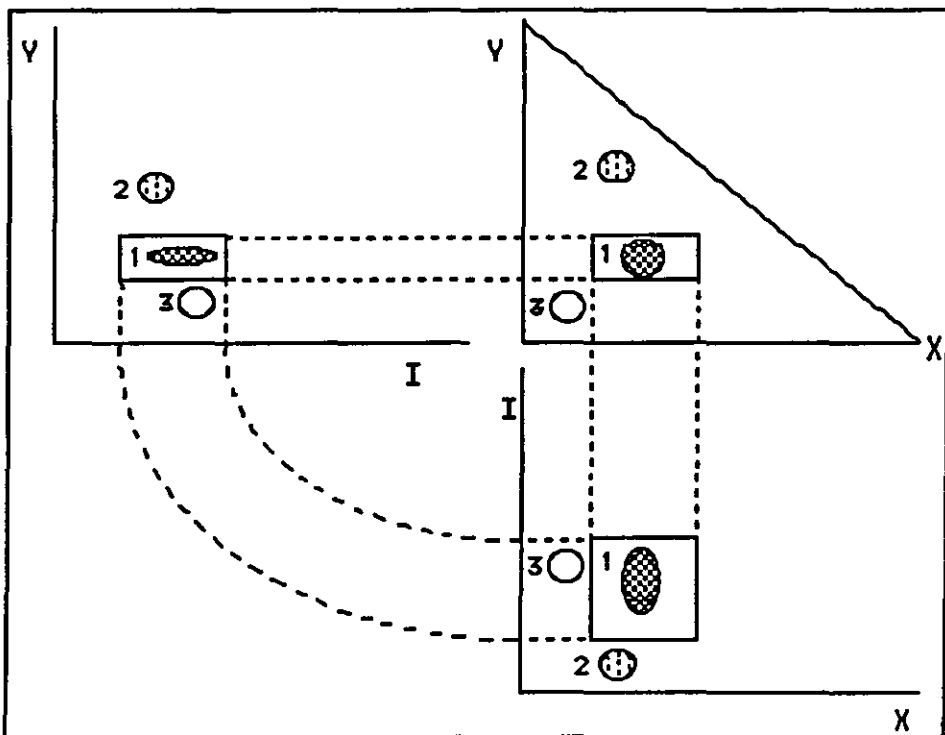
Figure 4.3 Colour distribution and rectangular decision surface with colour features.

99

interactively, the rectangular decision surface, which is then applied to the pixels of the image. The surface in Figure 4.3 is bounded so that feature points indicating the desired colour characteristics fall within the volume defined by the bounded surface. In this approach, the decision surfaces in the colour feature space obviously play an important role in separating regions in an image. However, for instance, if many colours of different regions in an image are distributed very closely, like a foggy rainbow, without clear borders amongst the colours in the colour feature space, it might be impossible to separate the colours with the decision surfaces, no matter how small their sizes are.

In general, a problem of separating colours in a three-dimensional colour feature space is, theoretically and practically, a three-dimensional clustering problem, neither a two-, nor one-dimensional clustering problem at all. It has usually been believed, in image analysis, that a three-dimensional process which operates on the whole image is computationally costly and that huge quantities of pixels cannot be processed even in a super computer since they need an enormous core memory capacity to process. One remedy for this problem is to project the colour feature space onto a two-dimensional space, employing the previous approach (Sarabi and Aggarwal, 1981). In fact, it might not be a general and perfect method to accommodate every possible case in the three-dimensional space, but only an immediate remedial technique to cover some portion of the whole cases in the space. Under this projection it is possible that some clusters which were separable in the three-dimensional space are no longer separable on any projection. A still more drastic method

of dimensionality reduction is, of course, to project the colour feature space onto a one-dimensional space such as one of the colour feature axes. The resulting projection is nothing more than the grey level histogram of one of the primary colour component intensities of an image. Although many chromatic features, for instance nine are used in Ohlander et al., (1978), eventually the number of dimensions for the process at a time is still one, not more than that. Sarabi and Aggarwal (1981) have developed a general interactive system which provides a means of solving this problem. The system allows the user to specify an initial number of clusters and then the clustering process continues until the number of clusters are generated. The colour feature (X, Y, I) histogram is examined to see if there are nodes which are not assigned to any cluster, if so, the user can increase the number of clusters or modify the tolerance, or terminate the cluster detection process. It is true that this approach has improved the level of the dimensionality from two to three. However rectangular parallelpiped box plays a key role in determining a cluster in the colour space. In colour science an ellipsoid tolerance is used to cluster the same colour features rather than a box shaped region. The above approach is an alternative to the Cluster Analysis in multivariate statistical methods.

4.3 CLUSTER ANALYSIS.

In this section Cluster Analysis will be reviewed not only to make a clear exposition of the concept and background of the analysis, but also to apply a proper clustering methodology, among the so many methodologies published thus far, to the image-segmentation problem. The pertinent point is that most researchers seem to believe that the Cluster Analysis procedure employed in colour image segmentation could produce a better result than any other approach such as one-dimensional histogramming methods; two-dimensional projecting methods; etc, &c. The primary obstacle to implementing this method is that it requires inordinate amounts of core memory; indeed in some situations this requirement exceeds the available memory of even super computers. It follows that most research in this area has been concerned with finding alternative implementations that do not require so much memory. Some methods published do however require very lengthy processing computation times. The underlying assumption in some of these efforts, has been that to reduce core memory requirements inevitably means an increase in processing time, and vice versa.

Consider 'Cluster Analysis' from the definition of the term cluster. Among the many proposed definitions of the term cluster, the definition by Zupan (1982) is clearer than others:

"Clusters are groups of objects linked together according to some rule. The goal of clustering is to find groups containing objects most homogeneous within these groups, while at the same time the groups are heterogeneous between themselves as much as possible. The terms 'homogeneous' and 'heterogeneous' are

102

referring to the common properties of the objects according to which we are trying to cluster the given set of data."

From the definition, Cluster Analysis seems to be quite a useful tool to solve the problem in image segmentation. However, in practice, applying this analysis to image segmentation has been avoided so far. Thus, the investigation has been concentrated on two aspects:

(1) What is the main difficulty of applying _` Cluster Analysis to _ ⸗ image segmentation?

(2) Which analysis, among several Cluster Analysis methods, is closely related to the image segmentation problem?

Cluster Analysis procedures have been classified into four types by Everitt (1974), as follows:

(1) Hierarchical Procedures

These procedures are sub-divided into agglomerative methods and divisive methods. The agglomerative methods are to merge individual entities into groups successively, where the entity has more than one attribute which describes the feature of the entity. The divisive methods are to partition the entire set of entities into individual elements.

(2) Partitioning Procedures

These procedures are used to partition the set of entities so as to optimise some predefined criterion. These approaches assume that the number of groups has been decided a priori by a user, although some do allow the number to be changed during the course of analysis.

(3) Density Search Procedures

Clusters are formed by searching for regions containing relatively high density in the data.

(4) Clumping Procedures

These procedures allow overlapping between the clusters. The feature of overlapping the clusters is in contrast to the other procedures since the results of other approaches are disjoint clusters.

Considering the important features of the procedures will be useful to a correct application. Note that the second procedures have some weak points, that is, they usually require large amounts of computing time, and a priori knowledge about how, for example, clustering criteria affects the efficiency and computing time as well. The third procedures have the disadvantage of relying on the values of various parameters which must be set by the user. The results obtained depend heavily on the values. A further difficulty lies in the assumption of multivariate normal distribution. The last procedures are suitable to specific areas such as language studies where words tend to have several meanings. On the other hand, the first procedures provide the user with a large number of options for the Cluster Analysis. Using the hierarchical procedures, the user can select clusters with different levels of clustering criteria. These procedures are also known as 'standard methods' (Zupan, 1982) in various fields of data handling. The hierarchical procedures with the features are best suited to the image segmentation. Thus let us take a close look at the algorithms of the several methods in the hierarchical procedures.

Hierarchical Procedures

As already illustrated, the hierarchical procedures are subdivided into agglomerative hierarchical methods and divisive hierarchical methods. Since the latter methods work in an opposite sense to the agglomerative methods, the investigation will be concentrated on the agglomerative hierarchical methods. Let us consider the agglomerative hierarchical methods in further detail. These methods start processing with the individual entities. Thus, there are initially as many clusters as the number of entities. Firstly, the process selects the most similar entities from the entities and merges the two entities into a group, and these initial groups are merged according to their similarities. Eventually, all subgroups are merged into a single heterogeneous cluster, where the similarity of the cluster decreases. The similarity which is used to determine a homogeneous group is measured by the Euclidian distance between entities or between subgroups, or between an entity and subgroup. According to how the calculation of the distance between two clusters is carried out, the agglomerative methods are also subdivided as follows:

(1) The Single Linkage or the Nearest Neighbour Method

This method (Sneath, 1957), which is probably one of the simplest clustering methods, can be used with similarities or distances between pair of clusters. In this method, the entities which are nearest to one another are merged into a new cluster. The procedure is as follows:

(i) In the first stage, calculate an n x n symmetric distance matrix from the initial set of n entities, where the distances

105

between entities are calculated using the Euclidian distance function.

(ii) In the second stage, search the distance matrix for the smallest distance.

(iii) In the third stage, merge the clusters with the smallest distance into a new cluster, and label the newly formed cluster. Then, update the entries in the distance matrix as follows:

(a) Delete the rows and columns corresponding to the clusters found in the second stage from the distance matrix.

(b) Calculate the smallest distances between the newly formed cluster and the remaining clusters, where the number of the smallest distances is that of the remaining clusters. For example, the smallest distance between the newly formed cluster and one of the remaining clusters is depicted in Figure 4.4.

(c) Add a row and column with the smallest distances to the distance matrix.

(iv) In the fourth stage, repeat stages (ii) and (iii) until all the clusters have been merged into the final single cluster.
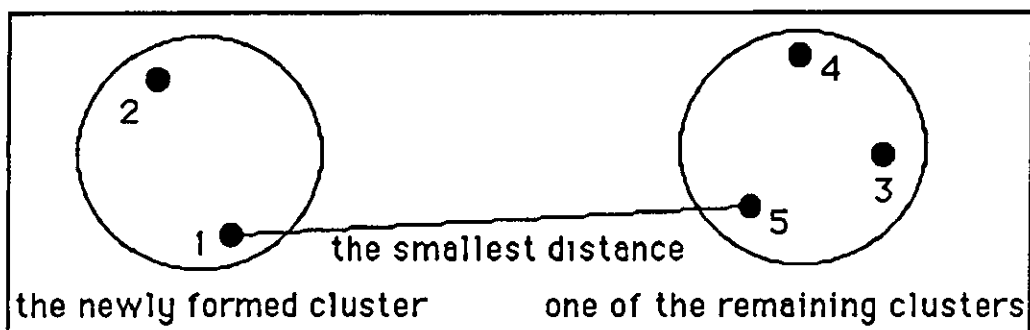
Figure 4.4 The smallest distance between the newly formed cluster and one of the remaining clusters.

(2) The Complete Linkage or the Furthest Neighbour Method

This method by Lance and Williams (1967) proceeds in much the same manner as single linkage, with one important exception. At each stage, the distance between clusters is determined by the longest distance between the clusters. This is in opposition to the single linkage method in which the distance between the clusters is determined by the smallest distance. As far as the algorithm is concerned, all the stages but the item (b) in the third stage in the algorithm of the single linkage can be applied. The item (b) is changed as follows:

Calculate the longest distances between the newly formed cluster and the remaining clusters, where the number of the longest distances is that of the remaining clusters. For example, the longest distance between the newly formed cluster and one of the remaining clusters is depicted in Figure 4.5.
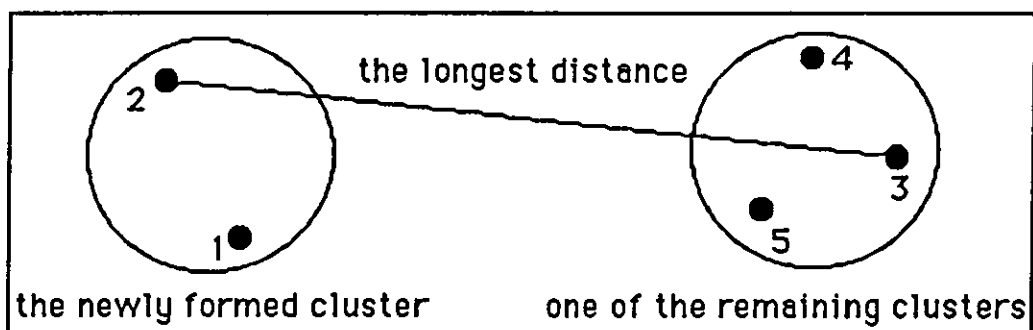
Figure 4.5 The longest distance between the newly formed cluster and one of the remaining clusters.

(3) The Average Linkage Method

This method by Sokal and Michener (1958) also proceeds in much the same manner as the single linkage and the complete linkage, with one important exception. At each stage, the distance between clusters is determined by the average distance between all pairs of entities where one member of a pair belongs to each cluster. All the stages but the item (b) in the third stage in the algorithm of both the single linkage and the complete linkage can be applied. The item (b) is changed as follows:

Calculate the average distances between the newly formed cluster and the remaining clusters. For example, the average distance between the newly formed cluster and one of the remaining clusters is depicted in Figure 4.6.
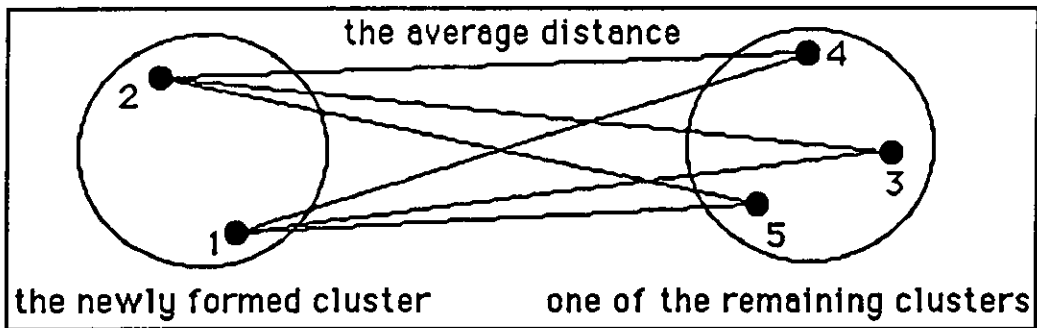
Figure 4.6 The average distance between the newly formed cluster and one of the remaining clusters.

(4) The Centroid Method

This method also proposed by Sokal and Michener (1958) also proceeds in much the same manner as the foregoing methods, but the difference lies in the calculation of the distance between clusters. As for the other algorithms, the

item (b) of the third stage is changed as follows:

Calculate the coordinates of the centroid, from where every entity in the cluster has an equal distance, of the newly formed cluster, and then calculate the distances between the coordinates and those of the centroids of the remaining clusters. For example, the distance between the coordinates of the centroid of the newly formed cluster and those of the one of the remaining cluster is depicted in Figure 4.7.
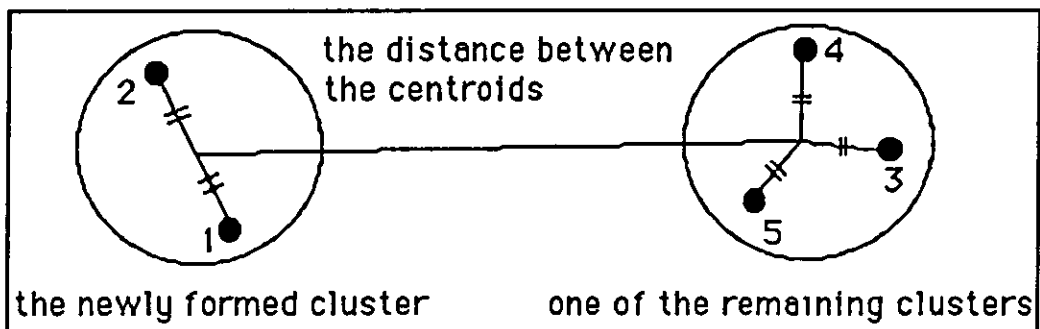
Figure 4.7 The distance between the centroids.

There are still a few other agglomerative methods that differ in the method used to calculate the distance between the clusters. However, the methods already discussed are dominately employed in many fields, and the further detailed investigation of other methods is out of the scope of this thesis because they are irrelevant to the colour image segmentation. Thus, the other methods will not be considered. Let us consider the basic problem occurring when Cluster Analysis is employed in ، colour-image analysis. There is no doubt that, in the Cluster Analysis methods discussed previously, the most important stage is the beginning of the procedure, that is, the first stage, where the $n \times n$ symmetric distance matrix is produced using the initial set of n entities. When one of the methods is adopted in ، colour image

109

segmentation, the entities are pixels forming an image. In order to produce the matrix containing the minimum distances between pixels, three different kinds of colour features such as R (red), G (green), B (blue), or X, Y, Z, or L*, a*, b*, or X, Y, I, or etc. are used as the attributes of each entity, that is, pixel. Imagine, for example, a colour image consisting of 100 x 100 pixels (which is in practice a tiny image). The number of initial entities will be 10,000, since each pixel with three colour features is regarded as an entity in the Cluster Analysis. In the first stage of ، ، Cluster Analysis, the procedure will produce the 10,000 x 10,000 symmetric distance matrix using the initial set of pixels. In fact, the procedure needs at least 100,000,000 (10,000 x 10,000) elements of core memory at the first stage. On the other hand, if the size of an image is, for another instance, 300 x 300, the minimum size of the core memory needed will be 8,100,000,000 (90,000 x 90,000). In general, if an image has n x n pixels, the size of the distance matrix to be calculated in the first stage of

Cluster Analysis is n^4, i.e. (n x n) x (n x n), since each of the pixels in an image is treated as an entity in ˉ Cluster Analysis. The main reason why Cluster Analysis has been avoided, so far, in the colour-image segmentation lies in the core memory problem from the first stage of the procedure. Due to this bottleneck, nearly all of the approaches, with considerable efforts, have pursued alternative ways. In one approach, Fukada (1978) divided a colour image with 256 x 256 pixels into sub-images of 8 x 8 pixels, and then applied Cluster Analysis to the sub-image. After getting the results a complex procedure for combining the incomplete clusters has to be employed. It could produce unexpected results or even poor quality results with a complicated colour image. This sort of approach would have a lot

110

of deficiencies and, may not be a reasonable way, but it is an alternative method.

Confronted with these circumstances, this thesis develops an improved algorithm for this area of investigation. This algorithm can directly apply   Cluster Analysis to the colour image segmentation with a colour image of various quality and sizes. The detailed algorithm developed will be illustrated in the next section.   · Cluster Analysis methods described previously are also discussed.

4.4 COLOUR PATTERN EXTRACTION.

As the title implies, in this section an algorithm to extract colour patterns from a colour image will be illustrated. In order to improve the quality of the results, the Cluster Analysis procedure is directly applied in the algorithm.

4.4.1 Auxiliary Means for Colour Image Segmentation.

For the correct concept of a colour feature space, first of all consider the relationship between a colour image and its colour feature space. Usually, a colour image consists of pixels with R, G and B values. These R, G and B values are transformed into the CIE L^*, a^* and b^* values for the further analysis as discussed in Chapter 2. On the other hand, a black-and-white image consists of pixels with grey levels. In the image segmentation of a black-and-white image, the grey levels are analysed using a one-dimensional histogram since the histogram reveals the composition of the various grey levels forming the image. When the grey levels with locations in the image are investigated, a two-dimensional histogram is efficiently used. On the other hand, a colour image is investigated in a three-dimensional colour feature space. Note the features of the histograms. The shape of a one-dimensional histogram physically shows a two-dimensional shape, i.e. various shapes of mountains projected onto a plane. The shape of the two-dimensional histogram is depicted as a three-dimensional shape, like cubic mountains with various heights and shapes. Thus, it can be concluded that the n-dimensional histogram can be displayed with the (n+1)-dimensional shape. Theoretically, a three-dimensional histogram is depicted as a four-dimensional shape.

However, it is impossible to display a four-dimensional shape in practice.

Consider the following examples with two hypothetical colour images. The image in Figure 4.8.(a) contains four squares filled with the red, green, blue, and yellow pixels of 10 x 10, respectively. Another image in Figure 4.8.(b) contains the same colours with 20 x 20 pixels. The compositions of the colour features in the image are depicted in the three-dimensional colour feature (The CIE L*, a* and b*) spaces in Figures 4.8.(c) and (d), respectively. As the graphs show, the two colour-feature spaces look the same, not different at all. As far as colour image segmentation is concerned, most of the required decision making may not be possible with the three-dimensional spaces. This could be a reason why there are not three-dimensional histograms, but
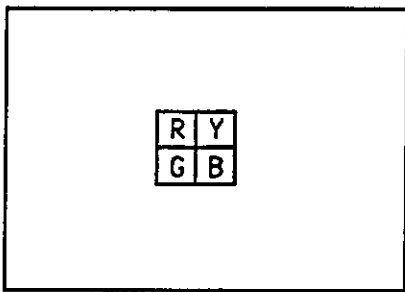
(a) Four squares of R, G, B and Y with 10 x 10 pixels.
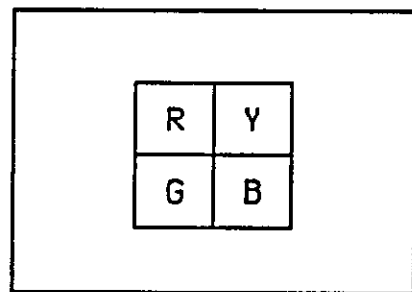
(b) Four squares of R, G, B and Y with 20 x 20 pixels.
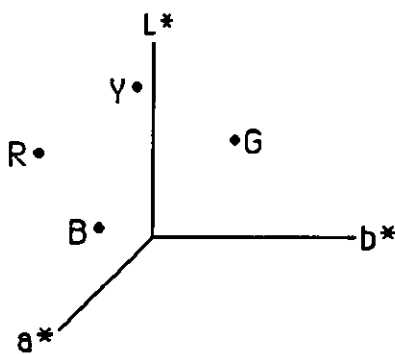
(c) The L*, a* and b* space.
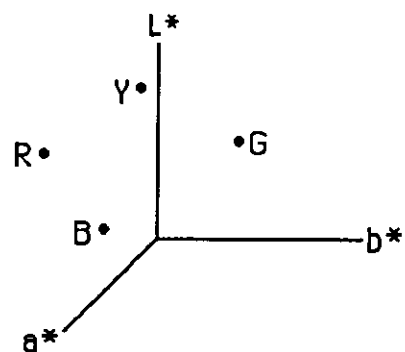
(d) The L*, a* and b* space.

Figure 4.8 Colour images and three-dimensional histograms.
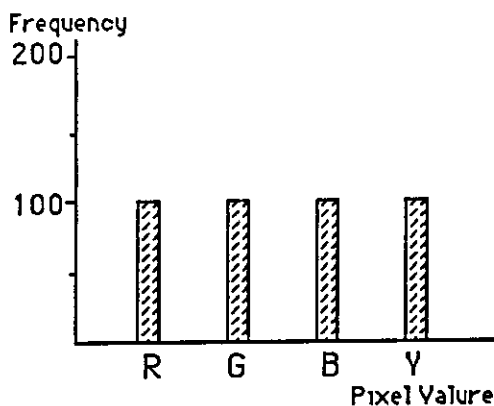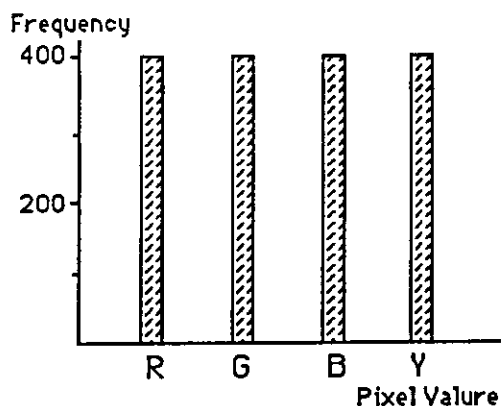
(e) Frequencies of pixels.   (f) Frequencies of pixels.

Figure 4.8 Colour images and three-dimensional histograms (continued).

three-dimensional spaces displaying locations of the four pixels graphically. This fact might be one of the important factors playing a major role in making the majority of the approaches to colour image segmentation difficult and complicated. Let us consider an Auxiliary Means which enables a three-dimensional histogram to be imaged in practice. Actually, every point in Figures 4.8.(c) and (d) is no longer a single point. Each point in Figure 4.8.(c) has 100 frequencies, and each point in Figure 4.8.(d) has 400 frequencies, but they are hidden. Thus, if the hidden frequencies are able to be displayed by a certain means, it may be regarded as an Auxiliary Means to make a three-dimensional histogram comprehensible. The Auxiliary Means devised uses the one-dimensional histograms depicted in Figures 4.8.(e) and (f), where the horizontal axes represent the values of pixels and the vertical axes frequencies. Note that the Auxiliary Means provides nothing but information about frequencies of pixels. Let us consider some reasonable methods to improve the Auxiliary Means so it can be used efficiently and actively in the further colour image segmentation procedure. First, extract the (x, y)

114

coordinates of pixels in the red square in Figure 4 8 (a) and put all of them in the bar on the R in Figure 4.8.(e); and carry out the same task with the green, blue and yellow squares in turn; and then with the squares in Figure 4.8.(b) and put them in the bar in Figure 4.8.(f), correspondingly. Second, after getting the results, assign one set of colour feature values (the CIE L*, a* and b*) into the bars on the R, G, B and Y, respectively. The Auxiliary Means in Figures 4.8.(e) and (f) are changed into those in Figures 4.9.(a) and (b), respectively. Now, it is desirable that the Auxiliary Means, with the three-dimensional colour feature space, can be used by the further colour image segmentation procedure. Let us consider the structural aspect of the Auxiliary Means in detail. Assume that each bar in Figure 4.9 is defined as a unit of the Auxiliary Means. Actually, each bar can obviously be considered as an entity in the Cluster Analysis. As Figure 4.10 shows, each unit consists of six items: (1) Cluster I.D., (2) I.D., (3) Pixel Value, (4) Colour Feature (the L*, a* and b*), (5) N.O.P., and (6) the (x, y) coordinates.
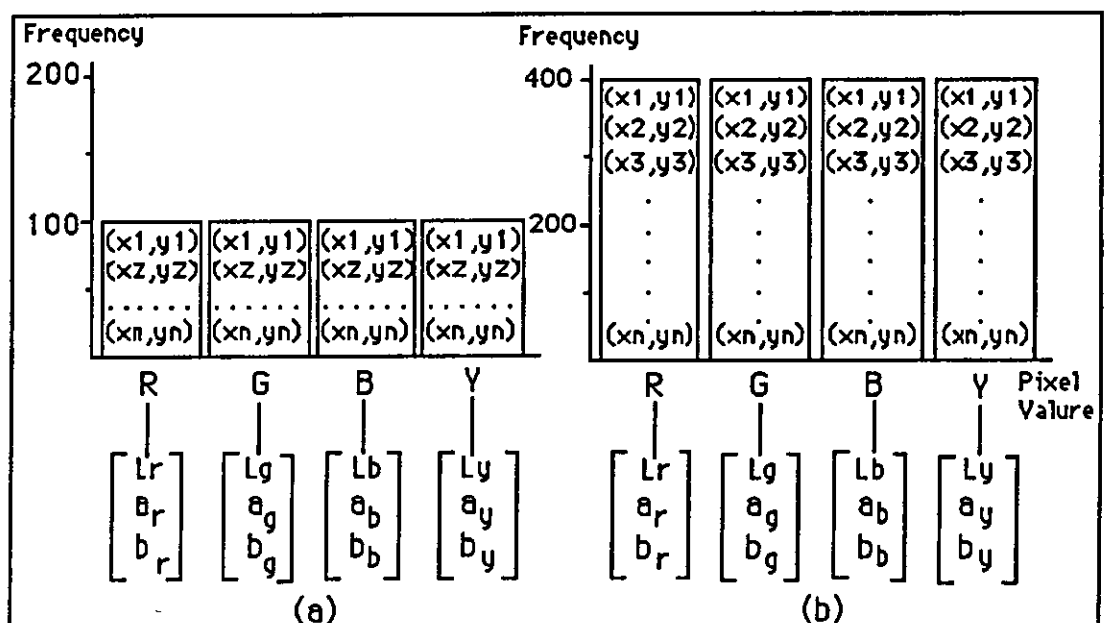
Figure 4.9 The Auxiliary Means (its hypothetical description).

115

The first item is an identification value of a cluster. After the Cluster Analysis is performed, a cluster value is assigned. The second item is an identification value for a set of pixels having the same pixel value. The I.D. for the red colour (R) in Figure 4.9.(a) is assigned 1, and that for the yellow colour (Y) is assigned 4. An important property to be remembered is that once a value is assigned to the I.D., it would not be changed any more during an operation since it should be used until the whole procedure for colour pattern extraction is finished. On the other hand, if there is noise, it is changed. A detailed discussion will be performed later. The third item is the value of a pixel which is an element displaying a colour image on a screen. The fourth item consists of three colour feature values, the L^*, a^* and b^*, which play a primary role, like attributes of an entity, in the Cluster Analysis. Note that the colour feature (the L^*, a^* and b^*) in colour image analysis usually occupies memory space three times as much as that of all the pixels in an image since each of them (the L^*, a^* and b^*) is created by being transformed from the R, G and B values of each pixel using the model developed in Chapter 2. However, employing the Auxiliary Means can dramatically reduce the memory space for the colour feature. The fifth item is the number of pixels with the same value. For example, the N.O.P. for one of the Auxiliary Means in Figure 4.9.(a) is 100 and the N.O.P. for that in Figure 4.9.(b) is 400. Finally, the sixth item contains the (x, y) coordinates of all the pixels of the same value in an image. These coordinates are used to display an actual pattern after the Cluster I.D. is determined.

The structure of the unit of the so-called Auxiliary Means and its components with functional aspects have been considered.

116

Item	
(1)	Cluster I.D.
(2)	I D
(3)	Pixel Value
(4)	L* | a* | b*
(5)	N.O P. (number of pixels)
(6)	(x1, y1) (x2, y2) (x3, y3) ⋮ (xn, yn)

Figure 4.10 The structure of a unit of the Auxiliary Means.

Then, the important question will be how many units should be created? Judd and Wyszecki (1975) have estimated that the number of different colours that we can distinguish is ten million. However, in practice, the number of different colours to be dealt with at a time by a computer is limited. In any system, the primary factor that can determine the number of different colours to be displayed and to be dealt with simultaneously depends upon the number of bits which are used to display colours on a screen. For example, for a screen which can display an image by six bits, the number of different colours to be displayed at the same time is 64 ($=2^6$). For a screen with eight bits, the possible maximum number of different colours 256 ($=2^8$). The number of bits to be dealt with is usually considered as the resolution of a displayed image. The majority of the colour image

117

handling systems, which have commonly been used, use six- or eight-bit machines. In the case of a six-bit display system, the maximum number of units of the Auxiliary Means is 64 since the number of different colours displayed and treated with the system is 64. On the other hand, the maximum number with an eight-bit screen is 256. Suppose a colour image of 500 x 500 pixels is coded by a six-bit system. Let's say the image contains forty different colours. Then, the number of units of the Auxiliary Means that should be created is forty. From the forty units, the same number of sets of the L*, a* and b* values are obtained, and used as input data to - Cluster Analysis. When a single linkage method is adopted, which is one of the hierarchical Cluster Analysis procedures, only a 40 x 40 symmetric distance matrix is created at the first stage. As soon as the result of . - Cluster Analysis is obtained, each cluster i.d. is assigned to the corresponding unit of the Auxiliary Means, where the number of clusters is determined depending upon the number of patterns with different colours in an image by visual decision. After assigning the cluster i.d., the units with the same cluster i.d. are merged into a group. The important feature of this improved algorithm is that . Cluster Analysis is performed, in this example, with only the forty different colour features, where all of the pixels are not involved. When the implementation of the Cluster Analysis procedure is completely finished, all of the pixels are only utilised in the assigning stage. The improved algorithm does not have to create a 250,000 x 250,000 symmetric distance matrix at all, nor must it segment the whole image into many pieces to manage a complex and inefficient partial Cluster Analysis.

In summary, the functional aspect of the Auxiliary Means derived from a three-dimensional histogram can be summarised as follows:

(1) The immediate motivation for devising the Auxiliary Means in this thesis is to explore a direct application of the Cluster Analysis technique to colour image segmentation.

(2) The function of the Auxiliary Means has been designed to reduce the memory space as much as possible. The majority of the existing methods for colour image segmentation inevitably have a tendency to waste the memory space. Thus, the Auxiliary Means can play an important role in breaking this tendency.

(3) When the Auxiliary Means is applied to _, image analysis, it dramatically reduces the execution time.

(4) This Auxiliary Means can be generally applied to Cluster Analysis problems arising in all relevant research areas.

4.4.2 A Procedure for Colour Pattern Extraction.

In the previous section, the motivation and background of the newly devised concept of the Auxiliary Means have been discussed. This has efficiently been used in colour image segmentation applying Cluster Analysis. In this section, a practical approach to colour image segmentation employing the Cluster Analysis procedure with the Auxiliary Means will be illustrated in detail from a design strategy to a procedural aspect. The basic strategy of this approach is as follows:

119

(1) The algorithm should directly apply the existing Cluster Analysis procedure to colour image segmentation without being restricted by image size.

(2) The algorithm should take advantage of existing Cluster Analysis procedures.

(3) The number of pixels in an image should be minimised to optimise the segmenting and merging procedures.

(4) The system should provide the user with sufficient opportunity for reasonable decision making in order that the colour pattern extracted by the system may be consistent with human vision.

The algorithm developed under the strategy is shown in Figure 4.11 and is to be illustrated in detail.

(i) In the first step, the image of an object is extracted from the image containing an object using the boundary data created in section 3.4. The boundary data have been extracted from the gradient plane (array) in the previous chapter and consist of the (x, y) coordinates and serial numbers starting from 1,000 which are larger than any pixel value in the image. The process creates a copy version of the original image and assigns the boundary data to the copy version. Thus, the copy version contains the image of the object surrounded by the serial numbers which can efficiently be used to extract the image of the object. Then, scan the image (array) from left to right and top to bottom with an attempt to detect one of the serial numbers. Note that since the serial numbers are larger than any other pixel value, they can be detected without any difficulty. As soon as one of the serial numbers is detected, pixels are extracted until another serial number is detected. On the other hand, the Cluster Analysis

120
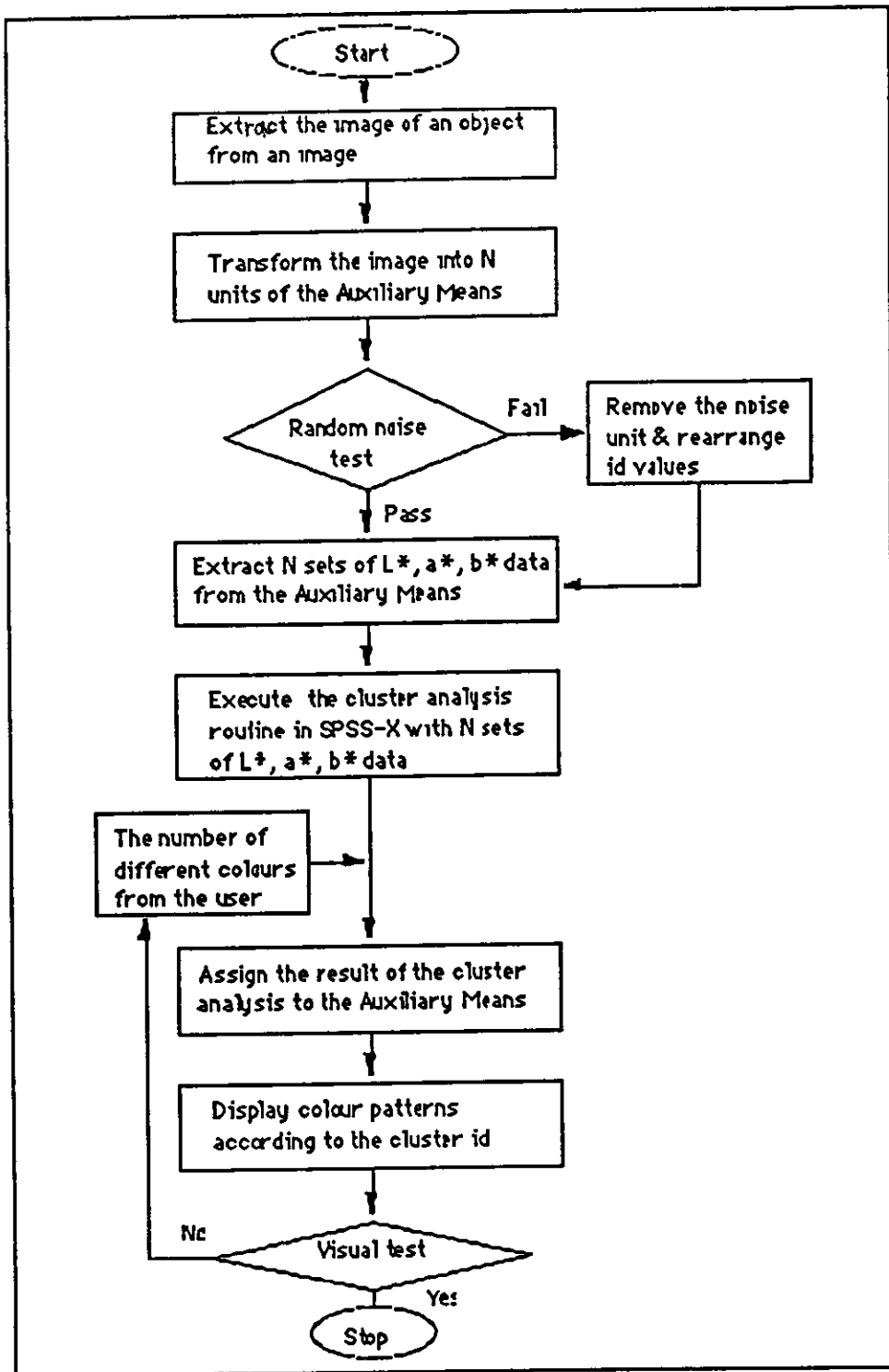
Figure 4.11 The algorithm of the colour pattern extraction.

procedure might also be applied to this step. However, if the colour of the pixels inside the object is the same as that of the

121

background, the pixels lying inside the object and the background will simultaneously be extracted. This will cause the situation to be complicated, and therefore the Cluster Analysis routine cannot be adopted in this step.

(ii) In the second step, the image of an object extracted in the previous step is segmented and then the segments are transformed into n different units of the Auxiliary Means. This is carried out according to the pixel value, where n is the number of different values of pixels in the image. When the first pixel value is detected, assign an i.d. value 1 to the I.D. of the first unit of the Auxiliary Means; assign the pixel value to the Pixel Value in the unit; transform the pixel value into the L*, a* and b* values and assign them into the corresponding item in the unit. These operations so far are performed only once whenever a new pixel group is detected. Finally assign the (x, y) coordinates of the pixel to the top of the item in the unit. Then, assign 1 to the N.O.P. in the unit; and remove the pixel value and the (x, y) coordinates of the pixel from the image. Search the extracted image for the same pixel value as that just detected. Whenever the same pixel value is detected, put the (x, y) coordinates of the pixel underneath the coordinates of the (x, y) coordinates of the pixel previously detected; increase the value by one in the N.O.P.; and remove the pixel value and the (x, y) coordinates of the pixel from the image. This task will be continued until the last pixel of the image is detected. When the task is finished, another pixel value can be easily detected and assign an i.d. value 2 to the I.D. of the second unit and then this process can be continued. When no pixel is left in the image, this step is complete. If the number of different values of pixels is n, then n units of the Auxiliary Means will be

122

created.

(iii) In the third step, check whether or not the Auxiliary Means contains random noise; and if any random noise is discovered, delete the corresponding unit, and rearrange the values of the item I.D. in the Auxiliary Means. In the first process, search every N.O.P. for the number of pixels that is less than, for example, one percent of the total number of pixels in the image of the object, where this percentage can be determined after analysing the image of each unit in the Auxiliary Means or the whole image (this problem will be discussed in the later part of this section again). If at least one unit which has less pixels than the predetermined criterion, for each unit calculate the average distance between _the unit and other units using the L*, a* and b* values. Then, calculate the mean and standard deviation of the average distances. Then, examine whether or not the average distance for the unit, which has less value of the N.O.P. than the criterion, is an outlier, that is, larger than [mean + 3 x standard deviation]. If at least one outlier is found, carry out the connectivity test for the pixels contained in the unit. If the pixels in a unit are noise according to the test, remove the corresponding unit and rearrange the i.d. values in the item I.D. of the Auxiliary Means. The further discussion will be performed in the later part of this section since the noise handling is very important in the Cluster Analysis employing the Auxiliary Means suggested in this thesis.

(iv) In the fourth step, n sets of the L*, a* and b* data are easily extracted from the Auxiliary Means, where n is the number of units. The important thing is that they should be extracted from every unit in the order of the i.d. values. The data set obtained in

this step is an n x 3 matrix and is to be used as an input data set to the SPSS-X Cluster Analysis procedure. The maximum size of n is 64 in a system of six-bit resolution or 256 with an eight-bit resolution.

(v) In the fifth step, execute the Cluster Analysis routine in the SPSS-X using the input data obtained in the previous step. In the routine, an n x n symmetric distance matrix is created, and additionally other operations illustrated in section 4.3 are performed., where the single linkage method is adopted. The routine produces lot of information which is useful for decision making. In particular, the Agglomeration Schedule, Cluster Membership of Cases, and the Dendrogram in the output are dominately used for clustering. The Cluster Membership of Cases is used as an input data set to the next step.

(vi) In the sixth step, the number of different colours found in the object is supplied by the user.

(vii) In the seventh step, the result of the Cluster Analysis is assigned to the first item of every unit of the Auxiliary Means.

(viii) In the eighth step, display the colour pattern using the pixel value and the (x, y) coordinates in the units having the same value of the Cluster I.D. Display the colour patterns equal to the number of clusters. The important thing to be noted is that if there is no noise, the value of the I.D. in each of the units of the Auxiliary Means is not changed once it is assigned in the second step. This means that the segmentation of pixels in the image is performed only once, and the pixels are not physically merged, but

124

temporally called when the Cluster I.D. which they belong to is called.

(viiii) In the last step, if the colour patterns displayed are consistent with those of human vision, then the procedure is stopped; otherwise, the procedure requires the new number of different colours to be specified by the user. The important feature of this algorithm is that after this step the Cluster Analysis routine no longer needs to be implemented and the output already produced is used. Once the routine stops at the end of the procedure, the Auxiliary Means assigned with the cluster values in the final stage is used in the colour pattern description in Chapter 6.

The handling of the random noise considered in the third step is an important problem that causes the image analysis to be disfunctional. The Cluster Analysis approach itself is not exempt from this tendency. The important fact to be noted is that, in the Cluster Analysis which has been designed to employ the Auxiliary Means, the pixels of an image are not involved directly in the Cluster Analysis procedure, but only unique colour values. If some pixels regarded as random noise have very strange features, the result of a clustering will be severely damaged by the pixels. The main idea to deal with the random noise is to strengthen this approach and to enable this procedure to produce the high quality of colour patterns consistent with that of ˙ human vision. In this procedure, it is assumed that some pixels that have all of the following features are determined as the random noise.

(1) The number of pixels with the same value is very small.

(2) The colour feature of the pixel is distinctly different from

125

those of other pixels.

(3) The pixels are scattered.

There is a problem with the above criteria, that is, can a small area of colour be defined as noise or as part of a pattern. In order to define the criteria, consider the butterfly domain, spot patterns in the wing of a butterfly are generally studied, where the area of a spot and the number of spots are among the important factors for the identification (Schwanwitsch, 1924; Nijhout, 1978; Brakefiel, 1979). This fact reveals that even a tiny spot in an image plays an important role and cannot be ignored at all. Taking into account this fact, the criterion for the small number in the first feature is determined as one percent of the total number of pixels in an image. If the criterion is determined with the number of pixels rather than the percentage, a severe problem is expected when the image of a butterfly is enlarged or reduced.

For the second criterion, for one pixel in each unit of the Auxiliary Means, calculate the distances between the pixel and pixels of the other units using the L^*, a^* and b^* values; and calculate the average distance. If the number of units of Auxiliary Means is n, the number of average distances obtained is n. Then, calculate the mean and standard deviation of the average distances. Let the average distances be m_1, m_2, m_3, ..., m_n, the mean, m_{avg}, and the standard deviation, S, of the average distances are respectively,

$$m_{avg} = (m_1 + m_2 + ... + m_n)/n,$$

$$S = [\ \Sigma(m_{avg} - m_i)^2\ ]^{1/2},$$

where, i=1, 2, 3, ..., n. In statistical analysis, the criterion for an outlier is usually [mean ± 3 x S] in the normal distribution.

126

Suppose that an average distance for a pixel regarded as random noise is m_j, and if the m_j is greater than $[m_{avg} + 3 \times S]$, it is concluded that the pixel is aberrant. Where, the meaning of this aberration is that the pixel has a very distinctive colour feature which is in contrast to other pixels. To clarify, note the following example with four pixels A, B, C and D, in Figure 4.12, where the figures between the pixels are distances. The average distances for the four pixels are 5.3, 11, 6.3 and 5.3, respectively, as shown in Table 4.1. The mean of the average distances is 6.9, the standard deviation of the average distances is 1.2, and the criterion for the outlier calculated is 10.5. The pixel B is considered as an outlier since the average distance of the pixel is 11 which is greater than the criterion 10.5. In other words, it is considered that the pixel B has a distinctly different colour feature. If only a few pixels with the colour feature are scattered, the result of clustering will not be consistent with human vision.
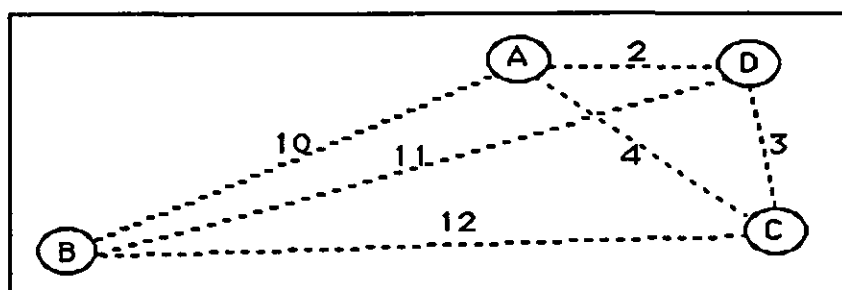
Figure 4.12 Pixels including noise.

The connectivity for the third feature is another important concept having been used to characterise a region in an image. The connectivity stands for the connection of pixels in an image. The connectivity test is performed using a 3 x 3 array. For instance, dark pixels in Figures 4.13.(b) and (c) are connected ones and, on

127

the other hand, dark pixels in Figure 4.13.(a) are completely unconnected. Note the 3 x 3 array containing a pixel with the dark feature in the middle as shown in Figure 4.13.(a'), each of the eight neighbours has a light feature, thus it is concluded that the pixel with the dark feature is isolated. On the other hand, each

Pixel	Distance	Average Distance (m_i)	The Mean of the Average Distances $(mavg)$	The Standard Deviation of Average Distances
A	AB=10 AC= 4 AD= 2	$m1 = \dfrac{10+4+2}{3}$ $= 5.3$	$mavg$ $= \dfrac{5.3+11+6.3+5.3}{4}$ $= 6.9$	$S = 1.2$
B	BA=10 BD=11 BC=12	$m2 = \dfrac{10+11+12}{3}$ $= 11$		
C	CD= 3 CA= 4 CB=12	$m3 = \dfrac{3+4+12}{3}$ $= 6.3$		
D	DA= 2 DB=11 DC= 3	$m4 = \dfrac{2+11+3}{3}$ $= 5.3$		
Criterion for the outlier: 6.9 + 3 x 1.2 = 10.5				

Table 4.1 The calculation of the outlier.

pixel centred at the array in Figure 4.13.(b') and (c') has two neighbours with dark features, respectively. Hence, it is concluded that the pixels in Figure 4.13.(b') and (c') are connected. In the actual process, first, assign any number larger than the maximum pixel value of a system, 1,000 for instance, to every cell of an array of the same size as the image, and assign the values of the pixels being examined to the array then each pixel value being examined can clearly be discriminated from other

pixel values. Second, carry out the connectivity test for each pixel being tested. Whenever an isolated pixel is detected during the test, count the number of isolated pixels. If the number is equal to the number of pixels being tested, it is concluded that the pixels are fully isolated. After the connectivity test, if some pixels
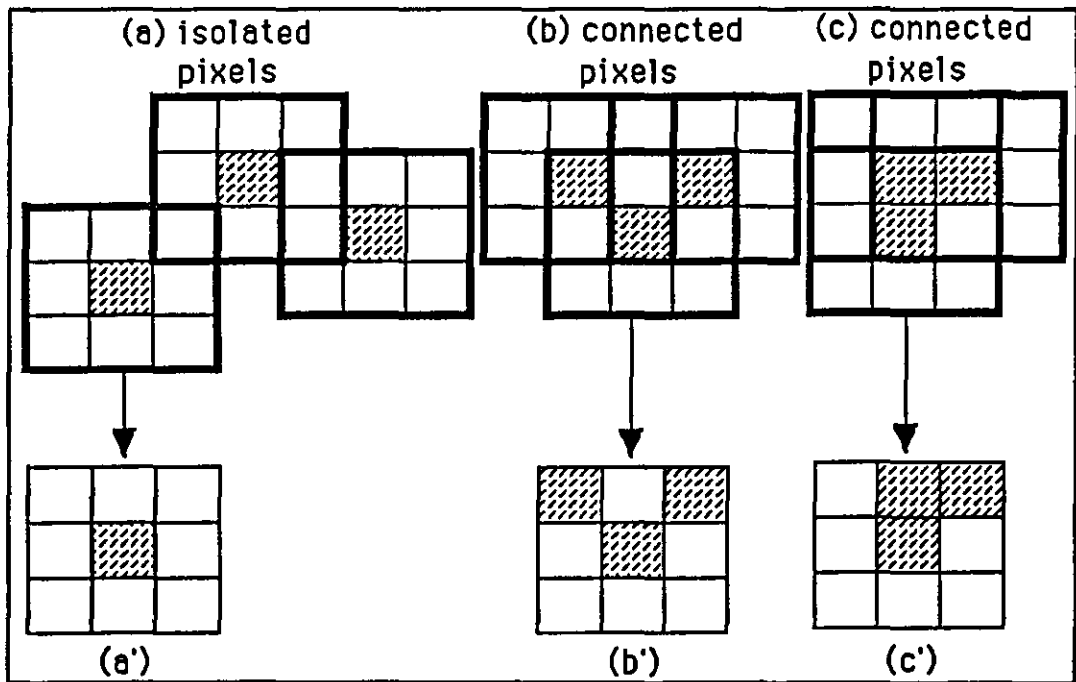
Figure 4.13 The connectivity test.

become clearly unconnected, have distinctly different colour features from each other, and are only a few in number, then it is concluded that the pixels are random noise and the corresponding unit is removed.

After the input data set to the Cluster Analysis is prepared, the Cluster Analysis is performed in the fifth step, where the single linkage method is applied. Let us investigate the suitability of the single linkage method. As already discussed in section 4.3, there are many techniques in the hierarchical methods of Cluster Analysis procedure, such as the single linkage method, the

129

complete linkage method, the average linkage method and the centroid method. Among these techniques, which method is most suitable to colour image segmentation? This is not a simple question since the quality of a result depends upon the method. Everitt (1974) has also pointed out that the major difficulty with the hierarchical techniques lies in the choice of one method from the many available and in the choice of which 'similarity' to use. The important thing to be noted is that in the average linkage method and the centroid method all of the data obtained from the whole pixels of an image should be involved in the calculation of the average or the centroid. However, the data prepared in the fourth step are a set of sample pixels representing each group of pixels having the same colour feature. Apart from the limitation, it is known that the two methods and the complete linkage method are likely to result in overlapping clusters (Lorr, 1983). The complete linkage method, as already explained in section 4.3, is that the longest distance between one of entities in one cluster and that in another cluster is calculated, thus the number of longest distances obtained is n(n-1)/2, where n is the number of clusters, Eventually, the two clusters having the minimum value are merged. However, This method leads to some problems when applied to image segmentation as shown in Figure 4.14. Let d1 be the longest distance between the clusters A and B, and d2 be the longest distance between the clusters A and C as shown in Figure 4.14.(a); and d3 be the shortest distance between the clusters A and B, and d4 be the shortest distance between the clusters A and C as shown in Figure 4.14.(b). According to the algorithm of the compete linkage method, the cluster A and the cluster B are merged because the distance d2 is shorter than the distance d1.

However, in fact, as Figure 4.14.(a) shows, the cluster B is located more closely to the cluster A than the cluster C, although the variance of the cluster B is larger than that of the cluster C. On the other hand, in the single linkage method, the cluster B is merged into the cluster A because the distance d3 is shorter than the distance d4. Consequently, comparing the two results undoubtedly reveals that the single linkage method produces the more reasonable result than the compete linkage method. In terms of the practical application of the single linkage method, Everitt (1974) has suggested that if one is looking for optimally connected clusters, the single linkage method may be useful.

(a) the complete linkage method   (b) the single linkage method
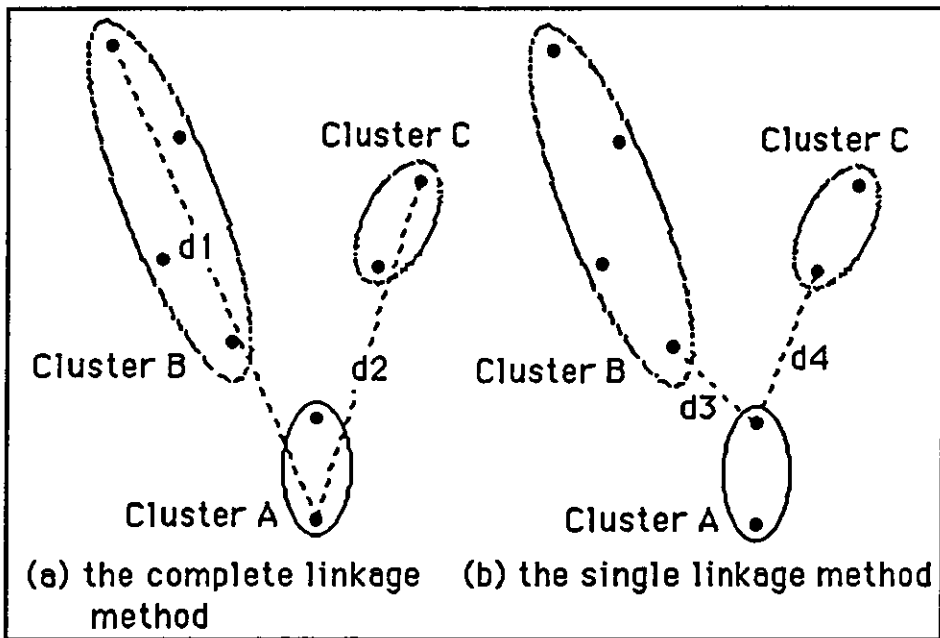
Figure 4.14 A comparison of the complete linkage method and the single linkage method.

For the time being, let us focus on the properties of the natural colours in the wing-patterns of butterflies. The important feature found in the empirical study of the wing-patterns of butterflies is that when the area near the border line between

131

two patterns of completely different colours is zoomed up, many different colours are easily detected. In particular, the colours are changed from one colour to another gradually rather than abruptly. Note the images of the wing-patterns of a butterfly in Figure 4.15.

(a)   (b)
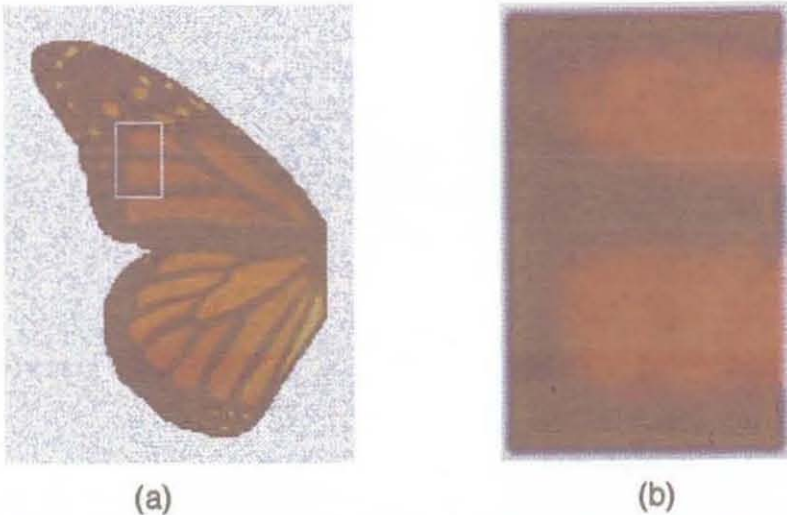
Figure 4.15 The original image and enlarged image. (a) An original image of the left-hand side wing of a butterfly. (b) The enlarged image of the image bounded by a box in (a).

The image on the left-hand side is the original image of the left wing of a butterfly and the image on the right-hand side is an enlarged image of the image inside the small box in Figure 4.15.(a). From the image on the left-hand side, we can detect two kinds of different colours one is dark brown and another is orange. Consequently, this fact found in the investigation suggests the important facts and directions of the colour image segmentation are as follows:

(1) When a natural image consists of more than two colour patterns, the distribution of the scanned colours composing each pattern in the L*a*b* colour feature space usually forms a chaining shape as Figure 4.16 shows.

132

(2) In the L*a*b* colour feature space, the shape of the cluster of the colours constructing a meaningful pattern may be quite different from the simple cube such as the ellipsoid or spherical shape which is commonly used for a tolerance limit to discriminate different colours in the colour feature space in the colour science domain.

(3) In a complex situation, that is,when an object image consists of more than two patterns of slightly different colours or with unclear borders among them, it is ambiguous to make a clear border line separating the groups (clusters) of similar colours composing the different patterns.

If the theoretical aspect of the single linkage method and the facts obtained in the investigation are put together, it will be undoubtedly concluded that a method to detect elongated or curved cluster structures is the single linkage method. The scatter diagrams shown in Figure 4.16 are the results obtained from applying the single linkage method to the extraction of colour patterns from the image of a butterfly, plexippus in Figure 4.15.(a) whose wing has two patterns of different colour groups. Each of the diagrams in Figure 4.16 is a two-dimensional scatter diagram projecting the clusters in the three-dimensional L*, a* and b* colour feature space onto an a*b* plane, an L*a* plane, or an L*b* plane. In the diagrams, each number surrounded by the closed curve represents the cluster i.d. As the diagrams show, the shape of each cluster is so complex that it is obviously difficult not only to simply describe it using a mathematical formula, but also to characterise it without the combination of the three diagrams.
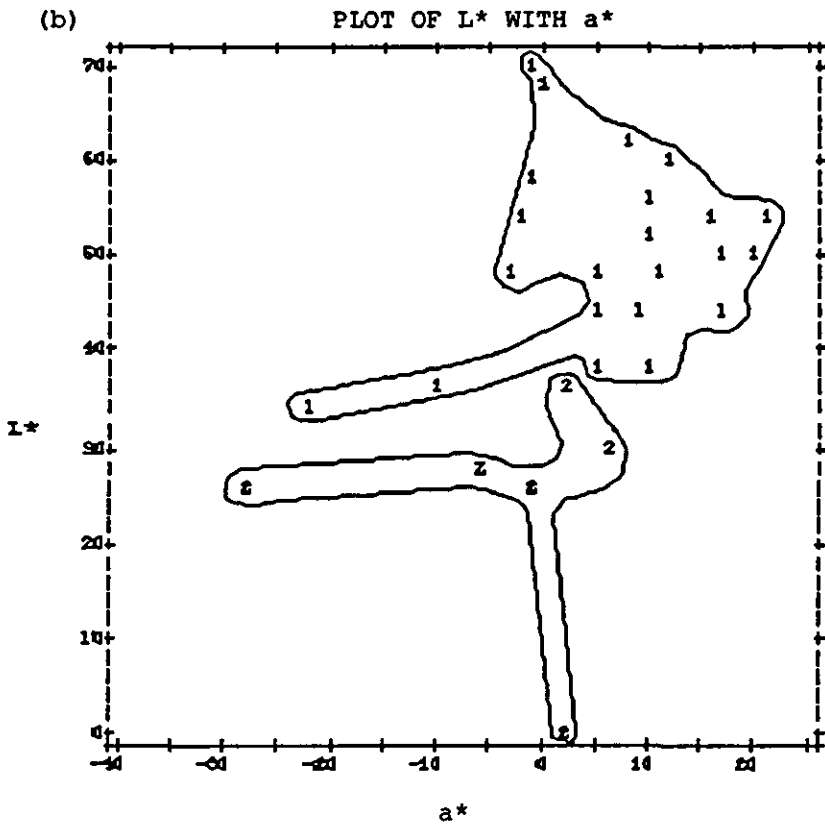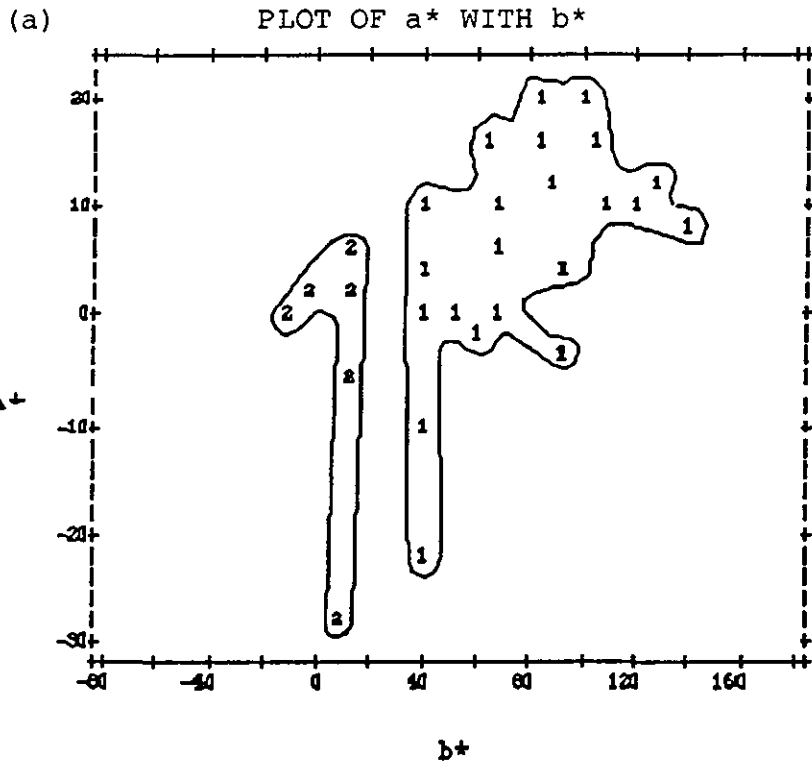
Figure 4.16 The scattered diagrams of clusters. (continued)

134

PLOT OF L* WITH b*
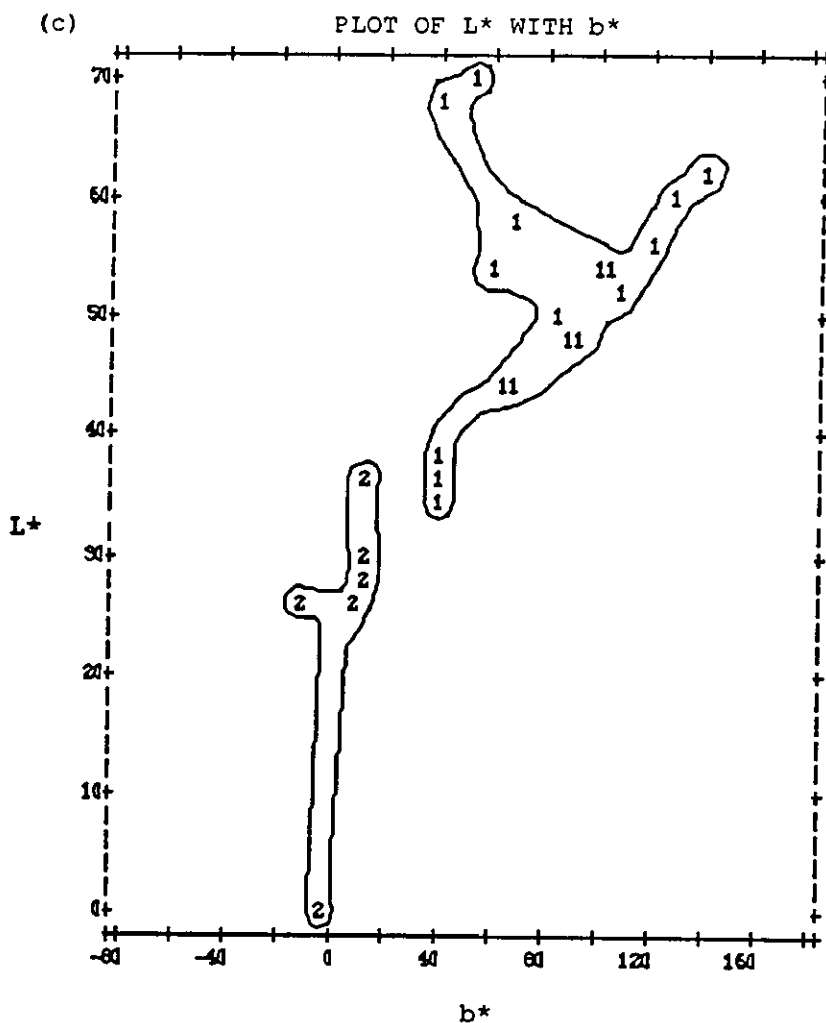
Figure 4.16 The scattered diagrams of clusters. (continued)

After the result of Cluster Analysis is obtained, the immediate problem in the sixth step is how many patterns with different colours should be extracted. If the image under processing consists of patterns with clearly different colours, and the patterns formulate simple blocks, the number of different colours to be supplied by the user will not be a problem. On the other hand, if patterns with similar colours are scattered without clear border lines among them, there will be a confusion or difficulty in deciding the number of different colours in the image

135

under processing. The sample image of a butterfly, plexippus, in Figure 4.15 shows one of the examples related to the above case. The reason for the difficulty in the decision making is because a similarity among the different colours and ambiguous border lines among them make a visual judgment difficult. As ⁻ human vision has difficulties in decision making with a complex image, so the determination of how many groups are present in the result of the Cluster Analysis has difficulties. The reason for the difficulties lies in the complex nature of multivariate sampling distributions. The problem of how many patterns with different colours should be extracted from an image obviously corresponds to a problem of how many clusters should be chosen from the result of the Cluster Analysis. In the social sciences, decision making for choosing the number of clusters is generally carried out using the tree structure of a dendrogram, which is one of the results obtained from the Cluster Analysis routine of the SPSS-X, as shown in Figure 4.17. The dendrogram obtained using the input data created from the image in Figure 4.15.(a) consists of three kinds of components:

(a) a hierarchical tree,

(b) labelled cases,

(c) distance level.

The tree which is a connected graph without cycles is used as a representation of the clustering hierarchy for the twenty-eight entities which are the different kinds of pixels of the image in Figure 4.15.(a). The root on the right-hand side of the tree is the initial vertex of the tree to which all other vertices (entities) are connected. Eventually, the tree is subdivided into binary trees, so it is possible to travel from any entity to another along the tree. The reason why the binary trees are used in the clustering

hierarchy is shown in the algorithm of merging clusters in section
4.3. The labelled cases on the vertical axis on the left-hand side
in Figure 4.17 include twenty-eight entities, where each of the
entities is labelled according to the sequence in the input data set
and is located in the corresponding clusters. The horizontal axis
represents the distance level between clusters. The number of
clusters is always associated with the distance level on the
horizontal axis. For instance, cut the tree along the vertical
direction at the distance level 23 as shown in Figure 4.17, then

```
* * * H I E R A R C H I C A L   C L U S T E R   A N A L Y S I S * * *

                     Dendrogram using Single Linkage

                    Rescaled Distance Cluster Combine
        C A S E   0         5        10        15        20      , 25
        Label  Seq  +--------+---------+---------+---------+--------+---+
                25   -+-----+                                      :
                26   -+     |                                      :
                22   -------+-+                                    :
                12   -------+ +-----------+                        :
                 6   ---------+           |                        :
                27   -----+           +-----------+                :
                28   -----+-------------+ |        |               :
                20   -----+           +-+ |        |               :
                19   -----------+-----+ | +-----+  :
                21   -----------+     +-+ |     |  :
                18   -----------------+   |     |    :      ; cut
                 8   -----------------+-----------+ |     |    :      ▼
                 9   ----------------+          +---+ |    :
                 4   ---------+----------+      |       +-----O---+
                17   ---------+       +-------+ |               |  :      |
                10   -+-------+       |         |               |  :      |
                14   -+     +-----------+       |               |  :      |
                24   ---------+                 |               |  :      |
                 1   ---+--------------+        |               |  :      |
                11   ---+            +-----------+               |  :      |
                13   -----------------+-----+                    |  :      |
                23   -----------------+                          |  :      |
                 3   -------+-------+                            |  :      |
                15   -------+       +-----------------+          |  :      |
                 7   ----------------+              +-+          |  :      |
                16   ------------------------------+ +-----+--:      |
                 5   -----------------------------------+    +O---+
                 2   -----------------------------------+ :    ◤
                                                           cut
```

Figure 4.17 A dendrogram.

137

there will be two subtrees. Collect the entities at the ends of each tree, then two clusters are obtained as follows:

cluster 1 = [25, 26, 22, 12, 6, 27, 28, 20, 19, 21, 18, 8, 9, 4, 17, 10, 14, 24, 1, 11, 13, 23],

cluster 2 = [3, 15, 7, 16, 5, 2].

If the tree is cut in the same manner at a different distance level, the number of clusters and the contents in each of the clusters are obviously changed. Consequently, the number of clusters and the contents in each of the clusters are determined depending upon the distance level. In fact, it is impossible for the ordinary user to get the distance level directly from an image. According to this fact, the system has been designed to enable the user to enter the number of different colours. When the original image of an object is displayed, the user decides the number of patterns with different colours in the image and enters the number of colours. On the other hand, it is possible to design a procedure to use the distance level instead of the number of different colours to determine the number of clusters. However, for the practical application, the system was designed to only handle the number of different colours. The seventh step in the process selects the number of clusters, corresponding to the number entered by the user, from the Cluster Membership of Cases which is one of the outputs of the Cluster Analysis routine of ˙ ⁻ SPSS-X in Figure 4.18. The Cluster Membership of Cases in Figure 4.18 is a sample output for the image in Figure 4.15.(a). It contains only part of the output, where the top line represents the number of clusters, the left most column represents the labelled cases, and the other columns below the number of clusters represent the cluster i.d. values. If the number entered by the user is 2, for instance, a column corresponding to 2 (the number of clusters) is selected.

The column surrounded by a dashed line in Figure 4.18 has cluster i.d. values which are arranged in the sequence of the labelled cases. Eventually, each of the cluster i.d. values is assigned individually to the item I.D. of the unit in the Auxiliary Means, in the sequence of the labelled cases.

* * * H I E R A R C H I C A L   C L U S T E R   A N A L Y S I S * * *

Cluster Membership of Cases using Single Linkage

Number of Clusters

Label	Case	10	9	8	7	6	5	4	3	2
	1	1	1	1	1	1	1	1	1	1
	2	2	2	2	2	2	2	2	2	2
	3	3	3	3	3	3	3	3	3	2
	4	4	4	4	4	4	4	4	1	1
	5	5	5	5	5	5	5	3	3	2
	6	6	6	6	6	4	4	4	1	1
	7	3	3	3	3	3	3	3	3	2
	8	7	7	7	4	4	4	4	1	1
	9	7	7	7	4	4	4	4	1	1
	10	8	4	4	4	4	4	4	1	1
	11	1	1	1	1	1	1	1	1	1
	12	6	6	6	6	4	4	4	1	1
	13	9	8	1	1	1	1	1	1	1
	14	8	4	4	4	4	4	4	1	1
	15	3	3	3	3	3	3	3	3	2
	16	10	9	8	7	6	3	3	3	2
	17	4	4	4	4	4	4	4	1	1
	18	6	6	6	6	4	4	4	1	1
	19	6	6	6	6	4	4	4	1	1
	20	6	6	6	6	4	4	4	1	1
	21	6	6	6	6	4	4	4	1	1
	22	6	6	6	6	4	4	4	1	1
	23	9	8	1	1	1	1	1	1	1
	24	8	4	4	4	4	4	4	1	1
	25	6	6	6	6	4	4	4	1	1
	26	6	6	6	6	4	4	4	1	1
	27	6	6	6	6	4	4	4	1	1
	28	6	6	6	6	4	4	4	1	1

Figure 4.18 Cluster Membership of Cases.

This concept of assigning the result of the Cluster Analysis to the Auxiliary Means is one of the important kernel points in this approach to the colour image segmentation. In terms of system efficiency, applying this concept actually dramatically reduces not only the computing time, but also the memory space since all of the pixels in an image are not involved in assigning the cluster i.d. The sample image in Figure 4.15.(a) has twenty-eight different kinds of pixels with different values and its size is, for instance, 200 x 200. In this case, the operation of assigning the cluster i.d. to the Auxiliary Means is performed only twenty-eight times, rather than 40,000 times. It needs only 28/40,000ths of the computing time and the corresponding memory space. When the image is enlarged, the values will be dramatically reduced. Let us have a close look at the process. The process picks the right most column from the Cluster Membership of Cases in Figure 4.18 according to the number of patterns with different colours from the user. In Figure 4.19, the top line is the Label Case where each labelled case is arranged in sequence from the left to right, and the next line includes the cluster i.d. values which correspond to the labelled cases, respectively. Below this line, the twenty-eight units of the Auxiliary Means are arranged in the sequence of the labelled cases. In the process, each of the cluster i.d. values in the second line is assigned to each of the units of the Auxiliary Means in sequence, one by one. After performing this process, the unit in the left most has been assigned 1, the next unit 2, the third unit 2, and finally the unit in the right most 1, as in Figure 4.19 shows. When the number of patterns with different colours entered by the user is 3, the first unit will be assigned 1, the second unit 2, the third unit 3, and the last unit 1. After all of the units in the Auxiliary Means have been assigned cluster i.d. values,

each of the patterns is displayed in the eighth step. Consider the procedure of displaying each of the patterns with the previous example. In the process of displaying an image, the major components of an image are (i) the size of an image, (ii) the value of each pixel, and (iii) the (x, y) coordinates of each pixel. In the procedure in Figure 4.20, the first parameter i, which is the number of patterns with different colours, has values of 1 and 2. The procedure of displaying a pattern is performed twice. In the next step, the image of 200 x 200 is cleared with the pixel value in the background. As soon as the image is cleared, each head of
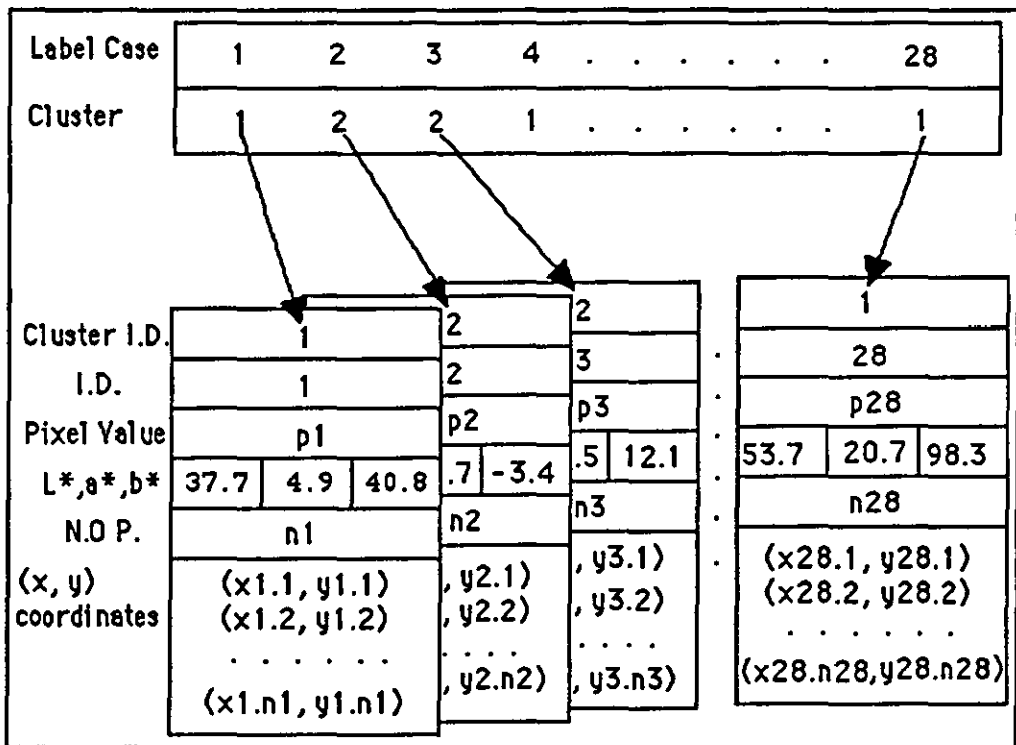
Figure 4.19 Assigning the cluster i.d. to the unit of the Auxiliary Means.

28 units of the Auxiliary Means is searched for the same value of i. When the cluster i.d. in the head of the unit in the Auxiliary Means is equal to the value of i, assign the pixel value to the (x, y)

141

of the image array, where x and y are each of the (x, y) coordinates in the unit. If all of the pixels in the units having the same cluster i.d. are assigned to the array, display the image. Each of the images containing the pattern obtained in this procedure is depicted in Figure 4.21. The important feature to be noted in the procedure is that since searching is performed only with the heads of the units in the Auxiliary Means, the computing time is also dramatically reduced.
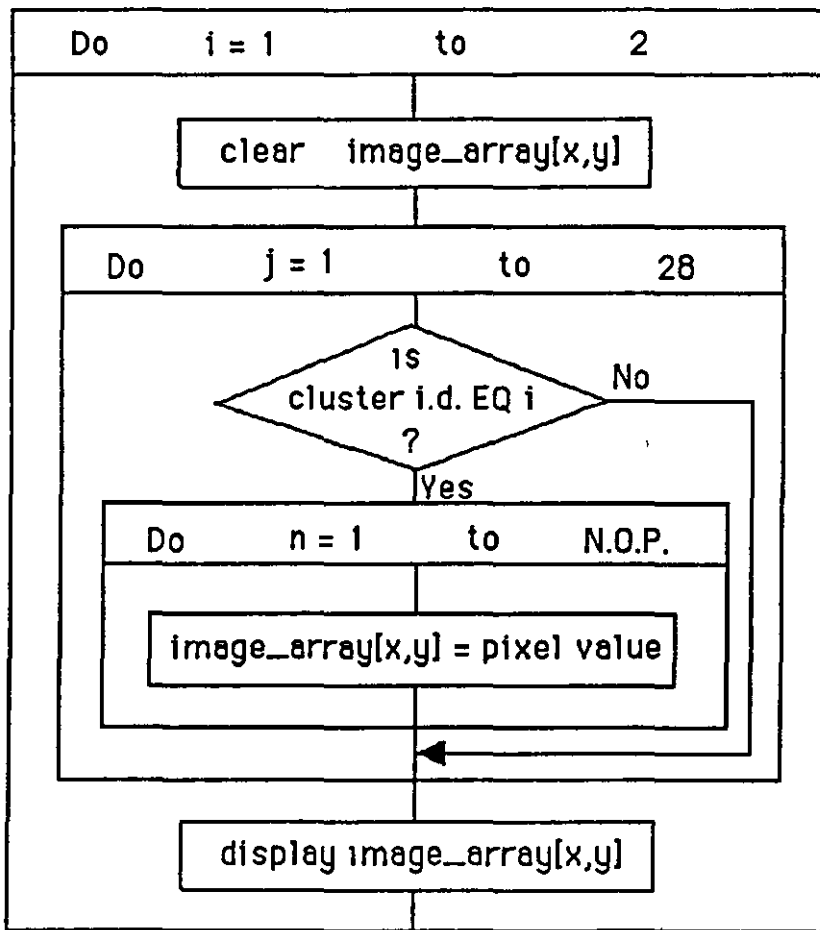
Figure 4.20 The procedure for displaying patterns.
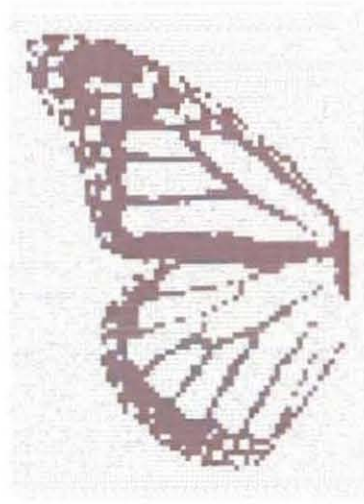
Pattern 1   Pattern 2

Figure 4.21 The patterns extracted.

4.5 CONCLUSION.

In the image analysis domain, the majority of approaches to segmenting a colour image into meaningful segments have been constrained by the problem of dealing with inordinate amounts of data, i.e. a large number of pixels of an image. In spite of this difficulty, many approaches from slightly different angles have been carried out to achieve the same goal. It has generally been realised that the majority of the approaches in the colour image segmentation could not be achieved other than by a roundabout route. However, they are clearly aware that a short cut exists, but they are also aware of a major difficulty with this short cut. This method suggested in this chapter provides such a short cut. The Auxiliary Means is a reasonable way to the short cut. To get through this short cut one must directly apply the Cluster Analysis to the colour image segmentation. In the practical applications which have been performed using sample images, the Auxiliary Means has successfully been used. To strengthen the function of the Auxiliary Means in the colour image segmentation a new algorithm has been added. In this algorithm, a method to remove random noise, which weakens the Auxiliary Means, has been considered.

During the development of the algorithm of this approach, Cluster Analysis has been thoroughly reviewed from the theoretical aspect to the practical application. Indeed, the application of the Cluster Analysis to colour image segmentation has led to a reasonable solution. The main reason is that the problem of the colour image segmentation is originally formulated in a three-dimensional colour feature space, not in

a one-dimensional domain, nor in a two-dimensional plane. Most of the existing approaches such as the mode-seeking method (Chow & Kaneko, 1972), the recursive region splitting method (Ohlander, Price & Reddy, 1978), and the decision surface method (Underwood & Aggarwal, 1977), etc., have tried to find the solution in a one-dimensional or two-dimensional domain in spite of an enormous use of computing time. It is believed that the designers of these approaches have done their best and the basic ideas have been brilliant within the circumstances, i.e. one- or two-dimensional domains. In fact, when one tries to solve a three-dimensional problem which is not simple in a one- or two-dimensional domain, the problem suddenly becomes more complex than imagined. In Cluster Analysis, the basic requirement is to calculate a distance matrix. If the matrix is calculated for an n x n image, the size of the matrix is (n x n) x (n x n) which usually exceeds the size of the core memory of existing main frames although the size of an image is small, for instance 100 x 100. It has been regarded as an obstacle like an incurable cancer in the medical domain. Eventually, the important fact to be noted is that it is impossible to carry out the application without employing the Auxiliary Means. Another desirable aspect of the Auxiliary Means is that it can be efficiently used in the operation of displaying each of the patterns extracted to reduce memory space as well as computing time. As far as system efficiency is concerned, the most important factors to be considered not only in the design stage, but also in the implementation stage are how to minimise the computing time and the memory space, and to produce the highest quality   output. From this point of view, the algorithm applying Cluster Analysis to the colour image segmentation with the Auxiliary Means in this thesis accommodates the important

145

factors.

In particular, the major concept of the Auxiliary Means developed in this thesis can be generally used in Cluster Analysis for any kinds of problems in the academic or the industrial research fields. For example, census data usually consist, of a huge number of observations, so it is not easy to perform Cluster Analysis. However, since most of the variables in the census data include categorical values, the concept of the Auxiliary Means can be applied without any difficulty.

Chapter 5

SHAPE DESCRIPTION METHODS.

5.1 Introduction.

5.2 Existing Shape Descriptors.

5.3 New Shape Description Method.

  5.3.1 The background and Basic Principle of this Method.

  5.3.2 The Algorithm for this Method.
    5.3.2.1 Detecting a Principal Axis.
    5.3.2.2 Calculation of Ratios.
      5.3.2.2.1 Rotation of a Contour.
      5.3.2.2.2 Calculation of Areas of Segments.
      5.3.2.2.3 Calculation of Ratios.

5.4 Conclusion.

5.1 INTRODUCTION.

Extracting the boundary of an object from an image is generally not a simple procedure. The main objective of extracting the boundary is to use the boundary in an object discrimination procedure. In this procedure, shape descriptors play the most important role. No matter how accurate the boundary may be, if a shape descriptor is inefficiently organised in its function, the effort which has been involved in producing the boundary will become meaningless, and the efficiency of a system which employs the descriptor will decrease. In some cases, the system might even produce unreasonable results. It is obvious that the importance of the shape descriptor in object discrimination procedures cannot be emphasised too much.

To date, many different approaches have been attempted for describing the boundary of an object. An investigation of some of the approaches which are closely related to the subject of this thesis will be carried out. The invariant moment method, the Fourier description method and the chain coding method are quite commonly used in the object discrimination domain. The investigation will concentrate on the theoretical background, the detailed procedure and the final product of each approach. Comparing, in parallel, the method to each other along functional lines. The main objective of the investigation is to understand the current state of the art of the existing methods, thus discovering any problems, pertinent to this thesis, that then need to be solved. An improved method for shape description will be clearly illustrated from the motivation for its development to its algorithm. One of the distinctive features of this method is that

148

it has been designed to be directly involved in object discrimination procedures.

5.2 EXISTING SHAPE DESCRIPTORS.

When the shape of an object is extracted from an image, the immediate task is how to describe the shape based on its external characteristics. In terms of biology, the external characteristics of an object are usually called morphological features. The methods for describing the morphological features are usually associated with tasks where the shape is important but that contained within it is of little or no interest. In this thesis, both the shape and its interior are of importance, so they are separately discussed. In this section, the existing shape description methods will be investigated. In particular, the investigation will focus on the invariant moment method, the Fourier descriptor, and the chain code, since they are commonly used in this domain. An important principle that should be considered at the design stage is to describe the features of an object in order to be independent of the starting point, scale, translation and orientation (Alt, 1962). Actually, it has been regarded as a basic condition for a shape descriptor. In practical applications, the variations are such that it is unlikely that the shapes, sizes, positions and orientations of two objects will be identical. In fact, the major difficulties in describing the features of an object arise because of these variations. Although only one of these variations is ignored, it will give rise to serious difficulty in an object identification process, because this can affect the various measurements of an object.

One scalar method using mathematical properties derived from the area within a shape contour is simple to implement. The descriptors usually take the form of numerical measures of the

shape rather than representing symbolic properties. It is known that in simple scalar techniques; area, perimeter length, diameter, the orientation of the major axis, and curvatures, etc. have been efficiently used for many years in the field of robotic vision and object recognition. The area of a shape is simply the number of pixels within a shape. A rough approximation of the perimeter length is obtained by counting the number of pixels along the contour. The diameter of a shape is defined by those two extrema on the boundary that have the greatest distance between them. The orientation of the major axis is an angle with a horizontal line of an image. The curvature of a shape is defined as the rate of change of slope. These descriptors are quite simply calculated, although some of them have a serious weakness in that they yield the same values for objects of distinctly different shapes.

To illustrate some problems with some of these descriptors, let us consider the following example. A rectangle of 1 x 20 in Figure 5.1.(a) is cut into three pieces, i.e. one rectangle of 1 x 18 and two squares of 1 x 1 as shown in Figure 5.1.(b). Put one of the squares on the rectangle slightly to the left-hand side and the other square underneath the rectangle slightly to the right-hand side. Then, an object in Figure 5.1.(c) is produced. On the other hand, put the two squares on the rectangle slightly apart from each other, then another object in Figure 5.1.(d) can be obtained. All of the numbers represent measurements of distances. Note the two objects of distinctly different shape in Figures 5.1.(c) and (d). The descriptor area yields 20 for each of the objects. The descriptor perimeter length yields 42 for each of the two objects. The diameter also yields the same value 18.03 for each of them. Although the three descriptors are used at the same time to

151

classify the two objects in Figures 5.1.(c) and (d) with widely different features, they show their limitations in the task by yielding the same values for the objects.
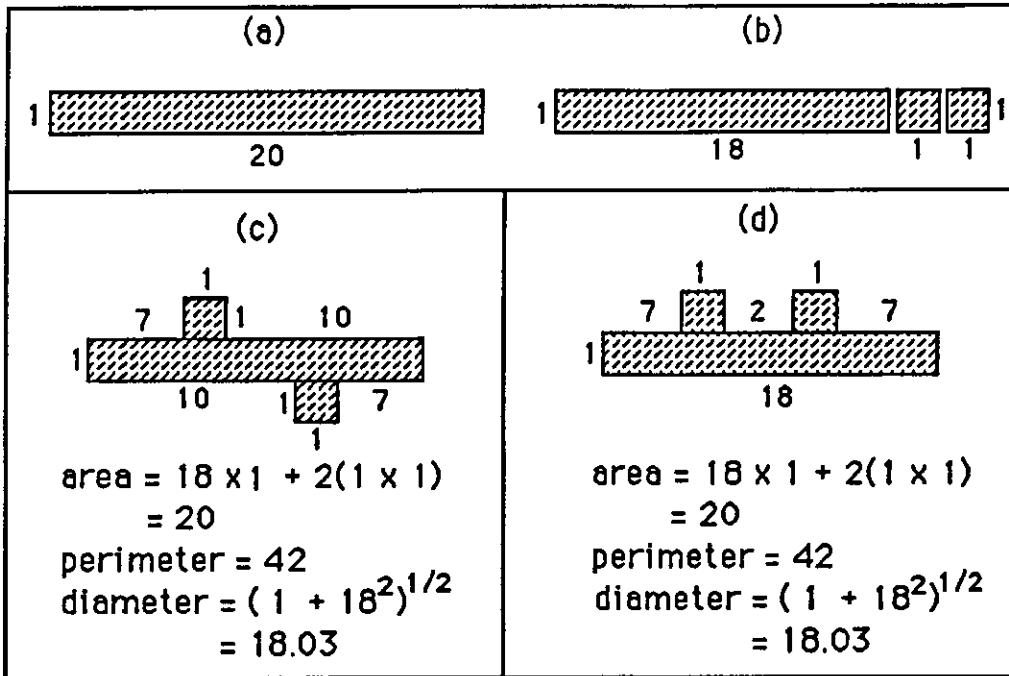
Figure 5.1 Descriptors and objects with different feature.

A shape can be described by the spatial moments of its intensity function, where this method is called the method of moments. The main paradigm of this method is that all possible measurement features of a shape can be represented in the set of moments. The term "moment" comes from the domain of statistics. The moments are easily calculated for an intensity function, f(x, y). The two-dimensional (p + q)th order moments which are called the (p + q)th generalised moments are:

$$m_{pq} = \sum_x \sum_y x^p y^p f(x, y),$$

(5.2-1)

where p, q = 0, 1, 2, 3, ..., and f(x, y) is the intensity function representing a shape. It should be noted from Equation (5.2-1) that since the generalised moments are scalars calculated from the

original data without any transformation, they are not independent of size, position and orientation. In other words, when two sets of the generalised moments are calculated for two different shapes, if the sizes, positions and orientations of the objects in the images are different, it is impossible to compare the objects using the sets. To accomplish this task successfully it is necessary to make the moments invariant to these conditions. What should be done in the first step is to transform the generalised moments into the central moments which are moments about the means of the x and y coordinates. If all of the x and y coordinates of the shape are shifted so that its origin coincides with $(\bar{x}, \bar{y})$, where $\bar{x}$ and $\bar{y}$ are the mean values of the image coordinates x and y, respectively, this translation results in a set of central moments. The two mean values are calculated by applying Equation (5.2-1):

$$\bar{x} = \frac{m_{10}}{m_{00}}, \qquad \bar{y} = \frac{m_{01}}{m_{00}}, \tag{5.2-2}$$

where $m_{00} = \sum_{x} \sum_{y} x^0 y^0 f(x, y)$

$$= \sum_{x} \sum_{y} f(x, y)$$

represents the total number of pixels in the image; and m_{10} and m_{01} are the first order moments which are the summations of the x and y coordinates, respectively:

$$m_{10} = \sum_{x} \sum_{y} x^1 y^0 f(x, y) = \sum_{x} \sum_{y} x f(x, y),$$

$$m_{01} = \sum_{x} \sum_{y} x^0 y^1 f(x, y) = \sum_{x} \sum_{y} y f(x, y).$$

Replacing $x^p y^q$ with $(x - \bar{x})^p (y - \bar{y})^q$ in Equation (5.2-1) results in the central moments μ_{pq}:

$$\mu_{pq} = \sum_{x} \sum_{y} (x - \bar{x})^p (y - \bar{y})^q f(x, y). \tag{5.2-3}$$

Equation (5.2-3) is usually called the central moment generation function. By applying the central moment generation function the central moments are expressed in terms of the ordinary moments for the first four orders (Hu, 1962):

$$\mu_{oo} = m_{oo} = n,$$

$$\mu_{10} = \mu_{o1} = 0,$$

$$\mu_{20} = m_{20} - n\bar{x}^2,$$

$$\mu_{11} = m_{11} - n\bar{x}\bar{y},$$

$$\mu_{02} = m_{02} - n\bar{y}^2,$$

$$\mu_{30} = m_{30} - 3m_{20}\bar{x} + 2n\bar{x}^3,$$

$$\mu_{21} = m_{21} - m_{20}\bar{y} - 2m_{11}\bar{x} + 2n\bar{x}^2\bar{y},$$

$$\mu_{12} = m_{12} - m_{02}\bar{x} - 2m_{11}\bar{y} + 2n\bar{x}\bar{y},$$

$$\mu_{03} = m_{03} - 3m_{02}\bar{y} + 2n\bar{y}^3.$$

The central moments are invariant only to the locations of the images. In the second step, by using the second- and third-order central moments the seven low-order invariant moments are known to be obtained. It is obvious that the invariant moments are functions of the central moments. The invariant moments proposed by Hu (1962) are:

$$M1 = \mu_{20} + \mu_{02},$$

$$M2 = (\mu_{20} - \mu_{02})^2 + 4\mu_{11}^2,$$

$$M3 = (\mu_{30} - 3\mu_{12})^2 + (3\mu_{21} - \mu_{03})^2,$$

$$M4 = (\mu_{30} + \mu_{12})^2 + (\mu_{21} + \mu_{03})^2,$$

$$M5 = (\mu_{30} - 3\mu_{12})(\mu_{30} + \mu_{12})[(\mu_{30} + \mu_{12})^2 - 3(\mu_{21} + \mu_{30})]^2$$
$$+ (3\mu_{21} - \mu_{03})(\mu_{21} + \mu_{03})[3(\mu_{30} + \mu_{12})^2 - (\mu_{21} + \mu_{03})^2],$$

$$M6 = (\mu_{20} - \mu_{02})[(\mu_{30} + \mu_{12})^2 - (\mu_{21} + \mu_{03})^2]$$
$$+ 4\mu_{12}(\mu_{30} + \mu_{12})(\mu_{21} + \mu_{03}),$$

$$M7 = (3\mu_{21} - \mu_{03})(\mu_{30} + \mu_{12})[(\mu_{30} + \mu_{12})^2 - 3(\mu_{21} + \mu_{03})^2]$$
$$- (\mu_{30} - 3\mu_{12})(\mu_{21} + \mu_{03})[3(\mu_{30} + \mu_{12})^2 - (\mu_{21} + \mu_{03})^2].$$

Hu (ibid.) has shown that the first six moments M1 through to M6 are invariant under rotation, while the seventh moment M7 is useful in distinguishing mirror images. This method has been used to accomplish pattern identification independently of position, size and orientation. Hall et al. (1975) have applied the method of moments to classify the radiographs of coal workers. In this study, only central moments were used, since it was determined that translation invariance was desirable, but size and rotation invariance was undesirable. Also, the moment computation was limited to the set of second order moments. Dudani et al. (1977) have also applied this method to an automatic recognition of aircraft types, using plastic models, from optical images. In this study, all of the seven invariant moment functions, M1 through to M7, were used. They found that it was difficult to arrive at any meaningful results regarding the relationship of recognition accuracy to the number of aircrafts in the given class because of the fact that similarity or dissimilarity in shapes of aircraft under consideration greatly affected the recognition accuracy. Smith and Wright (1971) have undertaken a study to determine the feasibility of the automatic interpretation of ship photographs using the method of moments. They used the invariant moments of up to the fifth order in their automatic identification system. Alt (1962) carried out the automatic recognition of printed characters employing the invariant moments from the third to the sixth order and demonstrated that a small number of moments is adequate to characterise certain patterns and discriminate among the patterns of a certain set, such as alphabetical and numerical characters. He explained the difficulty of deciding the number of moments and choosing the proper order among the moments in his

project was due to the fact that the effectiveness of the process of classification depends strongly on the order in which different moments are introduced. Hu (ibid.), who proposed the method of moments, has undertaken the representation of the printed characters on the two-dimensional space using the first and second order invariant moments to demonstrate the suitability of his method for its application to the classification of patterns. There have been lots of applications of this method to pattern classification as previously introduced. However, the important fact to be noted is that the number of different moments and the orders of the moments employed in those applications were different to each other. From this approach, one obvious question is how many different moments and which order of the moments should be selected to distinguish significantly different patterns? This question reveals that this method has some deficiency in its generality; generality being a desirable condition. It will be shown that this is a major problem with this method. White and Prentice (1988), in their study of discriminating leaf outlines, pointed out the problem that since this method summarised mainly the overall shape, it is difficult to interpret the result. Another criticism by Rohlf and Archie (1984) is that, using this approach, one cannot easily reconstruct an image from the descriptors.

Another approach to extracting a finite set of numerical features from a shape is the Fourier descriptor, first suggested by Cosgriff (1960). The main idea of this approach is that look-alike shapes are usually near each other in a space of Fourier descriptor features endowed with the Euclidian metric (Zahn & Roskies, 1972). The basic principle in this method is to

156

transform a continuous function f(x) into the Fourier integral F($\mathcal{F}$), which is called the Fourier transform of f , defined by the equation (Brigham, 1974):

$$F(\mathcal{f}) = F(\omega) = \int_{-\infty}^{\infty} f(x) \exp(-j2\pi\omega x)\, dx,$$

(5.2-4)

where $j = (-1)^{1/2}$. Before looking into this method in detail, consider the obvious question; What kind of factors make it possible to apply the Fourier transform to the image analysis? Let us consider some brief answers:

(1)   The first immediate factor would be that the closed curve of an object extracted from an image usually consists of a very complex form which cannot be transformed into an ordinary mathematical equation.

(2) The second factor will be that the Fourier transform frequency domain contains exactly the same information as that of the original function; they differ only in the manner of presentation of the information.

(3) The third factor which is very relevant to this inquiry can be found out from the properties of the two-dimensional Fourier transform described by Brigham (1974):

   (i) the translation property,

   (ii) the scaling property,

   (iii) the rotation property.

   (iv) the periodicity property.

These properties are thought to be closely related to the conditions which should be considered at the initial stage of describing the features of a shape independent of position, size and orientation as previously illustrated.

(4) Finally, once a function is transformed, the graphical form of the transformed function usually looks so different from that of

157

the original one that it is difficult to imagine the graphical form of the original function. However, when the Fourier transform of a function is given, the original function can be easily obtained by using the inverse Fourier transform (Brigham, 1972):

$$\mathbf{F}^{-1}\{\ \mathcal{F}\ \} = f(x) = \int_{-\infty}^{\infty} F(\omega) \exp(j2\pi\omega x)\ d\omega.$$

(5.2-5)

Replacing f(x), -j and dx in the right most part of Equation (5.2-4) with F(ω), j and dω, respectively, results in Equation (5.2-5). This shows the ease of obtaining the inverse. In fact, this is a very important property that enables a wide range of applications in the image processing domain. This property is in contrast to that of the method of moments. In practice, the Fourier transform of f in Equation (5.2-4) is a periodic function, sines and cosines, since the exponential term is expressed in the form:

$$\exp(-j2\pi\omega x) = \cos(2\pi\omega x) - j\sin(2\pi\omega x),$$

so it is not easy to imagine the graphical form of the original function with that of the transformed function. It is known that the Fourier transform of a real function f is generally complex, that is,

$$F(\omega) = R(\omega) + jX(\omega) = |F(\omega)|e^{j\phi(\omega)}$$

(5.2-6)

where R(ω) is the real component of F(ω),

X(ω) is the imaginary component of F(ω),

$|F(\omega)|$ is called the Fourier spectrum of f(x),

$\phi(\omega)$ is called the phase spectrum or phase angle of F(ω).

$|F(\omega)|$ can be denoted by $[R^2(\omega) + X^2(\omega)]^{1/2}$, $\phi(\omega)$ can be denoted by $\tan^{-1}(X(\omega)/R(\omega))$. The variable ω in the Fourier transform is often called the frequency variable. If f(x) is a one-dimensional discrete function, the one-dimensional discrete Fourier transform of f and its inverse function are given by (Brigham, 1972):

158

$$F(\omega) = \frac{1}{N} \sum_{x=0}^{N-1} f(x) \exp(-j2\pi\omega x/N) \quad , \tag{5 2-7}$$

for $\omega = 0, 1, 2, 3, \dots, N-1$, and $F(0)$, $F(1)$, $F(2)$, $\dots$, $F(N-1)$ are called the Fourier coefficients. In each of the coefficient calculations all the values of $f(x)$ are involved.

$$f(x) = \sum_{\omega=0}^{N-1} F(\omega) \exp(j2\pi\omega x/N) \tag{5.2-8}$$

for $x = 0, 1, 2, 3, \dots, N-1$.

In practice, images are typically digitised in square arrays, the two-dimensional discrete Fourier transform of $f(x, y)$ and its inverse function are:

$$F(u, v) = \frac{1}{N} \sum_{x=0}^{N-1} \sum_{y=0}^{N-1} f(x, y) \exp(-j2\pi(ux + vy)/N) \tag{5.2-9}$$

for $u, v = 0, 1, 2, 3, \dots, N-1$, and

$$f(x, y) = \frac{1}{N} \sum_{u=0}^{N-1} \sum_{v=0}^{N-1} F(u, v) \exp(j2\pi(ux + vy)/N) \tag{5.2-10}$$

for $x, y = 0, 1, 2, 3, \dots, N-1$.

Another important factor, although, which is not directly related to the description, is that when random noise corrupts the image signal during transmission through channels, the pixels in the image $f(x, y)$ are highly correlated but the elements of $F(u, v)$ are decorrelated (Huang & Schultheiss, 1963).

Thus far, the background and general aspect of the Fourier transform have been considered. Let us have a close look at the practical aspects of the Fourier descriptor of a shape from the definition to the procedure including the normalisation of the Fourier coefficients. The Fourier descriptor is clearly defined by Wesley et al. (1990):

"A closed curve may be represented by a periodic function of a continuous parameter, or alternatively, by a set of Fourier

159

coefficients of this function. The coefficients in this collection are referred to as 'Fourier descriptors'. The Fourier descriptors provide a means for representing the boundary of a two-dimensional shape."

In general, it is difficult to use the ordinary Fourier coefficients as input to a classifier because they contain factors dependent upon size, orientation, and starting point. In order to make the Fourier coefficients invariant to the size, orientation, and starting point of a contour it is necessary to perform a normalisation in the Fourier domain. Such Fourier-domain normalisation was initially developed by Granlund (1972). The procedure developed by him is as follows.

Consider a closed contour C in the complex plane as shown in Figure 5.2.
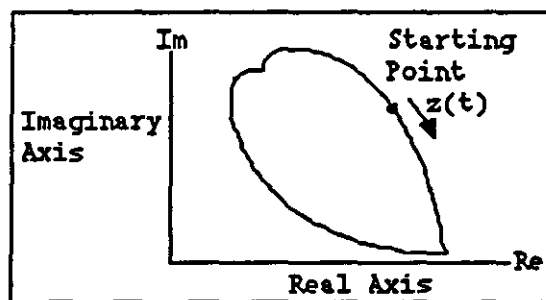
Figure 5.2 Contour function z(t).

Trace the contour from an arbitrary point in the clockwise direction at a constant speed v, and simultaneously, pick at every time t a complex number z, then the contour function is defined by

$$z = z(t), \qquad\qquad (5.2\text{-}11)$$

where the parameter t means a parameter of length along the contour. Choose v so that $T = 2\pi$. Traversing the contour more than once yields a periodic function:

$$z(t + nT) = z(t). \qquad\qquad (5.2\text{-}12)$$

160

T can be expressed as a complex Fourier series The Fourier descriptor of C is the complex Fourier series expansion of $z(t)$,

$$z(t) = \sum_{n=-\infty}^{\infty} F(\omega)e^{jnt} ,$$

(5.2-13)

where

$$F(\omega) = \frac{1}{2\pi} \int_{0}^{2\pi} z(t) e^{-jnt} dt .$$

(5.2-14)

This Fourier descriptor depends upon both the contour C and the starting point of $z(t)$. Since the contour C is in practice taken from a digitised image, $z(t)$ is not expressed as a continuous function. The normalisation process consists of translation, rotation, and change of scale. It is assumed that $F(\omega)^{*}$ is a specific set of Fourier coefficients from the original contour, and $Z(t)^{*}$ is the inverse of $F(\omega)^{*}$.

(a) Translation

The translation of a contour $Z(t)^{*}$ with the complex vector Z results in the following (Brigham, 1972):

$$Z(t) = Z(t)^{*} + Z = \sum_{-\infty}^{\infty} Z(t)^{*} e^{jnt} + Z.$$

The Fourier transform of the translated contour is expressed by:

$$F(\omega) = \begin{cases} F(\omega)^{*}, & \text{for } \omega \neq 0, \\ F(\omega)^{*} + Z, & \text{for } \omega = 0. \end{cases}$$

(5.2-15)

All coefficients except $F(0)$ are not dependent upon translation, $F(0)$ is simply the complex vector indicating the position of the centre of gravity of a contour.

(b) Rotation

To rotate a contour in the spatial domain simply requires multiplying $Z(t)^{*}$ by $e^{j\theta}$ (Brigham, 1972):

$$Z(t) = Z(t)^{*} e^{j\theta}$$

161

where θ is the angle of rotation. Due to linearity, the Fourier transform of the rotated contour is:

$$F(\omega) = F(\omega)^* e^{j\theta}. \qquad (5.2\text{-}16)$$

(c) Change of Scale

To change the scale of the contour, each of the Fourier coefficients is simply multiplied by a constant S (Brigham, 1972):

$$F(\omega) = SF(\omega)^*. \qquad (5.2\text{-}17)$$

(d) Change of a Starting Point

There are many different sets of Fourier coefficients for a certain contour depending upon the position of a starting point. The Fourier coefficients differ from one another with respect to a parameter τ. Assume that there exists a certain function

$$Z(t) = Z(t)^*$$

and, subsequently, the lower functions are given by

$$Z(t) = Z(t + \tau)^*.$$

The resulting Fourier coefficients become (Brigham, 1972):

$$F(\omega) = \frac{1}{2\pi} \int_0^{2\pi} Z(t + \tau)^* e^{-jnt} \, dt$$

$$= e^{jn\tau} \frac{1}{2\pi} \int_0^{2\pi} Z(t)^* e^{-jnt} \, dt$$

$$= e^{jn\tau} F(\omega)^*. \qquad (5.2\text{-}18)$$

When Equations (5.2-15) through to (5.2-18) are combined together, the general form for the Fourier transform of a contour which is invariant to translation, orientation, scale and starting point is given by (Granlund, 1972):

$$\begin{cases} F(\omega) = F(\omega)^* e^{jn\tau} S e^{j\theta}, & \text{for } \omega \neq 0, \\ F(\omega) = F(\omega)^* e^{jn\tau} S e^{j\theta} + Z, & \text{for } \omega = 0. \end{cases} \qquad (5.2\text{-}19)$$

162

In practice, when a point is selected during tracing the contour in Figure 5.2, a vector (x, y) is obtained. The x and y are, respectively,

$$\begin{cases} x = \mathrm{Re}\, Z(t), \\ y = \mathrm{Im}\, Z(t). \end{cases}$$

The computation of the Fourier coefficients of Re Z(t) and Im Z(t) is performed as follows (Granlund, 1972):

$$F(\omega) = \frac{1}{T}\int_0^T Z(t)\exp(-jn2\pi t/T)\,dt$$

$$= \mathrm{Re}\, F(\omega) + j\cdot\mathrm{Im}\, F(\omega),$$

where

$$\mathrm{Re}\, F(\omega) = \frac{1}{T}\int_0^T [\,\mathrm{Re}\, Z(t)\cos(n2\pi t/T) + \mathrm{Im}\, Z(t)\sin(n2\pi t/T)\,]\,dt,$$

$$(5.2\text{-}20)$$

$$\mathrm{Im}\, F(\omega) = \frac{1}{T}\int_0^T [\,\mathrm{Im}\, Z(t)\cos(n2\pi t/T) + \mathrm{Re}\, Z(t)\sin(n2\pi t/T)\,]\,dt.$$

$$(5.2\text{-}21)$$

Thus, the Fourier descriptor of a contour is obtained by applying Equations (5.2-20) and (5.2-21). Finally, to make the Fourier descriptor invariant to translation, orientation, scale and starting point apply Re F(ω) and Im F(ω) to Equation (5.2-19), respectively. At last, the Fourier descriptor obtained is ready to be used. The important fact to be noted here is that the previous procedure involving high level mathematical calculations of exponents of complex numbers, trigonometry and integrations obtains a N x 2 vector. This only contains a set of (u, v) coordinates in a two-dimensional Fourier plane for a certain contour. If the objective of a task is only boundary coding or reconstruction of a shape, a result is obtained but it requires unnecessarily time-consuming

163

effort. On the other hand, if the objective of a task is object identification, it is only the beginning of the task, although much effort has been involved in the procedure. It is necessary to extract some values such as maximal diameter of a shape, area, some angles, and perimeter length etc. from the vector for the object identification procedure. The majority of researchers who apply this approach use it mainly for shape description, since it is their final objective. Granlund (1972) has carried out the description of the shape of hand printed characters to validate the normalisation algorithm he developed. Rohlf and Archie (1984) have performed the description of the wing shape of mosquitoes applying this methods. Bookstein et al. (1982) have pointed out that a change in part of a shape (a 'local change') may result in changes in the values of many of the coefficients making them more complicated. It is obvious that the drawback of this approach is:

(1) The algorithm is simple, but not familiar to the designer and programmer because of several complex mathematical equations.

(2) This approach requires a large amount of computing time.

(3) It is not easy to modify some parts of the procedure when the results of an implementation are different to that expected.

The previous approaches are based on the description of a shape by means of scalars. The descriptors, as have already been discussed, have taken the form of numerical measures of the shape rather than representing symbolic features. From now on, the investigation of the description of a shape will focus on external space domain techniques. One of the techniques is the chain coding technique. This method was introduced by Freeman (1961) and has been, to date, widely used to describe a

shape. In this method, an arbitrary geometric contour is encoded so as to facilitate its analysis and manipulation by means of a digital computer. He has also proposed algorithms for normalisation to expand and rotate a given contour, and to redefine a starting point. As an illustration of the procedure developed by Freeman, consider the boundary of Figure 5.3.(b) drawn in the x-y plane. Trace the boundary from the point A in the clockwise direction and assign one of the directions in Figure 5.3.(a) to each segment connecting every pair of pixels.
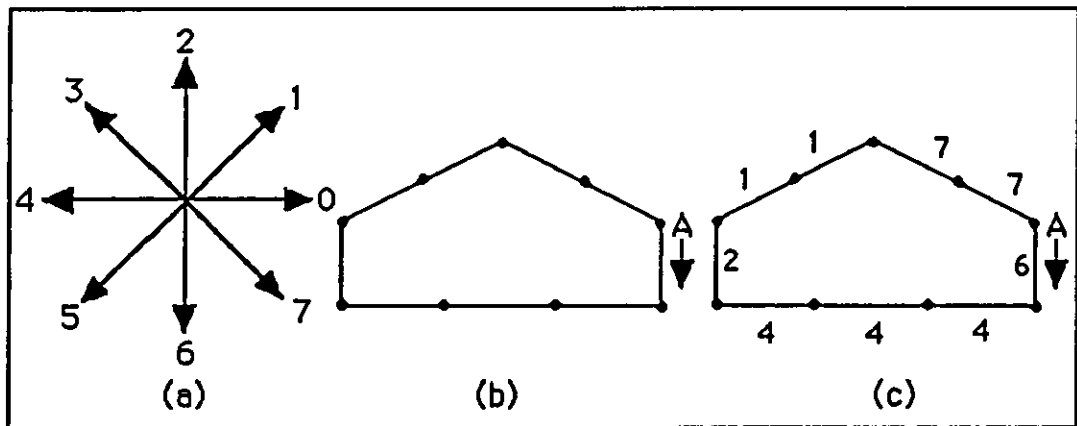
Figure 5.3 Chain code. (a) 8-directional chain code. (b) A boundary. (c) A chain coded boundary.

For a rectangular grid, if a point on a boundary is known, the next point will be only one of eight neighbours. If the decimal digits zero through to seven are assigned to these eight positions, starting with the one which is horizontally to the right and processing in a counter-clockwise direction, the code of Figure 5.3.(a) is obtained. Whenever a new segment is met during the tracing, select a proper direction which is approximately the same direction as the segment and assign it to the segment. The result of assigning directions is shown in Figure 5.3.(c) and is represented by the coded sequence:

165

6 4 4 4 2 1 1 7 7.

This sequence is called a chain code. The code can be represented in binary form:

110 100 100 100 010 001 001 111 111.

The important thing to be noted is that each code requires only three bits to specify. Freeman has argued that the required memory capacity for a continuous contour encoded in this way is then only 15 percent of that required for a contour which has all its points independently specified in a 1024 x 1024 point array. This is obviously one of the advantages of this method; it saves memory space. In this approach, there are some normalisation techniques for manipulating contours invariant to translation, scale, orientation and starting point.

(a) Expansion

A chain coded contour stored in the memory of a digital computer can be expanded without any difficulty. To expand a contour by a ratio N, each of the digits of the contour must be replaced by a set of N identical digits, where N should be an integer. For example, if the contour in Figure 5.3.(c) is to be expanded exactly twice the size, the expanded contour is given by the chain code:

6 6   4 4 4 4 4 4   2 2   1 1 1 1   7 7 7 7.

(b) Rotation

It is known that one of the advantages of the chain coding technique is to rotate a contour easily. The procedure of the rotation of a contour is to add any even number n to each of the digits in the decimal representation of a contour and divide the digit by 8, then the remainders of the calculation are the result.

166

The result is a rotation of 90° in a counter-clockwise rotation. The addition or subtraction of any even number n will cause a rotation equal to (n/2) x 90°. If '1' is added to each digit, a rotation of 45° is achieved; however, this rotation is nearly always accomplished with distortion. The main reason for the distortion (Freeman, 1961) is that in rotation by this approach only the angle is considered. In general, both the angle and the distance between the axis of rotation and each point of the contour are important parameters in the rotation of a contour. However, in this approach only one parameter, i.e. angle is considered. This obviously reveals the limitation of this approach.

(c) Translation

One of the important features of the chain coding technique is shifting a contour with ease. Each point on a curve is located relative to the previous one, thus, if the (x, y) coordinates of a starting point are determined on an x-y plane, the (x, y) coordinates of each of the remaining points are relatively determined. To shift a contour vertically or horizontally, only the (x, y) coordinates of the first point are required changing.

(d) Changing of Starting Point

The chain code obtained from a boundary depends upon the starting point. The procedure for normalising the code is very simple, that is, consider the code as a circular sequence of direction numbers and redefine the starting point in order to obtain the sequence of numbers having the minimum value. As an illustration, consider the chain code for Figure 5.3.(c). The original chain code is 6 4 4 4 2 1 1 7 7. To obtain the normalised code redefine the starting point and find the minimum magnitude:

167

6 4 4 4 2 1 1 7 7 (the original code)

4 4 4 2 1 1 7 7 6

4 4 2 1 1 7 7 6 4

4 2 1 1 7 7 6 4 4

2 1 1 7 7 6 4 4 4

1 1 7 7 6 4 4 4 2 (the normalised code)

1 7 7 6 4 4 4 2 1

7 7 6 4 4 4 2 1 1

7 6 4 4 4 2 1 1 7.

Since the string 1 1 7 7 6 4 4 4 2 has the minimum magnitude, it is the normalised code. Note that the computing time for this process mainly depends upon the length of the string. If the magnitude of a string exceeds the maximum number allowed in a computer, this process suddenly becomes complicated.

Marshall (1989) has pointed out some of disadvantages of this approach. The primary disadvantage of this code is that it is sensitive to noise as errors are cumulative, i.e., if one bit is in error, the remainder of the curve will be incorrectly reconstructed from the code. Another disadvantage pointed out by him is that the value of this code for recognition purposes is limited in this form. However, this approach has been widely used in the domain of boundary description.

Three shape-description methods have been investigated in detail. During the investigation the advantages as well as disadvantages of each method have been thoroughly considered. The important fact to be noted is that in all the approaches the final output is not features which can be directly used in the shape identification process, but the vector of a contour invariant

168

to the starting point, scale, translation and orientation of the contour. The vector obtained usually needs further processing to extract some features that are traditional measures, such as the length of an object, maximum width, perimeter length, ratios, angles, etc., which are frequently used by biologists attempting to quantify shape variation patterns. Apart from the advantages or disadvantages of these methods, none of them takes this aspect into account at all. The main reason is that the features required in the object identification process depend upon the kind of objects and domain. For instance, the features that have been used in the leaf species identification are completely different from those in fish species identification.

5.3 NEW SHAPE DESCRIPTION METHOD.

5.3.1 The Background and Basic Principle of this Method.

The foregoing section has clearly shown that the three existing shape description methods produce a vector, as a result of a complex process, which contains information only about the boundary of an object. The vector is invariant to location, scale, orientation and starting point factors. The vector produced by the Fourier descriptor or chain code cannot directly be used in the object identification process. In this section, a new shape description method will be introduced. The important facts that have been considered in the design stage are as follows:

(1) The shape descriptor should be created on a similar basis to that of object discrimination in human vision.

(2) The shape descriptor should be easily interpreted not only by visual assessment, but also by systematic methods.

(3) With a simple procedure, the shape descriptor which is independent of location, scale, orientation and starting point of a contour should be easily obtained.

(4) A reflected image (a mirror image) should be processable.

(5) The shape descriptor should be directly involved in the object identification procedure without any additional modification.

(6) The shape descriptor should be used as input data to the multivariate statistical analysis procedure for further study.

As an illustration of object identification using usual judgment, consider the objects in Figure 5.4. It is assumed that the major interest lies in the shapes of the objects without considering their size. When the shapes in Figure 5.4 are viewed

170

without any prejudice, it is easily recognised by human vision that the objects on the left-hand side have symmetrical shapes and those on the right-hand side asymmetrical shapes. It seems that the yardstick for this judgment would be the dotted line overlapped on the centre of each shape in the mind of the viewer. In the case of the objects on the left-hand side, each dotted line might divide the boundary into two curves. Then, the curves could be compared to each other top to bottom as shown in Figures 5.5.(a) and (c).
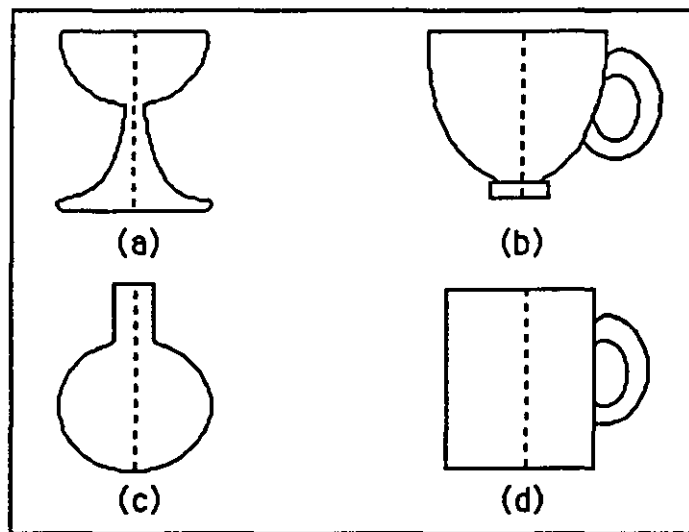
Figure 5.4 Objects shapes from the lateral view.

Since each pair of horizontal line segments have equal distances, it can be concluded that the objects have symmetrical shapes. On the other hand, in the case of the objects on the right-hand side, some pairs of horizontal line segments around the handle part differ from each other in length as shown in Figures 5.5.(b) and (d), hence it can be concluded that the objects have asymmetrical shapes. Let us consider a way of distinguishing symmetrical objects with different shapes. The objects in Figures 5.4.(a) and (c) have symmetrical shapes but are different from each other. A

171

property of the shape in Figure 5.4.(a) is that the area of the upper half is undoubtedly greater than that of the lower half. On the other hand, a property of the shape in Figure 5.4.(c) is in contrast to that of the shape in Figure 5.4.(a), i.e., the area of the lower half is greater than that of the upper half. These properties can obviously be used to distinguish the shape from each other.
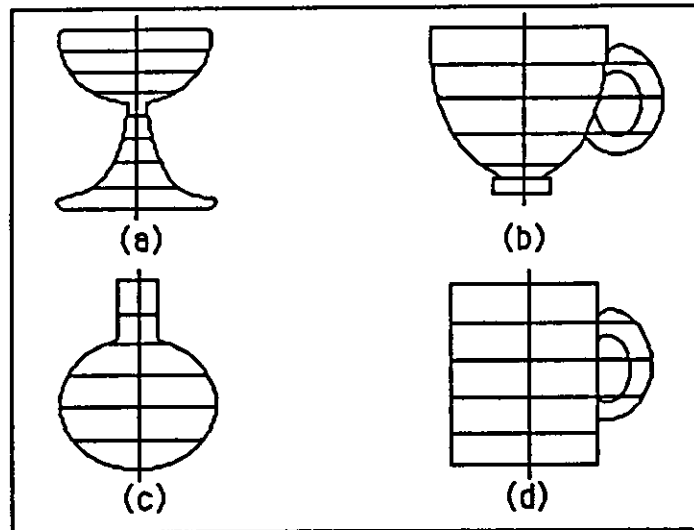
Figure 5.5 Comparison of each pair of horizontal line segments.

This can be quantified by calculating the area of each segment as shown in Figure 5.6. The straight line PQ in Figure 5.6 is an axis which divides the boundary into two curves of the same shape and the straight line MN is a perpendicular line to the line PQ at the middle point of the line PQ. Let the areas of the segments in Figure 5.6.(a) be S1, S2, S3 and S4, respectively; and the areas of the segments in Figure 5.6.(b) be R1, R2, R3 and R4, respectively. In fact, since the area of the object in Figure 5.6.(a) is different from that of the object in Figure 5.6.(b), it is meaningless to compare the two objects by the areas. Note that each object has a symmetrical shape, so it will be reasonable to consider one of the

172

curves for each object. Thus, to make the comparison, consider the ratios r11, r12, r21 and r22 defined by:

$$r11 = \frac{S1}{S1 + S2}, \qquad r12 = \frac{S2}{S1 + S2},$$

$$r21 = \frac{R1}{R1 + R2}, \qquad r22 = \frac{R2}{R1 + R2}, \tag{5.3.1-1}$$

where r11 is a ratio of the area of the upper half of the curve bounded by PQ over the area ⎯ of the curve bounded by PQ, r12 is that of the area of the lower half of the curve bounded by PQ over the area of the curve bounded by PQ, for the object in Figure 5.6.(a); and r21 and r22 are ratios for the object in Figure 5.6.(b).
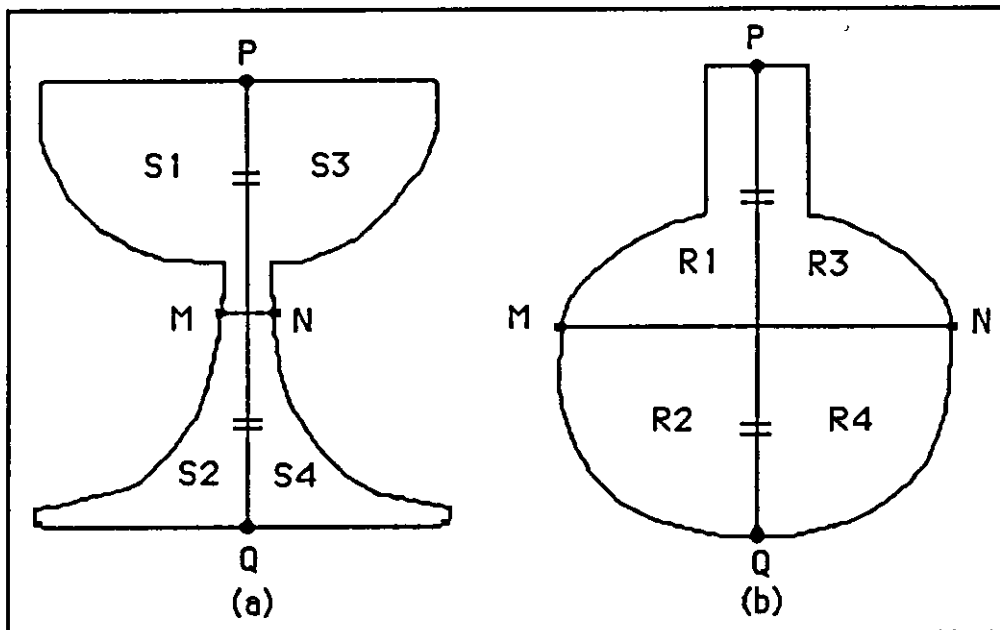
Figure 5.6 Areas of segments.

In the identification process, r11 is compared with r21 and r12 with r22. This method seems plausible for comparing shapes, since the ratios are independent of the scale, orientation, location and starting point of the contour of each object. However, taking a close look at the properties of the ratios gives rise to a further enhancement of the comparison process. As an illustration of this

173

fundamental problem, consider the two hypothetical objects that are different in shape as shown in Figure 5.7. Assume that each small box in the object is a unit square. As before, only the left half of each object is considered. Each area of the segment is: S1 = 2, S2 = 4, R1 = 4 and R2 = 8. The ratios r11, r12, r21 and r22 are respectively calculated by the following:

$$r11 = \frac{2}{2+4} = \frac{1}{3} \ , \quad r12 = \frac{4}{2+4} = \frac{2}{3} \ ,$$

$$r21 = \frac{4}{4+8} = \frac{1}{3} \ , \quad r22 = \frac{8}{4+8} = \frac{2}{3} \ .$$
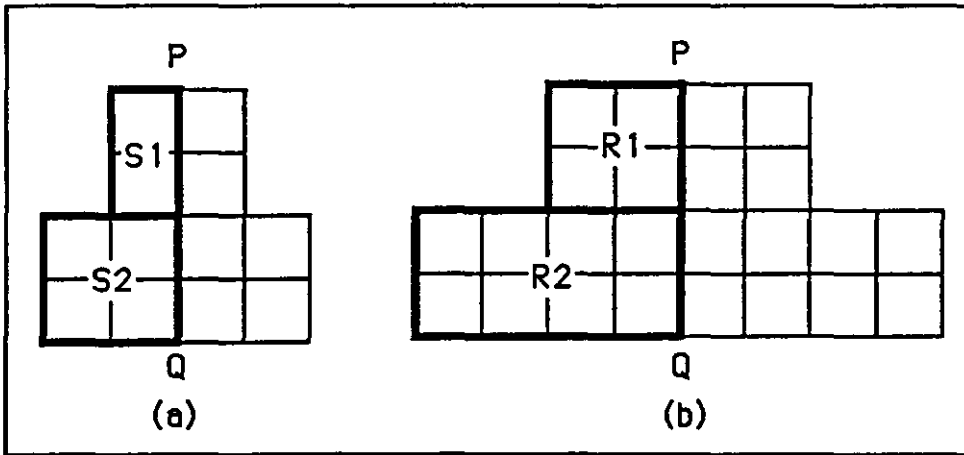
Figure 5.7 Areas of segments for hypothetical objects.

In the identification process, since r11 = r21 = 1/3 and r12 = r22 = 2/3, it can be concluded that the shape of the object in Figure 5.7.(a) is the same as that of the object in Figure 5.7.(b). However, in fact, the objects are completely different in shape, that is, the object on the left-hand side is thinner than that on the right-hand side although the ratios r11 and r12 are equal to r21 and r22, respectively. Consequently, it is obvious that the ratios obtained only from the areas cannot be used alone in the object discrimination process.

Thus, to discriminate the hypothetical objects in Figure 5.7,

174

the axis, the straight line PQ, should also be considered. The line PQ plays a major role in causing the ratios to form a close relationship with their respective objects. Suppose that A1 and A2 are defined by:

$$A1 = \frac{S1 + S2}{PQ^2}, \qquad A2 = \frac{R1 + R2}{PQ^2}, \qquad (5.3.1-2)$$

where A1 is a ratio of (S1 + S2) over PQ^2,

A2 is a ratio of (R1 + R2) over PQ^2

and PQ^2 is the area of a PQ x PQ square.

New ratios r11', r12', r21' and r22' are defined by:

$$r11' = A1 \times \frac{S1}{S1 + S2}, \qquad r12' = A1 \times \frac{S2}{S1 + S2},$$

$$r21' = A2 \times \frac{R1}{R1 + R2}, \qquad r22' = A2 \times \frac{R2}{R1 + R2}. \qquad (5.3.1-3)$$

Since the ratios r11', r12', r21' and r22' are properly linked with the $(axis)^2$, they can be involved in the discrimination process. This can be checked by carrying out the process with the practical data in Figure 5.8. The length of the axis PQ is 4 because the square is unity. The A1 and A2 are:

$$A1 = \frac{2 + 4}{4^2} = \frac{3}{8}, \qquad A2 = \frac{4 + 8}{4^2} = \frac{6}{8}.$$

Applying these values to Equation (5.3.1-3) results in:

$$r11' = A1 \times \frac{S1}{S1 + S2} = \frac{3}{8} \times \frac{2}{2 + 4} = \frac{1}{8},$$

$$r12' = A1 \times \frac{S2}{S1 + S2} = \frac{3}{8} \times \frac{4}{2 + 4} = \frac{2}{8},$$

$$r21' = A2 \times \frac{R1}{R1 + R2} = \frac{6}{8} \times \frac{4}{4 + 8} = \frac{2}{8},$$

$$r22' = A2 \times \frac{R2}{R1 + R2} = \frac{6}{8} \times \frac{8}{4 + 8} = \frac{4}{8}.$$

175

When r11' is compared with r21' and r12' with r22', it is concluded that the object in Figure 5.7.(a) is different in shape from that in Figure 5.7.(b) since r11' ≽ r21' and r12' ≽ r22'. In the process of the identification of the objects in Figure 5.6, Equations (5.3.1-2) and (5.3.1-3) can be efficiently used.
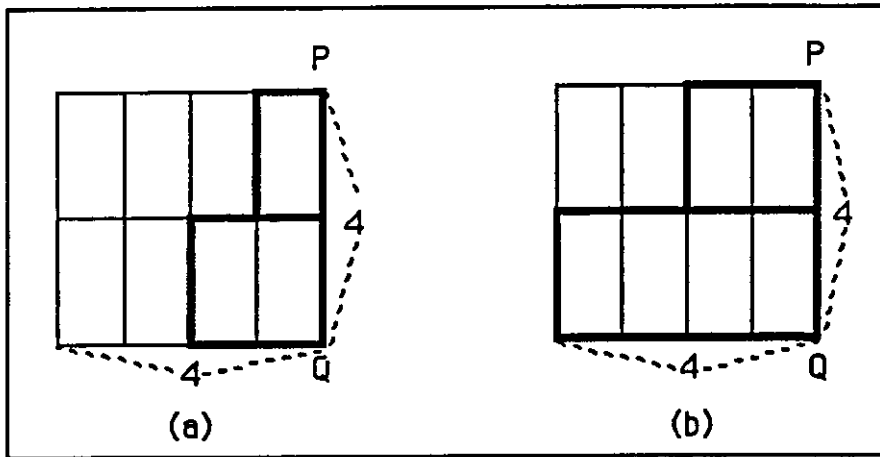
Figure 5.8 Reconstruction of the shapes using the components of shape descriptor.

Let us consider the effect of using the axis in the process by reconstructing the shapes of the objects in Figure 5.7. It is assumed that the reconstruction is limited to the left half of each shape. Firstly, draw two 4 x 4 squares as shown in Figure 5.8. Secondly, divide it into eight 2 x 1 rectangles. For the object in Figure 5.7.(a), since r11' = 1/8 and r12' = 2/8, select one rectangle on the extreme right of the upper half of the square and two rectangles on the right side of the lower half of the square. Performing a similar procedure results in reconstruction of the object in Figure 5.7.(b). The left half of each object has been reconstructed using the data of the axis, r11', r12', r21' and r22' as depicted in Figure 5.8. As the process has shown, the axis has played an important role in the shape description. Marr and

176

Nishihara (Marr & Nishihara, 1978) have also emphasised the necessity of an axis for the representation of a shape.

5.3.2 The Algorithm for this Method.

Thus far, the background and basic principles dominating the new shape description method developed in this thesis have been illustrated. Consider the algorithm for the general method which can be used in biological object identification in further detail. Usually, the shape of a biological object is too complex to be expressed in a mathematical formula. It is therefore essential to find a method which can replace mathematical formulation. The basic idea of this method is to transform a two-dimensional shape into a one-dimensional form, and to extract some descriptive elements, from this form. This is an alternative to mathematical formulation. In the dimensional transformation, the most important element is an axis. In an automatic system, it is a difficult task to define an axis. Thus, a straight line connecting two extreme points of a contour is usually regarded as an axis. For example, consider the contour in Figure 5.9.(a). The straight line connecting the two extreme points P and Q of the contour forms its axis. Another important element in the transformation are the ratios defined in equations (5.3.1-2) and (5.3.1-3). In the hypothetical-object identification in Figure 5.7, only two ratios for each segment have been used, however, if an object has a complex shape, the number of ratios should be increased. The accuracy of the identification depends upon the number of these ratios. The number of ratios is determined by the number of equal segments of an axis. For example, consider the segments in Figure 5.9. The axis PQ in Figure 5.9.(a) divides the contour into two

177

segments, one for the left-hand side, the other for the right-hand side. Their areas are respectively S_1 and S_2. This axis is divided into two equal segments as shown in Figure 5.9.(b). If a line perpendicular to PQ is drawn through the middle point of PQ, the contour is divided into four segments, where the areas of the segments are respectively S_{11}, S_{12}, S_{21} and S_{22}, i.e., S_{11} and S_{12} for the left-hand side, and S_{21} and S_{22} for the right-hand side. Dividing the axis in Figure 5.9.(C) into four equal segments results
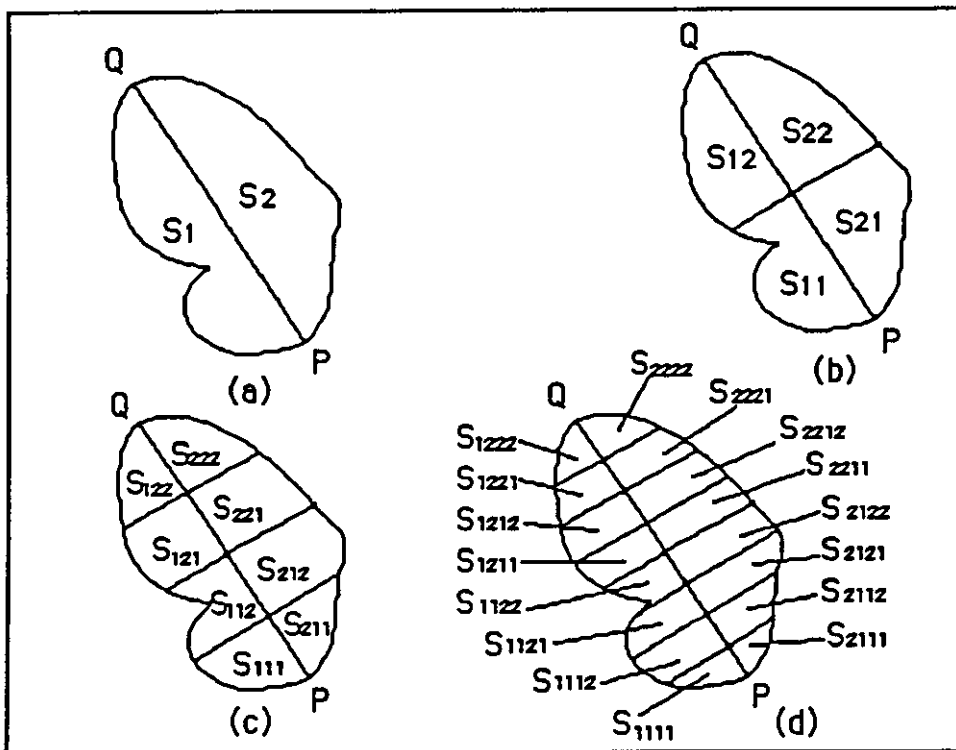
Figure 5.9 Contour segmentation.

in eight segments, where their areas are S_{111}, S_{112}, S_{121}, S_{122}, S_{211}, S_{212}, S_{221} and S_{222}, respectively. Further division of the axis will produce a large number of smaller segments. The ratio for each segment can be obtained as previously shown in Equations (5.3.1-2) and (5.3.1-3). The ratios for the segmentations in Figure 5.9.(a) are respectively:

178

$$r1 = A1 = \frac{S_1}{PQ^2}, \qquad r2 = A2 = \frac{S_2}{PQ^2}. \qquad (5.3.2\text{-}1)$$

The ratios for the segmentations in Figure 5.9.(b) are respectively:

$$r_{11} = A_1 \times \frac{S_{11}}{S_1}, \qquad r_{21} = A_2 \times \frac{S_{21}}{S_2},$$

$$r_{12} = A_1 \times \frac{S_{12}}{S_1}, \qquad r_{22} = A_2 \times \frac{S_{22}}{S_2}.$$

The ratios for the segments in Figure 5.9.(c) are respectively:

$$r_{111} = A_1 \times \frac{S_{111}}{S_1}, \qquad r_{211} = A_2 \times \frac{S_{211}}{S_2},$$

$$r_{112} = A_1 \times \frac{S_{112}}{S_1}, \qquad r_{212} = A_2 \times \frac{S_{212}}{S_2},$$

$$r_{121} = A_1 \times \frac{S_{121}}{S_1}, \qquad r_{221} = A_2 \times \frac{S_{221}}{S_2},$$

$$r_{122} = A_1 \times \frac{S_{122}}{S_1}, \qquad r_{222} = A_2 \times \frac{S_{222}}{S_2}.$$

The ratios for the segments in Figure 5.9.(d) are respectively:

$$r_{1111} = A_1 \times \frac{S_{1111}}{S_1}, \qquad r_{2111} = A_2 \times \frac{S_{2111}}{S_2},$$

$$r_{1112} = A_1 \times \frac{S_{1112}}{S_1}, \qquad r_{2112} = A_2 \times \frac{S_{2112}}{S_2},$$

$$r_{1121} = A_1 \times \frac{S_{1121}}{S_1}, \qquad r_{2121} = A_2 \times \frac{S_{2121}}{S_2},$$

$$r_{1122} = A_1 \times \frac{S_{1122}}{S_1}, \qquad r_{2122} = A_2 \times \frac{S_{2122}}{S_2},$$

$$r_{1211} = A_1 \times \frac{S_{1211}}{S_1}, \qquad r_{2211} = A_2 \times \frac{S_{2211}}{S_2},$$

179

$$r_{1212} = A_1 \times \frac{S_{1212}}{S_1}, \qquad r_{2212} = A_2 \times \frac{S_{2212}}{S_2},$$

$$r_{1221} = A_1 \times \frac{S_{1221}}{S_1}, \qquad r_{2221} = A_2 \times \frac{S_{2221}}{S_2},$$

$$r_{1222} = A_1 \times \frac{S_{1222}}{S_1}, \qquad r_{2222} = A_2 \times \frac{S_{2222}}{S_2}.$$

Consequently, the ratio for each segment can be obtained using the ratio A1 or A2, and area S1 or S2 and the area of the segment itself. After the ratios are obtained, the ratios can be represented in the tree-type hierarchical structure as shown in Figure 5.10.
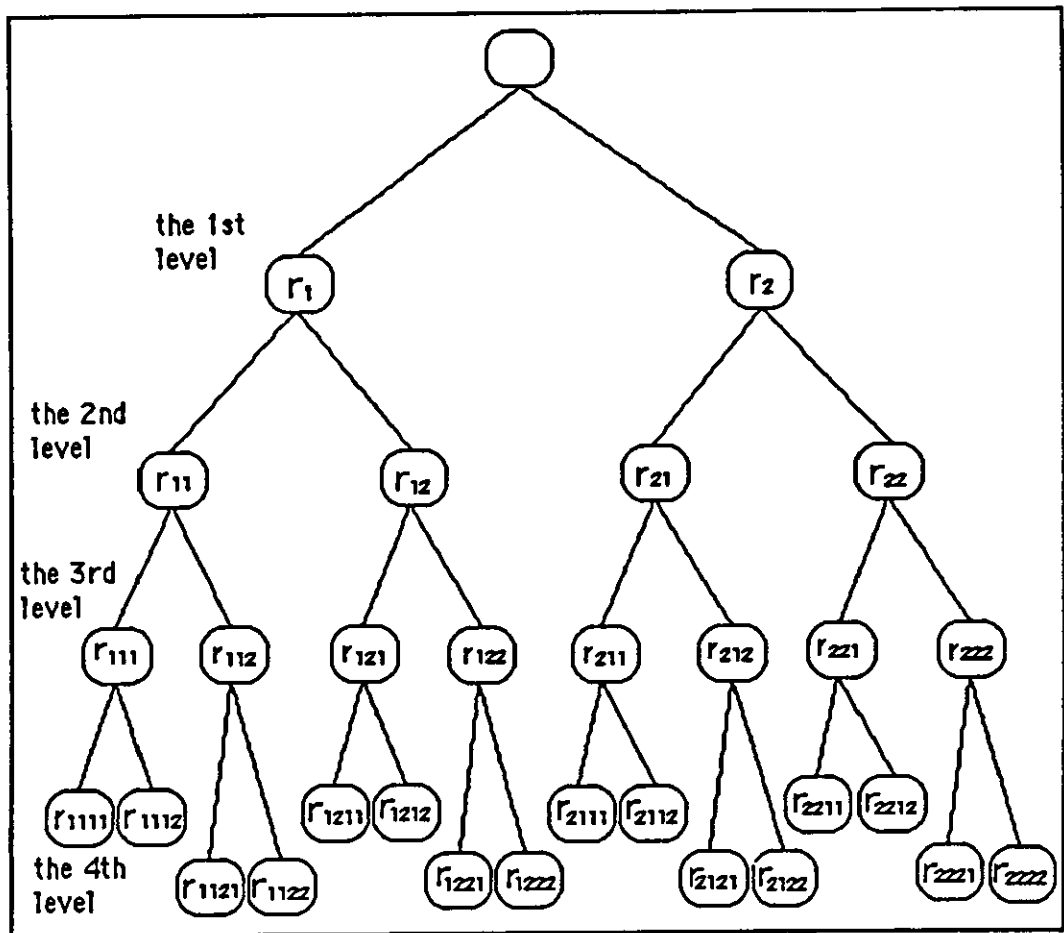
Figure 5.10 The tree of ratios.

In the object identification process, the ratio tree can be efficiently used. Let us take a close look at this process. When a new ratio tree is compared with the library data, the comparison is performed from the first level in Figure 5.10. Let a set of ratios in the library data be a set of d's and newly calculated ratios be r's. In the first level, if $r1 \neq d1$ or $r1 \neq d2$, it is concluded that the new object is different from the object in the library. On the other hand, if $r1 = d1$ and $r2 = d2$, the process moves to the second level. If $r11 \neq d11$, $r12 \neq d12$, $r21 \neq d21$ or $r22 \neq d22$, it is concluded that the object differs from that of the library in shape. Otherwise, i.e., $r11 = d11$, $r12 = d12$, $r21 = d21$ and $r22 = d22$, the process moves down to the next level, where a similar operation is undertaken. This process is a top-down method; alternatively if the process is performed from the lowest level, it becomes a bottom-up method. Either method can be employed depending upon the situation. As far as the result is concerned, there will be no difference between the methods. However, the main difference will be in computing time. If the majority of the objects under consideration have completely different shapes, the top-down method will be quicker. This is because most of the results can be obtained in the upper levels. On the other hand, if the majority of the objects have very similar shapes, the bottom-up method will be better. The reason is that in most cases when the top-down method is adopted, the dissimilarity is determined around the bottom level.

Let us focus on the library data for biological objects. For example, in a species of butterfly there will be some variation among the shapes of butterflies. When the library data are built, this variation should be considered. In image analysis, this

181

variation is usually called a tolerance. This tolerance should be considered at every level of the ratio tree in Figure 5.10. If the variation for each ratio is obtained, each node of the ratio tree in the library data will have upper and lower limits of a ratio. In the object identification process, the comparison is performed using the upper, lower limits and newly obtained ratio. In the first level, if $d_1^L < r_1 < d_1^U$ and $d_2^L < r_2 < d_2^U$, the process moves down to the next level; otherwise, it is determined that the new object has a different shape, where d_i^L represents the lower limit and d_i^U the upper limit.

Additionally, consider how to identify the shape of a reflected image (a mirror image). In this method, the task can be easily accomplished using the ratio tree. In the first level, if $d_1^L < r_2 < d_1^U$ and $d_2^L < r_1 < d_2^U$, the process moves down to the next level; otherwise, it is determined that the new object has a different shape. This process only differs from the previous process, in the comparison of ratios. The ratio r1 is replaced by the ratio r2, and vice versa.

In practice, how can an axis and the ratio, which play a major role in object identification, be obtained?

5 3.2.1 Detecting a Principal Axis.

Firstly, note the procedure for searching a principal axis. The simple traditional method to obtain the axis of a contour consisting of N points is as follows:
(i) For each point in a contour, calculate distances from the point to the other points in the contour, and select two points forming

the longest distance.

(ii) N longest distances were obtained in the step (i). Select the maximum distance from the N longest distances.

In this method, the number of distances calculated is N(N-1). Let us consider the number of distance calculations using the nine points in Figure 5.11.(a). For the point A, eight distances of the solid lines will be calculated, and for the point B, another eight distances of the dotted lines will be calculated. Likewise, this calculation will be repeated for the other seven points. The number of distances calculated in this case is 9 x (9-1) = 72.
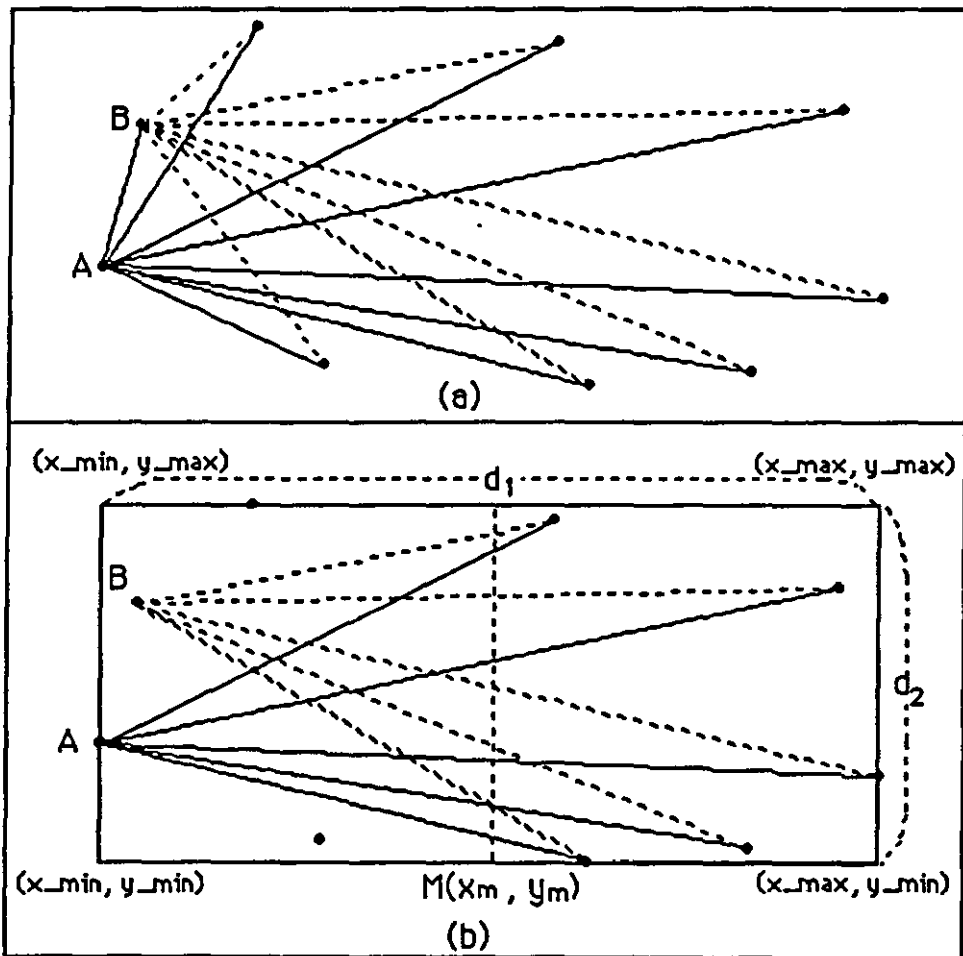
Figure 5.11 Calculations of distances for finding a diameter.

The more efficient method, which was devised in this thesis, to obtain the axis of a contour is as follows:

(1) Draw the smallest circumscribing rectangle whose sides are chosen to be parallel to the coordinate axes as shown in Figures 5.12.(a) and (b).

(2) Select the longer side of the rectangle and find the middle point of the side.

(3) Divide the contour into two curves using the x- or y-coordinate of the middle point. If the longer side is parallel to the x-axis as shown in Figure 5.12.(a), the x-coordinate should be used; otherwise, as shown in Figure 5.12.(b), the y-coordinate should be used.

(4) Let the curve on one side be Curve A, and that on the other side be Curve B. For each point on the Curve A, calculate the distance from the point to every point on the Curve B, and select the longest distance with the (x, y) coordinates of the two points forming this distance. Then, the number of the longest distances selected is equal to the number of points on the Curve A.

(5) Select the maximum distance from the longest distances with the (x, y) coordinates of the two points forming this distance. The maximum distance obtained is a diameter and the two points of the axis are the extreme points.

As an illustration of this method, consider the procedure with the contour consisting of nine points in Figure 5.11.(b) which is the same as that in Figure 5.11.(a). (1) Search the x-coordinates for the minimum and maximum values, and also search the y-coordinates for the minimum and maximum values. Let the minimum and maximum values of the x-coordinates be respectively x_min and x_max, and those of the y-coordinates

y_min and y_max, respectively. Thus, the smallest circumscribing rectangle as shown in Figure 5.11.(b) is obtained. (2) The sides of the rectangle which are parallel to the x-axis are the longer sides, since d1 > d2. The middle point $M(x_m, y_m)$ is obtained by:

x_m = x_min + (x_max - x_min)/2,

y_m = y_min + (y_max - y_min)/2.

(2) Since the longer sides are parallel to the x-axis, the x-coordinate x_m is used to divide the contour into two curves, i.e., Curve A and Curve B.

If $x_i <= x_m$, (x_i, y_j) ε Curve A,

otherwise, (x_i, y_j) ε Curve B.

The four points on Curve A are located on the left-hand side of the dashed vertical line in Figure 5.11.(b) and the remaining five points are located on the right-hand side. (4) For each point on Curve A, five distances are calculated, and the longest distance is selected. Likewise, the number of distances calculated is 4 x 5 = 20. (5) The maximum distance can be selected from the longest distances.
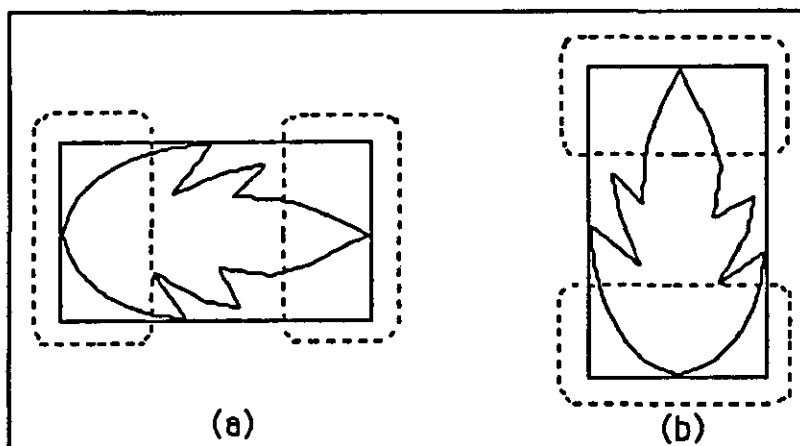
Figure 5.12 Circumscribing rectangles.

185

Consequently, this method can reduce the computing time. If a contour consists of a larger number of points, the traditional method causes a serious problem in the operation with time-consuming calculations. The basic paradigm behind this method is that the approximate locations of the extreme points of a contour can be found out in advance using a simple method. In a circumscribing rectangle in Figure 5.12.(a) or (b), the extreme points of a contour are obviously located around the end parts of the longer side, respectively, as depicted by the dotted zones in Figures 5.12.(a) and (b). Once the locations are determined, the curve in one of the zones can be separated from the curve in the other zone. Dealing with the separated curves to find a diameter can reduce the number of calculations where all of the points are involved. The maximum number of calculations for distances involving N points is (N/2) x (N/2). The weakness in this approach is that it is only applicable in the case of a rectangle. Another weakness of this approach is that it is no longer applicable if a contour has more than one axis.

5.3.2.2 Calculation of Ratios.

In a procedure for calculating ratios, an important task to be undertaken is calculating the area of each segment. In practice, the image of an object is arbitrarily located in an image plane, so the orientation of an image is usually different from that of the other image. Thus, this makes the task complex.

5.3.2.2.1 Rotation of a Contour.

To simplify this task the first operation to be carried out is to rotate a contour, formed by an object, using one of the extreme

points obtained in the previous procedure. The major objective of the rotation is to make a principal axis, connected between two extreme points of the contour, parallel to the x-axis. The method for rotating the contour at the centre of rotation is to rotate every point on the contour by an angle formed with the principal axis and the x-axis. This centre of rotation is one of the extreme points. The procedure for the rotation is as follows:

(1) Choose one of the extreme points obtained, which is to be regarded as the centre of rotation. Assume that the extreme point chosen is P, and the other extreme point is Q. Let the (x, y) coordinates of the points P and Q be (x_P, y_P) and (x_q, y_q), respectively.

(2) Once the centre of rotation is determined, the rotation of every point $C(x_c, y_c)$ on the contour is performed on the centre of rotation $P(x_P, y_P)$. Firstly, an angle θ_r for the rotation which is formed with the principal axis PQ and the x-axis is calculated.
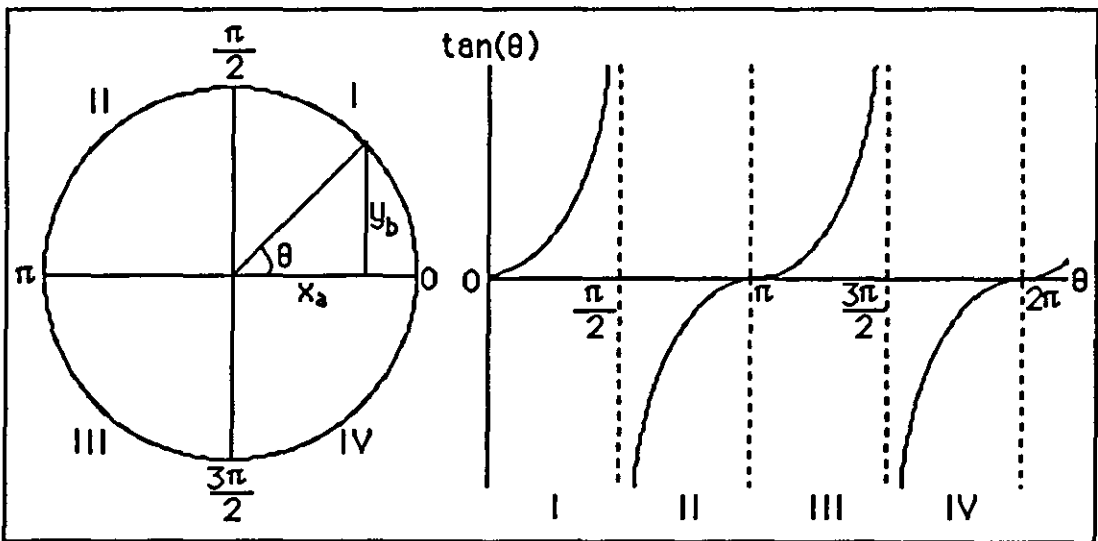
Figure 5.13 The property of tan(θ).

Secondly, an angle θ_c formed with a straight line PC and the x-axis is calculated, where the straight line PC is a line connected between the point $P(x_p, y_p)$ and each point $C(x_c, y_c)$ on the contour. In general, an angle θ formed with a straight line, connected between the origin $O(0, 0)$ of the x-y plane and an arbitrary point $A(x_a, y_a)$, and the x-axis is calculated by applying the trigonometric function, e.g., $\theta = \arctan(y_a/x_a)$. It is necessary to note the property of the function $\tan(\theta)$ before applying it. As Figure 5.13 shows, the value of $\tan(\theta)$ is determined by an angle θ and a quadrant to which a point belongs. Since the property of this function is well known, it does not need a detailed explanation. Thus, it is necessary to consider the location of a point $Q(x_q, y_q)$ in order to obtain a correct angle by applying the arctangent function. The angle θ_r for rotation can be calculated as follows:

It is assumed that the point $P(x_p, y_p)$ is regarded as an origin of the x-y plane.

(i) When the point $Q(x_q, y_q)$ is located in the quadrant I, the angle θ_r is obtained by $\theta_r = \arctan[(y_q - y_p)/(x_q - x_p)]$.

(ii) When the point $Q(x_q, y_q)$ is located in the quadrant II, the angle θ_r is obtained by $\theta_r = \pi + \arctan[(y_q - y_p)/(x_q - x_p)]$.

(iii) When the point $Q(x_q, y_q)$ is located in the quadrant III, the angle θ_r is obtained by $\theta_r = \pi + \arctan[(y_q - y_p)/(x_q - x_p)]$.

(iv) When the point $Q(x_q, y_q)$ is located in the quadrant IV, the angle θ_r is obtained by $\theta_r = 2\pi - \arctan[(y_q - y_p)/(x_q - x_p)]$.

In all cases of (i), (ii), (iii) and (iv), a case when the straight line PQ is parallel to either the x- or y-axis is not included. Note that this case will be treated by particular method which will be illustrated in detail in the step (4) below.

188

(3) In this step, the angle, denoted by θ_c, formed with the straight line PC and the x-axis is calculated. In fact, this calculation is performed for every point on the contour. Thus, the number of angles to be obtained is equal to [the number of points on a contour - 1] since the point P is fixed. This calculation is performed by the same method as in step (2), but only the two cases (v) and (vi) are added.

(i) When the point $C(x_c, y_c)$ is located in the quadrant I, the angle θ_c is obtained by $\theta_c = \arctan[(y_c - y_p)/(x_c - x_p)]$.

(ii) When the point $C(x_c, y_c)$ is located in the quadrant II, the angle θ_c is obtained by $\theta_c = \pi + \arctan[(y_c - y_p)/(x_c - x_p)]$.

(iii) When the point $C(x_c, y_c)$ is located in the quadrant III, the angle θ_c is obtained by $\theta_c = \pi + \arctan[(y_c - y_p)/(x_c - x_p)]$.

(iv) When the point $C(x_c, y_c)$ is located in the quadrant IV, the angle θ_c is obtained by $\theta_c = 2\pi + \arctan[(y_c - y_p)/(x_c - x_p)]$.

(v) When the point $C(x_c, y_c)$ is located on the border line between the quadrants I and II, the angle θ_c is obtained by $\theta_c = \pi/2$.

(vi) When the point $C(x_c, y_c)$ is located on the border line between the quadrants III and IV, the angle θ_c is obtained by $\theta_c = 3\pi/2$.

(4) The method of rotation is subdivided into two categories depending upon a feature of the straight line PQ: (i) the first category corresponds to a case when the straight line PQ is parallel to either the x- or y-axis, (ii) the second category corresponds to a case when the straight line PQ is not parallel to any axis, i.e., the x- or y-axis.

(i) In the first category, when the straight line PQ is parallel to the x-axis, it is unnecessary to rotate the contour because the objective of the rotation is to make the straight line PQ parallel

to the x-axis. On the other hand, when the straight line PQ is parallel to the y-axis, the x-coordinates of every point on the contour are simply replaced by the y-coordinate of the point, and vice versa.

(ii) In the second category, every point $C(x_c, y_c)$ on the contour is rotated with the angle of rotation θ_r, which has been calculated in the step (2), on the centre of rotation P in the counter-clockwise direction. For instance, if the points $C(x_c, y_c)$, $Q(x_q, y_q)$ and $C'(x_c', y_c')$ are located in the quadrant I, as shown in Figure 5.14, where $C'(x_c', y_c')$ is a point resultant from the rotation of the point $C(x_c, y_c)$, the angle $\angle C'PX$ will play an important role in calculating the (x, y) coordinates of the point C'. Since the angle $\angle CPX = \theta_c$ and the rotating angle $\angle QPX = \theta_r$, the rotated angle $\angle CPC' = \theta_r$. Thus, the angle $\angle C'PX = \angle CPX - \angle CPC' = \theta_c - \theta_r$. Using this angle $\angle C'PX$ ($\theta_c - \theta_r$), the x-coordinate of the point C', denoted by x_c', and the y-coordinate of the point C', denoted by y_c' are respectively calculated by the following equations:

$$x_c' = x_p + PC' \cos(\theta_c - \theta_r), \qquad (5.3.2.2.1\text{-}1)$$

$$y_c' = y_p + PC' \sin(\theta_c - \theta_r). \qquad (5.3.2.2.1\text{-}2)$$
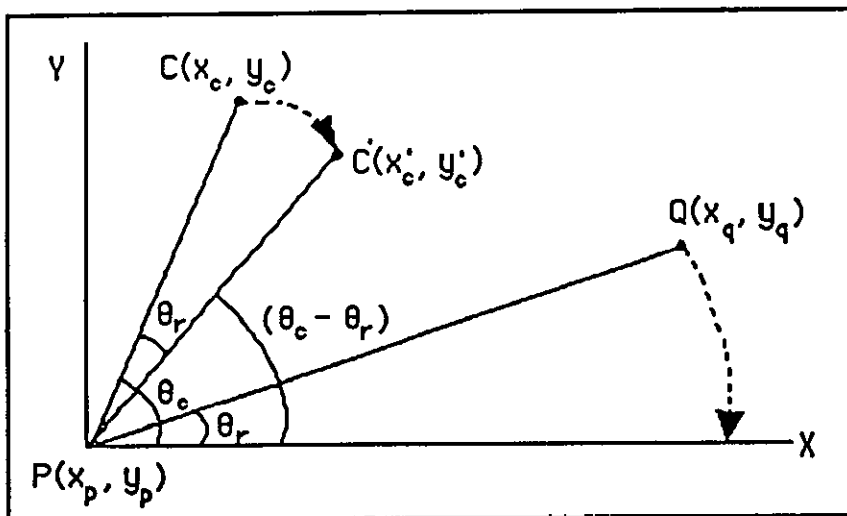
Figure 5.14 Rotation of points.

190

The (x, y) coordinates of every point rotated can be obtained by applying Equations (5.3.2.2.1-1) and (5.3.2.2.1-2) with the values of the angles θr and θc calculated in steps (1) and (2).

5.3.2.2.2 Calculation of Areas of Segments.

Once the principal axis of a contour has been rotated parallel to the x-axis, calculation of the area of each segment is performed. Before performing the calculation, consider the different types of contours which appear in biological object analysis, as shown in Figure 5.15. In the type of contours shown in Figures 5.15.(a) and (b), the contour is divided into two curves: one is above the principal axis PQ and the other is below the axis. On the other hand, in the type of a contour in Figure 5.15.(c), the contour is not divided by the axis PQ. In this case, the whole contour is located above the axis PQ.
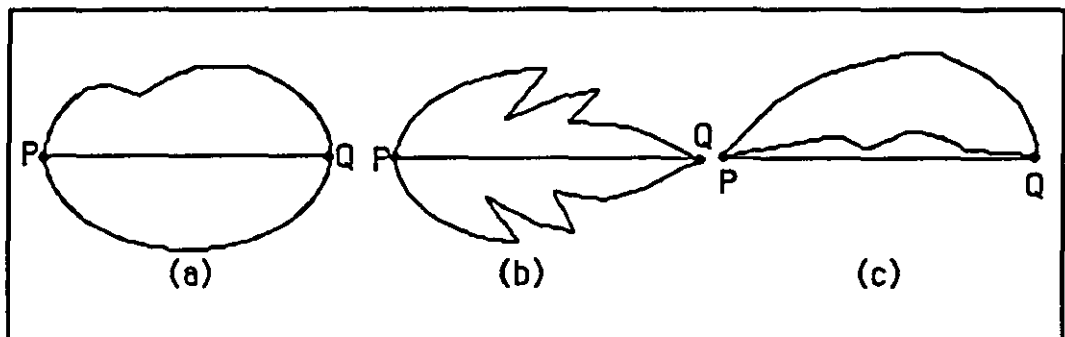
Figure 5.15 Contours of biological objects.

This shows that a principal axis PQ of a contour does not always divides the contour into two segments. The procedures for calculating areas of segments are as follows:

(1) The first task is to select every point whose y-coordinate is greater than or equal to the y-coordinate of the point P or Q, and

191

to select every point whose y-coordinate is less than or equal to the y-coordinate of the point P or Q. In cases of the contours in Figures 5.15.(a) and (b), two vectors are obtained: one for the upper part and the other part for the lower part. On the other hand, in the case of Figure 5.15.(c), only one vector is obtained, since the whole contour is located in the upper part. The vector contains (x, y) coordinates of every point in the upper part or lower part of the axis.

(2) In the second step, rearrange the vectors so that the point P or Q may be put first. The vectors are represented by:

the vector for the upper part	the vector for the lower part
(x_p, y_p)	(x_p, y_p)
(x_{u1}, y_{u1})	(x_{L1}, y_{L1})
(x_{u2}, y_{u2})	(x_{L2}, y_{L2})
.	.
.	.
.	.
(x_{ui}, y_{ui})	(x_{Lj}, y_{Lj})
.	.
.	.
.	.
(x_q, y_q)	(x_q, y_q)

(3) In the third step, divide the principal axis PQ into N equal segments, where N should be 2^n, where $n >= 0$. $N = 2^n$ is selected for the convenience of constructing a ratio tree. The accuracy of discriminating objects mainly depends upon the N. Two arrays, e.g., $S_1[k]$ and $S_2[k]$, where $k = 1, 2, 3, \ldots\ldots, N$, which can be used to assign the area of each segment are needed. The arrays $S_1[k]$ and $S_2[k]$ are for the upper part and the lower part, respectively.

(4) The area of each segment is calculated by applying a trapezoidal method. In this method, the number of parameters required is four: x_i, x_{i+1}, $f(x_i)$, and $f(x_{i+1})$ as shown in Figure 5.16.(a). The area S of each diagram in Figures 5.16 (a) and (b) is calculated by the following equations:

$$S = (1/2) \ (f(x_i) + f(x_{i+1})) \ (x_{i+1} - x_i),$$ (5.3.2.2.2-1)

where   if $x_{i+1} > x_i$, $S > 0$, (5.3.2.2.2-1a)

   if $x_{i+1} < x_i$, $S < 0$. (5.3.2.2.2-1b)

In the case of the diagram in Figure 5.17.(a), the area is calculated by Equation (5.3.2.2.2-1a), since $x_{i+1} > x_i$. On the other hand, in the case of the diagram in Figure 5.16.(b), the shaded area is calculated by applying Equations (5.3.2.2.2-1a) and (5.3.2.2.2-1b). Let us have a closer look at the process of calculating the area in the latter case. Assume that the lines AB and CD in Figure 5.16.(b) are straight lines, respectively. Firstly, calculate the area of trapezoid ABFE, S_α, by applying Equation (5.3.2.2.2-1a). Secondly, calculate the area of trapezoid CDEF, S_β, by applying Equation (5.3.2.2.2-1b), where the area S_β is less than zero, since the point C appears earlier than the point D in a vector obtained in the step (2). Thus, the shaded area is $S_\alpha + S_\beta$.
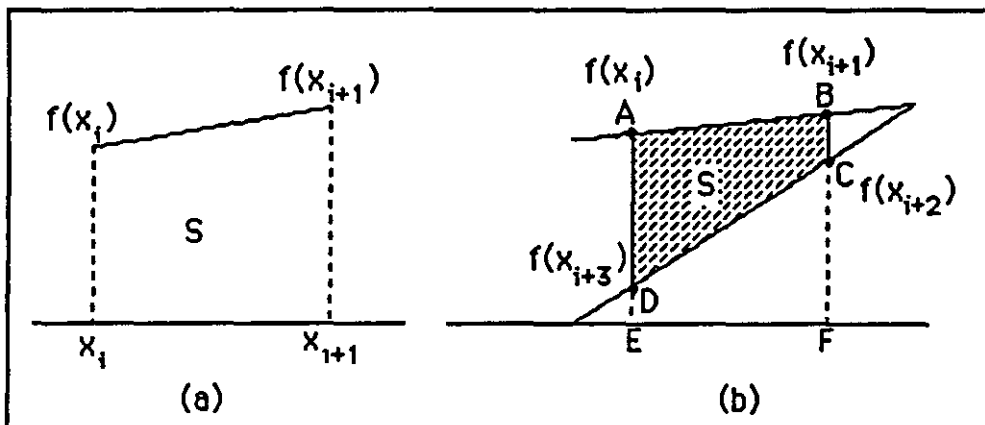
Figure 5.16 The areas of segments.

193

In practice, areas of segments in the upper part or the lower part of a principal axis PQ are calculated by the following equations, respectively:

For the area of each segment in the upper part:

$$S_1 = (1/2)\ [(y_{ui} - y_p) + (y_{ui+1} - y_p)](x_{ui+1} - x_{ui}), \qquad (5.3.2.2.2-2)$$

where (x_{ui}, y_{ui}) and (x_{ui+1}, y_{ui+1}) are (x, y) coordinates of the two adjacent points on the curve in the upper part as shown in Figure 5.17. For the area of each segment in the lower part:

$$S_2 = (1/2)\ [(y_p - y_{Lj}) + (y_p - y_{Lj+1})](x_{Lj+1} - x_{Lj}), \qquad (5.3.2.2.2-3)$$

where (x_{Lj}, y_{Lj}) and (x_{Lj+1}, y_{Lj+1}) are (x, y) coordinates of the two adjacent points on the curve in the lower part as shown in Figure 5.17.
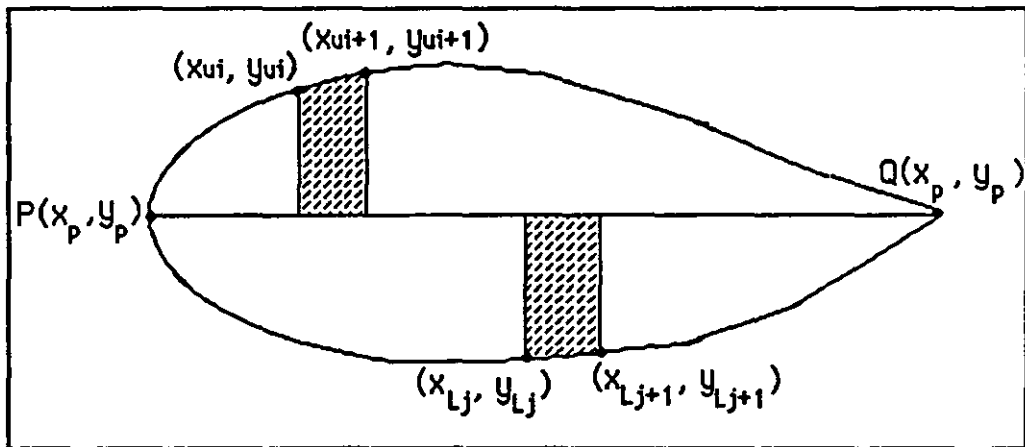
Figure 5.17 Area of a segment in the upper or lower part.

Whenever the area of a minor segment within a specific range, e.g., from x_A to x_B as shown in Figure 5.18, which has been determined in step (3), is obtained, this area is assigned to the corresponding array, e.g., $S_1[k]$ or $S_2[k]$, where k is an index for the kth segment. The range of k is from x_A to x_B. Once the area of every minor segment is assigned to the corresponding array, the result is as follows:

194

For the segments in the upper part of a contour, the array $S_1[k]$, where $k = 1, 2, 3, \ldots, N$, containing areas is:

S_1	$S_1[1]$	$S_1[2]$	$S_1[3]$	$S_1[4]$	$\cdots\cdots$	$S_1[k]$	$\cdots\cdots$	$S_1[N]$
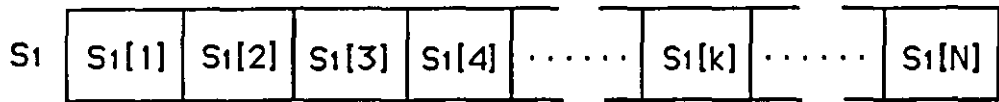
For the segments in the lower part of a contour, the array $S_2[k]$, where $k = 1, 2, 3, \ldots, N$, containing areas is:

S_2	$S_2[1]$	$S_2[2]$	$S_2[3]$	$S_2[4]$	$\cdots\cdots$	$S_2[k]$	$\cdots\cdots$	$S_2[N]$
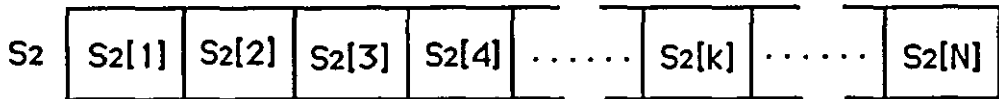
Let the total area of the upper part of a contour be S_1^T and the total area of the lower part of a contour be S_2^T. The S_1^T and S_2^T are respectively calculated by:

$$S_1^T = \sum_{k=1}^{N} S_1[k],$$

$$S_2^T = \sum_{k=1}^{N} S_2[k].$$
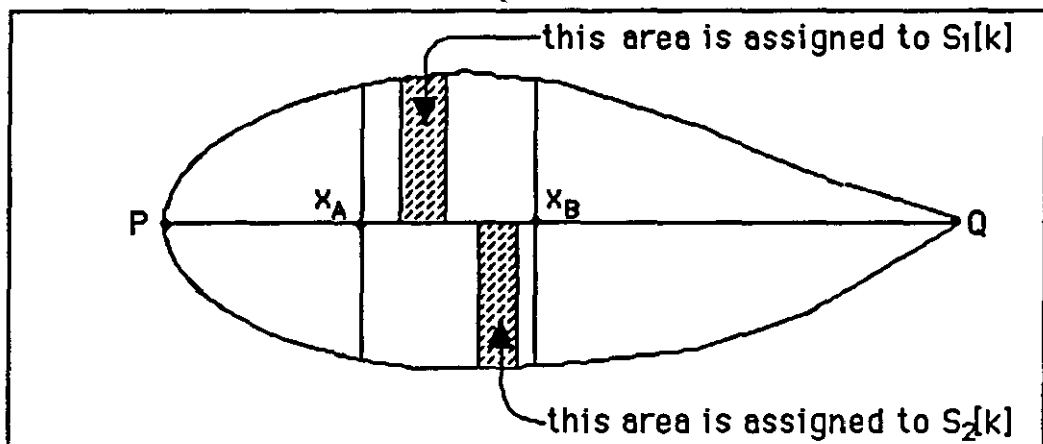
Figure 5.18 Assigning areas into $S_1[k]$ and $S_2[k]$.

5.3.2.2.3 Calculation of Ratios.

An efficient way of establishing a ratio tree is to use a bottom-up method in which the tree is built up from the bottom

level to the top level. This approach saves computing time in calculating areas. The process is as follows:

(1) Firstly, calculate the ratios A1 and A2. The ratio A1 is a ratio of the area of the upper part of a contour S1 over the area of a PQ x PQ square which can be drawn on the straight line PQ as shown in Figure 5.19. The ratio A2 is a ratio of the area of the lower part of a contour S2 over the area of a PQ x PQ square which can be drawn underneath the straight line PQ as shown in Figure 5.19. The ratios A1 and A2 are respectively calculated by Equation (5.3.1-2):

$$A1 = \frac{S1}{PQ^2}, \qquad A2 = \frac{S2}{PQ^2}.$$

Let the ratios A1 and A2 be r1 and r2, respectively.
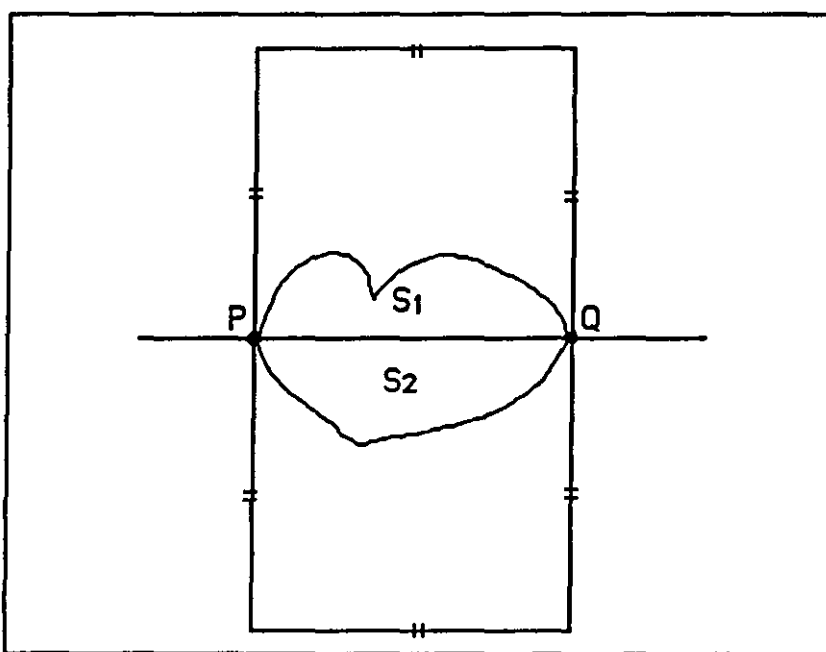
Figure 5.19 Diagrammatical representation of ratios.

(2) In the second step, the ratios from the bottom level to the second level are calculated. Let the ratios for the segments in the

196

upper part of the bottom level be $r_1[1]$, $r_1[2]$, $r_1[3]$, ..., $r_1[N]$, and the ratios for the segments in the lower part of the same level be $r_2[1]$, $r_2[2]$, $r_2[3]$, ..., $r_2[N]$. The ratios are calculated by:

$$r_1[1] = A_1 \times \frac{S_1[1]}{S_1{}^T} , \qquad r_2[1] = A_2 \times \frac{S_2[1]}{S_2{}^T} ,$$

$$r_1[2] = A_1 \times \frac{S_1[2]}{S_1{}^T} , \qquad r_2[2] = A_2 \times \frac{S_2[2]}{S_2{}^T} ,$$

$$r_1[3] = A_1 \times \frac{S_1[3]}{S_1{}^T} , \qquad r_2[3] = A_2 \times \frac{S_2[3]}{S_2{}^T} ,$$

$$\vdots \qquad\qquad\qquad \vdots$$

$$r_1[k] = A_1 \times \frac{S_1[k]}{S_1{}^T} , \qquad r_2[k] = A_2 \times \frac{S_2[k]}{S_2{}^T} ,$$

$$\vdots \qquad\qquad\qquad \vdots$$

$$r_1[N] = A_1 \times \frac{S_1[N]}{S_1{}^T} , \qquad r_2[k] = A_2 \times \frac{S_2[N]}{S_2{}^T} .$$

In the upper part, the ratios for the segments of the level one level above the bottom level are calculated by:

$$r_1[1, 2] = A_1 \times \frac{S_1[1] + S_1[2]}{S_1{}^T} , \qquad r_2[1, 2] = A_2 \times \frac{S_2[1] + S_2[2]}{S_2{}^T} ,$$

$$r_1[3, 4] = A_1 \times \frac{S_1[3] + S_1[4]}{S_1{}^T} , \qquad r_2[3, 4] = A_2 \times \frac{S_2[3] + S_2[4]}{S_2{}^T} ,$$

$$r_1[5, 6] = A_1 \times \frac{S_1[5] + S_1[6]}{S_1{}^T} , \qquad r_2[5, 6] = A_2 \times \frac{S_2[5] + S_2[6]}{S_2{}^T} ,$$

$$\vdots \qquad\qquad\qquad \vdots$$

$$r_1[k, k+1] = A_1 \times \frac{S_1[k] + S_1[k+1]}{S_1{}^T} , \qquad r_2[k, k+1] = A_2 \times \frac{S_2[k] + S_z[k+1]}{S_2{}^T} ,$$

$$\vdots \qquad\qquad\qquad \vdots$$

$$r_1[N-1, N] = A_1 \times \frac{S_1[N-1] + S_1[N]}{S_1{}^T}, \quad r_2[N-1, N] = A_2 \times \frac{S_2[N-1] + S_2[N]}{S_2{}^T}$$

Likewise, the ratios for each level of the tree can be calculated. The process for building up the tree is graphically illustrated in Figure 5.20.
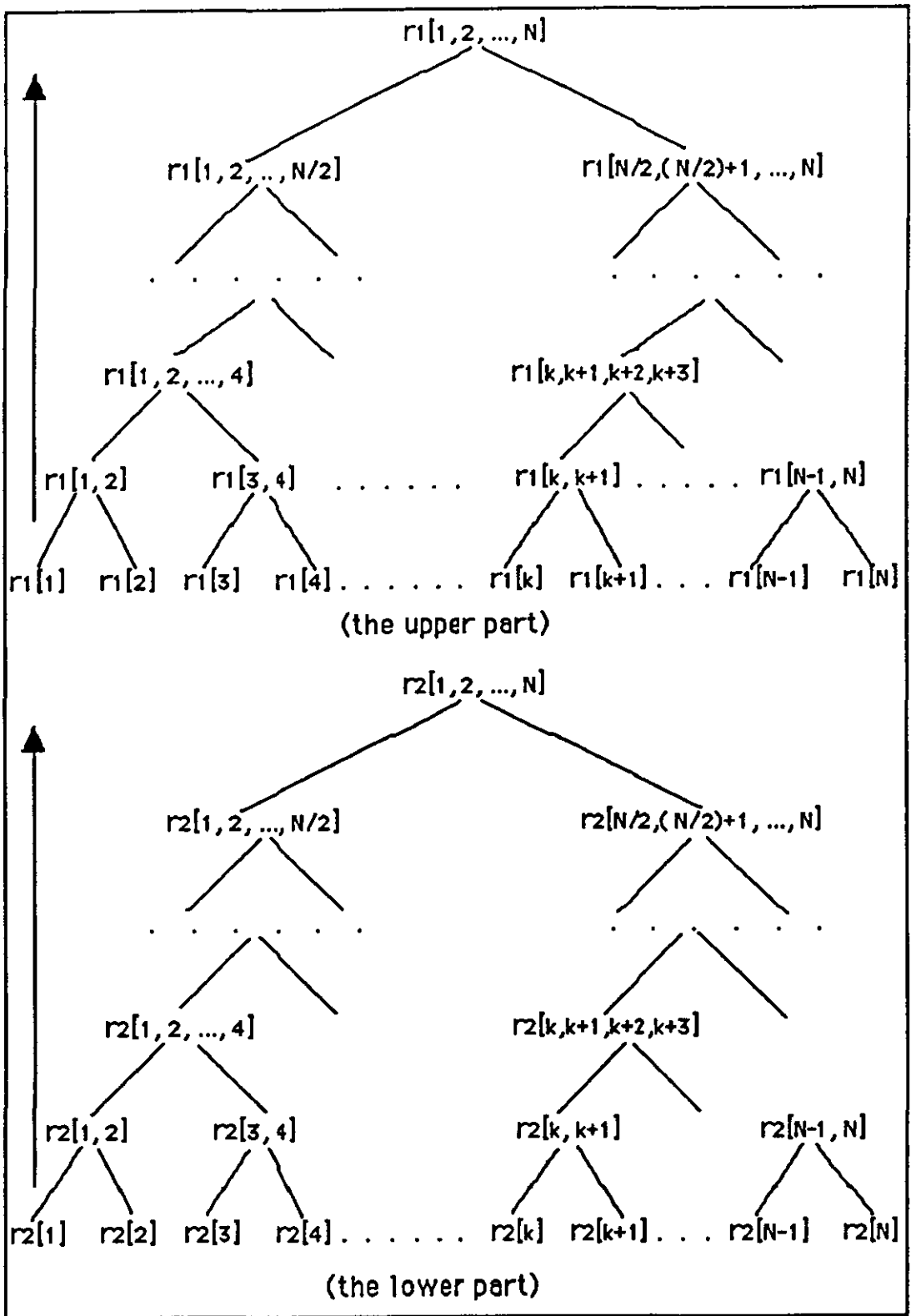
Figure 5.20 The bottom-up process for a ratio tree.

199

5.4 CONCLUSION.

It is well known that the result of a computerised object discrimination system mostly relies on the shape descriptor. This means that "how well is a shape descriptor organised in its function?" corresponds to "how well can an object discrimination system operate?". The most important factors which have been emphasised for an object discrimination system are accuracy, efficiency and generality. With this view point in mind, an investigation has been carried out on the existing shape description methods. Among them, three methods such as the invariant moment, the Fourier descriptor and the chain code have been considered, since they have been commonly used in the shape description domain. Each method has been reviewed from the theoretical background and detailed procedure to the final product. Some case studies, applying each method, have been investigated to correctly evaluate the functional aspects of each method. The investigation has revealed the following important facts. The first is that the latter two methods cannot directly be involved in the object discrimination procedure. The second important fact is that two of them have commonly been designed to produce only a vector that can represent a normalised contour which is invariant to location, orientation and starting point factors. In practice, some important attributes such as diameters, widths, ratios and angles, etc. are extracted from the vector in the object discrimination procedure. On the other hand, most case studies applying the invariant moment method have commonly argued that seven different kinds of invariant moments do not provide a practical description and this causes confusion when selecting the optimum number of invariant moments for use with

200

an object discrimination procedure.

Consequently, it was necessary to develop a new shape descriptor which could be directly involved in an object discrimination procedure. This improved method is to transform a two-dimensional contour of an object into two one-dimensional curves; and to calculate ratios using the area of each segment, the area of a curve bounded by an axis, and the area of a [length of an axis] x [length of an axis] square. A hierarchical tree which is established by ratios can be directly involved in an object discrimination procedure. The most important feature of this improved method is that it is an attempt to discriminate an object using the similar method to that of human vision. This shape descriptor accommodates the basic requirements that a shape descriptor should be independent of location, orientation and starting point of a contour. In addition, this shape descriptor can easily be used in discriminating a reflected image, i.e., a mirror image. On the other hand, this method has a deficiency in discriminating an object which has more than one axis.

Chapter 6

COLOUR PATTERN DESCRIPTION METHODS.

6.1 Introduction.

6.2 Major Factors for Colour Pattern Description.

6.2.1 The Number of Different Colour Patterns.

6.2.2 Colour Feature of Each Colour Pattern.

6.2.3 The Ratio of the Area of Each Colour Pattern Over the Total Area of an Object.

6.2.4 Normalised Centre of Gravity of Each Colour Pattern.

6.2.5 The Slope of the Regression Line of Each Colour Pattern.

6.2.6 The Ratios for Segments of Each Colour Pattern.

6.3 Colour Pattern Description.

6.3.1 Calculation of the Major Factors.

6.3.1.1 The L*a*b* Colour Feature of Colour Pattern.

6.3.1.2 The Ratio (the Area of Colour Pattern/the Total Area).

6.3.1.3 Normalised Centre of Gravity of Colour Pattern.

6.3.1.4 The Slope of the Regression Line of Each Colour Pattern.

6.3.1.5 The Ratios for Segments of Each Colour Pattern.

6.3.2 Hierarchical Organisation of Factors.

6.4 Conclusion.

202

6.1 INTRODUCTION.

In a biological object identification process the information which is obtained from each object's shape is not always good enough to discriminate one object from another. If however, each object also consists of complicated patterns with distinctively different colours, the information obtained from the various colour patterns within each object is added to the information from the shape, the object identification is likely to be improved. In the real world, a great majority of biological objects have the same shape but contain various colour patterns. Thus it is necessary to consider the colour patterns in the object identification process. It may not be too much to say that the success of the object identification depends upon the information from the colour patterns which form the surface of an object. An important task which immediately arises is how to describe the information in such a way that it can be successfully utilised in the object identification process. From this point of view, the colour pattern description is worthy of investigation.

The literature survey which has been performed in this thesis has revealed that a great amount of research has already been accomplished in the shape description domain, but, on the other hand, only a little research has been performed in the colour pattern description domain. The reason for this might be that since most algorithms for colour pattern extraction which have been published require laborious effort, they are not good enough to be generally applied in other academic or industrial research fields. In practice, because colour pattern extraction requires a complicated methodology in which a colour pattern has first to be

decided on, it was considered unreasonable to expect active research in this field in an object classification procedure. The colour image capturing devices were not generally available to deal with colour pattern extraction. Pattern descriptors which have been commonly used are a measure of compactness of a pattern which is defined as $(perimeter)^2/area$, the area of a pattern, the orientation of the principal axis, the mean of the grey levels, and the variance of a pattern, etc. In fact, colour patterns in an object cannot be completely described by any one of these descriptors alone. The reason for this will be discussed in detail.

In this chapter, several important factors which are required to represent the features of each colour pattern within an object are defined. The background and motivation of the definition of these factors will be discussed. In particular the organisation of these factors for the object identification will be discussed.

6.2 MAJOR FACTORS FOR COLOUR PATTERN DESCRIPTION.

In the great majority of butterflies, wings usually consist of colour patterns. Some species of butterflies have no colour pattern on their wings, but most species do. The colour pattern is defined as a region which is composed of picture cells having similar colour features which are connected to each other (Duda & Hart, 1973). Each colour pattern varies depending upon characteristics such as colour feature, size feature, location feature and shape feature. The colour feature is a property of colour sensation which each colour pattern shows. The size feature is a property representing the area of each colour pattern in relation to the total area of an object to which each colour pattern belongs. The location feature is a property representing the position of each pattern within an object. The shape feature is a morphological property which each pattern forms. These features play an important role in species discrimination, and they can be used as major factors for colour pattern description. The colour patterns obtained by applying the algorithm in Chapter 4 are represented by these major factors which can be used to classify objects. In the object discrimination procedure, all the major factors should be simultaneously considered because if any one of the factors fails to be assessed it is difficult to successfully carry out the discrimination. The background and necessity of each factor will be illustrated. An important fact to be noted is that these factors will dominate the algorithm for the discrimination of butterfly species with colour-patterned wings.

6.2.1 The Number of Different Colour Patterns.

As an illustration, consider three different wing patterns of butterflies as shown in Figure 6.1. The wings in Figure 6.1 are those of childrenae, lycimenes and dardanus. At first glance, they look similar. However, they have completely different wing pattern features. How then can one make it possible for an automatic object discrimination system to classify their different features? This question implies a necessity for a systematic organisation of these features in a colour pattern description. Let us only consider the colour patterns on the wings in Figure 6.1, not their shapes. The wings in Figures 6.1.(a) and (b) contain three different colour patterns. On the other hand, the wings in Figure 6.1.(c) contain two different colour patterns. All of the wings have a similar colour feature on the background. Thus, it is possible to simply discriminate the wings in Figures 6.1.(a) and (b) from the wings in figure 6.1.(c) using the number of different colour patterns. However, it is impossible to discriminate the wings in Figure 6.1.(a) from the wings in Figure 6.1.(b) using the number of different colour patterns because they have   equal number. Consequently, the number of different colour patterns can be regarded as a factor for colour pattern description although it does not completely discriminate objects. Using this factor in the actual discrimination procedure can obviously reduce the number of cases, when searching in library data by excluding objects whose number of different colour patterns is not equal to that of the object under consideration.

6.2.2 Colour Feature of Each Colour Pattern.

If the number of different colour patterns cannot discriminate the object in Figure 6.1.(a) from the object in Figure 6.1.(b), let us consider the easiest way of the discriminating these objects. An immediate method for the discrimination is to consider the colour feature of each pattern. The colour of the small pattern in the upper part of the wings in Figure 6.1(a) is yellow. The colour of the pattern in the middle part of the wings in Figure 6.1.(a) is yellow-green. The colour of the lower part is red. The colours of the upper and the lower parts of the wings in Figure 6.1.(b) are respectively the same as those of the upper and the lower parts of the wings in Figure 6.1.(a). On the other hand, the colour of the middle part of the wings in Figure 6.1(b) is green. When the colours of the patterns in Figure 6.1.(a) are respectively compared with those of the patterns in Figure 6.1.(b), it can be concluded that the two objects are different because of the colour difference between the pattern in the middle part of the object in Figure 6.1.(a) and that in the middle part of the object in Figure 6.1.(b). Consequently, this colour feature undoubtedly plays an important role in a colour object discrimination procedure. Thus, this colour feature can obviously be regarded as the second factor of colour pattern description. The important fact to be noted is that there are many factors such as environmental conditions, film speed, the size of the aperture and shutter speed of a camera, etc. which affect the colour representation of a photograph. If an image is obtained from a photograph, there are some variations in the colour features of an object due to these factors. Thus, the variations of a colour feature should be considered in the description.

207

(a)   (b)   (c)
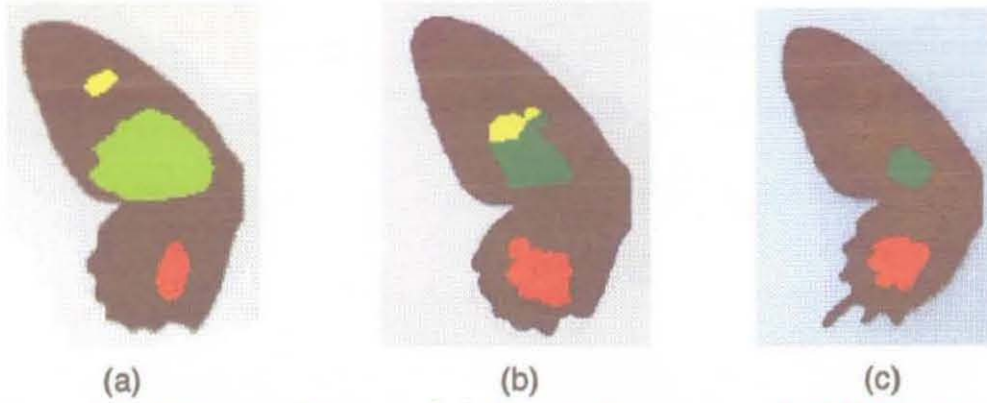
Figure 6.1 Wing patterns. (a) The left wings of childrenae. (b) The left wings of lycimenes. (c) The left wings of dardanus.

(a)   (b)
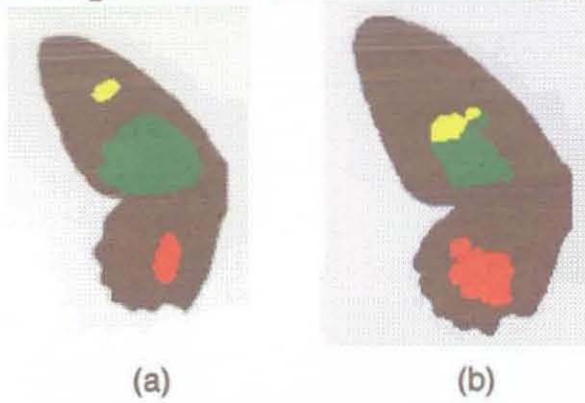
Figure 6.2 Wing patterns.

(a)   (b)
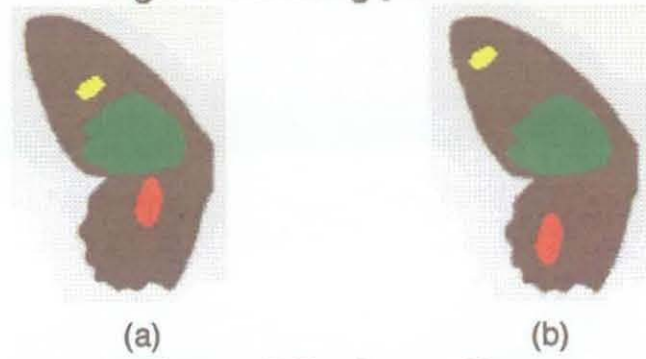
Figure 6.3 wing patterns.

(a)   (b)
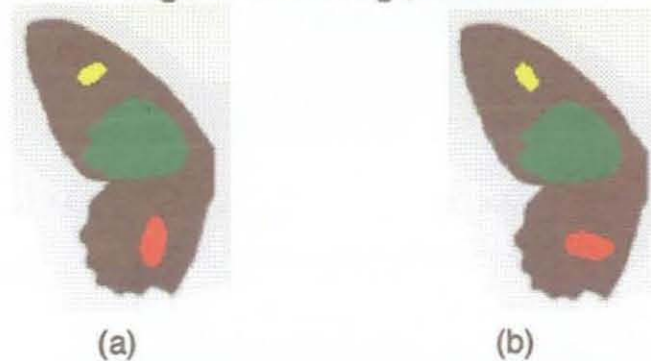
Figure 6.5 Wing patterns.

208

6.2.3 The Ratio of the Area of Each Colour Pattern Over the Total Area of an Object.

As Figure 6.2 shows, if the colour features do not make a difference, the alternative to using the colour feature is to use the size of each colour pattern relative to the size of the whole object. This means that the size of an object varies depending upon the photograph size, but also upon the size of an object itself. Thus, a reasonable way of using the size of each colour pattern is to use the ratio of the area of each colour pattern over the area of an object. Let the ratio of the area of the yellow pattern over the total area of the wings be r_{a1}; the ratio of the area of the green pattern over the total area be r_{a2}; and the ratio of the area of the red pattern over the total area be r_{a3}, in Figure 6.2.(a). Likewise, let the ratios of the areas of the colour patterns over the total area of the wings in Figure 6.2.(b) be respectively r_{b1}, r_{b2} and r_{b3}. These ratios should be arranged, in descending order as $r_{a2} > r_{a3} > r_{a1}$ and $r_{b2} > r_{b3} > r_{b1}$. In the discrimination procedure, this pair of ratios with the same order can be efficiently used. In fact, the arrangement of the different colour patterns in an object, as shown in Figure 6.2.(a) or (b) is so random that a reasonable arrangement of the ratios in descending order is necessary, since this arrangement is invariant to irregular arrangement of the patterns within an object. The basic idea of this arrangement is that a certain colour pattern which has the largest area can initially be denoted by human vision, and each colour pattern can also be detected in the order of its size. In the discrimination procedure, if $r_{a2} = r_{b2}$, $r_{a3} = r_{b3}$, and $r_{a1} = r_{b1}$, it is concluded that the two objects have patterns with the same number, same colour features, and same ratios; otherwise, it is

209

concluded that the two objects have different colour patterns. In fact, in the case of Figure 6.2, $r_{a2} \approx r_{b2}$, $r_{a3} \approx r_{b3}$ and $r_{a1} \approx r_{b1}$, thus it is concluded that these wings have different patterns. Consequently, the ratio of the area of each colour pattern over the total area of an object can be regarded as the third factor of colour pattern description.

6.2.4 Normalised Centre of Gravity of Each Colour Pattern.

As Figure 6.3 shows, each object has three different colour patterns, where each pair of colour patterns have similar colour features and similar ratios, but different locations within each object. These objects in Figure 6.3 cannot be discriminated by the three previous factors of colour pattern description, i.e., the number of different colour patterns, the colour feature, and the ratio of the area of each colour pattern over the total area of an object. Thus, employing a locational factor should additionally be considered in order to discriminate such objects as in Figure 6.3. To describe the location of a colour pattern is not a simple task because the orientation of the principal axis, location and size of an object to which the colour pattern belongs varies. The basic procedure for describing the location of a colour pattern is to describe its location such that it is independent of the orientation, location and size of an object. In the region description domain, the location of the centre of gravity has commonly been used. However, the location of the centre of the gravity of a pattern depends upon the orientation of the principal axis, location and size of an object. Therefore, the centre of gravity of a colour pattern cannot be used without any kind of

210

normalisation. There should be two kinds of normalisation , i.e., the normalisation of the orientation of the principal axis of an object, and the normalisation of the location and size of an object. The normalisation of the orientation is carried out by a similar method to that which has been developed in the previous chapter. Since this normalisation has an important effect on the other factors which will be discussed in the following stages, the detailed calculation method will be illustrated in section 6.3. Once this normalisation is performed, the result will be obtained as shown in Figure 6.4. Let the length of the principal axis PQ in Figure 6.4 be d. For the normalisation of the (x, y) coordinates of the centre of gravity, two d x d squares should be drawn as shown in Figure 6.4. Then, calculate the (x, y) coordinates of the centre of gravity for each colour pattern. Let the (x, y) coordinates of the centre of gravity for one of the colour patterns be ($\bar{x}_r$, $\bar{y}_r$) as shown in Figure 6.4.
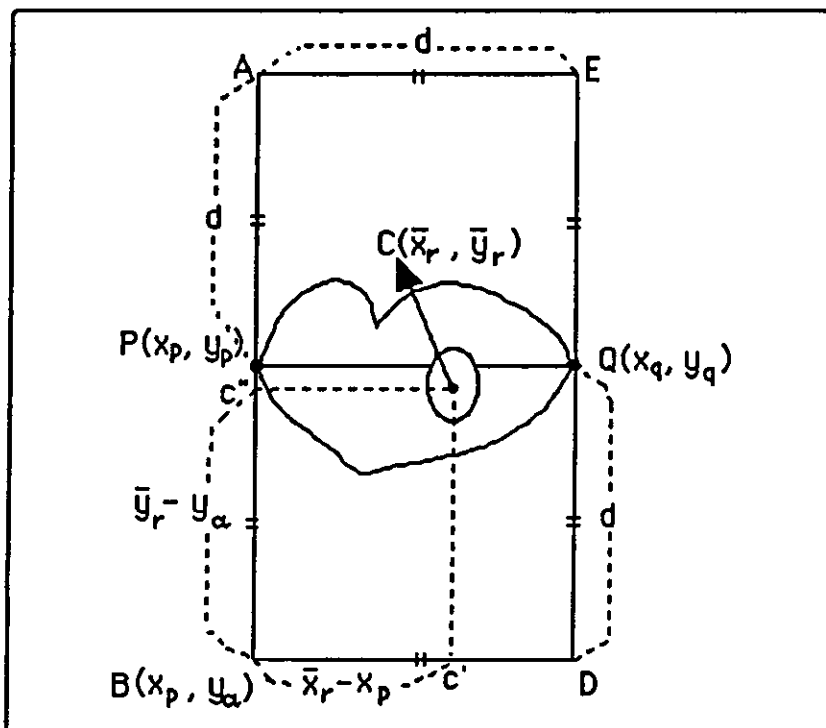
Figure 6.4 Normalisation of the centre of gravity.

211

Let the (x, y) coordinates of the lower left corner of the rectangle in Figure 6.4 be (x_P, y_α). Note that the centre of gravity is a point $C(\bar{x}_r, \bar{y}_r)$ which can easily be changed depending upon the location and size of the whole image. Thus, it is necessary to make the centre of gravity invariant to the location and size of the whole image. The most convenient and efficient way of doing this is to make use of the (x, y) coordinates of the centre of gravity, (x_P, y_α), the (d + d) x d rectangle, and the (x, y) coordinates of the lower left corner as shown in Figure 6.4. The basic principle of this normalisation is to describe the point $C(\bar{x}_r, \bar{y}_r)$ in relation to the rectangle and the (x, y) coordinates of the lower left corner, (x_P, y_α). Note that the rectangle, ABDE, in Figure 6.4, is determined by the length of the principal axis of an object, and is invariant to the location of the object. Let the (x, y) coordinates of the normalised centre of gravity be ($\bar{x}_n$, $\bar{y}_n$). The (x, y) coordinates of the normalised centre of gravity, ($\bar{x}_n$, $\bar{y}_n$), are calculated as follows:

$$\bar{x}_n = \frac{\bar{x}_r - x_p}{d} \quad ,$$

(6.2.4-1)

$$\bar{y}_n = \frac{\bar{y}_r - y_\alpha}{d + d} \quad .$$

(6.2.4-2)

As Equations (6.2.4-1) and (6.2.4-2) show, $\bar{x}_n$ and $\bar{y}_n$ are ratios, i.e., $\bar{x}_n$ is the ratio of ($\bar{x}_r$ - x_p) over d and $\bar{y}_n$ is the ratio of ($\bar{y}_r$ - y_α) over (d + d). These ratios are calculated in relation to the rectangle and the (x, y) coordinates of the lower left corner in Figure 6.4, therefore they are invariant to the location and size of an object. This normalised centre of gravity can be used in the object discrimination procedure. Consider, for example, the colour

patterns in each object in Figure 6.3. The normalised centre of gravity of the green pattern in each object will have a similar value. On the other hand, the normalised (x, y) coordinates of the centre of gravity of the yellow pattern in Figure 6.3.(a) will be quite different from those of the yellow pattern in Figure 6.3.(b); and the normalised (x, y) coordinates of the centre of gravity of the red pattern in Figure 6.3.(a) will also be quite different from those of the red pattern in Figure 6.3.(b). Note that since variation in the normalised centres of gravity for the target colour patterns is usual even in the same species, this variation should be considered in a practical implementation. Consequently, the normalised centre of gravity of each colour pattern can be used as the fourth factor of colour pattern description.

6.2.5 The Slope of the Regression Line of Each Colour Pattern.

The yellow and red patterns in Figure 6.5.(b) are respectively those in Figure 6.5.(a) rotated through 90° in the counter-clockwise direction. As Figure 6.5 shows, each object has an equal number of different colour patterns, where each pair of colour patterns have similar colour features, similar ratios of their areas over the total area, and similar normalised centres of gravity, but different orientations of the principal axis. These objects cannot be discriminated by the four factors of colour pattern description, i.e., the number of different colour patterns, the colour feature, the ratio of the area of each colour pattern over the total area of an object, and the normalised centre of gravity. Therefore, it is necessary to additionally consider the morphological aspects of each pair of colour patterns in order to

213

classify the objects in Figure 6.5. The shapes of the colour patterns in Figure 6.5 could be considered to be simple in their description. However, the description of the shape of a colour pattern in an object usually is a complicated task as the previous chapter has shown. Note that the main objective of the colour pattern description in this system is not for detailed morphological analysis relevant to a particular domain, but for a computerised object discrimination procedure which can generally be adopted in the biological object discrimination domain. For this purpose, four important factors of colour pattern description have already been introduced. Applied simultaneously in an object searching procedure, they should dramatically reduce the number of likely candidates in a sample space. Thus, if only a few basic factors for shape description are added to the previous factors, they will be able to cover a wide range of various cases. The first sub-factor of shape description for a colour pattern which is commonly used in the region description domain is the orientation of the principal axis of a colour pattern. Since this orientation usually varies depending upon the orientation of an object to which the colour pattern belongs, the normalisation of this orientation is inevitably required. The normalisation is performed by rotating the principal axis such that it becomes parallel to the horizontal line, as already illustrated in the normalisation of the centre of gravity. Once the principal axis is rotated, the orientation of the principal axis of each colour pattern is approximated by applying simple regression analysis. In this regression analysis, a simple regression equation is usually represented by:

$$Y_i = \beta_0 + \beta_1 X_i + \varepsilon_i \, , \tag{6.2.5-1}$$

where

X_i is the independent variable which is the x-coordinate of each pixel in colour pattern,

Y_i is the dependent variable which is the y-coordinate of each pixel in a colour pattern,

β_0 is the intercept of the Y-axis,

β_1 is the regression coefficient which represents the slope of the regression line,

ϵ_i is the error term.

An important fact to be noted is that since β_0 varies depending upon the location and size of an object itself, this value cannot directly be used as a factor of colour pattern description. In particular, since the normalised centre of gravity can efficiently be used to represent the location of a certain colour pattern and the regression line usually passes through the centre of gravity of the rotated pattern, β_0, which represents the intercept of the Y-axis, does not need to be involved in the shape description.

Consider, for example, the colour patterns in Figure 6.5. Let the β_1 for the red pattern in Figure 6.5.(a) be β_{1a}, the β_1 for the red pattern in Figure 6.5.(b) be β_{1b}. The value of β_{1a} is different from that of β_{1b}, since the red pattern in Figure 6.5.(b) is the red pattern in Figure 6.5.(a) rotated through 90° in the counter clockwise direction. For simplicity of illustration, compare β_{1a} with β_{1b}. Since β_{1a} is different from β_{1b}, it can be concluded that the two objects are different from each other. Consequently, the slope of a simple regression line can be regarded as the fifth factor of colour pattern description.

215

6.2.6 The Ratios for Segments of Each Colour Pattern.

Suppose that two objects have an equal number of different colour patterns, where the corresponding colour patterns have similar values for all of the corresponding factors previously discussed, but still look different from each other in their shapes. In order to solve the additional problem of classifying the shapes of the colour patterns, consider the second sub-factor of shape description for a colour pattern which is the ratios of areas of segments over the area of a colour pattern. Since the orientation
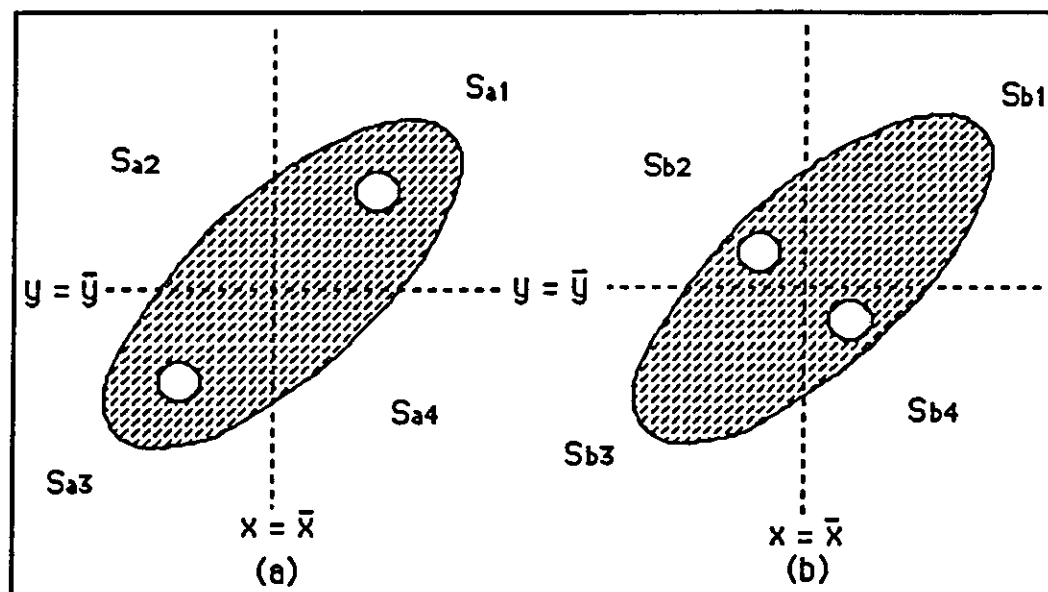
Figure 6.6 The hypothetical patterns.

of the principal axis of a colour pattern usually varies depending upon the orientation of an object to which the colour pattern belongs, the normalisation of this orientation should be performed as shown previously. In general, the ratios of areas are invariant to the size of an object, so the size factor does not need to be considered in the ratios. The basic principle behind the ratio calculation is similar to that of the ratio calculation in the

216

previous chapter. The ratio calculation which is now under consideration is performed using the (x, y) coordinates of the centre of gravity of a colour pattern. Suppose, for example, two hypothetical colour patterns as shown in Figure 6.6, where all the corresponding factors, which have been considered, have similar values. In order to discriminate these patterns, draw dashed lines, at the centre of gravity, each of which is parallel to the horizontal or the vertical line and then split each pattern into four segments, as shown in Figure 6.6. Count the number of pixels in each segment. Let the area of each segment for the pattern in Figure 6.6.(a) be S_{a1}, S_{a2}, S_{a3} and S_{a4}; the area of each segment for the pattern in Figure 6.6.(b) be S_{b1}, S_{b2}, S_{b3} and S_{b4}; and the total area of each pattern be S_{aT} and S_{bT}. The ratio of the area of the upper half over the total area of the pattern in Figure 6.6.(a) is:

$$H_{a1} = \frac{S_{a1} + S_{a2}}{S_{aT}} , \qquad (6.26\text{-}1)$$

and the ratio of the area of the lower half over the total area of the pattern in Figure 6.6.(a) is

$$H_{a2} = \frac{S_{a3} + S_{a4}}{S_{aT}} . \qquad (6.26\text{-}2)$$

Likewise, the ratios for the upper half and the lower half of the pattern in Figure 6.6.(b) are respectively:

$$H_{b1} = \frac{S_{b1} + S_{b2}}{S_{bT}} , \qquad (6\ 2.6\text{-}3)$$

$$H_{b2} = \frac{S_{b3} + S_{b4}}{S_{bT}} . \qquad (6.2.6\text{-}4)$$

Since it has been assumed that all the corresponding factors have had the same values, if each hole in Figure 6.6 has equal area, H_{a1} = H_{b1} and H_{a2} = H_{b2}. These ratios cannot discriminate these patterns. Thus, consider the ratio for each segment to

217

discriminate these patterns. The ratios of the area of each segment over the total area of the patterns are:

$$Q_{a1} = \frac{S_{a1}}{S_{aT}} , \qquad\qquad Q_{b1} = \frac{S_{b1}}{S_{bT}} ,$$

$$Q_{a2} = \frac{S_{a2}}{S_{aT}} , \qquad\qquad Q_{b2} = \frac{S_{b2}}{S_{bT}} ,$$

$$Q_{a3} = \frac{S_{a3}}{S_{aT}} , \qquad\qquad Q_{b3} = \frac{S_{b3}}{S_{bT}} ,$$

$$Q_{a4} = \frac{S_{a4}}{S_{aT}} , \qquad\qquad Q_{b4} = \frac{S_{b4}}{S_{bT}} , \qquad\qquad (6.2.6\text{-}5)$$

where Q_{a1} through Q_{a4} are ratios for the segments in Figure 6.6.(a) and Q_{b1} through Q_{b4} are ratios for the segments in Figure 6.6.(b). Under the previous assumption, the corresponding ratios are different from each other. Thus, these four ratios such as Q_{j1}, Q_{j2}, Q_{3} and Q_{j4} will successfully be used as shape descriptors, where j is a subscript for the different patterns. Although the previous two ratios such as H_{j1} and H_{j2} could not discriminate these patterns, they will also be used as shape descriptors because every descriptor does not always discriminate different patterns. Consequently, these ratios, i.e., H_{j1}, H_{j2}, Q_{j1}, Q_{j2}, Q_{j3} and Q_{j4} can obviously be regarded as the sixth factor of colour pattern description.

So far, the six factors of colour pattern description have been defined. The background and motivation of each factor has been also illustrated. In fact, these factors can play an important role in describing any colour pattern in an object because they have been designed to accommodate the basic requirement which a colour pattern descriptor should be invariant to the size, orientation and location of an object to which each colour pattern belongs.

6.3 COLOUR PATTERN DESCRIPTION.

In the previous section, six major factors which are important when discriminating objects have been defined, where each object usually consists of patterns with various colour features, sizes, locations and shapes. It has also been shown that each factor has its own limitations in describing the various colour patterns, thus all the factors should simultaneously be involved in the object discrimination process. In the following sub-sections, the detailed procedure for calculating each factor will be illustrated, and then object representation with various colour patterns will also be discussed. Once all the factors are obtained, these factors should be hierarchically organised to reduce computing time when searching library data for an optimum solution.

6.3.1 Calculation of the Major Factors.

6.3.1.1 The L*a*b* Colour Feature of Colour Pattern.

Suppose, for example, that an object is described by these factors as shown in Table 6.1. This object consists of three different colour patterns. The colour of each pattern is described by the L*a*b* colour features. Note that each colour pattern has been obtained by applying Cluster Analysis as in Chapter 4. Thus, there are two possible cases in which a colour pattern is described by the L*a*b* colour features. One case is that of a colour pattern constructed by pixels of completely homogeneous L*a*b* colour features. The other case is that of a colour pattern constructed by pixels which have slightly different L*a*b* colour features, where this set of pixels forms a certain shape of

pattern which is clearly distinguished from its neighbouring pixels. In the former case, this pattern can be described by one set of the $L^*a^*b^*$ colour features. In the latter case, this pattern can be described by the centre of gravity of $L^*a^*b^*$. This value can be easily obtained by simply calculating the mean value of each of the L^*, a^* and b^* from the units having equal Cluster i.d.s of the Auxiliary Means created in Chapter 4. In Table 6.1, the colour features for each pattern are represented by the centres of gravity, i.e., Lm_j, Am_j and Bm_j, where j represents each pattern.

Factor / Pattern	Colour Feature	Area of Pattern Over Total Area	Normalised Centre of Gravity	Slope of Regression Line	Ratios	
A	Lma Ama Bma	ra	$\bar{X}$na $\bar{y}$na	βa1	Ha1 Ha2	Qa1 Qa2 Qa3 Qa4
B	Lmb Amb Bmb	rb	$\bar{X}$nb $\bar{y}$nb	βb1	Hb1 Hb2	Qb1 Qb2 Qb3 Qb4
C	Lmc Amc Bmc	rc	$\bar{X}$nc $\bar{y}$nc	βc1	Hc1 Hc2	Qc1 Qc2 Qc3 Qc4

Table 6.1 Object representation by factors.

6.3.1.2 The Ratio (the Area of Colour Pattern/the Total Area).

The third column in Table 6.1 shows the ratios of the area of each colour pattern over the total area of the object. Each ratio can be obtained by using the Auxiliary Means created in Chapter 4. For each ratio, simply add all the values in the NOP of every unit having an equal Cluster i.d. in the Auxiliary means; and divide the result by the total number of pixels in this object. Then, the ratios obtained are ra, rb and rc. As already illustrated in the

previous section, these ratios should be arranged in descending order. Hence, these ratios are arranged as $r_a > r_b > r_c$. If these ratios are equal to each other, they should be rearranged by considering the (x, y) coordinates of the normalised centre of gravity. This will be discussed in detail later.

6.3.1.3 Normalised Centre of Gravity of Colour Pattern.

The fourth column in Table 6.1 shows the normalised centre of gravity of each colour pattern. This normalised centre of gravity of each colour pattern in an object is obtained by the following steps:

(1) If a principal axis of an object is not parallel to the x-axis, every point in the object should be rotated by an angle which is formed with the principal axis and the x-axis on the centre of rotation, i.e., one of the principal axis.

(2) Once the principal axis has been rotated to be parallel to the x-axis, the centre of gravity of each pattern in the object is calculated.

(3) The (x, y) coordinates of the centre of gravity of each pattern which have previously been obtained are normalised.

In the first step, the angle which is formed with the principal axis PQ which has been obtained in section 5.3, and the x-axis is calculated using the method in section 5.3. If the angle is equal to zero, the rotation of every point is unnecessary otherwise every point in the object should be rotated by the method in section 5.3. In practice, the (x, y) coordinates of the rotated points are obtained by applying the (x, y) coordinates of every point in each unit which has an equal Cluster i.d. in the Auxiliary Means, to

221

Equations (5.3-5) and (5.3-6).

In the second step, the centre of gravity of each rotated pattern is calculated. Let the (x, y) coordinates of every point in the pattern be (x_{ri}, y_{ri}), and the centre of gravity of the pattern be $(\bar{x}_r, \bar{y}_r)$. The centre of gravity is calculated by

$$\bar{x}_r = \frac{\sum_{i=1}^{n} x_{ri}}{n},$$

$$\bar{y}_r = \frac{\sum_{i=1}^{n} y_{ri}}{n},$$

where n is the number of pixels in the pattern.

In the third step, the normalised centre of gravity is calculated. In this step, the most important (x, y) coordinates of the lower left corner of the rectangle ABDE in Figure 6.7 are respectively calculated as follows: the x-coordinate is the same as the x-coordinate of the point P, i.e., x_p, whereas the y-coordinate y_α is:

$y_\alpha = y_p - d,$

where d is the length of the principal axis PQ which is calculated by:

$d = (y_q - y_p).$

The distance d_2 between two points B and C' in Figure 6.7 is:

$d_2 = \bar{x}_r - x_p,$

where the point C' is the crossing point of the straight line DB and the vertical line from the point C which is the centre of

222

gravity of the pattern. The distance d3 between two points B and C" in Figure 6.7 is:

$$d_3 = \bar{y}_r - y_\alpha = \bar{y}_r - (y_p - d),$$

where the point C" is the crossing point of the straight line AB and the horizontal line from the point C. The normalised (x, y) coordinates of the centre of gravity of the rotated pattern ($\bar{x}_n$, $\bar{y}_n$) are calculated by:

$$\bar{x}_n = \frac{d_2}{d} = \frac{\bar{x}_r - x_p}{d}$$

$$\bar{y}_n = \frac{d_3}{d + d} = \frac{\bar{y}_r - y_\alpha}{d + d} = \frac{\bar{y}_r - (y_p - d)}{2d}$$
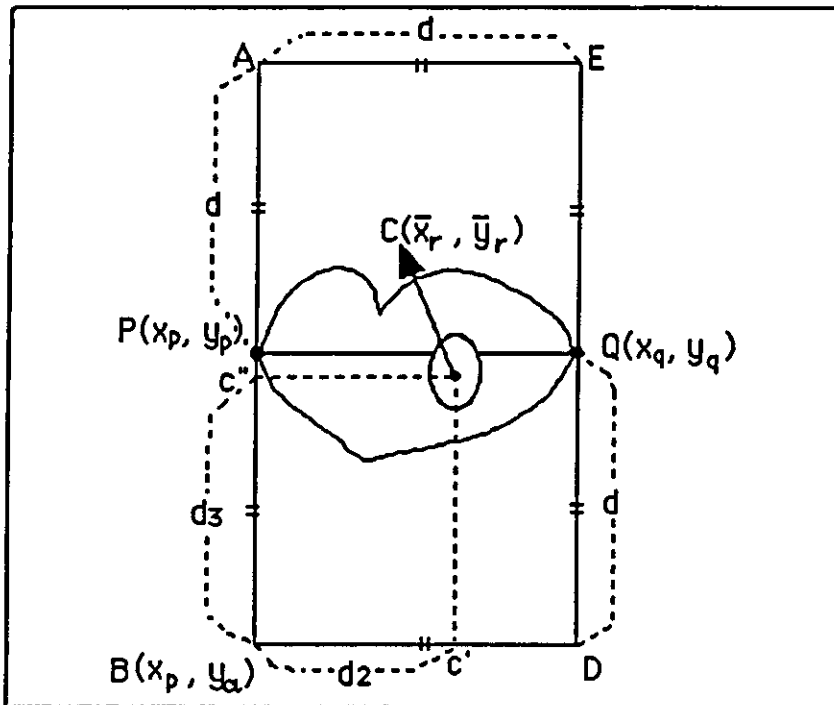
Figure 6.7 Calculation of the normalised centre of gravity.

6.3.1.4 The Slope of the Regression Line of Each Colour Pattern.

Since every point of the object has already been rotated in the previous process of the normalisation of the centre of gravity of a

223

pattern, the calculation of the slope of a regression line can be carried out immediately. In simple regression analysis, the regression line is represented by Equation (6.2 5-1):

$$Y_i = \beta_0 + \beta_1 X_i + \epsilon_i .$$

The intercept of the Y-axis, β_0, does not need to be involved in the shape description as illustrated in section 6.2.5, so the regression coefficient, β_1, which is generally regarded as a slope of a regression line is only considered in this stage. The regression coefficient is simply calculated by:

$$\beta_1 = \frac{n \sum_{i=1}^{n} x_i y_i - (\sum_{i=1}^{n} x_i)(\sum_{i=1}^{n} y_i)}{n \sum_{i=1}^{n} x_i^2 - (\sum_{i=1}^{n} x_i)^2}$$

$$= \frac{\sum_{i=1}^{n} (x_i - \bar{x}_r)(y_i - \bar{y}_r)}{\sum_{i=1}^{n} (x_i - \bar{x}_r)^2} ,$$

where x_i and y_i are respectively the x- and y-coordinate of every point in the rotated pattern, and $\bar{x}_r$ and $\bar{y}_r$ are respectively the x- and y-coordinate of the centre of gravity of the rotated pattern.

6.3.1.5 The Ratios for Segments of Each Colour Pattern.

Divide a pattern, which has already been rotated in the previous step, into four segments as shown in Figure 6.8, where the horizontal and vertical lines cross at the centre of gravity of the pattern. Let the area of each segment be S_1, S_2, S_3 and S_4. The area of each segment is obtained by simply counting the number of pixels in each segment. Let the area of the upper half of the

224

pattern be S_{H1}, and the area of the lower half of the pattern be S_{H2}. S_{H1} is $S_1 + S_2$, and S_{H2} is $S_3 + S_4$. The total area of the pattern, S_T, is $S_1 + S_2 + S_3 + S_4$.
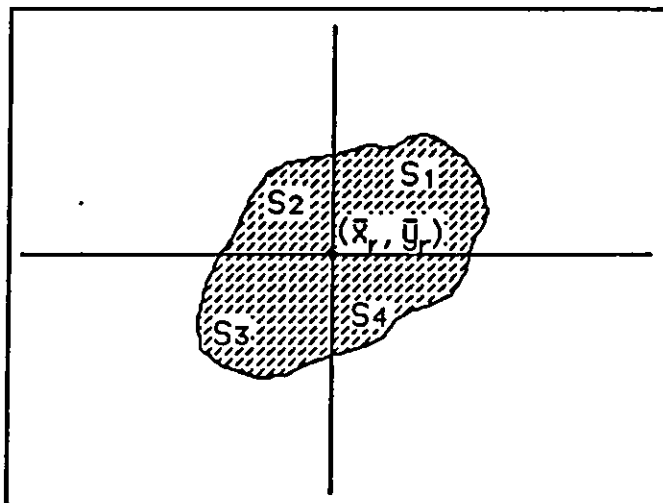
Figure 6.8 Segments of a pattern.

The ratio of the area of each segment over the total area of the pattern is:

$$Q_1 = \frac{S_1}{S_T}, \quad Q_2 = \frac{S_2}{S_T}, \quad Q_3 = \frac{S_3}{S_T}, \quad \text{and } Q_4 = \frac{S_4}{S_T}.$$

The ratio of the area of the upper half of the pattern over the total area is $H_1 = S_{H1}$, and the ratio of the area of the lower half of the pattern over the total area is $H_2 = S_{H2}/S_T$.

6.3.2 Hierarchical Organisation of Factors.

As briefly stated in the early stages of this section, once all the factors for colour pattern description have been obtained, these factors should hierarchically be organised in order to be efficiently used in the object identification stage. This hierarchical organisation is required not only for the object in the

225

library data but also for an object under consideration. Before performing the organisation, consider the following facts which are essential to optimise this organisation. The number of sets of factors by which an object is represented depends absolutely upon the number of patterns with distinctively different colours of which the object consists. Since the number of different colour patterns dominates the structure of the colour pattern descriptor, this factor can be used as an important variable. A crucial fact to be noted is that if an object image is obtained from a photograph, each colour element of the image is usually affected by many factors such as environmental conditions, film speed, the size of the aperture and shutter speed of a camera, etc. (Hunt, 1987). Consequently, the colour features of the image which are obtained from the photographs of an object with different environmental factors are not always identical to each other. However, if an image is captured under the ordinary environment, the number of different colour patterns is invariant to the environment. The reason for this is that the intrinsic nature of the colour features of a material of which the surface of an object consists is not changed with different environmental factors, but are viewed differently. This fact shows that the number of different colour patterns is obviously invariant to environmental change. The important point is that the same kind of objects, i.e., the same species of butterflies, usually have variations of value for each of factors except the number of different colour-pattern factors. Thus, the number of different colour pattern factors can be regarded as a primary factor for colour pattern description.

If the number of different colour patterns has been determined, the area of each colour pattern is determined in

226

relation to the total area of an object to which each pattern belongs. This factor is the ratio of the area of each colour pattern over the total area of an object. If an object consists of N different colour patterns, the number of ratios is N. To improve the efficiency of an identification process, it is necessary to arrange these ratios in descending order. If these ratios are not arranged in this order, the process will unnecessarily spend time on searching the library data for a corresponding ratio. Once these ratios are arranged in the descending order, other factors such as the normalised centre of gravity, slope of regression line and ratios for the shape of each colour pattern should accordingly be arranged. On the other hand, since the colour feature factor has variations depending upon environmental factors, it is reasonable to place this factor at the end of the hierarchy. Thus, these factors are arranged in the hierarchical structure as shown in Figure 6.9. Finally, the name of an object is put on the bottom of the structure. For example, if an object has three different colour patterns, and the descending order of the ratios for these patterns is $r_a > r_b > r_c$, then the factors are organised as shown in Figure 6.9. On the top of the Figure 6.9, the number of colour patterns is placed, r_a, r_b and r_c on the second level are the ratios, where each ratio r_j is obtained by:

$$r_j = \frac{\text{(the number of pixels in each colour pattern)}}{\text{(the number of pixels in an object)}} \quad .$$

227
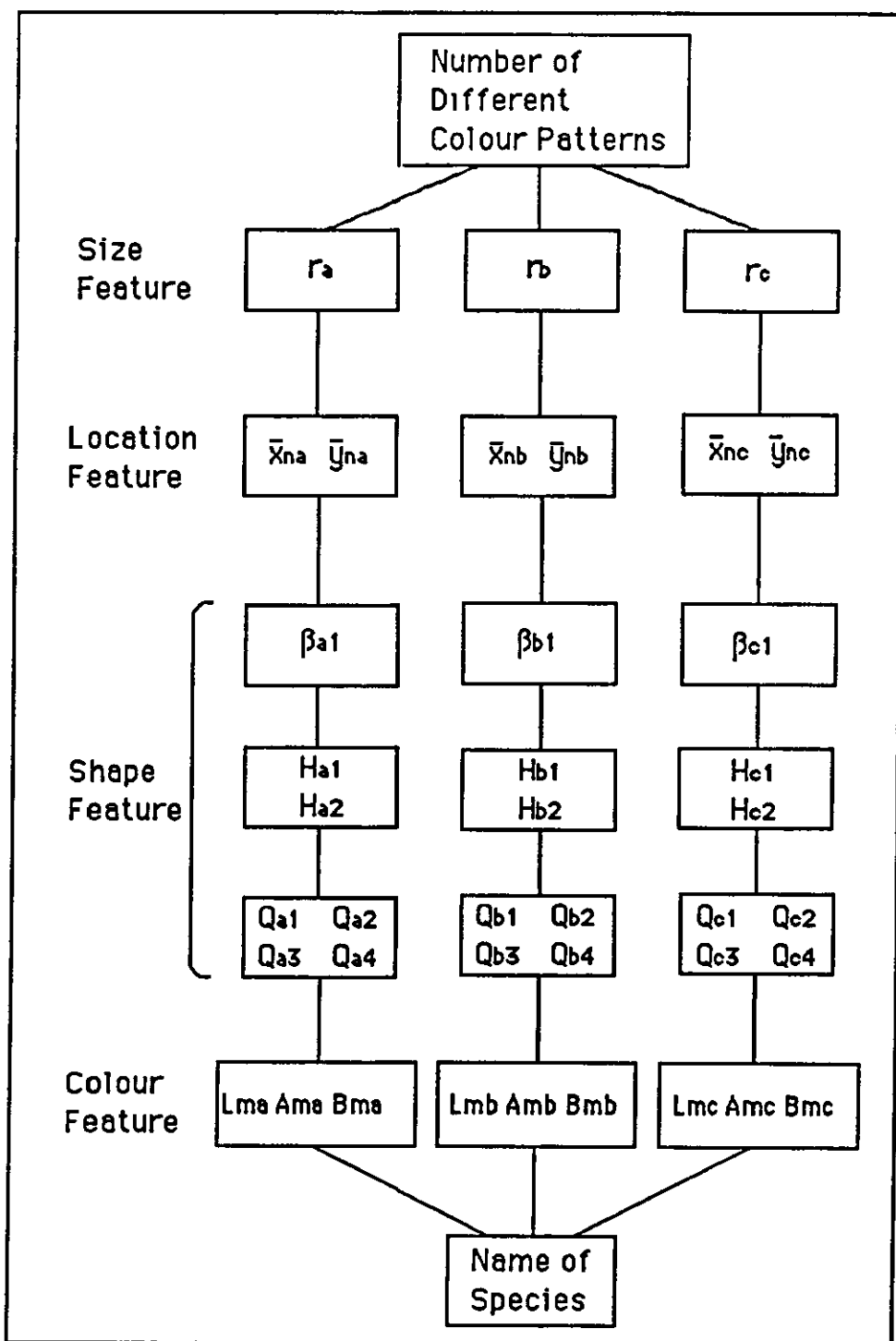
Figure 6.9 The hierarchical organisation of factors.

On the third level, $(\bar{X}_{na}, \bar{Y}_{na})$, $(\bar{X}_{nb}, \bar{Y}_{nb})$ and $(\bar{X}_{nc}, \bar{Y}_{nc})$ are the normalised centre of gravity of each colour pattern. On the fourth level, β_{a1}, β_{b1} and β_{c1} are the slope of a regression line of each

228

colour pattern. On the fifth level, [Ha_1, Ha_2], [Hb_1, Hb_2] and [Hc_1, Hc_2] are ratios, where each ratio H$_j1$, where j=1, 2, 3, is obtained by:

$$H_{j1} = \frac{(\text{the number of pixels in the upper half segment})}{(\text{the number of pixels in each object})}$$

and each ratio H$_j2$ is obtained by:

$$H_{j2} = \frac{(\text{the number of pixels in the lower half segment})}{(\text{the number of pixels in each object})}$$

On the sixth level, Q$_j1$, Q$_j2$, Q$_j3$ and Q$_j4$, where j=1, 2, 3, are ratios, where each ratio is obtained by:

$$Q_j = \frac{(\text{the number of pixels in a segment})}{(\text{the number of pixels in an object})}$$

On the seventh level, [Lm_j, Am_j, Bm_j], where j=1, 2, 3, are respectively the centre of gravity of L*a*b* of each colour pattern. On the bottom level, the name of the species is placed. An important fact to be noted is that all the factors are invariant to the size, orientation and location of an object.

6.4 CONCLUSION.

It is well known in the region description domain that most pattern (region) descriptors should satisfy the basic requirements that every pattern descriptor should be invariant to the size, orientation and location of an object to which each pattern belongs. Among the descriptors which have been commonly used in the description of each pattern of an object in a black-and-white image, such descriptors as a measure of compactness, which is defined as $(perimeter)^2/area$, and the Euler number, i.e., the number of holes in an object, are invariant to the size, orientation and location of an object. On the other hand, the majority of pattern descriptors such as the area, orientation of the principal axis and centre of gravity of each pattern are variant on the size, orientation and location of an object, thus they do not satisfy the basic requirements.

These requirements are particularly important in colour pattern descriptors for biological objects because the images of these objects are usually obtained from photographs or video films. When these objects are taken by camera, the sizes, orientations and locations of these objects are not always constant. In the biological objects, each colour pattern has its own features such as colour feature, size feature, location feature and shape feature. Since these features are constant within an object, if the size, orientation and location of the object image is changed these features except the colour features are accordingly changed. In this chapter, the six major factors which are required to represent these features of each colour pattern of an object have been defined. These factors have been

designed to accommodate the basic requirements. These factors can be generally used in the colour pattern description domain. Additionally, these factors have been hierarchically organised in order to be efficiently used in the object identification process.

Chapter 7

THE STRUCTURE OF THE SPECIES IDENTIFICATION SYSTEM.

7.1 Introduction.

7.2 Configuration of Hardware and Software.

7.3 Species Identification System.

    7.3.1 Learning System.

    7.3.2 Implementation System.

    7.3.3 Leaf Species and Butterfly Species Identification Systems.

        7.3.3.1 Leaf Species Identification System.

        7.3.3.2 Butterfly Species Identification System.

7.4 Conclusion.

7.1 INTRODUCTION.

In the previous chapters, the representation methods for biological objects which were developed in this thesis have been discussed. In this chapter, all the representation methods are integrated into a prototype system. There are two prototype systems: one for leaves and another for butterflies. The system for leaves was designed to evaluate the algorithms for shape description. On the other hand, the system for butterflies was designed to evaluate the algorithms for shape description, colour pattern extraction and colour pattern description. Each prototype system consists of two subsystems:-

o a learning system, and

o an implementation system.

The learning system was designed to calculate variations of the external features of biological objects such as size, shape and colour pattern within a species. The implementation system was designed to identify a species under test by referring the lower and upper limits of each descriptor determined by the learning system. These systems were designed to be easily expanded into an actual system which would be used for various purposes such as discovering a new species and so on in biology.

Each system was tested using sample species in the validation stage. The results of the experiment were discussed based on two aspects:

(1) the identification ability of each system, and

(2) the effectiveness of the descriptors in the discrimination of the sample data.

7.2 CONFIGURATION OF HARDWARE AND SOFTWARE.

In this section, the configuration of the hardware and software which are basically required for a prototype system is illustrated. The prototype system was established based on the configuration in Figure 7.1. The main body of ˷ this system was built using the C programming language installed on a Hewlett Packard workstation running under Unix version 8B, where the X-window system was utilised to display a colour image on a VDU.
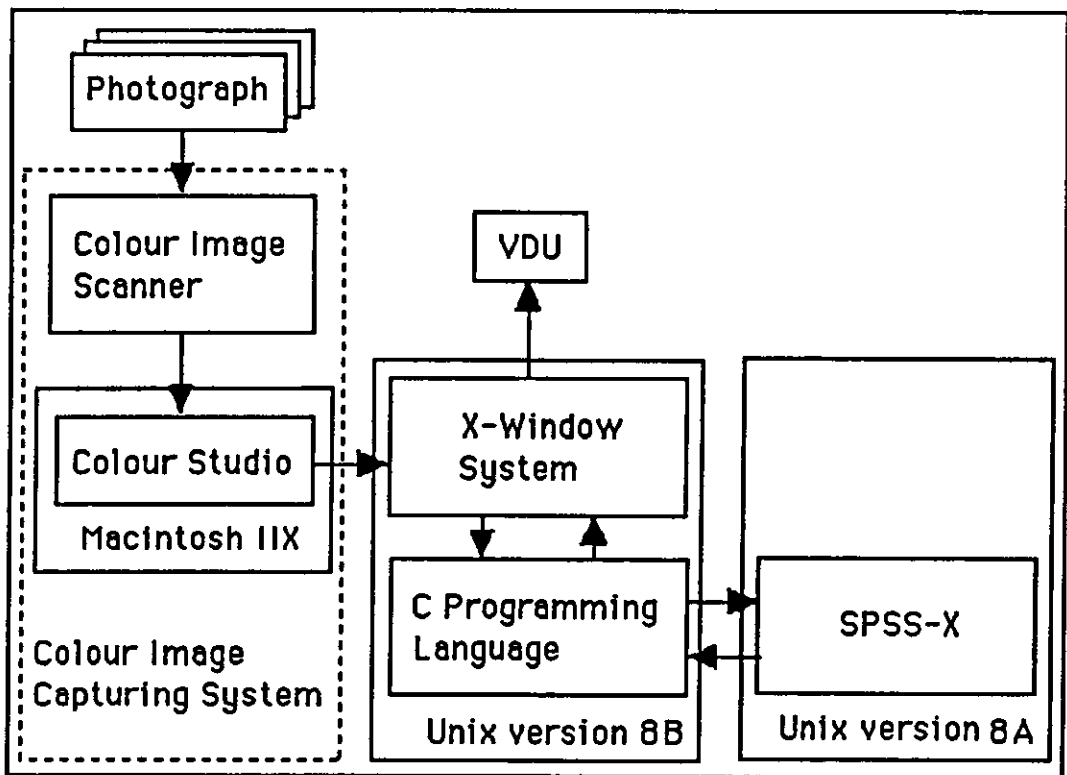
Figure 7.1 Configuration of hardware and software.

The colour image of an object is captured by a colour image scanner (JX600) connected to a Macintosh IIX system, where the Colour Studio application, installed on the Macintosh system, is utilised to digitise a scanned image. A digitised colour image is

234

transferred to Unix version 8B. This digitised colour image is used as input data to the prototype system. In the processing stage for colour pattern extraction, input data to the Cluster Analysis are transferred to Unix version 8A where the SPSS-X application, a statistical package, is installed. A Cluster Analysis routine in the SPSS-X produces the result using thise input data. This result is transferred to Unix version 8B and is used for colour pattern extraction.

7.3 SPECIES IDENTIFICATION SYSTEM.

A species identification system consists of two subsystems:

o a learning system, and

o an implementation system.

The learning system was designed to calculate variations of the external features of biological objects such as size, shape and colour pattern within a species. The implementation system was designed to identify a species under test, based on the lower and upper limits of each descriptor determined by the learning system.

There are two species identification systems which were separately designed to evaluate the representation methods, which were developed in this thesis, by applying sample objects: leaves and butterflies. The prototype system for leaves was designed to evaluate the algorithms for shape description. On the other hand, the prototype system for butterflies was designed to evaluate the algorithms for shape description, colour pattern extraction and colour pattern description. These prototype systems were designed only to examine basic functions such as the calculation of each descriptor since the main objective of this thesis lies in the development of biological object description methods. However, these systems are easily expanded into actual systems which can be used for various purposes such as discovering a new species and so on. For the actual system, an expertise in the relevant domain and plenty of sample images to cover each species are required.

7.3.1 Learning System.

As discussed in Chapter 1, the external features of biological objects vary in size, shape and colour pattern within a species, thus a species identification system should accommodate these variations. In order to satisfy this principle, a learning system was designed to calculate the variation of each descriptor which was extracted from the images of the sample species. For each descriptor, the lower and upper limits are determined by a statistical normalisation method. The normalisation method consists of two steps:

(1) Calculate the mean and standard deviation of each descriptor using the images of the sample species.

(2) Infer the lower and upper limits of a population distribution using the sample mean and standard deviation.

Let the sample mean value of a descriptor be M, the sample standard deviation S. The lower and upper limits are inferred by using the sample mean and standard deviation as follows:

o the lower limit: M - 3S,

o the upper limit: M + 3S,

where the lower and upper limits cover the 99.74 % of the normal distribution with the mean M and standard deviation S. The reason for this statistical normalisation using the sample mean and standard deviation is that even for an actual system it is impossible to collect all of the images of objects in every species.

7.3.2 Implementation System.

Once the lower and upper limits of each descriptor for each species is determined by a learning system using given samples,

an object image which is under test is examined by an implementation system. This implementation system was designed to evaluate values of every descriptor, that is, to examine whether or not each value was within the lower and upper limits of the corresponding descriptor previously calculated by the learning system. If a value of a descriptor is within the ranges, it is decided that the value of the descriptor is identical to that of the corresponding ratio previously learned. Otherwise, it is decided that the value of the descriptor is different from that of the corresponding descriptor. Thus this implementation system was designed to summarise the detailed results of the examination which would be utilised in further analysis in a relevant domain.

7.3.3 Leaf Species and Butterfly Species Identification Systems.

7.3.3.1 Leaf Species Identification System.

A leaf species identification system was designed to identify leaf species based on the shape of the leaf. This system consists of a learning system and an implementation system. The learning system was designed to build up library data using the images of the sample species. The library data were designed to contain the lower and upper limits of each ratio in a ratio tree for each species and the name of the species. The implementation system was designed to identify leaf species by examining whether or not the value of each ratio in a ratio tree was within the ranges of the corresponding ratio in the library data, which were built up by the learning system.

238
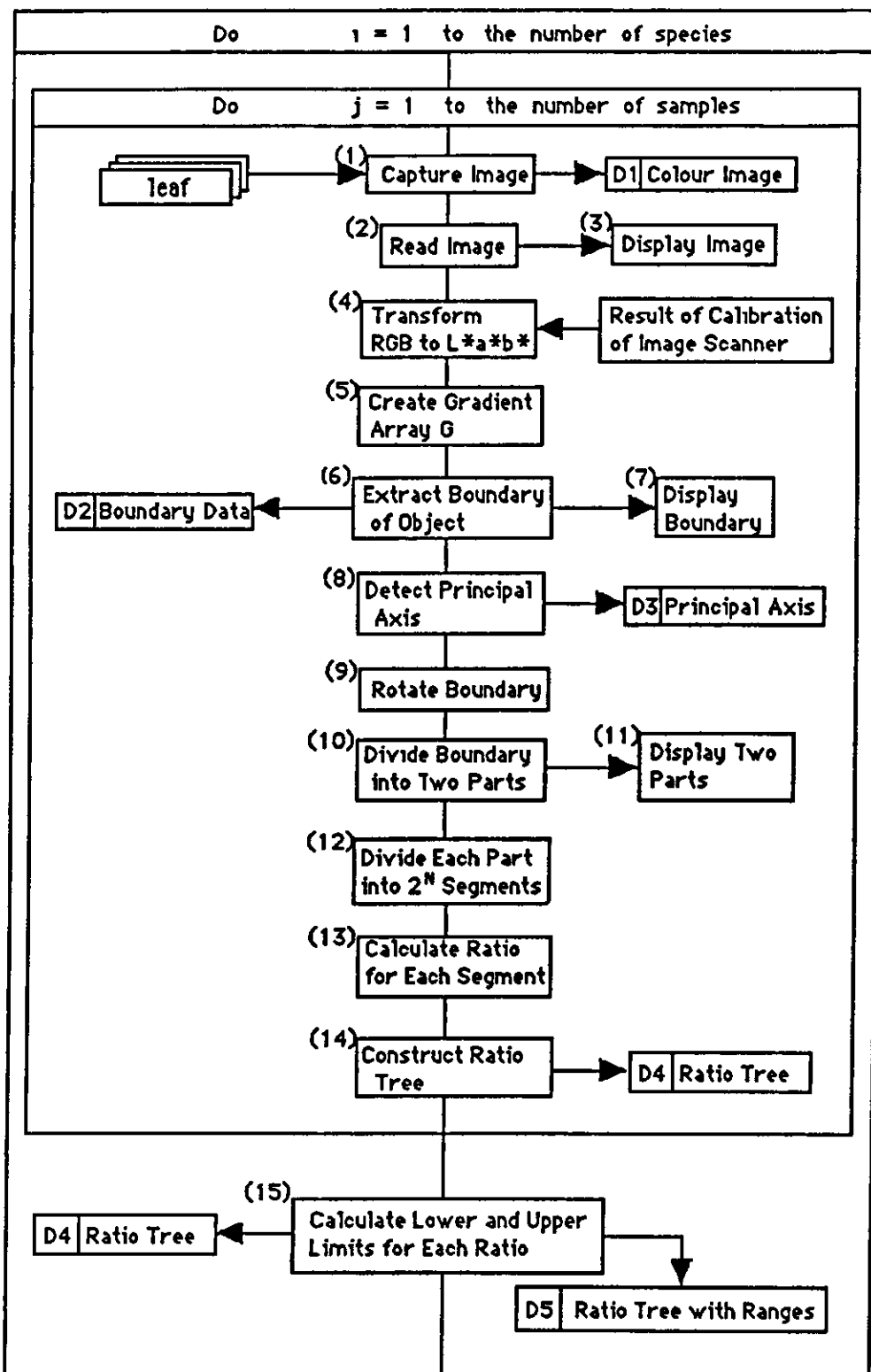
Figure 7.2 A flow chart of a learning system for a leaf species identification system.

Let us consider the detailed procedure of the learning system as shown in Figure 7.2, for leaf species identification. In Figure 7.2, a number in parentheses on the upper left corner of a box represents a process; and a D and a number in a box at the left-hand end represents a file. In process 1, each leaf is scanned using a colour image scanner which is connected to a Macintosh IIX, where a colour image D1, which is composed of R, G and B values, is created. This image is transferred to Unix version 8B. In process 2, this image is read. Thus, this image is displayed on the CRT screen to verify that it is the correct image. In process 4, the R, G and B values of each pixel in the image are transformed into L^*, a^* and b^* values, where the result of the calibration of the image scanner is employed. In process 5, a gradient array G is created by applying L^*, a^* and b^* values of each pixel in the image. In process 6, the boundary of an object in the image is extracted using the gradient array G. The extracted boundary data are stored in file D2 and this boundary image is displayed, again for verification. In process 8, a principal axis of the boundary is detected, where two (x, y) coordinates of the extreme points, which form the principal axis of the boundary, are obtained. These (x, y) coordinates are stored in file D3. In process 9, the boundary is rotated in order to make the principal axis parallel to the x-axis. In process 10, the rotated boundary is divided into two parts, that is, the upper part and the lower part. To verify this process, the boundary with the principal axis is displayed on the CRT screen. In process 12, each part is divided into 2^N segments. In process 13, the ratio for each segment is calculated. In process 14, a ratio tree is constructed using the ratio calculated in the previous process. This ratio tree is stored in file D4 each time through the loop. That is for 10 samples D4 would contain 10 ratio

240

trees. If all the sample images of a species are processed, the lower and upper limits of each ratio are calculated in process 15. These lower and upper limits for each species are stored in file D5. This file is used as the library data in the implementation system and thus contains a single ratio tree with ranges.

Let us consider the detailed procedure of the implementation system in Figure 7.3, for a leaf species identification system. The functions of the processes 1 through to 14 in Figure 7.3 are exactly the same as those of the processes 1 through to 14 in Figure 7.2. The contents of the files D1 through to D4 in Figure 7.3 are similar to those of the files D1 through to D4 in Figure 7.2. As soon as a ratio tree is produced in process 14 in Figure 7.3, each ratio is examined, in process 15, whether or not it is within the lower and upper limits of its corresponding ratio in D5 which has been created in the learning stage. Finally, in process 16, the result of the comparison is displayed.

Start

(1) Capture Image → D1 | Colour Image

leaf →

(2) Read Image → (3) Display Image

(4) Transform RGB to L*a*b* ← Result of Calibration of Image Scanner

(5) Create Gradient Array G

D2 | Boundary Data ← (6) Extract Boundary of Object → (7) Display Boundary

(8) Detect Principal Axis → D3 | Principal Axis

(9) Rotate Boundary

(10) Divide Boundary into Two Parts → (11) Display Two Parts

(12) Divide Each Part into 2^N Segments

(13) Calculate Ratio for Each Segment

D4 | Ratio Tree ← (14) Construct Ratio Tree

D5 | Ratio Tree with Ranges

(15) Compare Each Ratio in D4 with That in D5

(16) Display the Result of Comparison

End

Figure 7.3 A flow chart of an implementation system for a leaf species identification system.

242

In the validation stage, two different kinds of leaf species, as shown in Figure 7.4, were chosen to test the system. As Table 7.1 shows, ten samples of Species A and sixteen samples of Species B were randomly selected from the given samples for the learning stage; and five samples for Species A and ten samples for Species B were selected for the implementation stage.

Species	No. of Samples in the Learning Stage	No. of Samples in the Implementation Stage	Total
Species A	10	5	15
Species B	16	10	26
Total	26	15	41

Table 7.1 The number of samples involved in the validation stage.

The original image of each species is shown in Figures 7.4.(a) and (b). In process 6, the boundary of each sample as shown in Figures 7.4.(c) and (d) was extracted. As Figures 7.4.(e) and (f) show, a principal axis of each boundary was detected. As the shapes of the species show, the shape of each species is completely different. Thus, in process 12, the upper and lower parts of the boundary were divided into 2^3 segments as shown in Figures 7.4.(i) and (j). After a calculation of the ratio for each segment using samples involved in the learning stage, the library data containing the lower and upper limits of each ratio were created.

In the implementation stage, the ratio for each segment of individual test species was calculated and examined whether or not it was within the lower and upper limits of its corresponding ratio of each species in the library data which had been created in the learning stage. The result of the test undertaken is shown in

Species A   **Species B**

(a)   (b)

(c)   (d)

(e)   (f)

(g)   (h)

(i)   (j)
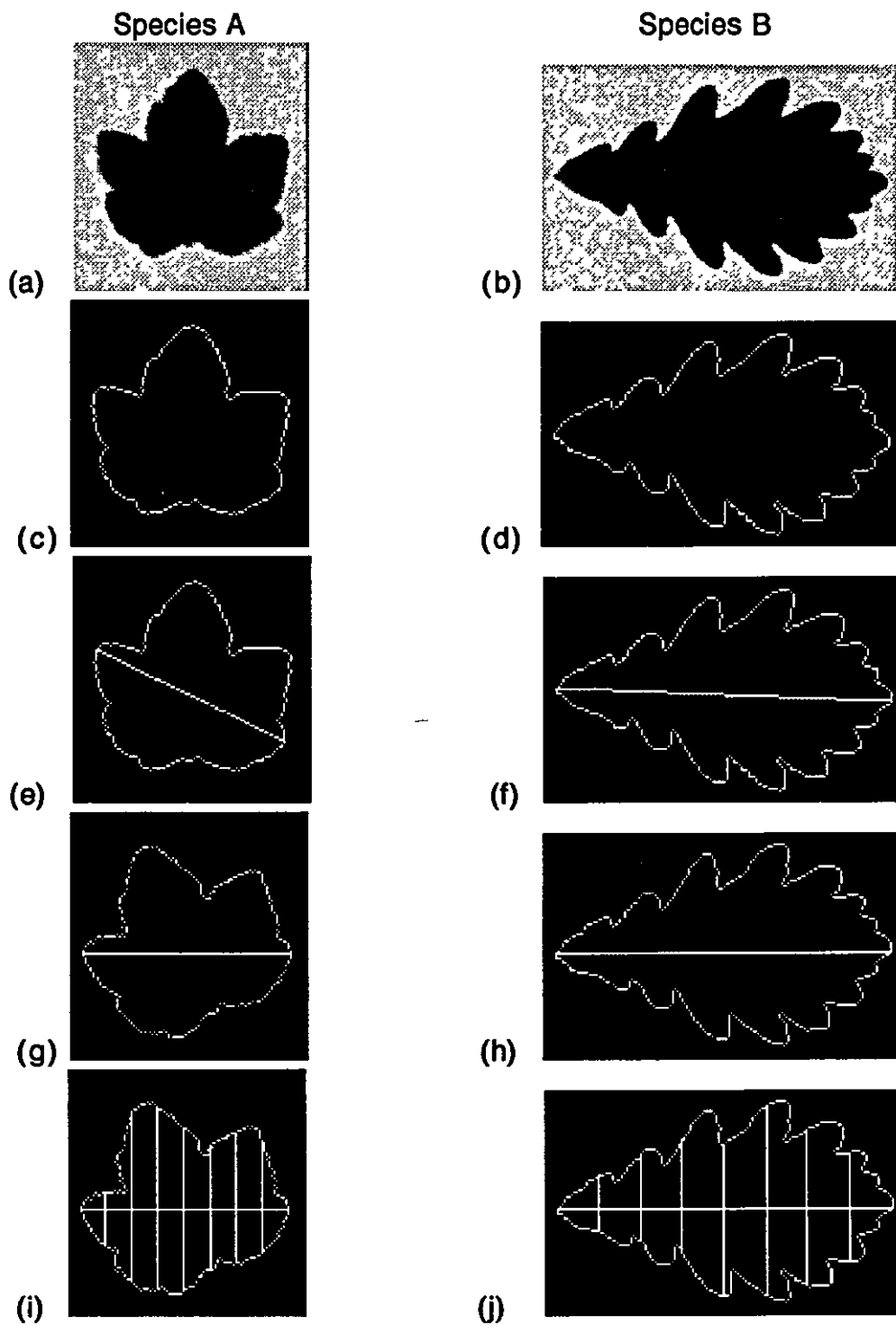
Figure 7.4 Sample images. (a) and (b) Original images. (c) and (d) Boundaries extracted. (e) and (f) Principal axes. (g) and (h) Rotated boundaries. (i) and (j) Segmented boundaries.

Table 7.2. The method for the test was that if the ratio for every segment calculated using a test sample species was within the range of its corresponding ratio of a species in the library data, it was considered as the same species that was in the library data. In the test with five samples of Species A, four samples were correctly identified as Species A, while one sample was not identified, because only one ratio was determined as an outlier. In the test with ten samples of Species B, nine samples were identified as Species B, while one sample was not identified. Consequently, 87% (13 out of 15) of the samples were correctly identified.

Species	No. of Test Samples	Identified	Failed
Species A	5	4	1
Species B	10	9	1
Total	15	13	2

Table 7.2 The result of the identification test.
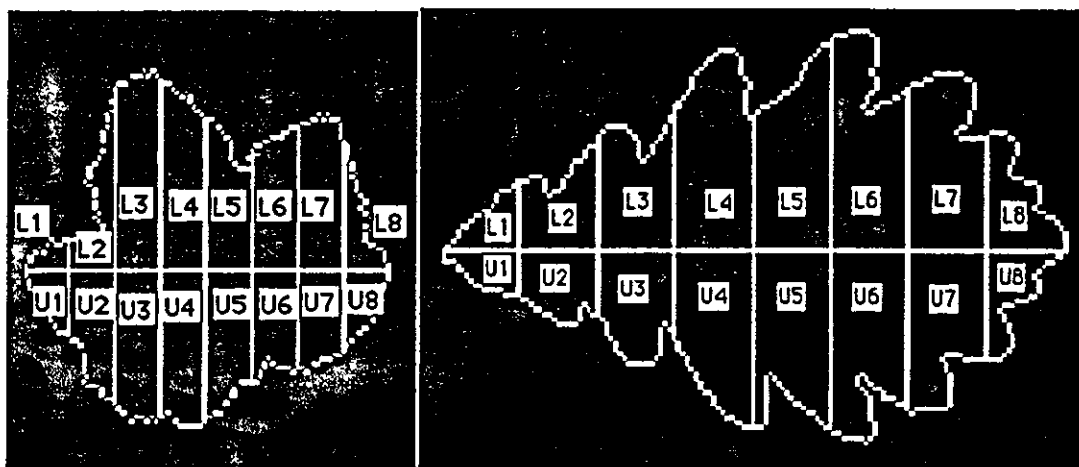
Figure 7.5 The ratio for each segment.

In order to examine the effectiveness of these descriptors (ratios) in the leaf species classification using distributions of sample species, 16 samples were selected from each species. Let

the samples of Species A be group 1 and those of Species B group 2. Let the ratio for each segment in the lower part be U1, U2, U3, ..., U8 and that in the upper part be L1, L2, L3, ..., L8 as shown in Figure 7.5. The diagrams in Figure 7.6 show the distribution of the sample species. The diagram in Figure 7.6.(a) is a scatter diagram of the U1 values against the L1 values; that in Figure 7.6.(b) is a scatter diagram of the U3 values against the L3 values. In each diagram, each of the points represents individual sample species; and the number '1' represents group 1 and the number '2' group 2. The diagrams in Figures 7.6.(c) and (d) are respectively the same diagrams in Figures 7.6.(a) and (b), where one-dimensional distribution of the values corresponding to each axis is added to each axis. The points in Figure 7.6.(a) can be categorised into their corresponding groups by a vertical line against the U1-axis, as Figure 7.6.(c) shows, since the one-dimensional distributions of the U1 values of both groups can be clearly separated; however these points cannot be categorised into their corresponding groups by a vertical line against the L1-axis because the one-dimensional distributions of the L1 values of both groups are completely overlapped, as Figure 7.6.(c) shows. On the other hand, the points in Figure 7.6.(b) can be categorised into their corresponding groups by a vertical line and a horizontal line, as Figure 7.6.(d) shows, because the one-dimensional distributions of the U3 values of both groups can be clearly separated and those of the L3 values of both groups can be clearly separated. This reveals that the points cannot be separated into their corresponding groups by the ratio L1, but they can be clearly separated by the ratios U1, L3 and U3. It can be concluded that if all of the ratios are simultaneously used in the identification stage, as already explained in Chapter 5, these samples can be completely

categorised into their corresponding groups.

Additionally, in an actual system with various shapes of species, the number of segments of the upper and lower parts of the boundary should be increased depending upon the accuracy of the result which is required.
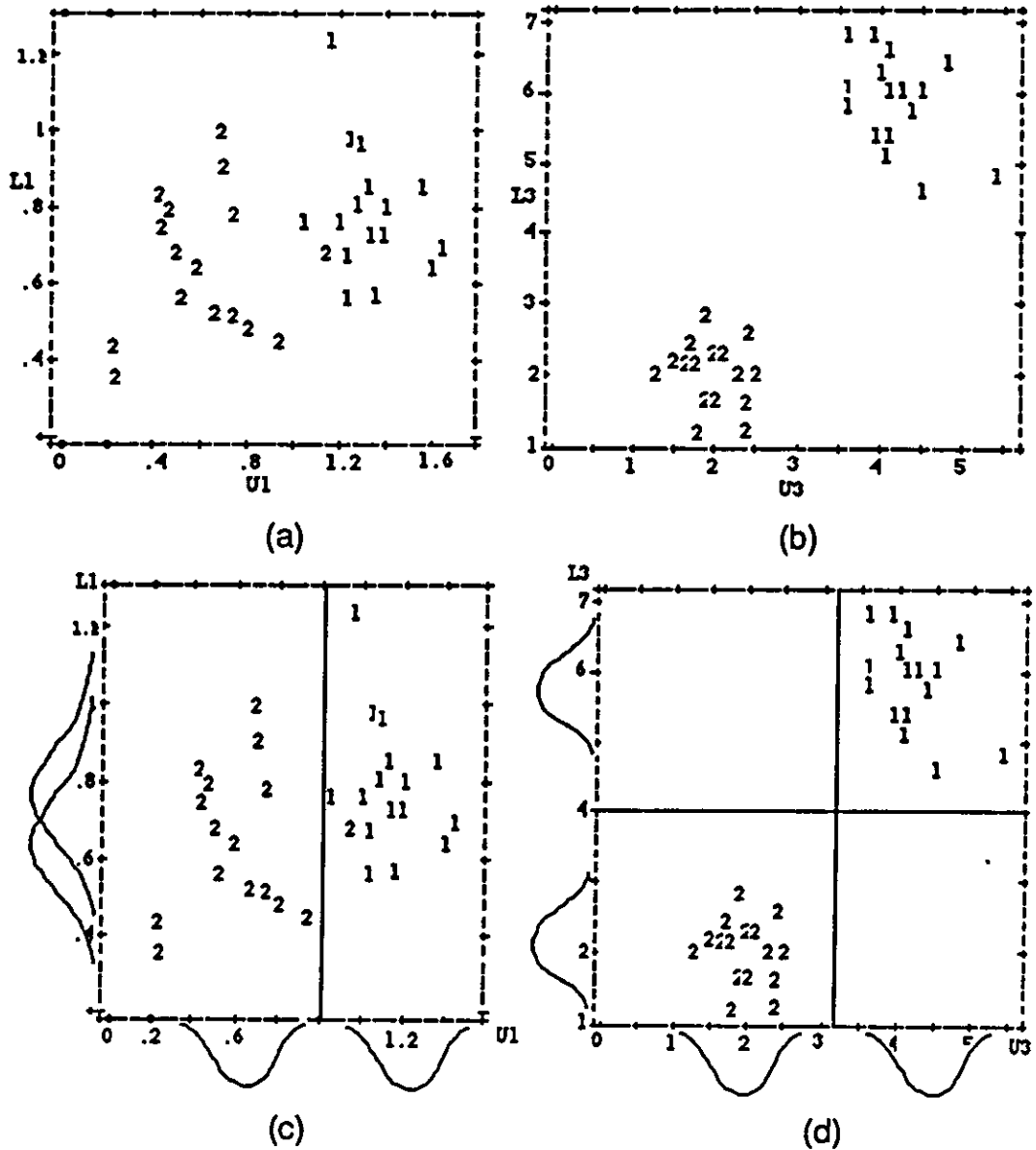
Figure 7.6 Scatter diagrams. (a) and (c) Scatter diagrams of the U1 values against the L1 values. (b) and (d) Scatter diagrams of the U3 values against the L3 values.

7.3.3.2 Butterfly Species Identification System.

A butterfly species identification system was designed to identify butterfly species based on the wing shape and colour pattern on the wings. This system also consists of a learning system and an implementation system. Due to the variations of the shape and the colour pattern in a species, the learning system was designed to build up library data using the images of the same species. The library data were designed to contain the lower and upper limits of each descriptor for each species and the name of the species. The implementation system was designed to identify butterfly species by examining whether or not the value of each descriptor was within the ranges of the corresponding descriptor in the library data, which were built up by the learning system. In the butterfly domain, both the colour pattern and the wing shape are commonly used for butterfly species classification. Thus, the implementation system was designed to identify butterfly species by alternatively using the shape of the wings.

Let us consider the detailed procedure of the learning system as shown in Figure 7.7 and 7.8, for butterfly identification. The functions of the processes 1 through to 14 in Figure 7.7 are exactly the same as those of the processes 1 through to 14 in Figure 7.2. The contents of the files D1 through to D5 in Figure 7.7 are similar to those of the files D1 through to D5 in Figure 7.2. In process B in Figure 7.7, colour patterns are extracted from an image created in process 1. The detailed procedure for this process is depicted in Figure 7.8. As soon as process 14 in Figure 7.7 is carried out, the image of an object is extracted from the

248

colour image stored in file D1 in process 15 in Figure 7.8, where the boundary data stored in file D2 are used. The image extracted in process 15 is displayed on the CRT screen. In process 17, this image is rotated to make the principal axis parallel to the x-axis. In process 19, the Auxiliary Means is created by using the rotated image. After a random noise test, N sets of L*, a* and b* data are extracted from the Auxiliary Means in process 22, where N is the number of pixels with different colour features in the image of an object. File D8 is transferred to Unix version 8A where the SPSS-X is available. A Cluster Analysis routine in the SPSS-X is executed in process 23. The result of the Cluster Analysis is transferred to Unix version 8A. In process 24, this result of the Cluster Analysis is assigned to the Auxiliary Means, where the number of colour patterns supplied by the user is used to determine the number of clusters. In process 24, each colour pattern extracted is displayed for a visual test. After the visual test, in process 26, five different kinds of major factors for description are calculated. This calculation is repeated as many times as the number of colour patterns. In process 27, major factors calculated in process 26 are arranged in descending order according to the value of the size factor. The major factors arranged are stored in file D15. If all the sample images of a species are processed, the lower and upper limits of each descriptor are calculated in process 28. This process produces two important files D5 and D16. The D5 is used as the library data for colour pattern description in the implementation system.
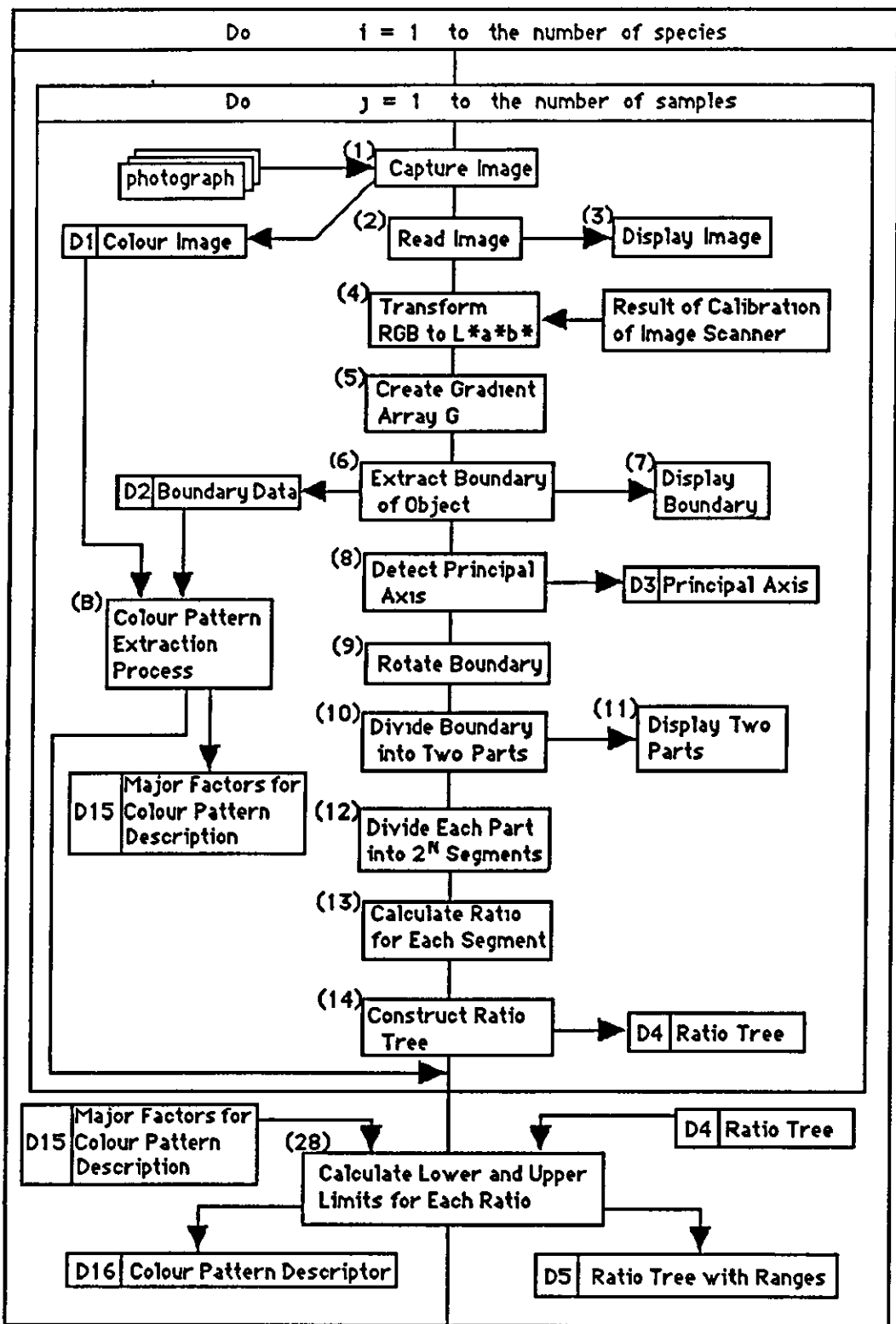
Figure 7.7 A flow chart of a learning system for a butterfly species identification system.
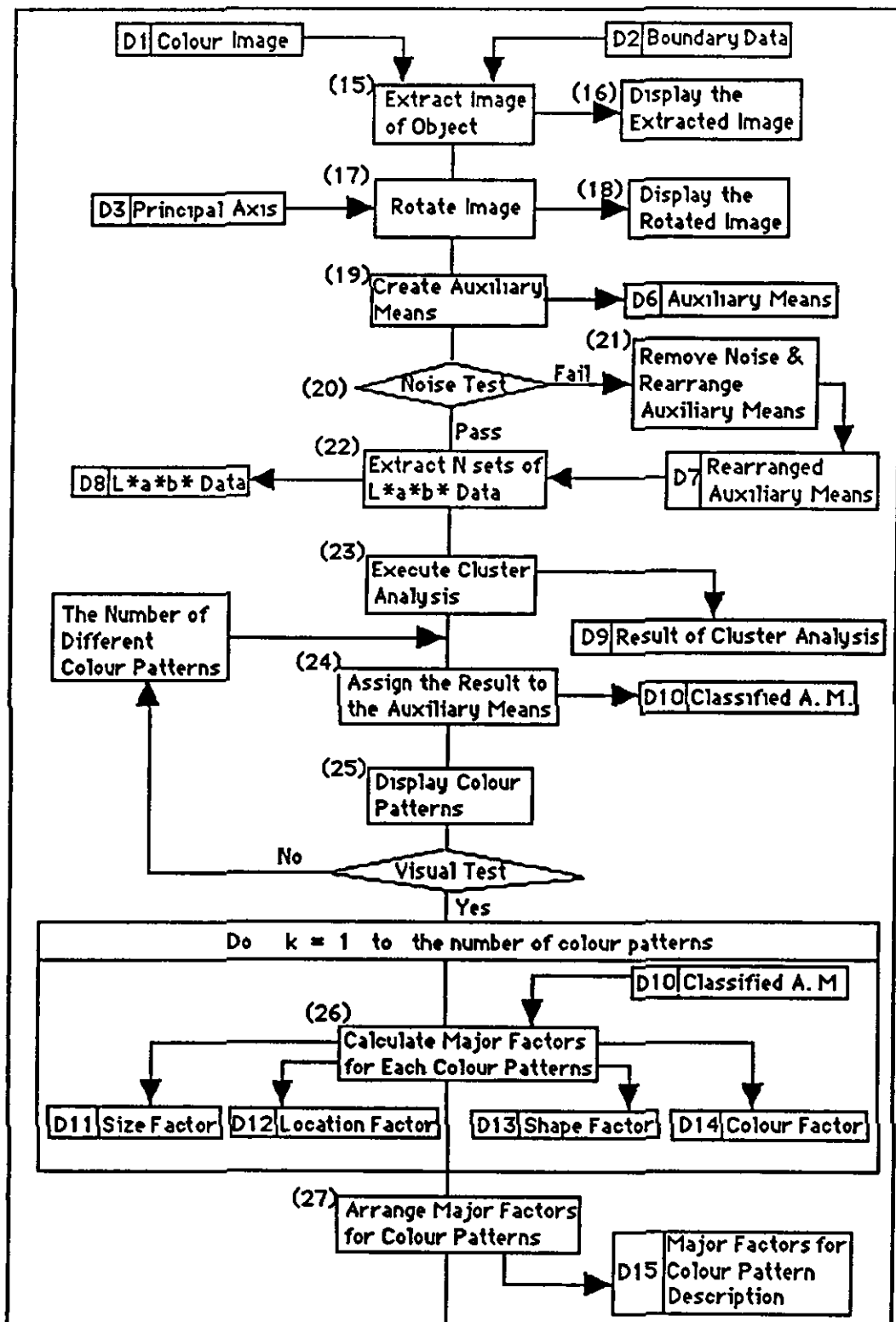
Figure 7.8 A flow chart of a colour pattern extraction process.

251

Let us consider the detailed procedure of the implementation system for a butterfly species identification system. In the case of a butterfly species identification system relying on the wing shapes, the implementation system is exactly the same as that for the leaf species identification in Figure 7.3. On the other hand, for a butterfly species identification system relying on the colour patterns on the wings, the flow chart of the implementation system is depicted in Figure 7.9. The functions of the processes 1 through to 7 in Figure 7.9 are exactly the same as those of the processes 1 through to 7 in Figure 7.7. The contents of the files D1, D2 and D15 in Figure 7.9 are similar to those of the files D1, D2 and D15 in Figure 7.7. Whereas, the detailed procedure for the process B in Figure 7.9 is also exactly the same as that in Figure 7.8. In process 28 in Figure 7.9, each major factor value stored in file D15 is compared with the corresponding major factor value in file D16 in the hierarchical order in Figure 6.8 in Chapter 6. Finally, the result of the comparison is displayed.
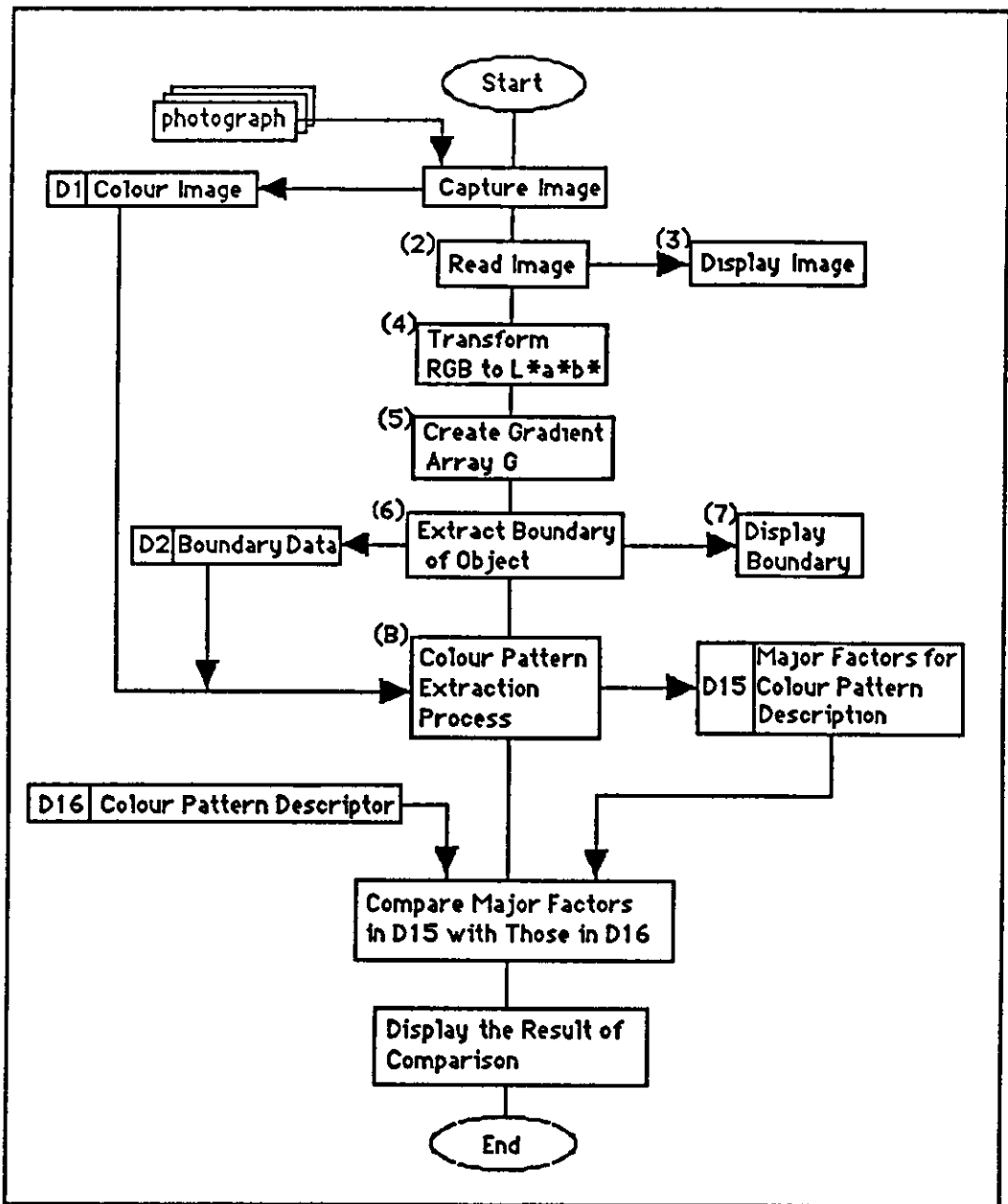
Figure 7.9 A flow chart of an implementation system for a butterfly species identification system with colour patterns.

In the validation stage, two different kinds of butterfly species, as shown in Figure 7.10.(a) and Figure 7.11.(a), were chosen to test the system. As Table 7.3 shows, ten samples for each species were randomly selected from the given samples for the learning stage; and five samples for each species were selected for the implementation stage.

Species	No. of Samples in the Learning Stage	No. of Samples in the Implementation Stage	Total
Species A	10	5	15
Species B	10	5	15
Total	20	10	30

Table 7.3 The number of samples involved in the validation stage.

As the images show, the wing shapes of each species were completely different. The species identification by shape had been performed in the leaf species identification, therefore in this validation stage the butterfly species identification was carried out based on the colour pattern of the wings. The butterfly has four wings: two wings on the left-hand side and another two on the right-hand side. The shapes and patterns of the one-side wings are exactly the same as those of the other-side wings. In the butterfly domain, one-sided wings are generally used for species classification. Thus, in this experiment the images of the left-hand-side wings were manually extracted to concentrate on the validation test of the algorithms for colour pattern extraction and its description. In process 15 in Figure 7.8, two different colour patterns for species A, as shown in Figures 7.10.(b) and (c), were extracted; three different colour patterns for species B, as shown in Figures 7.11.(b), (c) and (d), were extracted. As Figures
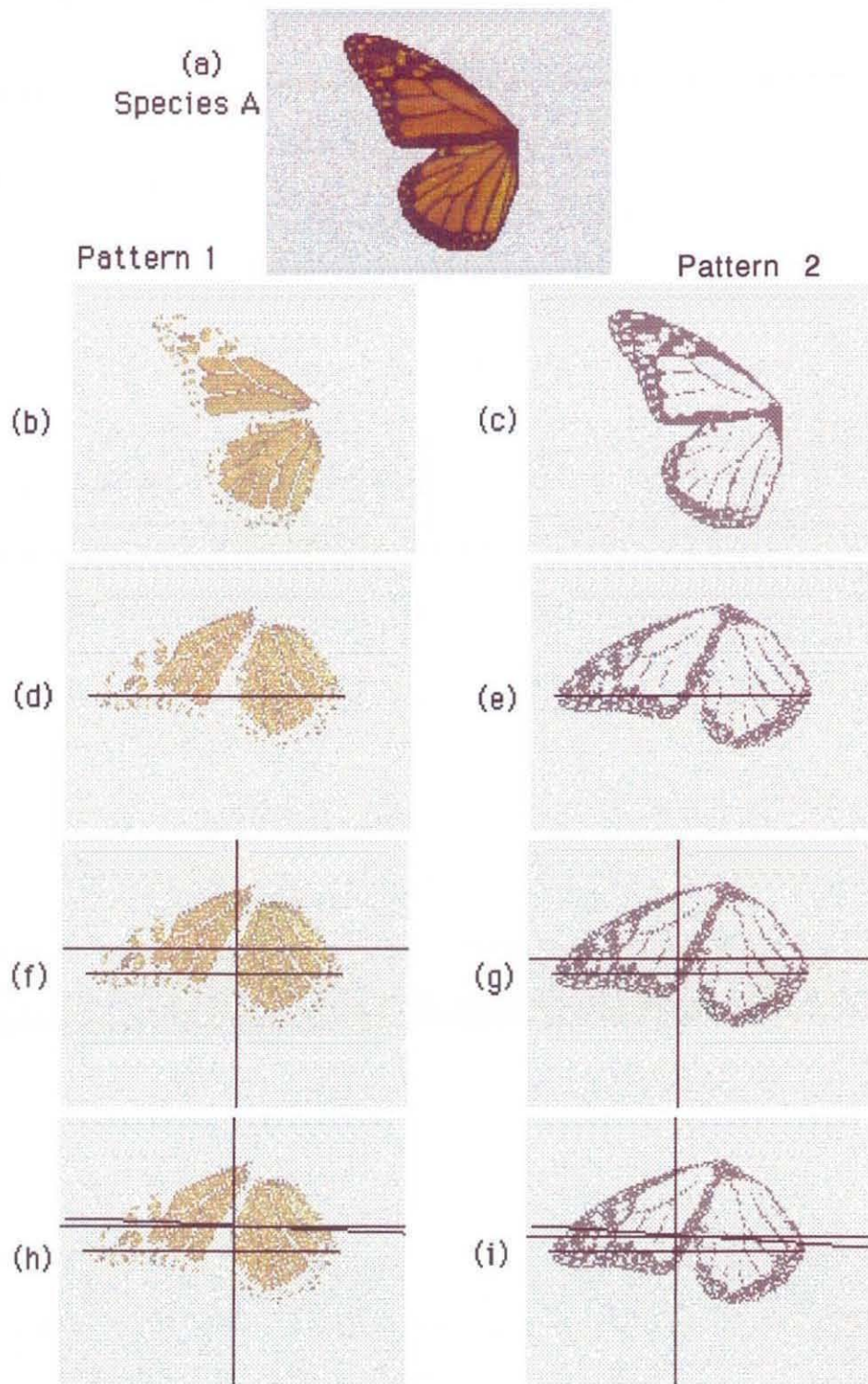
Figure 7.10 Wing patterns and major factors for each pattern of Species A. (a) The left-hand side wings. (b) and (c) Colour patterns. (d) and (e) Rotated patterns and principal axis. (f) and (g) Centre of gravity and four quadrants. (h) and (i) Regression lines.

255

(a) Species B

Pattern 3   Pattern 4   Pattern 5

(b)   (c)   (d)

(e)   (f)   (g)

(h)   (i)   (j)

(k)   (l)   (m)
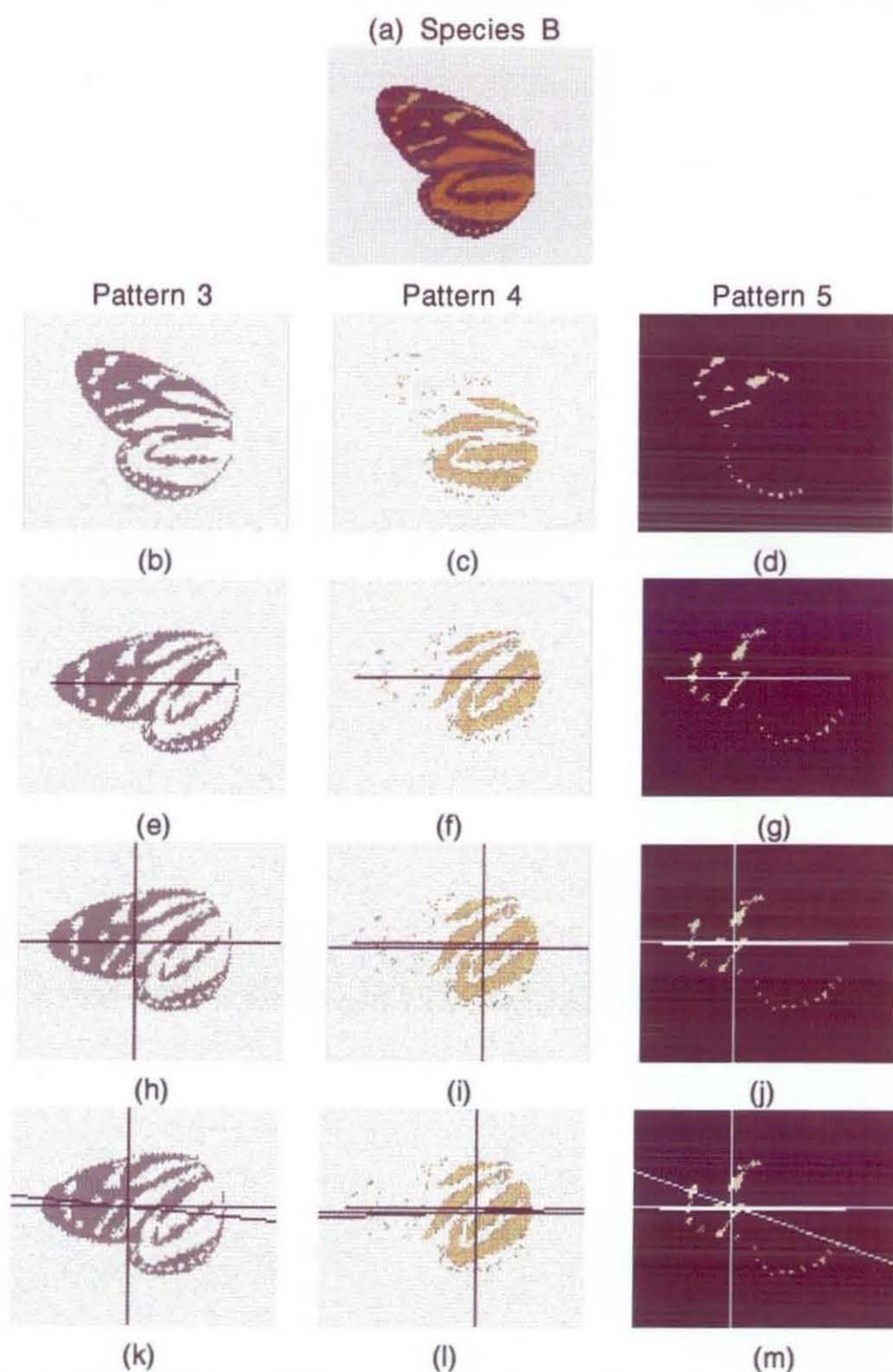
Figure 7.11 Wing patterns and major factors for each pattern of Species B. (a) The left-hand side wings. (b)-(d) Colour patterns. (e)-(g) Rotated patterns and principal axis. (h)-(j) Centre of gravity and four quadrants. (k)-(m) Regression lines.

256

7.10.(d) and (e) and Figures 7.11.(e), (f) and (g) show, each colour pattern was rotated using a principal axis. In process 26 in Figure 7.8, major factors, which were designed for colour-pattern description, were calculated. The number of descriptors calculated for each colour pattern was 14. Although these descriptors were already illustrated in Chapter 6, some of them are depicted in Figures 7.10 and 7.11 for clear understanding. Figures 7.10.(f) and (g) and Figures 7.11.(h), (i) and (j) show the centre of gravity and four quadrants for each colour pattern. As Figures 7.10.(h) and (i) and Figures 7.11.(k), (l) and (m) show, a regression line for each colour pattern, which represents a slope of a pattern, was calculated. After the calculation of the descriptors for each colour pattern using sample species involved in the learning stage, the library data containing the lower and upper limits of each descriptor were created.

In the implementation stage, the descriptors for each colour pattern of individual test species were calculated and arranged in descending order according to the size of each colour pattern. Since the number of colour patterns of Species A is different from that of Species B, the result of the comparison between species is apparent. Thus, in this test each colour pattern of a test species was compared with each of five colour patterns (2 for Species A, 3 for Species B) in the library data, that is, the comparison was performed between the colour patterns rather than between the species. If every descriptor of a test colour pattern was within the range of its corresponding descriptor of a colour pattern in the library data, it was considered as the same colour pattern that was in the library data. In the case of the test with five samples of Species A, there were two different kinds of

colour patterns. Let the colour pattern with a larger number of pixels, as shown in Figure 7.10.(b), be Pattern 1 and that with a smaller number of pixels, as shown in Figure 7.10.(c), Pattern 2. These patterns were correctly identified as shown in Table 7.4. In the case of the test with five samples of Species B, there are three different kinds of colour patterns. Let the colour pattern of the larger size, as shown in Figure 7.11.(b), be Pattern 3, that of the medium size, as shown in Figure 7.11.(c) Pattern 4, and that of the smaller size, as shown in Figure 7.11.(d), Pattern 5. As Table 7.4 shows, all of the test colour patterns corresponding to Pattern 3 were correctly identified; three of the test colour patterns corresponding to Pattern 4 were correctly identified, while two of them were not identified; and four of the test colour patterns corresponding to Pattern 5 were correctly identified, while one of them was not identified. Consequently, 88 % (22 out of 25) of the colour patterns were correctly identified.

Species	Pattern	No. of Test Samples	Identified	Failed
Species A	Pattern 1 Pattern 2	5 5	5 5	0 0
Species B	Pattern 3 Pattern 4 Pattern 5	5 5 5	5 3 4	0 2 1
Total	5	25	22	3

Table 7.4 The result of the identification test.

In order to examine the effectiveness of the colour-pattern descriptors in the colour pattern classification, let us look into the distributions of all the samples. Among 14 different kinds of descriptors, a descriptor for the size of a colour pattern and

258

descriptors for the location of a colour pattern were chosen to be examined. A diagram in Figure 7.12 shows ranges of the descriptor for the size of each pattern, where Pattern 5 can be clearly separated from the other Patterns. However, Patterns 2 and 4 as well as Patterns 1 and 3 are duplicated. Thus, Pattern 2 cannot be separated from Pattern 4 and Pattern 1 cannot be separated from Pattern 3 using this descriptor. On the other hand, Patterns 2 and 4 can be clearly separated from Patterns 1 and 3.
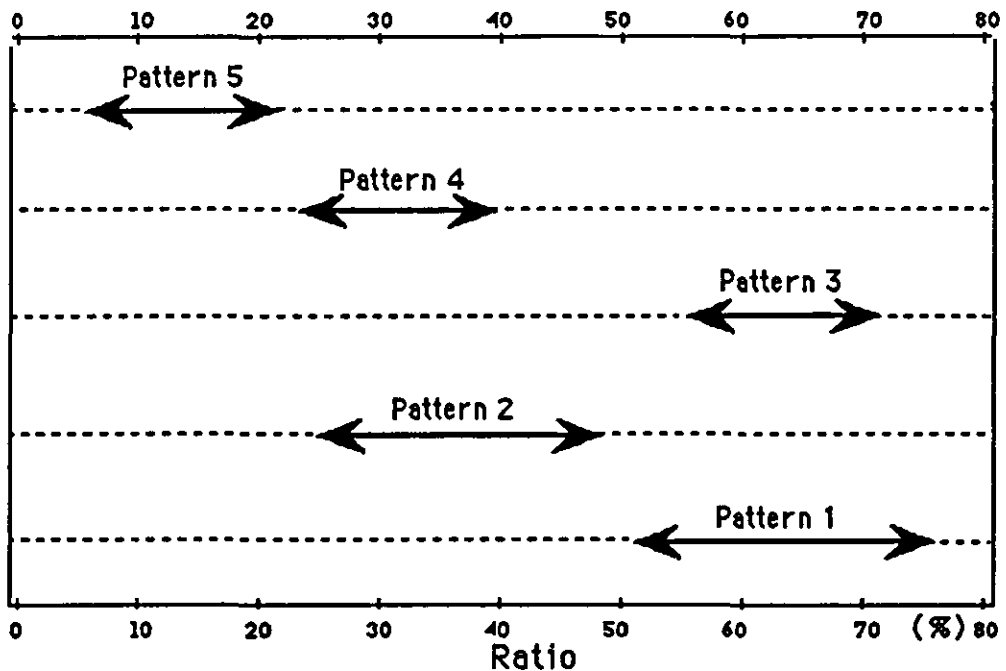
Figure 7.12 Range of each descriptor for the size of each colour pattern.

To examine the clear separation of the Patterns 2 and 4 as well as the Patterns 1 and 3, let us look into another diagram in Figure 7.13. The diagram in Figure 7.13 is a scatter diagram of the values of the normalised centre of gravity x against the values of the normalised centre of gravity y. As this scatter diagram shows, Pattern 2 can be clearly separated from Pattern 4. However, it is still difficult to judge the discrimination of Pattern 1 from

259

Pattern 3 using this scatter diagram because three different kinds of Patterns are mixed in the central part of the scatter diagram. Thus, let us look into another scatter diagram in Figure 7.14, where only Patterns 1 and 3 are plotted. As this scatter diagram shows, Pattern 1 can be clearly separated from Pattern 3. As leaf species classification showed, this reveals that if all of the descriptors are involved in the colour-pattern classification, each colour pattern can be clearly separated into its corresponding group.
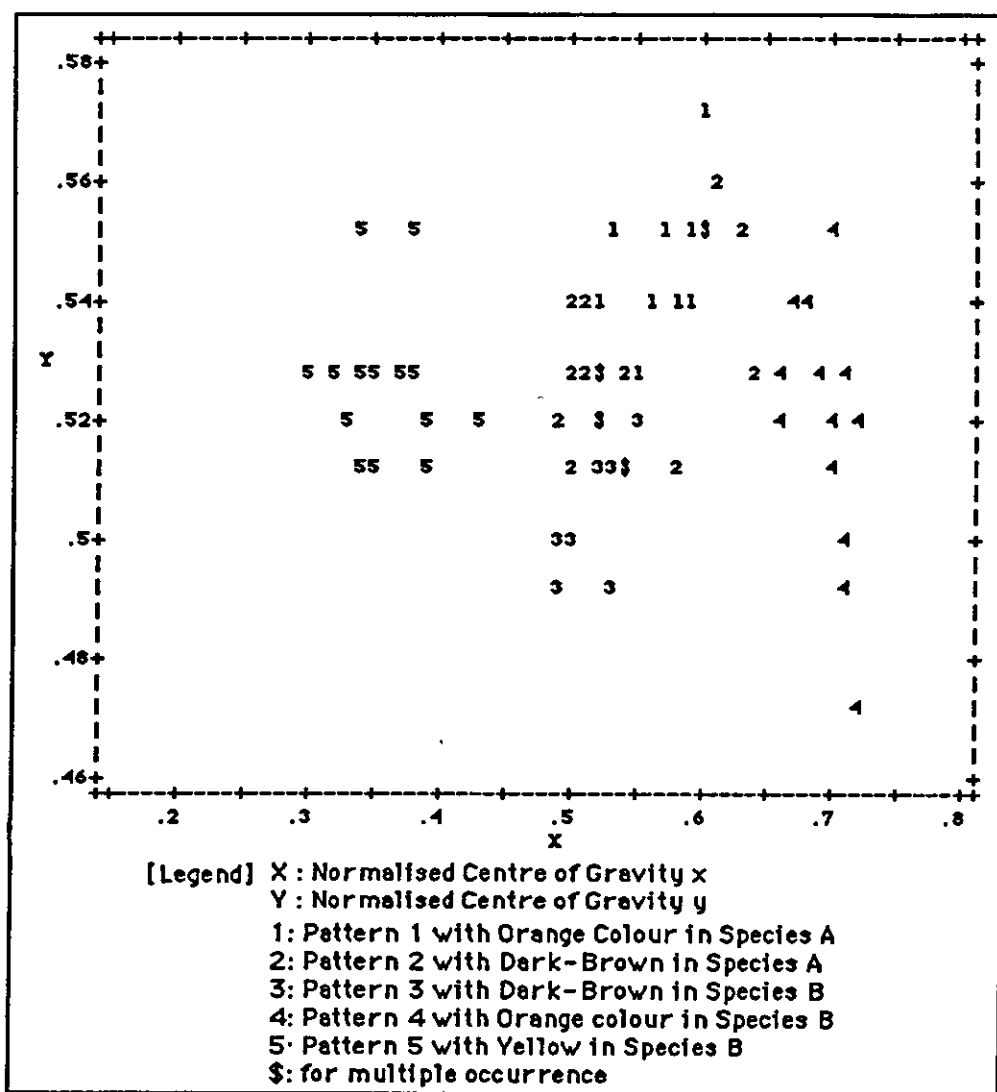
Figure 7.13 A scatter diagram of the normalised centre of gravity x values against the normalised centre of gravity y values for each colour pattern.
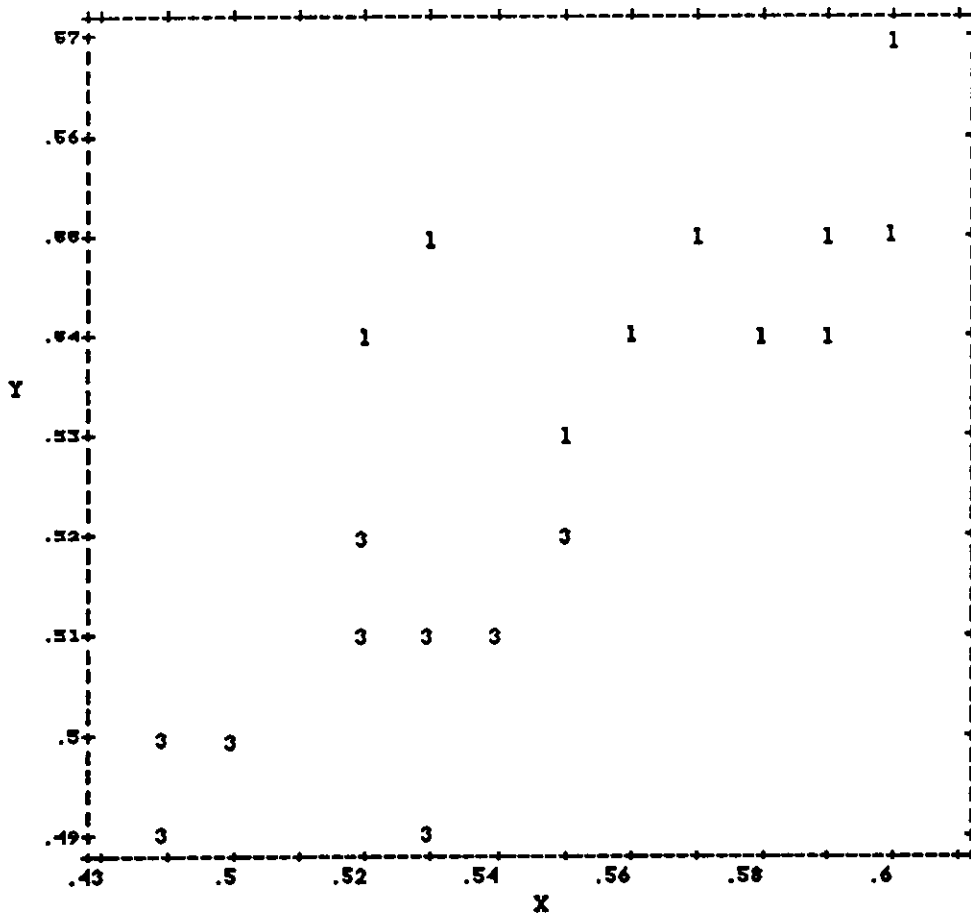
Figure 7.14 A scatter diagram for the location of colour
patterns (1 and 3).

7.4 CONCLUSION.

The presentation methods for biological objects which have been developed in this thesis are categorised into two domains:-

(1) the shape description domain, and

(2) the colour pattern description domain.

In this chapter, all the procedures which were required to create each of these descriptors were considered by establishing a prototype system. One prototype system for a leaf identification system was designed to evaluate the shape description method. Another prototype system for a butterfly species identification system was designed to evaluate the colour pattern description method. In particular, the colour pattern extraction method applying a Cluster Analysis routine in the SPSS-X was utilised to extract colour patterns from the images of butterflies in the latter prototype system.

In the validation stage, the main focus of the experiment was on the effectiveness of shape and colour pattern descriptors in the classification of sample data. The experiment was undertaken utilising two prototype systems: one for leaf species identification and the other for colour pattern classification, where images of leaves and butterflies were respectively used for the validation. In brief, both the descriptors produced sufficient information which could be used for species classification. Whenever the system provided the output of an execution, it could be interpreted and assessed without difficulty.

In addition, as the diagram for the ranges of the size of each Pattern in Figure 7.12 and the scatter diagram for the location of each colour pattern in Figure 7.13 show, colour patterns having similar features form groups. This reveals that the algorithm for colour pattern extraction which was discussed in Chapter 4 works properly.

8 CONCLUSIONS.

This thesis has primarily been concerned with the problem of how to represent a biological object for computerised identification. Images of biological objects have been generally characterised by shapes and colour patterns in the biological domain and the pattern recognition domain. Thus, it was necessary to represent the biological object using descriptors for the shape and the colour pattern. In the pattern recognition domain, many description methods for shapes and colour patterns have been published. The basic requirements which a description method should satisfy are those such as invariance of scale, location and orientation of an object; direct involvement in the identification stage; easy assessment of results and so on. The literature survey undertaken in this thesis revealed that the majority of existing methods were well designed to meet some the requirements but not sufficient to meet all of them. Thus, it was necessary to develop improved methods not only for shape description, but also for colour pattern description. The major task to deal with in this thesis was to develop a shape-description method and a colour-pattern description method which could accommodate all of the basic requirements and could be generally applied in the biological and pattern recognition domains. The main principle of the shape-description method is theoretically the same as that of the colour-pattern description method with respect to the following:

(1) A principal axis of an object is considered as a major parameter which dominates most of the values of the descriptors, because they are calculated based on the rotated principal axis;

(2) Most of the descriptors are ratios, because they can

264

accommodate the important requirement previously discussed.

However, the shape-description method which was discussed in Chapter 5 was designed slightly differently from the colour-pattern description method which was discussed in Chapter 6. The main reason for this is that the shape of a biological object can be simply characterised based on the boundary of an object; on the other hand the colour pattern of a biological object can be characterised based on the interior of the image of an object. The important information to characterise each colour pattern consists of various factors such as size, location, shape and colour as already discussed in Chapter 6.

From the view point of the user, important aspects of a description method might be accuracy, efficiency, flexibility, simplicity and so on. However, no matter how well a method is designed to cover all of these aspects, if the method has difficulty in interpretation or assessment of the result obtained by applying the method, it might not be easy to avoid criticisms. When considering this aspect of the description methods developed in this thesis, each descriptor was designed to represent practical component of an image of factor which could be interpretable, the result obtained by this method could be immediately interpreted or assessed. In the validation stage, these description methods proved highly effective for those objects with one principal axis. For objects with more than one principal axis system problems will arise when these methods are applied. The author suggests a further study for improving this aspect of these methods.

In the colour-pattern description stage, an important task was to segment a colour image into meaningful segments. The most efficient method for this task is to apply the Cluster Analysis. In the image analysis and pattern recognition domains, the majority of approaches to this method have been constrained by the problem of dealing with inordinate amounts of data, i.e. a large number of pixels of an image. In order to directly apply the Cluster Analysis to the colour image segmentation, the Auxiliary Means which is a kind of data structure was devised in this thesis. However, the method employing the Auxiliary Means had a serious problem with random noise. To overcome this problem a method to remove random noise was considered. In the validation stage, this method employing the Auxiliary Means was successfully applied. One of the important features of this approach was to utilise the Cluster Analysis routine of the SPSS-X. It is desirable to build the Cluster Analysis routine in a practical system for the system's flexibility since the routine in the SPSS-X has a limit on the number of cases it can manage, for example 150 cases in an 80K workspace.

Additionally, a calibration method for a colour scanner digitising system in the CIE L*A*B* colour space, which was developed utilising the Macbeth colour chart in this thesis, can be widely applied, because the spectral sensitivity of one device is usually different from that of another.

Chapter 9

REFERENCES.

9 REFERENCES.

Agoston, G.A. 1979. Colour Theory and Its Application in Art and Design. Springer-Verlag, Berlin.

Alt, F. 1962. "Digital pattern recognition by moments," Journal of the ACM, vol.9, pp.240-258.

Ali, M. and Aggarwal, J.K. 1977. "Automatic interpretation of infrared aerial colour photographs of citrus orchards having infestations of insect pests and diseases," IEEE Transactions on Geoscience and Electronics, vol.15, pp.170-179.

Ali, M., Martin, W.N. and Aggarwal, J.K. 1979."Colour-based computer analysis of aerial photographs," Computer Graphics and Image Processing, vol.9, pp.282-293.

Anderson, T.W. 1958. Introduction to Multivariate Statistics. John Wiley & Sons, New York.

Ballard, D. H. and Brown, C.M. 1982. Computer Vision. Prentice-Hall, New Jersey.

Blum, H. and Nagel, R.N. 1978. "Shape description using weighted symmetric axis features," Pattern Recognition, vol.10, pp.167-180.

Bookstein, F.L., Chernoff, B. R.L., Humphries, J.M., Smith, G.R. and Strauss, R.E. 1985. Morphometrics in Evolutionary Biology. Academy of Natural Sciences of Philadelphia, P.A..

Bookstein, F.L., Strauss, R.E., Humphries, J.M., Chernoff, B., Elder, R.L. and Smith, G.R. 1982. "A comment on the uses of Fourier methods in systematics," Systematic Zoology, vol.31, pp.85-92.

Bouma, P.J. 1971. Physical Aspects of Colour. Macmillan & Co..

Brakefield, P. 1979. "Spot-number in Maniola jurtina-variation between generations and selection in marginal populations," Heredity, vol.42, pp.259-266.

Castleman, K.R. 1979. Digital Image Processing. Prentice-Hall, New Jersey.

Celenk, M. 1988. "An adaptive machine learning algorithm for colour image analysis and processing," International Journal of Robotics & Computer-Integrated Manufacturing, vol.4, pp.403-412.

Chen, C.H. 1973. Statistical Pattern Recognition. Hayden, Washington, D.C.

Chow, C.K. and Kaneko, T. 1972. "Automatic boundary detection of the left ventricle from cineangiograms," Computers and Biological Research, vol.5, pp.388-410.

CIE Publication No.15.2. 1986. Colorimetry. Central Bureau of the CIE.

Cosgriff, R.L. 1960. Identification of Shape. Ohio State University Research Foundation, Report 820-11, Columbus.

Cover, T.M. and Hart, P.E. 1967. "Nearest neighbour pattern classification," IEEE Transactions on Information Theory, vol.13, pp.21-27.

Davis, L.S. 1975. "Survey of edge detection techniques," Computer Graphics and Image Processing, vol.4, pp.248-270.

Duda, R.O. and Hart, P.E. 1973. Pattern Classification and Scene Analysis. John Wiley & Sons, New York.

Dudani, S.A., Breeding, K. and McGhee, R. 1977. "Aircraft identification by moment invariants," IEEE Transactions on Computers, vol.26, pp.39-45.

Ehrlich, P.R. and Raven, P.H. 1965. "Butterflies and plants: a study in coevolution," Evolution, vol.18, pp.586-608.

Evance, R.M. 1974. The Perception of Colour. Wiley, New York.

Everitt, B. 1974. Cluster Analysis. Heinemann Educational Books, New York.

Ferson, S., Rohlf, F.J. and Koehin, R.K. 1985. "Measuring shape variation of two-dimensional outlines," Systematic Zoology, vol.34, pp.59-68.

Freeman, H. 1961. "On the encoding of arbitrary geometric configurations," IRE Transactions on Electronic Computers, vol.10, pp.260-268.

Fu, K.S. 1974. Syntactic Methods in Pattern Recognition, Academic Press, New York.

Fu, K. S. 1982. Syntactic Pattern Recognition and Applications. Prentice-Hall, New Jersey.

Fu, K.S. Gonzalez, R.C. and Lee, C.S.G. 1987. Robotics: Control, Sensing, Vision and Intelligence. McGraw-Hill, New York.

Fu, K.S. and Mui, J.K. 1981. "A survey of image Segmentation," Pattern Recognition, vol.13, pp.3-16.

Fukada, Y. 1978. "Spatial clustering procedures for region analysis," Proceedings of the 4th International Joint Conference on Pattern Recognition, Kyoto, Japan, pp.329-331.

Fukunaga, K. 1972. Introduction to Statistical Pattern Recognition. Academic Press, New York.

Goldmark, R.C. and Hollywood, J.M. 1951. "A new technique for improving the sharpness of television pictures," Proceedings of IRE, vol.39, pp.1314-1322.

Gonzalez, R.C. and Wintz, P. 1987. Digital Image Processing. Addison-Wesley.

Granlund, G.H. 1972. "Fourier preprocessing for hand print character recognition," IEEE Transactions on Computers, vol.21, pp.195-201.

271

Guild, J. 1931. "The colorimetric properties of the spectrum," Philosophical Transactions of the Royal Society of London, A230, pp.149-187.

Hall, E.L., Crawford, W.O. and Roberts, F.E. 1975. "Computer classification of pneumoconiosis from radiographs of coal workers," IEEE Transactions on Biomedical Engineering, vol.22, pp.518-527.

Haralick, R.M. 1983. Pictorial Data Analysis. Springer-Verlag, New York.

Ho. Y.C. and Kashyap, R.L. 1965. "An algorithm for linear inequalities and its applications," IEEE Transactions on Electronic Computers, vol.14, pp.683-688.

Hu, M.K. 1962. "Visual pattern recognition by moment invariants," IRE Transactions on Information Theory, vol.8, pp.179-187.

Huang, T.T.Y. and Schultheiss, P.M. 1963. "Block quantization of correlated Gaussian random variables," IRE Transactions on Communication Systems, vol.11, pp.289-296.

Hunt, R.W.G. 1989. Measuring Colour. John Wiley & Sons, New York.

Hunt, R.W.G. 1987. The Reproduction of Colour in Photography, Printing and Television. Fountain Press, U.K.

Hurvich, L.M. 1981. Colour Vision. Sinauer Associates, Mass.

Ito, T. and Fukushima, M. 1976. "Computer analysis of colour information with applications of picture processing," The 3rd International Joint Conference on Pattern Recognition, Coronado, California, pp.833-837.

Judd, D.B. and Wyszecki, G. 1975. Colour in Business, Science and Industry. 3rd ed. John Wiley & Sons, New York.

Kanade, T. 1977. Computer Recognition of Human Faces. ISR-47, Birkhauser.

Kirsh, R.A. 1971. "Computer determination of the constituent structure of biological images," Computer and Biological Research, vol.4, pp.315-328.

Kuehni, R.G. 1977. "An analysis of the HATRA acceptability data," Colour Research and Application, vol.2, pp. 85-87.

Lace, G.N. and Williams, W.T. 1967. "A general theory of classificatory sorting strategies: hierarchical systems," Computer Journal, vol.9, pp.373-380.

Ledley, R.S. 1964. "High-speed automatic analysis of biomedical pictures," Science, vol.146, pp.216-223.

Levine, M.D. 1985. Vision in Man and Machine. McGraw-Hill, New York.

Liu, H.K. 1977. "Two- and three-dimensional boundary detection," Computer Graphics and Image Processing, vol.6, pp.123-134.

Lorr, M. 1983. Cluster Analysis for Social Science. Jossey-Bass Publishers.

Lozano, R.D. 1977. "Evaluation of different colour-difference formulae by means of an experiment on colour scaling-preliminary report," Colour Research and Application, vol.2, pp.13-18.

Marr, D. 1980. "Theory of edge detection," Proceedings of Royal Society London, B207, pp.187-217.

Marr, D. 1982. Vision, a Computational Investigation into the Human Representation and Processing of Visual Information. W. H. Freeman.

Marr, D. and Nishihara, H.K. 1978. "representation and recognition of the spatial organisation of three-dimensional shape," Proceedings of the Royal Society of London, Series B, Vol.200, pp.269-294.

Marshall, S. 1989. "Review of shape coding techniques," Image and Vision Computing, vol.7, pp.281-294.

McCamy, C.S., Marcw, H. and Davidson, J.G. 1976. "A color-rendition chart," Journal of Applied Photographic Engineering, vol.2, pp.95-99.

McLaren, K. 1983. The Colour Science of Dyes and Pigments. Adam Hilger Ltd., Bristol.

McLaren, K. 1981. "The development of improved colour-difference

equations by optimisation against acceptability data," Golden Jubilee of Colour in the CIE. Bradford, Society of Dyers and Colourists, pp.156-173.

Nevatia, R. 1982. Machine Perception. Prentice-Hall, New Jersey.

Nevatia, R. 1977. "A color edge detector and its use in scene segmentation," IEEE Transactions on Systems, Man and Cybernetics. vol.7, pp.820-826.

Nijhout, H.F. 1978. "Wing pattern formulation in lepidoptera," Journal of Experimental Zoology, vol.206, pp.119-136.

Nilsson, N.J. 1965. Learning Machines. McGraw-Hill, New York.

Ohlander, R., Price, K. and Reddy, D.R. 1978. "Picture segmentation using a recursive region splitting method," Computer Graphics and Image Processing, vol.8, pp.313-333.

Ohta, Y., Kanade, T. and Sakai, T. 1980. "Colour information for region segmentation," Computer Graphics and Image Processing, vol.13, pp.222-241.

Parpert, S. 1973. Use of Technology to Enhance Education. Technical Report 298, AI Lab, MIT.

Pointer, M.R. 1981. "A comparison of the CIE 1976 colour space," Colour Research and Application, vol.6, pp.108-117.

Pratt, W.K. 1978. Digital Image Processing. John Wiley, New York.

Prewitt, J.M.S. 1970. "Object enhancement and extraction," Lipkin, B.S. and Rosenfeld, A. eds., <u>Picture Processing and Psychopictorics</u>, Academic, New York.

Roberts, L.G. 1965. "Machine perception of three-dimensional solids," Tippet, J.T. ed., <u>Optical and Electro-Optical Information Processing</u>. MIT Press, Mass.

Robertson, A.R. 1977. "The CIE 1976 Colour-difference formulae," <u>Colour Research and Application</u>, vol.2, pp.7-12.

Robinson, G.S. 1977. "Colour edge detection," <u>Optical Engineering</u>, vol.16, pp.479-484.

Robinson, G.S. 1977. "Edge detection by compass gradient masks," <u>Computer Graphics and Image Processing</u>, vol.6, pp.492-501.

Rodieck, R.W. 1973. The Vertebrate Retina, Principles of Structure and Function. Freeman, San Francisco.

Rohlf, F.J. and Archie, J.W. 1984. "A comparison of Fourier methods for the description of wing shape in mosquitoes," <u>Systematic Zoology</u>, vol.33, pp.302-317.

Rosenfeld, A. 1969. Picture Processing by Computer. Academic Press.

Rosenfeld, A. and Kak, A.C. 1976. Digital Image Processing. Academic Press, New York.

Sankar, P.V. 1978. Colour Edge Detection: a Comparative Study. Technical Report TR-66, Computer Science, University of Maryland.

Sarabi, A. and Aggarwal, J.K. 1981. "Segmentation of chromatic images," Pattern Recognition, vol.13, pp.417-427.

Schwanwitch, B.N. 1924. "On the ground plan of wing-pattern in Nymphalidae and certain other families of the rhopalocerous lepidoptera," Proceedings of zoology Society London, 1924, pp.509-528.

Smith, F.W. and Wright, M.H. 1971. "Automatic ship photo interpretation by the method of moments," IEEE Transactions on Computers, vol.20, pp.1089-1095.

Sokal, R.R. and Michener, C.D. 1958. A Statistical Method for Evaluating Systematic Relationships. University of Kansas Science Bulletin, vol.38, pp.1409-1438.

SPSS Inc., 1988. SPSS-X User's Guide, 3rd ed. SPSS inc. Michigan, III.

Strachan, N.J., Nesvadva, P. and Allen, A.R. 1990. "Calibration of a video camera digitising system in the CIE L*U*V* colour space," Pattern Recognition Letters, vol.11, pp.771-777.

Tomina, S. 1988. "A colour classification algorithm for colour images," Kittler, J. ed., Pattern Recognition 4th International Conference, Cambridge, U.K., pp.163-172.

Underwood, S.A. and Aggarwal, J.K. 1977. "International computer analysis of aerial colour infrared photographs," _Computer Graphics Image Processing_, vol.6, pp.1-24.

Wesley, E., Arbter, L., Burkhardt, H. and Hirzinger, G. 1990. "Application of affine-invariant Fourier descriptors to recognition of 3-D objects," _IEEE Transactions on Pattern Analysis and Machine Intelligence_, vol.12, pp.640-647.

White, R.J. 1988. "Comparison of shape description methods for biological outlines," Bock, H.H. ed., _Classification and Related Methods of Data Analysis_. Elsevier Science Publishers, pp.395-402.

West, J.G. and Noble, I.R. 1984. "Analysis of digital leaf images of the Dodonaea Viscosa complex in Australia," _Taxon_, vol.33, pp.595-613.

White, R. J. and Prentice, H.C. 1988. "Comparison of shape description methods for biological outlines," Bock, H.H. ed., _Classification and Related Methods of Data Analysis_, pp.395-402.

Wright, W.D. 1928. "A trichromatic colorimeter with spectral primaries," _Transactions on Optical Society, London_, vol.29, pp.225-230.

Wyszecki, G. 1981. "Uniform colour spaces," _Golden Jubilee of Colour in the CIE_. the Society of Dyers and Colourists, Bradford, pp.53-77.

Wyszecki, G. and Stiles, W.S. 1982. Colour Science: Concepts and Methods, Quantitative Data and Formulae. 2nd ed., John Wiley & Sons.

Zahn, C.T. and Roskies, R.Z. 1972. "Fourier descriptors for plane closed curves," IEEE Transactions on Computers, vol.21, pp.269-281.

Zupan, J. 1982. Clustering of Large Data. John Wiley & Sons.

APPENDIX

A. LEAF SPECIES IDENTIFICATION.

B. BUTTERFLY SPECIES IDENTIFICATION.

A. LEAF SPECIES IDENTIFICATION.

In this Appendix, the data and the result of the analysis which were obtained during the validation stage for leaf species classification are described. There were two different kinds of leaf species involved in the test. For species A in Figure A.1.(a), the number of samples was 16, where 10 samples was randomly selected from the given samples for the learning stage; and 6 for the implementation stage. For species B in Figure A.1.(b), the number of samples was 26, where 16 samples were randomly selected from the given samples for the learning stage; and 10 for the implementation stage.

Species A   Species B

(a)   (b)
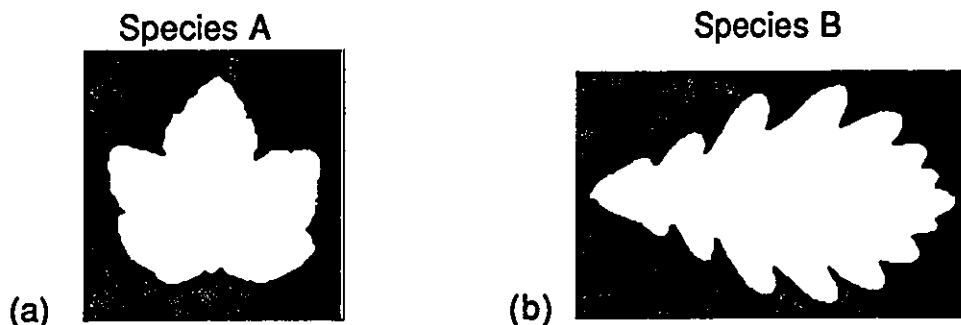
Figure A.1 The images of sample species.

After rotation of the boundary of each sample using a principal axis, the upper and lower parts were divided into 2^3 segments as shown in Figure A.2.(a), and the ratio for each segment was calculated. Another ratio for each segment of 2^2 segments for the upper and lower parts, as shown in Figure A.2.(b), was calculated using the ratios for 2^3 segments. The ratio for each segment of 2^1 segments for the upper and lower parts, as shown in Figure A.2.(c), was calculated using the ratios for 2^2 segments. Finally, the ratios for the upper and lower parts, as shown in Figure A.2.(d), were calculated using the ratios for 2^1 segments. Thus,

A-2

the number of ratios (descriptors) for each part is 15. The value of each ratio (descriptor) for each sample involved in the validation stage is shown in Table A.1. through to Table A.6.

(a)

(b)

(c)

(d)
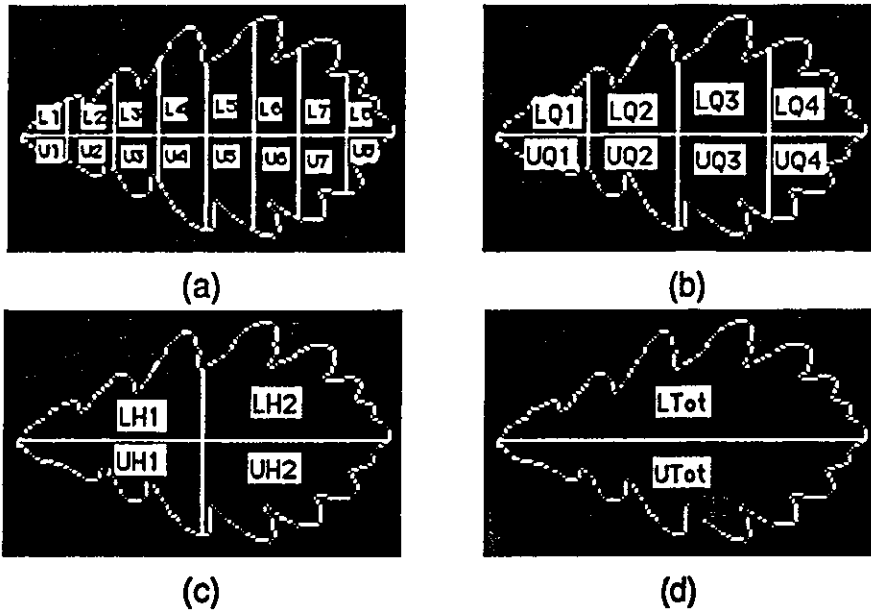
Figure A.2 The ratio for each segment.

The main objective of the experiment was to examine the function of the descriptor which was designed to discriminate one group from another. Two-dimensional scatter diagrams usually show the relationship between observations of each group. As most of the scatter diagrams in Figure A.3 through Figure A.19 show, each sample group can be clearly separated from the other group.

Table A.1.(a) The ratios for the upper part for 10 samples of Species A involved in the learning stage.

LTot	LH1	LH2	LQ1	LQ2	LQ3	LQ4	L1	L2	L3	L4	L5	L6	L7	L8
27 63	14 08	13 55	3 19	10 89	7.67	5 88	.69	2 50	5.76	5 13	3 68	3.99	4.43	1.45
26.54	13.11	13.43	1.60	11.51	8.38	5.05	.66	.94	6 02	5.49	4 32	4.06	3 69	1.36
26.50	14.70	11.80	4.30	10 40	6.38	5.42	1.23	3 07	5.75	4 65	3.12	3 26	3 53	1 89
35.17	17.67	17.50	4 60	13.07	9.97	7.53	.83	3.77	5 95	7.12	6.12	3.85	4.58	2.95
32.42	16.51	15 91	2 84	13.67	9.35	6 56	.77	2.07	6.78	6 89	5.20	4.15	4.31	2.25
33 99	16.73	17 26	5.14	11.59	9.68	7.58	.80	4 34	6.28	5.31	5 07	4.61	4 95	2 63
34.80	17.08	17.72	3.88	13 20	9 88	7.84	.57	3 31	6.81	6.39	5 27	4.61	5.34	2.50
25.32	10.97	14 35	1 33	9 64	7.64	6 71	.55	.78	4.50	5.14	4.42	3.22	4.31	2.40
28.67	12.79	15 88	2 69	10.10	9.05	6 83	.82	1 87	5.16	4.94	4.50	4 55	4.99	1.84
25.73	12.74	12 99	2.16	10.58	6.99	6.00	.76	1.40	5 90	4.68	3 85	3.14	3.48	2.52

Table A.1.(b) The ratios for the lower part for 10 samples of Species A involved in the learning stage.

UTot	UH1	UH2	UQ1	UQ2	UQ3	UQ4	U1	U2	U3	U4	U5	U6	U7	U8
23.59	12.84	10.75	3.96	8 88	6.70	4.05	1.23	2 73	4.35	4.53	3.79	2 91	2 68	1.37
22.60	13.51	9.09	4.84	8.67	5.50	3.59	1.63	3.21	4.46	4.21	2.89	2.61	2.50	1.09
18.67	11.07	7.60	4.05	7 02	5.01	2 59	1.17	2.88	3 59	3.43	2.83	2.18	1 89	.70
20.29	12.14	8.15	4.55	7.59	4.81	3.34	1.54	3 01	3.58	4 01	2.74	2.07	2.25	1.09
19.22	11.21	8.01	3.65	7.56	5.03	2.98	1.18	2 47	3 61	3.95	2.96	2.07	2.07	.91
19.28	12 23	7.05	4 20	8 03	4.39	2.66	1 29	2 91	4.02	4.01	2.64	1.75	1.68	98
23 37	12.21	11.16	4.13	8.08	6 98	4.18	1.25	2.88	3.91	4 17	4 41	2 57	2 43	1.75
24.92	13.75	11.17	4.29	9.46	7.30	3.87	1.36	2 93	4.48	4 98	4 67	2.63	2 53	1.34
21.43	12.51	8.92	4.12	8 39	5.44	3.48	1.31	2.81	4.07	4.32	3.11	2.33	2.24	1.24
22.79	12.07	10.72	3 59	8.48	6.60	4.12	1.02	2 57	4.18	4 30	3.55	3.05	2.58	1.54

Table A.2.(a) The mean of each ratio for the upper part using 10 samples of Species A involved in the learning stage.

LTot	LH1	LH2	LQ1	LQ2	LQ3	LQ4	L1	L2	L3	L4	L5	L6	L7	L8
29.68	14 64	15 04	3 17	11.46	8.50	6 54	0 77	2 40	5 89	5 57	4 55	3 94	4 36	2.18

Table A.2.(b) The standard deviation of each ratio for the upper part using 10 samples of Species A involved in the learning stage.

LTot	LH1	LH2	LQ1	LQ2	LQ3	LQ4	L1	L2	L3	L4	L5	L6	L7	L8
3 98	2.26	2 10	1 29	1.41	1.28	0.95	0 19	1 21	0.69	0 90	0.88	0.57	0 64	0.52

Table A.2.(c) The mean of each ratio for the lower part using 10 samples of Species A involved in the learning stage.

UTot	UH1	UH2	UQ1	UQ2	UQ3	UQ4	U1	U2	U3	U4	U5	U6	U7	U8
21.62	12.35	9.26	4.14	8.22	5.78	3.49	1.30	2 84	4.02	4.19	3 36	2.42	2.28	1.20

Table A.2.(d) The standard deviation of each ratio for the lower part using 10 samples of Species A involved in the learning stage.

UTot	UH1	UH2	UQ1	UQ2	UQ3	UQ4	U1	U2	U3	U4	U5	U6	U7	U8
2.16	0.86	1 57	0.38	0.71	1.03	0 59	0.18	0.21	0 35	0.40	0.72	0.41	0.32	0.31

A-5

Table A.3.(a) The ratios for the upper part for 6 samples of Species A involved in the implementation stage.

LTot	LH1	LH2	LQ1	LQ2	LQ3	LQ4	L1	L2	L3	L4	L5	L6	L7	L8
31.75	16 84	14 91	4.44	12 40	8 23	6 68	.71	3.73	6 50	5 90	4 41	3 82	4.32	2 36
33.55	17.15	16.40	5.96	11.19	9.05	7.35	.95	5 01	5.44	5 75	4.69	4.36	4.44	2.91
28.01	13.17	14 84	1.79	11 38	8.22	6 62	.62	1.17	5 63	5 75	4.98	3.24	4.08	2 54
33 72	17.22	16 50	5 05	12.17	9.30	7.20	.78	4.27	6 48	5 69	5 11	4.19	4 54	2.66
27.02	12 69	14 33	2.32	10.37	7.95	6.38	.71	1 61	4.71	5 66	4.41	3.54	4 29	2 09
35.43	17.75	17 68	6 00	11.75	9.71	7.97	.97	5 03	5.90	5 85	5.35	4.36	5.34	2 63

Table A.3.(b) The ratios for the lower part for 6 samples of Species A involved in the implementation stage.

UTot	UH1	UH2	UQ1	UQ2	UQ3	UQ4	U1	U2	U3	U4	U5	U6	U7	U8
22.75	12 43	10 32	3.91	8.52	5.77	4.55	1.35	2.56	4.12	4 40	2 97	2 80	3 09	1.46
18.35	11.59	6.76	3 65	7.94	3.89	2.87	1.24	2.41	3.96	3.98	1.98	1.91	1.82	1.05
24.93	13.80	11.13	4.16	9.64	7.14	3.99	1.58	2.58	4.33	5 31	4 63	2.51	2.30	1.69
25.04	13.64	11.40	3.97	9.67	6.80	4.60	1.39	2.58	4.78	4.89	3.90	2 90	3 08	1.50
26 26	15.32	10 94	4.64	10.68	7.26	3 68	1.30	3.34	5.37	5.31	4.46	2.80	2.34	1.34
21.26	12.44	8 82	3.90	8.54	5 49	3 33	1.26	2.64	4 06	4.48	3.37	2.12	2.26	1.07

LTot	LH1	LH2	LQ1	LQ2	LQ3	LQ4	L1	L2	L3	L4	L5	L6	L7	L8
17 52	7.44	10 08	2.77	4.67	6 28	3 80	.93	1 84	2 18	2.49	3 07	3 21	2 68	1.12
14.93	7.38	7.55	2.51	4.87	5.00	2.55	.34	2.17	2.29	2.58	2.80	2.20	1.85	.70
16.31	7.72	8.59	2 42	5 30	5 42	3.17	.81	1 61	2 26	3 04	2.85	2 57	2 28	.89
14.32	6.65	7 67	2 44	4 21	4 98	2.69	84	1.60	2.09	2.12	2.70	2 28	1 97	.72
16.51	8.01	8.50	2.63	5.38	5.72	2.78	1.01	1.62	2.53	2.85	2.88	2.84	2.10	68
16.84	7.14	9.70	2.23	4.91	6.32	3.38	.69	1.54	1.95	2.96	3 20	3.12	2.48	.90
13.71	5.97	7.74	1.78	4.19	5.23	2.51	.62	1.16	1.57	2 62	2.70	2 53	1 93	.58
15.83	7.47	8 36	2.53	4 94	5.63	2.73	.74	1.79	2.44	2.50	2.81	2.82	2.15	.58
19 67	8 46	11.21	2.54	5.92	6.66	4.55	80	1.74	2.72	3.20	3 22	3 44	3.13	1.42
15.15	5 80	9.35	1.65	4.15	6.20	3.15	.51	1.14	1.96	2.19	3.13	3.07	2.24	.91
15.56	6 54	9.02	1.94	4.60	5.95	3.07	66	1.28	2 28	2.32	3.19	2.76	2.23	.84
10.88	4 40	6.48	1.45	2.95	4.09	2 39	.53	.92	1.18	1.77	2.06	2.03	1.76	.63
17.01	5.63	11.38	1.35	4.28	6 94	4 44	.43	.92	2.15	2.13	3.58	3.36	3.16	1.28
14 55	5.57	8 98	1.43	4.14	5 63	3.35	.45	.98	1.51	2.63	2.50	3.13	2.38	97
12.96	4 27	8.69	1.25	3.02	5.53	3.16	.47	.78	1.23	1.79	2.65	2.88	2.21	.95
14.31	6.73	7.58	2.07	4.66	4.88	2.70	.56	1.51	2.17	2.49	2 50	2.38	1.86	.84

Table A.4.(b) The ratios for the lower part for 16 samples of Species B involved in the learning stage.

UTot	UH1	UH2	UQ1	UQ2	UQ3	UQ4	U1	U2	U3	U4	U5	U6	U7	U8
16.13	6 58	9 55	1.93	4.65	6.11	3 44	.70	1.23	1.79	2 86	2 94	3.17	2 56	.88
14 22	6.63	7.59	1.44	5.19	4 70	2.89	.23	1.21	2.05	3.14	2 56	2.14	2 02	.87
15 01	5.73	9 28	1.45	4.28	5.67	3 61	.46	.99	1.65	2 63	2.50	3.17	2.47	1.14
12.43	4 44	7.99	1.24	3 20	4 84	3.15	.42	82	1.27	1.93	2.45	2 39	2.15	1.00
16.58	6 89	9 69	2.10	4.79	5.99	3.70	.70	1.40	2.38	2 41	3.10	2.89	2 62	1.08
19.93	8.42	11.51	2 82	5 60	7.08	4.43	1.15	1 67	2.51	3.09	3 63	3.45	3 09	1.34
16 34	7.29	9 05	2 01	5.28	5.75	3.30	.60	1.41	2 02	3 26	2.94	2.81	2.25	1.05
15.91	6.23	9.68	1.49	4.74	5.93	3.75	.43	1.06	1.66	3.08	2.79	3.14	2 57	1.18
13 55	6.15	7.40	2.17	3.98	5.09	2.31	.75	1.42	1.87	2.11	2.48	2 61	1.80	.51
19.02	8.42	10.60	2.48	5.94	6.67	3.93	.71	1.77	2.33	3 61	3.25	3.42	2.94	.99
15.82	6 29	9.53	1.50	4 79	6 24	3.29	.51	.99	1.70	3.09	3.05	3.19	2.41	.88
14.91	6.42	8.49	2 01	4.41	5.52	2.97	.66	1.35	1.81	2.60	2.78	2.74	2.12	.85
15 23	6 43	8.80	1 50	4.93	5.64	3.16	.23	1.27	2.02	2.91	2.58	3.06	2.38	.78
17.99	8.40	9.59	2.87	5.53	6.44	3.15	.97	1.90	2.43	3.10	3.13	3.31	2.45	.70
18.17	8 20	9.97	2.57	5.63	6.68	3 29	.79	1.78	2.40	3.23	3.37	3.31	2.61	.68
11.53	5.74	5.79	1.89	3.85	3.98	1.81	.50	1.39	1.50	2.35	2.08	1.90	1.39	.42

Table A.5.(a) The mean of each ratio for the upper part using 16 samples (Species B) involved in the learning stage.

LTot	LH1	LH2	LQ1	LQ2	LQ3	LQ4	L1	L2	L3	L4	L5	L6	L7	L8
15 38	6 57	8 81	2.06	4.51	5 65	3 15	0 65	1.41	2 03	2.48	2 87	2 79	2 28	0 88

Table A.5.(b) The standard deviation of each ratio for the upper part using 16 samples of Species B involved in the learning stage.

LTot	LH1	LH2	LQ1	LQ2	LQ3	LQ4	L1	L2	L3	L4	L5	L6	L7	L8
2.04	1.22	1.33	0 51	0.78	0.73	0.64	0.19	0 40	0.45	0 42	0.36	0.42	0.42	0 24

Table A.5.(c) The mean of each ratio for the lower part using 16 samples of Species B involved in the learning stage.

UTot	UH1	UH2	UQ1	UQ2	UQ3	UQ4	U1	U2	U3	U4	U5	U6	U7	U8
15.80	6.77	9.03	1.97	4.80	5.77	3.26	0.61	1.35	1.96	2 84	2.85	2.92	2.36	0.90

Table A.5.(d) The standard deviation of each ratio for the lower part using 16 samples of Species B involved in the learning stage.

UTot	UH1	UH2	UQ1	UQ2	UQ3	UQ4	U1	U2	U3	U4	U5	U6	U7	U8
2.28	1.13	1.36	0.51	0.74	0 82	0.61	0.25	0.31	0.37	0.46	0.40	0.46	0.42	0.24

Table A.6.(a) The ratios for the upper part for 10 samples of Species B involved in the implementation stage.

LTot	LH1	LH2	LQ1	LQ2	LQ3	LQ4	L1	L2	L3	L4	L5	L6	L7	L8
16 52	7.01	9 51	2 19	4 82	6 20	3 31	.53	1 66	1 91	2 91	2 85	3 35	2 64	.67
14 32	5 91	8 41	1.90	4.01	5.17	3.24	.66	1.24	1.54	2.47	2 26	2.91	2.16	1.08
15 27	6.10	9.17	1.85	4.25	5.82	3.35	.62	1.23	1.78	2.47	2 93	2.89	2 48	.87
14.98	6.90	8 08	2 20	4 70	5.30	2.78	.54	1.66	2 01	2.69	2 80	2 50	2.01	.77
17.35	6 51	10 84	1.88	4.63	6.49	4.35	.70	1.18	1.50	3.13	2.83	3 66	2 93	1 42
14.49	6.36	8.13	1 79	4 57	5.13	3 00	.52	1 27	1.94	2 63	2.41	2.72	2.16	84
16.70	7.84	8 86	2 65	5.19	6.01	2.85	.86	1.79	2 43	2.76	3.07	2 94	2.02	.83
14.38	5.85	8.53	1 83	4 02	5.39	3.14	.60	1 23	1.79	2 23	2 62	2.77	2.17	.97
13.34	5.65	7.69	1.57	4 08	4 83	2.86	.42	1.15	1.71	2.37	2.56	2.27	2.07	.79
16.99	6 96	10.03	1.98	4.98	6 02	4.01	.64	1.34	1.87	3.11	2.98	3.04	2.78	1.23

Table A.6.(b) The ratios for the lower part for 10 samples of Species B involved in the implementation stage.

UTot	UH1	UH2	UQ1	UQ2	UQ3	UQ4	U1	U2	U3	U4	U5	U6	U7	U8
17.00	7.30	9.70	1 87	5.43	6.40	3 30	.56	1.31	2.13	3.30	3 08	3.32	2.29	1.01
13.29	5.67	7.62	1.70	3.97	4.81	2 81	.59	1.11	1.64	2.33	2.16	2 65	1.96	.85
21.40	10.75	10 65	3.69	7.06	7.19	3.46	1.17	2 52	3.00	4.06	3.59	3 60	2.65	.81
15.15	6.33	8 82	2.14	4.19	5.44	3.38	.71	1.43	1.66	2.53	2.83	2.61	2.45	.93
14.71	6.65	8.06	2.31	4.34	5 32	2.74	.75	1.56	1.79	2.55	2.96	2.36	1.98	.76
12.96	6.60	6.36	2.11	4.49	4.57	1.79	.57	1.54	1.94	2.55	2.44	2.13	1.31	.48
17.04	6.21	10.83	1.58	4.63	6.52	4.31	.56	1.02	2.15	2.48	3 22	3 30	2.96	1.35
13 84	6 00	7 84	1.99	4 01	5.44	2.40	77	1.22	1.65	2.36	2.75	2.69	1.90	.50
15.96	6.61	9.35	2.26	4.35	5.85	3.50	.68	1.58	2.01	2.34	2.79	3.06	2.42	1.08
14.37	5.86	8.51	1.66	4.20	5.39	3.12	.55	1.11	1.62	2 58	2.69	2.70	2.30	.82

Figure A.3 A scatter diagram of the LTot values against the UTot values.
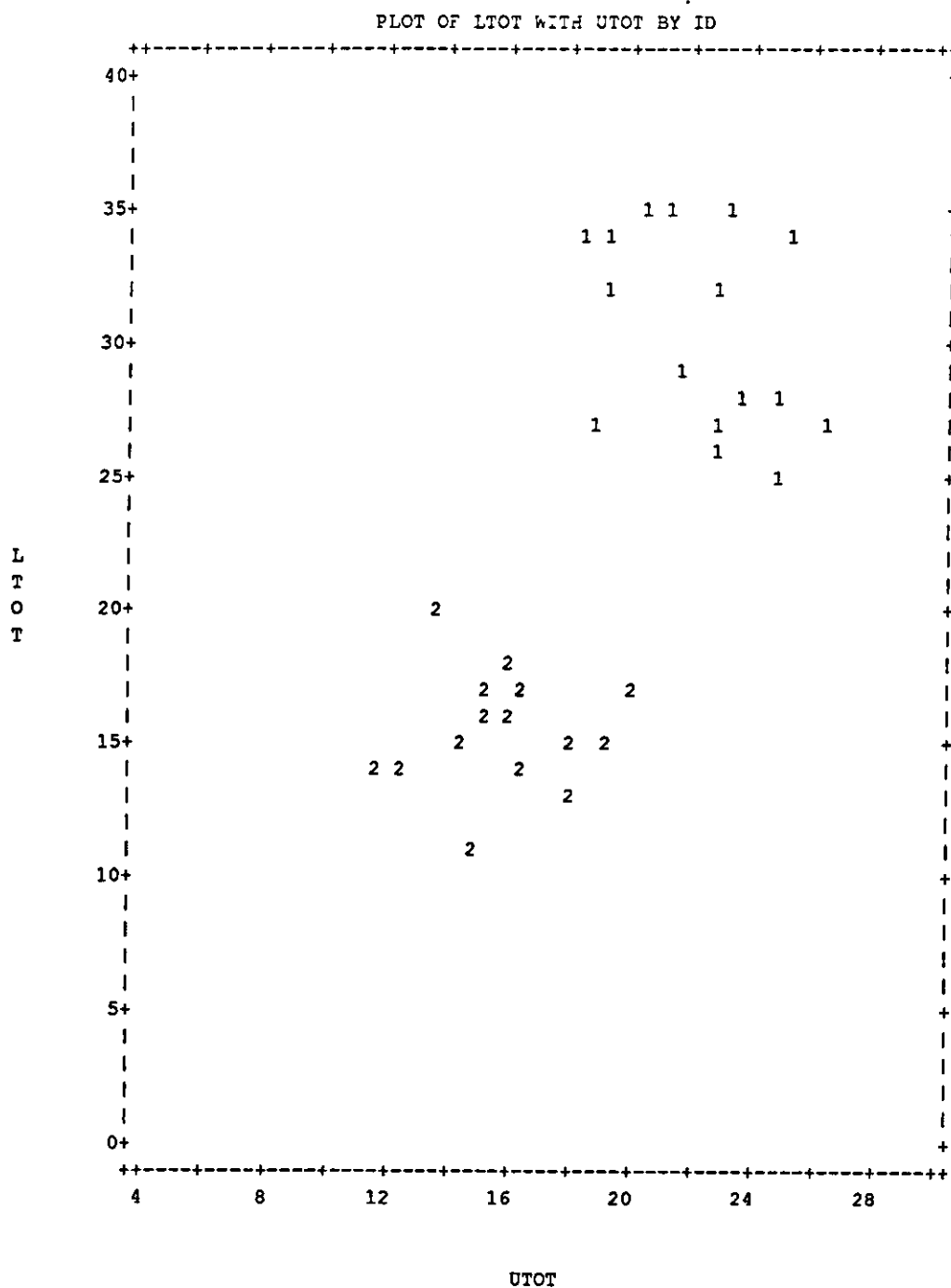
```
                         PLOT OF LTOT WITH UTOT BY ID
         ++----+----+----+----+----+----+----+----+----+----+----+----++
    40+                                                                  +
      |                                                                  |
      |                                                                  |
      |                                                                  |
      |                                                                  |
    35+                                  1 1     1                       +
      |                              1 1         1                       |
      |                                                1                  |
      |                                  1           1                   |
      |                                                                  |
    30+                                                                  +
      |                                        1                         |
      |                                            1 1                   |
      |                                  1         1         1           |
      |                                            1                     |
    25+                                            1                     +
      |                                                                  |
      |                                                                  |
  L   |                                                                  |
  T   |                                                                  |
  O 20+                       2                                          +
  T   |                                                                  |
      |                          2                                       |
      |                        2 2             2                         |
      |                        2 2                                       |
    15+                      2             2 2                           +
      |                2 2             2                                 |
      |                                2                                 |
      |                                                                  |
      |                    2                                             |
    10+                                                                  +
      |                                                                  |
      |                                                                  |
      |                                                                  |
      |                                                                  |
     5+                                                                  +
      |                                                                  |
      |                                                                  |
      |                                                                  |
      |                                                                  |
     0+                                                                  +
         ++----+----+----+----+----+----+----+----+----+----+----+----++
          4        8        12       16       20       24       28
```

UTOT

       32 cases plotted.
Use first digit of ID as plotting symbol and $ for multiple
occurrence.

A-11

Figure A.4 A scatter diagram of the LH1 values against the UH1 values.
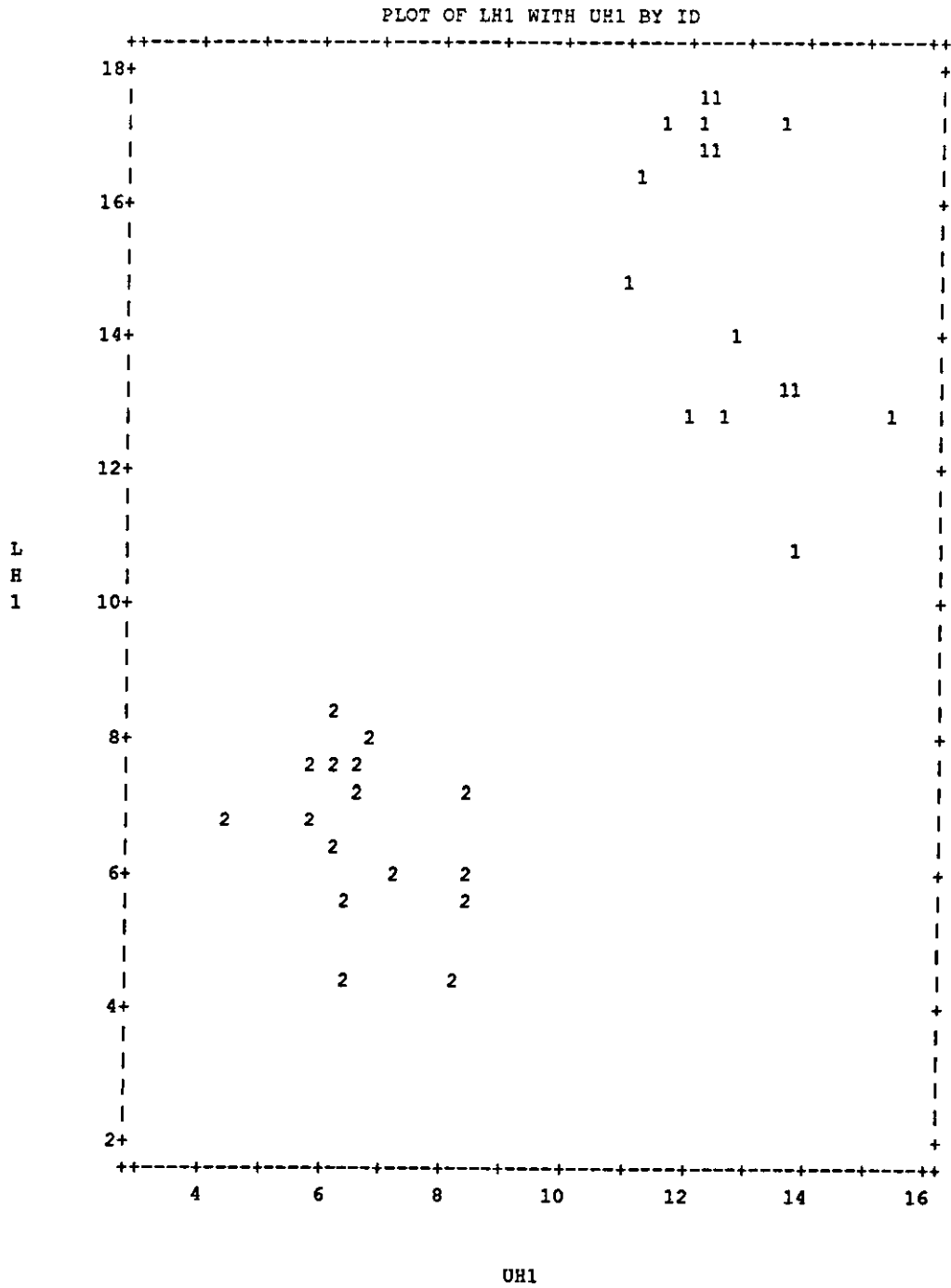
PLOT OF LH1 WITH UH1 BY ID

32 cases plotted.
Use first digit of ID as plotting symbol and $ for multiple occurrence.

Figure A.5 A scatter diagram of the LH2 values against the UH2 values.
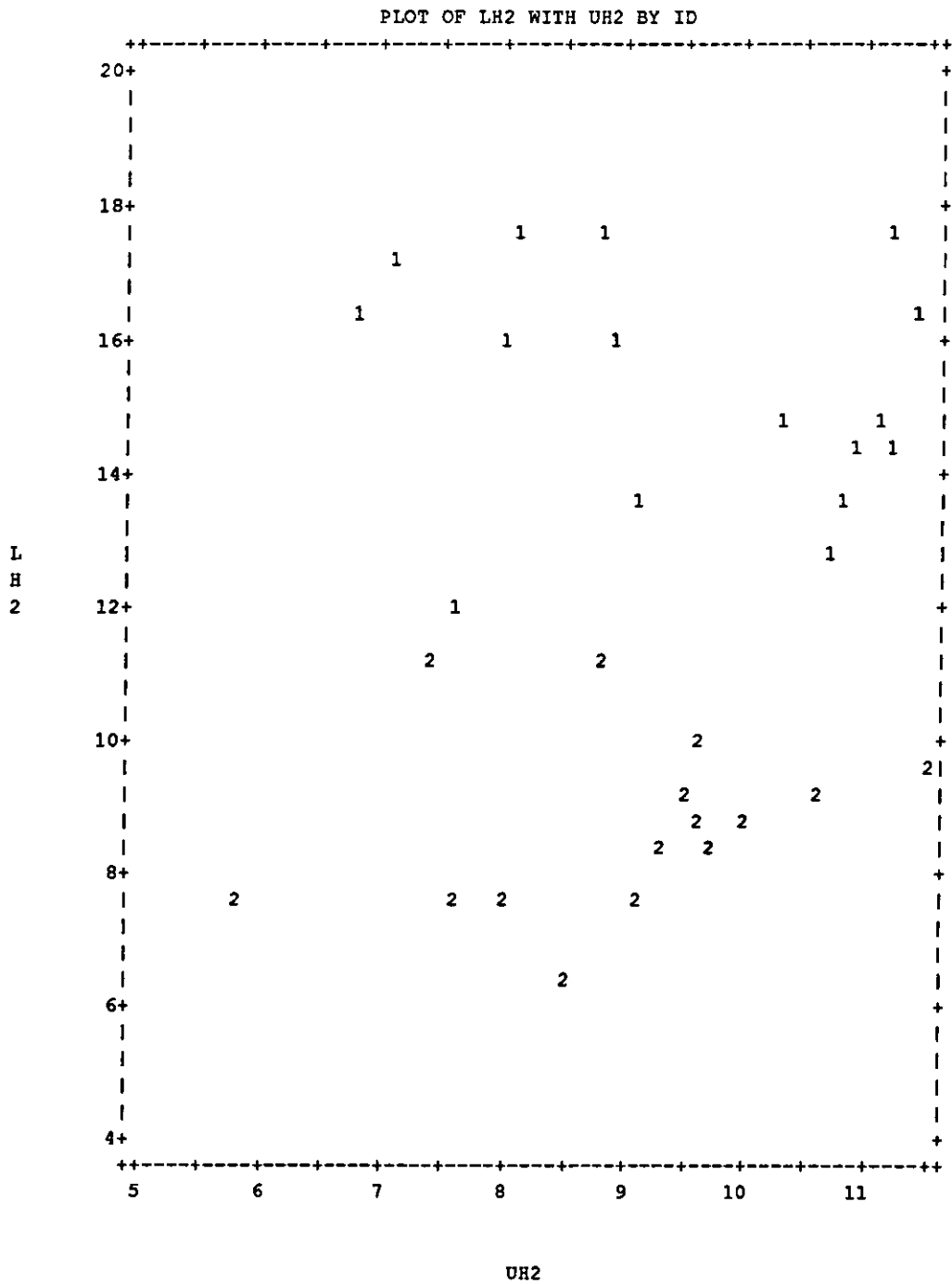

```
                              PLOT OF LH2 WITH UH2 BY ID
        ++----+----+----+----+----+----+----+----+----+----+----+----+----++
     20+                                                                    +
       |                                                                    |
       |                                                                    |
       |                                                                    |
       |                                                                    |
     18+                                                                    +
       |                            1         1                   1         |
       |                      1                                             |
       |                                                                    |
       |                 1                                          1       |
     16+                            1         1                             +
       |                                                                    |
       |                                                                    |
       |                                                  1         1       |
       |                                                      1   1         |
     14+                                                                    +
       |                                    1                     1         |
       |                                                                    |
  L    |                                                        1           |
  H    |                                                                    |
  2  12+                        1                                           +
       |                                                                    |
       |                   2               2                                |
       |                                                                    |
       |                                                                    |
     10+                                          2                         +
       |                                                                  2 |
       |                                   2           2                    |
       |                                     2   2                          |
       |                                  2    2                            |
      8+                                                                    +
       |           2                2   2           2                       |
       |                                                                    |
       |                                                                    |
       |                              2                                     |
      6+                                                                    +
       |                                                                    |
       |                                                                    |
       |                                                                    |
       |                                                                    |
      4+                                                                    +
        ++----+----+----+----+----+----+----+----+----+----+----+----+----++
         5         6         7         8         9        10        11
```

UH2

32 cases plotted.
Use first digit of ID as plotting symbol and $ for multiple occurrence.

A-13

Figure A.6 A scatter diagram of the LH1 values against the LH2 values.
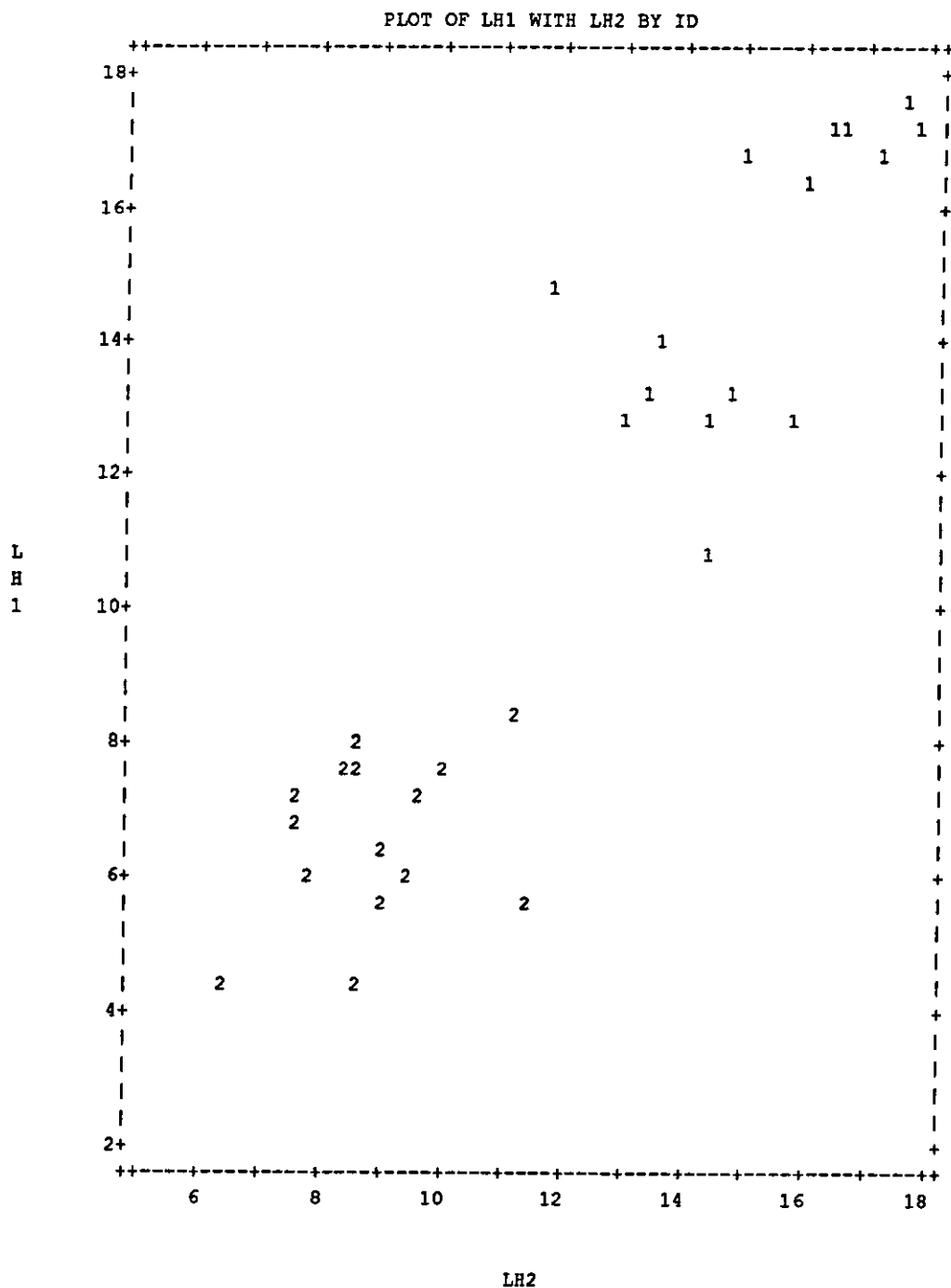
```
                              PLOT OF LH1 WITH LH2 BY ID
        ++----+----+----+----+----+----+----+----+----+----+----+----++
    18+                                                              1   +
     |                                                                  1 |
     |                                                       11        1  |
     |                                                  1          1     |
    16+                                                     1           +
     |
     |
     |                                      1
     |
    14+                                          1                      +
     |
     |                                      1      1                    |
     |                                   1      1        1              |
     |
    12+                                                                 +
     |
     |
 L   |                                             1                    |
 H   |
 1  10+                                                                 +
     |
     |
     |
     |                                  2
    8+                           2                                     +
     |                           22      2                             |
     |                     2          2                                |
     |                     2                                           |
     |                        2                                        |
    6+                  2        2                                     +
     |                        2          2                             |
     |
     |
     |           2              2                                      |
    4+                                                                 +
     |
     |
     |
    2+                                                                 +
        ++----+----+----+----+----+----+----+----+----+----+----+----++
            6         8        10        12        14        16        18

                                   LH2
```

           32 cases plotted.
     Use first digit of ID as plotting symbol and $ for multiple
occurrence.

A-14

Figure A.7 A scatter diagram of the UH1 values against the UH2 values.
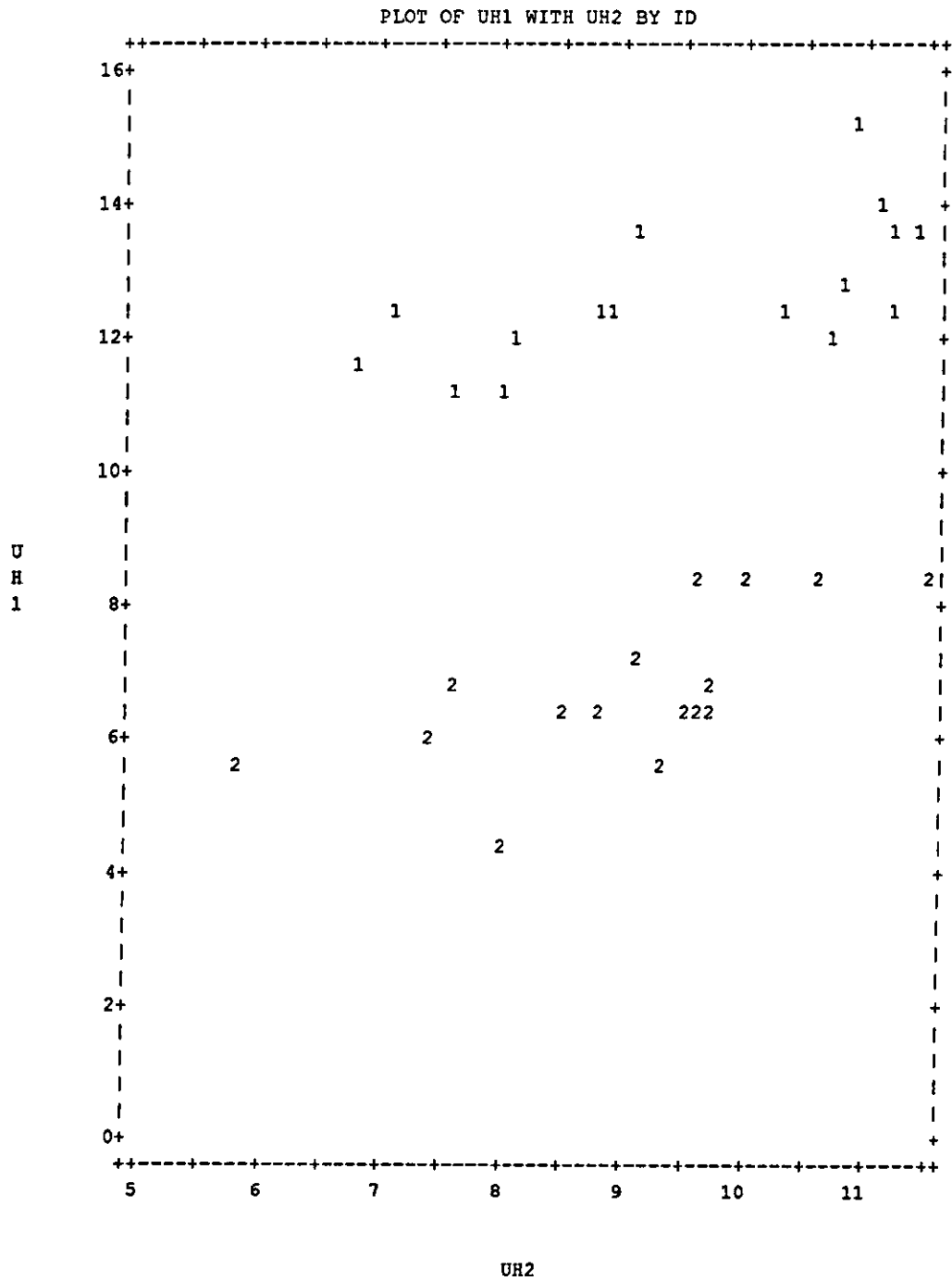
```
                          PLOT OF UH1 WITH UH2 BY ID
          ++----+----+----+----+----+----+----+----+----+----+----+----++
      16+                                                               +
        |
        |                                                    1          |
        |                                                               |
        |                                                               |
      14+                                                      1        +
        |                                        1                 1 1  |
        |                                                               |
        |                                                    1          |
        |                    1                11             1       1   |
      12+                                 1                      1       +
        |                 1                                             |
        |                       1    1                                  |
        |                                                               |
        |                                                               |
      10+                                                               +
        |                                                               |
        |                                                               |
  U     |                                                               |
  H     |                                  2    2      2          2     |
  1   8+                                                               +
        |                                                               |
        |                              2                                |
        |                       2                 2                     |
        |                             2  2      222                     |
      6+                        2                                       +
        |            2                          2                       |
        |                                                               |
        |                                                               |
        |                  2                                            |
      4+                                                               +
        |                                                               |
        |                                                               |
        |                                                               |
        |                                                               |
      2+                                                               +
        |                                                               |
        |                                                               |
        |                                                               |
        |                                                               |
      0+                                                               +
          ++----+----+----+----+----+----+----+----+----+----+----+----++
          5         6         7         8         9        10        11

                                    UH2
```

        32 cases plotted.
    Use first digit of ID as plotting symbol and $ for multiple
occurrence.

A-15

Figure A.8 A scatter diagram of the LQ1 values against the UQ1 values.

```
                        PLOT OF LQ1 WITH UQ1 BY ID
        ++----+----+----+----+----+----+----+----+----+----+----+----++
      7+                                                              +
       |                                                              |
       |                                                              |
       |                                                              |
       |                                                              |
      6+                                       1 1                    +
       |                                                              |
       |                                                              |
       |                                                              |
       |                                           1                  |
      5+                                         1                    +
       |                                                              |
       |                                             1                |
       |                                         1 1                  |
       |                                                              |
      4+                                                              +
       |                                         1                    |
       |                                                              |
    L  |                                                              |
    Q  |                                         1                    |
    1  3+                                                             +
       |                   2                 1                        |
       |                22       22              1                    |
       |             2  2                            1                |
       |                             2       1                        |
      2+                2   2                                         +
       |                   2                     1                    |
       |                      2                      1                |
       |             2   2       2               1                   |
       |                   2                                          |
      1+                                                              +
       |                                                              |
       |                                                              |
       |                                                              |
       |                                                              |
      0+                                                              +
       |                                                              |
       |                                                              |
       |                                                              |
       |                                                              |
     -1+                                                              +
        ++----+----+----+----+----+----+----+----+----+----+----+----++
          0    1    2    3    4    5    6
```

UQ1

      32 cases plotted.
  Use first digit of ID as plotting symbol and $ for multiple
occurrence.

Figure A.9 A scatter diagram of the LQ2 values against the UQ2 values.

PLOT OF LQ2 WITH UQ2 BY ID

32 cases plotted.
Use first digit of ID as plotting symbol and $ for multiple occurrence.

Figure A.10 A scatter diagram of the LQ3 values against the UQ3 values.

```
                        PLOT OF LQ3 WITH UQ3 BY ID
       ++----+----+----+----+----+----+----+----+----+----+----+----+----++
   11+                                                                    +
     |                                                                    |
     |                                                                    |
     |                                                                    |
     |                                                                    |
   10+                        1                                           +
     |                            1                    1                  |
     |                   1                                                |
     |                        1                    1                      |
     |                                                                    |
    9+              1          1                                          +
     |                                                                    |
     |                                                                    |
     |                             1                                      |
     |                                1              1                    |
    8+                                                  1                 +
     |                                                                    |
     |                                        1      1                    |
  L  |                                                                    |
  Q  |                                                                    |
  3  7+                             2            1                        +
     |                                                                    |
     |                          2                                         |
     |                        1                        2                  |
     |                                    2      2                        |
    6+                                      2                             +
     |                                    2                               |
     |                                  2      2  2                       |
     |                               2                                    |
     |                                 2                                  |
    5+                    22                                              +
     |              2                                                     |
     |                                                                    |
     |                                                                    |
     |                                                                    |
    4+                                  2                                 +
     |                                                                    |
     |                                                                    |
     |                                                                    |
     |                                                                    |
    3+                                                                    +
       ++----+----+----+----+----+----+----+----+----+----+----+----+----++
        2         3         4         5         6         7         8
```

UQ3

32 cases plotted.
Use first digit of ID as plotting symbol and $ for multiple occurrence.

A-18

Figure A.11 A scatter diagram of the LQ4 values against the UQ4 values.


```
                      PLOT OF LQ4 WITH UQ4 BY ID
        ++----+----+----+----+----+----+----+----+----+----+----+----++
      9+                                                              +
       |                                                              |
       |                                                              |
       |                                                              |
       |                                                              |
      8+                              1                               +
       |                                              1               |
       |                1                 1                           |
       |                  1                                           |
       |                                                         1    |
      7+                                                              +
       |                               1     1                        |
       |                      1           1        1           1      |
       |                                      1                       |
       |                                                              |
      6+                                          1                   +
       |                                          1                   |
       |                                                              |
   L   |            1                                                 |
   Q   |                                                              |
   4  5+                                 1                            +
       |                                                              |
       |          2                                                   |
       |                     2                                        |
       |                                                              |
      4+                                                              +
       |                          2                                   |
       |                                                              |
       |                     2                               2        |
       |                       2    2     2                           |
      3+                       2                                      +
       |      2                             22                        |
       |                 2   2  2                                     |
       |                 2                                            |
       |                                                              |
      2+                                                              +
       |                                                              |
       |                                                              |
       |                                                              |
       |                                                              |
      1+                                                              +
        ++----+----+----+----+----+----+----+----+----+----+----+----++
        1.5        2        2.5       3        3.5       4        4.5

                                    UQ4

          32 cases plotted.
     Use first digit of ID as plotting symbol and $ for multiple
   occurrence.
```

A-19

Figure A.12 A scatter diagram of the L1 values against the U1 values.

```
                            PLOT OF L1 WITH U1 BY ID
        ++----+----+----+----+----+----+----+----+----+----+----+----++
   1.4+                                                                +
      |                                                                |
      |                                                                |
      |                                                                |
      |                                      1                         |
   1.2+                                                                +
      |                                                                |
      |                                                                |
      |                                                                |
      |                                                                |
     1+                         2                                      +
      |                                          11                    |
      |                         2                                      |
      |                                                                |
      |               2                    1    1                      |
    .8+                2        2          1  1                        +
      |                2              1   1                            |
      |                                    11                          |
      |            2               2 1               1                 |
   L  |              2                             1                   |
   1     .6+                                                           +
      |            2                 1  1                              |
      |              22                                                |
      |                2                                               |
      |        2                 2                                     |
    .4+                                                                +
      |        2                                                       |
      |                                                                |
      |                                                                |
      |                                                                |
    .2+                                                                +
      |                                                                |
      |                                                                |
      |                                                                |
      |                                                                |
     0+                                                                +
      |                                                                |
      |                                                                |
      |                                                                |
      |                                                                |
  -.2+                                                                 +
        ++----+----+----+----+----+----+----+----+----+----+----+----++
        -.4      0       .4       .8      1.2      1.6       2

                                   U1
```

32 cases plotted.
Use first digit of ID as plotting symbol and $ for multiple occurrence.

Figure A.13 A scatter diagram of the L2 values against the U2 values.

```
                         PLOT OF L2 WITH U2 BY ID
        ++----+----+----+----+----+----+----+----+----+----+----+----+----++
      6+                                                                    +
       |                                                                    |
       |                                                                    |
       |                                                                    |
       |                                                                    |
      5+                                           1       1                +
       |                                                                    |
       |                                                                    |
       |                                                     1              |
       |                                                 1                  |
      4+                                                                    +
       |                                             1              1       |
       |                                                                    |
       |                                                   1                |
       |                                                                    |
      3+                                                   1                +
       |                                                                    |
       |                                               1                    |
       |                                                                    |
  L    |                   2                                                |
  2   2+                                         1                          +
       |                2     2   2                        1                |
       |        2    2           2        2                               11|
       |                                             1                      |
       |        2            2        2          1                          |
      1+              2 2              2                                   1+
       |                        2                          1                |
       |                                                                    |
       |                                                                    |
       |                                                                    |
      0+                                                                    +
       |                                                                    |
       |                                                                    |
       |                                             .                      |
       |                                                                    |
     -1+                                                                    +
       |                                                                    |
       |                                                                    |
       |                                                                    |
       |                                                                    |
     -2+                                                                    +
        ++----+----+----+----+----+----+----+----+----+----+----+----+----++
          .8        1.2       1.6        2        2.4       2.8       3.2

                                    U2
```

      32 cases plotted.
  Use first digit of ID as plotting symbol and $ for multiple occurrence.

A-21

Figure A.14 A scatter diagram of the L3 values against the U3 values.


```
                        PLOT OF L3 WITH U3 BY ID
      ++----+----+----+----+----+----+----+----+----+----+----+----++
    7+ +                                                           +
     I                                    1    1                   I
     I                                         1                   I
     I                                                   :         I
     I                                         1                   I
    6+                                    1      11   1            +
     I                                    1         1              I
     I                                             1               I
     I                                         1                   I
     I                                         1                   I
    5+                                                             +
     I                                                  1          I
     I                                         1                   I
     I                                                             I
     I                                                             I
    4+                                                             +
     I                                                             I
     I                                                             I
     I                                                             I
 L   I                                                             I
 3  3+                                                             +
     I                          2                                  I
     I                             2                               I
     I                       2                                     I
     I                     2 22 22                                 I
    2+                   2           2 2                           I
     I                                                             I
     I                       2     2                               I
     I                                                             I
     I                       2     2                               I
    1+                                                             +
     I                                                             I
     I                                                             I
     I                                                             I
     I                                                             I
    0+                                                             +
     I                                                             I
     I                                                             I
     I                                                             I
     I                                                             I
   -1+                                                             +
      ++----+----+----+----+----+----+----+----+----+----+----+----++
       0         1         2         3         4         5         6
```

U3

32 cases plotted.
Use first digit of ID as plotting symbol and $ for multiple
occurrence.

A-22

Figure A.15 A scatter diagram of the L4 values against the U4 values.

PLOT OF L4 WITH U4 BY ID

```
        ++----+----+----+----+----+----+----+----+----+----+----+----++
     8+                                        1                        +
      |
      |
      |
      |                                      1
     7+                                      1                          +
      |
      |
      |                                        1
      |
     6+                                      1                          +
      |                                    1     1        1             +
      |                                              1   1
      |                                    1 1
      |                                        1   1
     5+                                        1                        +
      |
      |                          1           1
      |
  L   |                                                                 |
  4  4+                                                                 +
      |
      |
      |
      |                    2
     3+                        2     2                                  +
      |                      2
      |                              2 2
      |                  2       2 2
      |              2           2           2
     2+                                                                 +
      |                      2       2
      |
      |
      |
     1+                                                                 +
      |
      |
      |
     0+                                                                 +
        ++----+----+----+----+----+----+----+----+----+----+----+----++
        0         1         2         3         4         5         6
```

U4

32 cases plotted.
Use first digit of ID as plotting symbol and $ for multiple
occurrence.

A-23

Figure A.16 A scatter diagram of the L5 values against the U6 values.

PLOT OF L5 WITH U6 BY ID

32 cases plotted.
Use first digit of ID as plotting symbol and $ for multiple occurrence.

Figure A.17 A scatter diagram of the L6 values against the U6 values.


```
                        PLOT OF L6 WITH U6 BY ID
         ++----+----+----+----+----+----+----+----+----+----+----+----++
      5+                                                                 +
       |                                                                 |
       |                                                                 |
       |                                                                 |
       |              1              1        1                          |
    4.5+                                                                 +
       |                 1    1                                          |
       |                                                                 |
       |                    1                         1                  |
       |                                    1                            |
      4+          -                                  1                   +
       |                                                                 |
       |                    1                    1                       |
       |                                                                 |
       |                                                                 |
    3.5+                                         1                       +
       |                                2              2                 |
       |                         1                                       |
       |                            1  1            2                    |
    L  |                                        1        2  2            |
    6  3+                                                    2           +
       |                                                 2               |
       |                                    2       22                   |
       |                                                                 |
       |                                             2                   |
    2.5+                                         2                       +
       |              2                                                  |
       |                          2                                      |
       |                    2                                            |
      2+                                        2                        +
       |                                                                 |
       |                                                                 |
       |                                                                 |
       |                                                                 |
    1.5+                                                                 +
       |                                                                 |
       |                                                                 |
       |                                                                 |
       |                                                                 |
      1+                                                                 +
         ++----+----+----+----+----+----+----+----+----+----+----+----++
         1.2      1.6       2      2.4      2.8      3.2      3.6
```

U6

        32 cases plotted.
  Use first digit of ID as plotting symbol and $ for multiple
occurrence.

A-25

Figure A.18 A scatter diagram of the L7 values against the U7 values.

```
                          PLOT OF L7 WITH U7 BY ID
          ++----+----+----+----+----+----+----+----+----+----+----+----+--++
      5.5+                                                                  +
         |                                                                  |
         |                                  1    1                          |
         |                                                                  |
         |                                                                  |
       5+                                      1                            +
         |                         1                                        |
         |                                                                  |
         |                                                                  |
         |                                   1                              |
     4.5+                                                          1        +
         |                             1              1                     |
         |                               1       1   1              1       |
         |                                                                  |
         |                                      1                           |
       4+                                                                   +
         |                                                                  |
         |                                                                  |
         |                                         1                        |
   L     |                                                                  |
   7   3.5+                           1                1                     +
         |                                                                  |
         |                                                                  |
         |                                      2                           |
         |                         2                                        |
       3+                                                                   +
         |                                                                  |
         |                                            2                     |
         |                                                                  |
     2.5+                                                        2          +
         |                                         2                        |
         |                                          2                       |
         |                                     2    22        2             |
         |                                           2                      |
       2+                                      2                            +
         |               2                  2    2                          |
         |                                  2                               |
         |                                                                  |
     1.5+                                                                   +
          ++----+----+----+----+----+----+----+----+----+----+----+----+--++
          .8      1.2      1.6       2       2.4      2.8      3.2

                                    U7
```

32 cases plotted.
Use first digit of ID as plotting symbol and $ for multiple occurrence.

A-26

Figure A.19 A scatter diagram of the L8 values against the U8 values.

```
                          PLOT OF L8 WITH U8 BY ID
          ++----+----+----+----+----+----+----+----+----+----+----+----++
     3.5+                                                               +
        !
        |
        |
        |
      3+                              1                                  +
        |                             1
        |
        |                                      1
        |                           1 1
     2.5+                                        1   1 1                 +
        !                                      1  1
        |                         1
        |
        |                                      1
      2+                                                                 +
        |                    1
        |                                 1
        |
  L     |
  8   1.5+                                      1                        +
        !                1             1
        |                    1
        |                        1
        |
      1+                   22                                            +
        |                       2   2   2                                +
        |             2         2
        |                     2  2 2
        |                   2    2   2
      .5+                                                                +
        |
        !
        |
        |
      0+                                                                 +
        |
        |
        |
        |
    -.5+                                                                 +
          ++----+----+----+----+----+----+----+----+----+----+----+----++
          -.4      0      .4      .8      1.2      1.6      2

                                     U8
```

32 cases plotted.
Use first digit of ID as plotting symbol and $ for multiple occurrence.

A-27

B. COLOUR PATTERN IDENTIFICATION.

In this Appendix, the data and result of analysis which were obtained during the validation stage for colour pattern classification are described. There were two different kinds of butterfly species, as shown in Figures B.1.(a) and (d), involved in the test. Since the number of colour patterns of Species A is different from that of Species B, the result of comparison between species is apparent. Thus, in this test each colour pattern of a test species was compared with each of five colour patterns (2 for Species A, 3 for Species B) in the library data. For each species the number of samples was 15, where 10 samples for each species were randomly selected from the given samples for the learning stage; and 5 for the implementation stage. Each colour pattern extracted from each species is shown in Figures B.1.(b), (c), (e), (f) and (g). After rotation of each pattern 13 descriptors for each pattern were calculated. Each descriptor is illustrated as following:

Size : the number of pixels in a pattern/total number of pixels

N_cx : the normalised centre of gravity x of a pattern

N_cy : the normalised centre of gravity y of a pattern

Beta : the slope of a pattern

H1 : the number of pixels in the upper part/total number of pixels in a pattern

H2 : the number of pixels in the lower part/total number of pixels in a pattern

Q1 : the number of pixels in the quadrant I/ total number of pixels in a pattern

Q2 : the number of pixels in the quadrant II/ total number of pixels in a pattern

Q3 : the number of pixels in the quadrant III/ total number of

pixels in a pattern

Q4   : the number of pixels in the quadrant IV/ total number of
pixels in a pattern

L_m : the average value of L* contained in a pattern

A_m : the average value of A* contained in a pattern

B_m : the average value of B* contained in a pattern

(a)
Species A

Pattern 1

Pattern 2

(b)

(c)

(d) Species B

Pattern 3

Pattern 4

Pattern 5

(e)

(f)

(g)
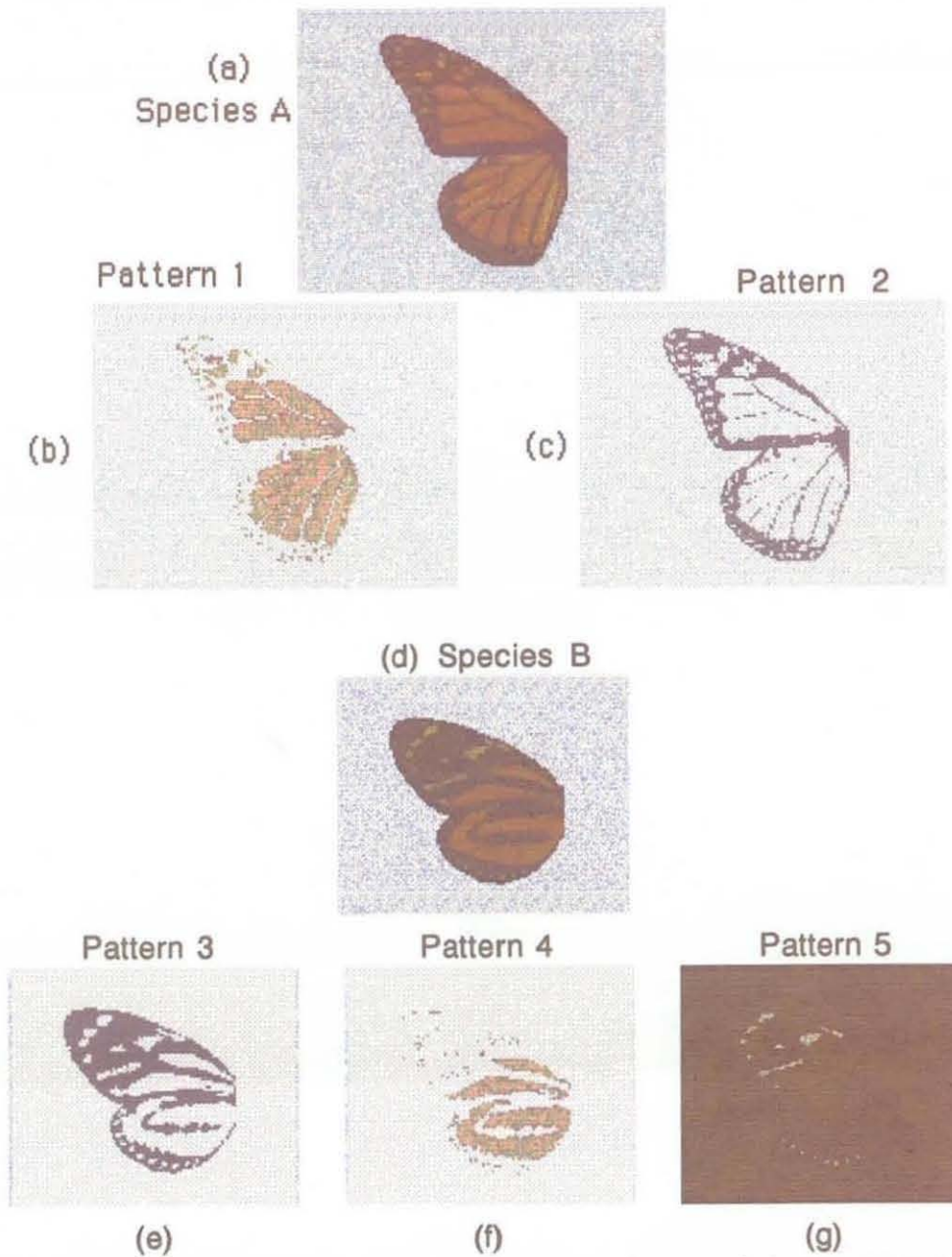
Figure B.1 Wing patterns and colour patterns. (a) The left-hand side wings of Species A. (b) and (c) Colour patterns of Species A. (d) The left-hand side wings of species B. (e)-(g) Colour patterns of Species B.

Table B.1.(a) The values of descriptors for 10 samples of Pattern 1 involved in the learning stage.

Size	N_cx	N_cy	Beta	H1	H2	Q1	Q2	Q3	Q4	L_m	A_m	B_m
52.34	0.59	0.55	0.04	0.49	0.51	0.25	0.24	0.20	0.31	51.78	6.87	87.42
65.54	0.53	0.55	0.04	0.46	0.54	0.24	0.22	0.23	0.31	18.62	-4.65	6.75
75.05	0.52	0.53	0.04	0.49	0.51	0.26	0.23	0.24	0.27	34.23	-1.58	24.91
64.39	0.52	0.54	0.07	0.46	0.54	0.24	0.22	0.24	0.30	31.29	-3.16	19.54
58.29	0.60	0.57	0.01	0.48	0.52	0.24	0.24	0.21	0.31	48.84	12.71	80.06
71.52	0.52	0.53	0.06	0.47	0.53	0.25	0.22	0.23	0.30	35.64	-2.57	28.79
52.98	0.57	0.55	0.03	0.47	0.53	0.25	0.22	0.22	0.31	41.62	8.22	55.87
62.21	0.57	0.55	0.04	0.50	0.50	0.24	0.26	0.20	0.30	51.88	7.52	85.48
61.03	0.56	0.54	0.06	0.49	0.51	0.22	0.28	0.20	0.31	49.44	12.56	81.68
57.42	0.59	0.54	0.03	0.48	0.52	0.24	0.24	0.21	0.31	52.27	7.45	89.27

Table B.1.(b) The values of descriptors for 5 samples of Pattern 1 involved in the implementation stage.

Size	N_cx	N_cy	Beta	H1	H2	Q1	Q2	Q3	Q4	L_m	A_m	B_m
59.63	0.60	0.55	0.05	0.50	0.50	0.25	0.25	0.18	0.32	51.81	9.06	94.77
55.81	0.55	0.53	0.06	0.48	0.52	0.19	0.28	0.24	0.28	45.84	6.71	76.61
53.23	0.58	0.54	0.07	0.46	0.54	0.21	0.24	0.21	0.33	45.31	9.17	72.46
63.96	0.53	0.55	0.02	0.48	0.52	0.25	0.23	0.24	0.28	41.34	3.12	59.09
61.74	0.59	0.55	0.05	0.49	0.51	0.22	0.27	0.20	0.30	51.13	9.24	94.96

Table B.2.(a) The values of descriptors for 10 samples of Pattern 2 involved in the learning stage.

Size	N_cx	N_cy	Beta	H1	H2	Q1	Q2	Q3	Q4	L_m	A_m	B_m
47.66	0.51	0.53	0.08	0.45	0.55	0.22	0.23	0.24	0.31	22.30	-4.6	8.13
34.46	0.61	0.56	0.04	0.48	0.52	0.25	0.24	0.21	0.30	49.39	8.08	79.73
24.95	0.64	0.53	0.08	0.50	0.50	0.29	0.21	0.15	0.35	57.22	7.67	123.94
35.61	0.60	0.55	0.08	0.51	0.49	0.23	0.28	0.19	0.30	0.00	0.00	0.00
41.71	0.50	0.54	0.04	0.44	0.56	0.22	0.22	0.25	0.31	28.27	-5.11	10.57
28.48	0.63	0.55	0.07	0.51	0.49	0.24	0.27	0.17	0.32	0.00	0.00	0.00
47.02	0.54	0.51	0.13	0.42	0.58	0.18	0.24	0.20	0.38	28.63	-2.42	10.99
37.79	0.52	0.52	0.15	0.47	0.53	0.20	0.27	0.19	0.34	28.73	-1.59	10.83
38.97	0.51	0.54	0.07	0.47	0.53	0.25	0.21	0.23	0.31	28.94	-0.38	11.25
42.58	0.54	0.53	0.06	0.46	0.54	0.25	0.21	0.24	0.30	28.19	-6.00	10.42

Table B.2.(b) The values of descriptors for 5 samples of Pattern 2 involved in the implementation stage.

Size	N_cx	N_cy	Beta	H1	H2	Q1	Q2	Q3	Q4	L_m	A_m	B_m
40.37	0.50	0.53	0.06	0.46	0.54	0.23	0.23	0.25	0.29	28.45	-3.57	10.81
44.19	0.50	0.51	0.08	0.41	0.59	0.20	0.21	0.26	0.33	28.63	-2.48	10.98
46.77	0.49	0.52	0.08	0.44	0.56	0.21	0.23	0.24	0.32	28.28	-4.93	10.59
36.04	0.58	0.51	0.10	0.39	0.61	0.22	0.17	0.25	0.36	28.91	-1.00	11.02
38.26	0.49	0.52	0.07	0.40	0.60	0.18	0.22	0.27	0.33	28.46	-3.42	10.85

Table B.3.(a) The values of descriptors for 10 samples of Pattern 3 involved in the learning stage.

Size	N_cx	N_cy	Beta	H1	H2	Q1	Q2	Q3	Q4	L_m	A_m	B_m
57.43	0.52	0.52	-0.02	0.47	0.53	0.25	0.22	0.25	0.28	28.16	-5.59	10.54
57.60	0.49	0.49	0.13	0.54	0.46	0.23	0.31	0.18	0.28	28.68	-4.91	11.38
63.66	0.54	0.51	0.04	0.48	0.52	0.25	0.24	0.22	0.30	28.54	-4.33	11.27
57.06	0.53	0.49	0.11	0.50	0.50	0.24	0.27	0.19	0.31	28.08	-6.15	10.46
65.84	0.52	0.52	-0.01	0.48	0.52	0.23	0.24	0.25	0.27	29.51	-4.79	14.79
61.45	0.52	0.51	-0.02	0.47	0.53	0.25	0.22	0.26	0.27	29.23	-5.60	14.40
59.19	0.52	0.52	-0.02	0.47	0.53	0.24	0.23	0.26	0.27	28.09	-6.10	10.47
65.32	0.55	0.52	0.01	0.49	0.51	0.25	0.24	0.23	0.29	28.91	-4.42	12.73
58.40	0.50	0.50	0.08	0.52	0.48	0.23	0.28	0.21	0.28	28.25	-4.95	10.63
68.74	0.53	0.51	0.05	0.50	0.50	0.24	0.25	0.23	0.27	30.51	-2.15	17.08

Table B.3.(b) The values of descriptors for 5 samples of Pattern 3 involved in the implementation stage.

Size	N_cx	N_cy	Beta	H1	H2	Q1	Q2	Q3	Q4	L_m	A_m	B_m
58.67	0.49	0.50	0.09	0.51	0.49	0.23	0.28	0.23	0.26	28.27	-4.90	10.64
57.59	0.52	0.52	0.00	0.50	0.50	0.25	0.25	0.24	0.27	28.25	-4.99	10.62
58.12	0.52	0.51	0.05	0.49	0.51	0.24	0.25	0.22	0.29	28.24	-4.96	10.63
62.68	0.54	0.51	0.07	0.49	0.51	0.25	0.24	0.21	0.30	28.50	-4.90	11.08
56.64	0.52	0.53	-0.02	0.46	0.54	0.25	0.21	0.25	0.29	28.08	-6.15	10.46

Table B.4.(a) The values of descriptors for 10 samples of Pattern 4 involved in the learning stage.

Size	N_cx	N_cy	Beta	H1	H2	Q1	Q2	Q3	Q4	L_m	A_m	B_m
31.85	0.71	0.53	-0.06	0.50	0.50	0.26	0.24	0.25	0.25	51.11	11.50	97.99
34.64	0.72	0.47	-0.04	0.47	0.53	0.24	0.23	0.27	0.26	52.57	9.63	106.05
27.13	0.70	0.52	-0.09	0.49	0.51	0.25	0.24	0.28	0.23	51.24	13.06	96.83
28.72	0.71	0.50	-0.10	0.50	0.50	0.26	0.24	0.27	0.23	51.07	13.44	93.86
29.08	0.68	0.54	-0.06	0.50	0.50	0.26	0.24	0.25	0.25	53.45	12.22	105.37
31.83	0.66	0.53	-0.04	0.50	0.50	0.26	0.24	0.24	0.26	51.58	13.40	96.88
34.33	0.67	0.54	-0.05	0.49	0.51	0.26	0.23	0.24	0.26	52.21	11.50	98.49
29.35	0.69	0.53	-0.09	0.50	0.50	0.26	0.24	0.25	0.24	51.96	11.35	100.45
33.01	0.70	0.51	-0.03	0.49	0.51	0.25	0.24	0.26	0.25	54.54	13.40	109.84
25.46	0.70	0.51	-0.06	0.49	0.51	0.25	0.24	0.27	0.24	54.24	13.35	108.44

Table B.4.(b) The values of descriptors for 5 samples of Pattern 4 involved in the implementation stage.

Size	N_cx	N_cy	Beta	H1	H2	Q1	Q2	Q3	Q4	L_m	A_m	B_m
36.48	0.71	0.49	-0.04	0.48	0.52	0.26	0.22	0.26	0.26	49.45	9.55	90.35
34.45	0.69	0.53	-0.08	0.50	0.50	0.27	0.22	0.26	0.24	50.37	10.87	92.26
33.60	0.66	0.52	0.01	0.49	0.51	0.25	0.24	0.23	0.27	47.69	13.90	77.67
24.89	0.72	0.52	-0.02	0.49	0.51	0.24	0.25	0.25	0.25	52.06	13.78	99.33
30.51	0.70	0.55	-0.14	0.51	0.49	0.28	0.23	0.25	0.24	46.72	11.59	75.15

Table B.5.(a) The values of descriptors for 10 samples of Pattern 5 involved in the learning stage.

Size	N_cx	N_cy	Beta	H1	H2	Q1	Q2	Q3	Q4	L_m	A_m	B_m
10.72	0.35	0.51	0.18	0.50	0.50	0.21	0.29	0.26	0.23	66.40	-1.22	37.77
7.76	0.34	0.51	0.13	0.54	0.46	0.31	0.23	0.28	0.18	71.73	-0.38	33.29
9.21	0.35	0.53	0.00	0.50	0.50	0.34	0.15	0.27	0.23	64.44	2.95	45.34
14.22	0.39	0.52	0.15	0.56	0.44	0.30	0.26	0.28	0.17	64.52	-0.16	38.85
5.08	0.32	0.53	0.02	0.51	0.49	0.31	0.21	0.24	0.24	71.19	-2.84	55.89
6.72	0.37	0.53	0.10	0.52	0.48	0.21	0.31	0.28	0.20	66.66	-2.58	50.53
6.47	0.33	0.52	0.19	0.49	0.51	0.28	0.22	0.27	0.23	67.50	0.76	83.03
5.34	0.30	0.53	0.14	0.51	0.49	0.33	0.18	0.36	0.13	68.66	-3.71	20.12
8.59	0.43	0.52	0.27	0.53	0.47	0.15	0.38	0.27	0.20	56.75	-1.25	49.05
5.81	0.38	0.55	0.16	0.54	0.46	0.41	0.14	0.25	0.20	65.91	-5.04	45.94

Table B.5.(b) The values of descriptors for 5 samples of Pattern 5 involved in the implementation stage.

Size	N_cx	N_cy	Beta	H1	H2	Q1	Q2	Q3	Q4	L_m	A_m	B_m
4.85	0.39	0.51	0.35	0.56	0.44	0.30	0.26	0.22	0.22	65.13	-5.09	44.02
7.96	0.33	0.52	0.15	0.49	0.51	0.30	0.19	0.25	0.26	66.88	0.17	61.26
8.28	0.34	0.53	0.20	0.53	0.47	0.31	0.22	0.24	0.23	65.79	-5.20	46.28
12.43	0.38	0.53	0.16	0.55	0.45	0.32	0.23	0.25	0.20	63.81	0.84	65.36
12.85	0.34	0.55	-0.09	0.49	0.51	0.36	0.13	0.25	0.26	70.77	-9.26	30.61

Table B.6.(a) The mean and standard deviation of each descriptor using 10 samples of each Pattern involved in the learning stage.

Pattern n	M SD	Size	N_cx	N_cy	Beta	H1	H2	Q1	Q2	Q3	Q4	L_m	A_m	B_m
1	M	62.08	0.56	0.55	0.04	0.48	0 52	0 24	0 24	0.22	0 30	41.56	4.34	55 98
	SD	7 38	0 03	0 01	0 02	0.01	0 01	0 01	0 02	0 02	0 01	11.36	6 66	32.77
2	M	37.92	0.56	0.54	0.08	0.47	0 53	0.23	0.24	0.21	0.32	27.17	-0.44	26.59
	SD	7.38	0 05	0 02	0.04	0.03	0.03	0.03	0.03	0.03	0 03	17.97	4.89	41 23
3	M	61.47	0 52	0 51	0 03	0 49	0.51	0.24	0 25	0.23	0 28	28 80	-4.90	12.38
	SD	4.18	0.02	0 01	0.06	0 02	0.02	0.01	0.03	0 03	0.01	0.78	1.16	2.31
4	M	30.54	0.69	0 52	-0 06	0.49	0.51	0.25	0.24	0.26	0.25	52.40	12 29	101.42
	SD	3.07	0 02	0.02	0 02	0.01	0 01	0 01	0 00	0 01	0.01	1.28	1.28	5.55
5	M	7.99	0 36	0.52	0.13	0.52	0.48	0.29	0.24	0.28	0.20	66.38	-1.35	45.98
	SD	2.83	0.04	0.01	0.08	0 02	0.02	0 08	0 07	0.03	0.03	4.20	2 32	16 5

Figure B.2 A diagram for the ranges of Size of each pattern.

```
                          PLOT OF ID WITH X1
        ++----+----+----+----+----+----+----+----+----+---------+----+----++
    5+            154221                                                    +
     I                                                                      I
     I                                                                      I
     I                                                                      I
     I                                                                      I
    4+                       1123251                                        +
     I                                                                      I
     I                                                                      I
     I                                                                      I
     I                                                                      I
Pattern 3+                                        171212                    +
     I                                                                      I
     I                                                                      I
     I                                                                      I
     I                                                                      I
    2+                         1 1   12312112                               +
     I                                                                      I
     I                                                                      I
     I                                                                      I
     I                                                                      I
    1+                                         21121321  1 1                +
        ++----+----+----+----+----+----+----+----+---------+----+----++
        -30       -10        10        30        50        7C        90
                                      Size
```
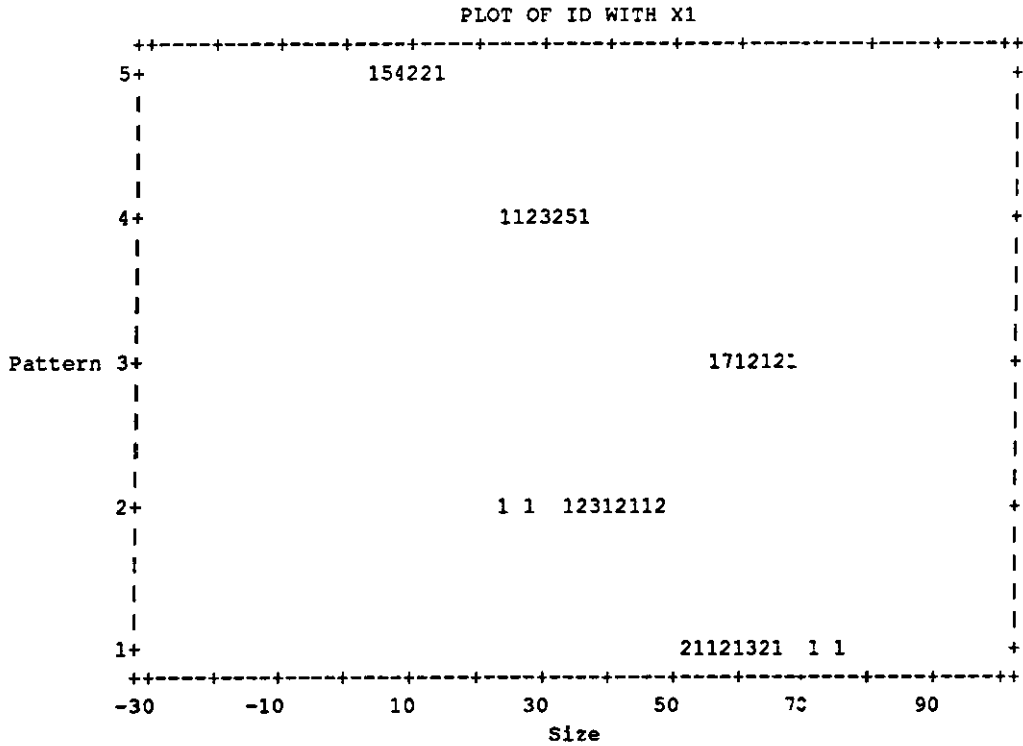
Figure B.3 A diagram for the ranges of Beta of each pattern.

```
                          PLOT OF ID WITH X4
        ++----+----+----+----+----+----+----+----+----+---------+----+----++
    5+                 1        1 1        1  1122 111        1          1   +
     I                                                                      I
     I                                                                      I
     I                                                                      I
     I                                                                      I
    4+            1    121 31311  1                                         +
     I                                                                      I
     I                                                                      I
     I                                                                      I
     I                                                                      I
Pattern 3+                 4111   12 111 1 1                                +
     I                                                                      I
     I                                                                      I
     I                                                                      I
     I                                                                      I
    2+                          2 235 1  1 1                                +
     I                                                                      I
     I                                                                      I
     I                                                                      I
     I                                                                      I
    1+                        1124232                                       +
        ++----+----+----+----+----+----+----+----+----+---------+----+----++
        -.25      -.15      -.05       .05       .15       .25       .35
                                      Beta
```

B-10
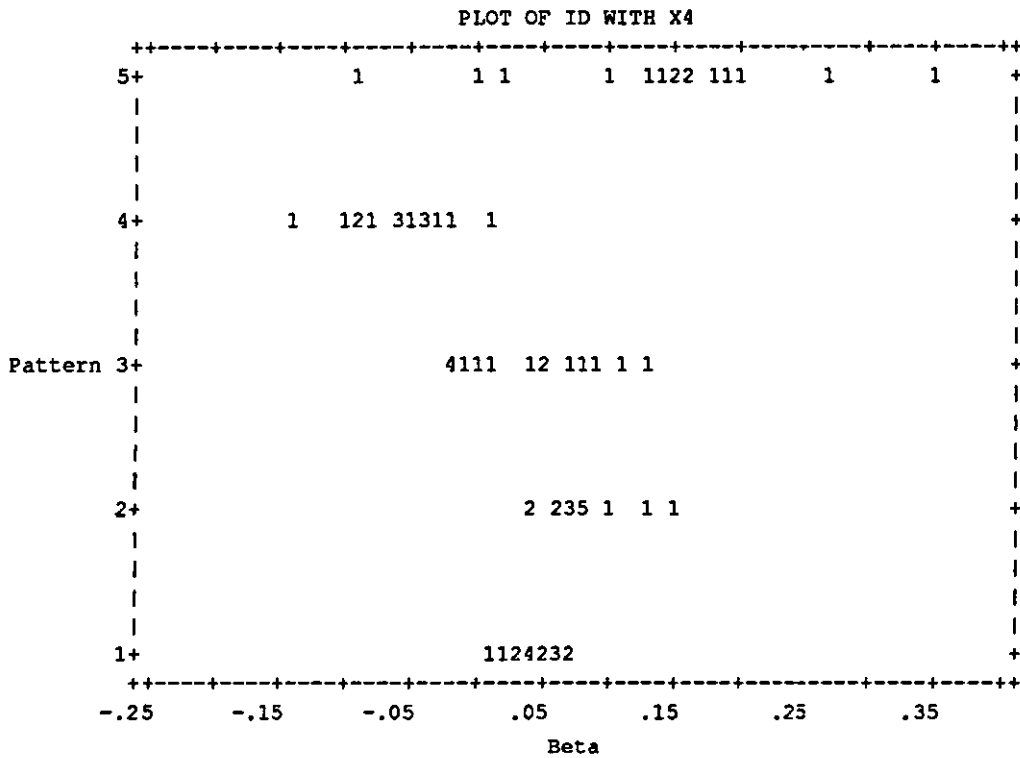
Figure B.4 A scatter diagram of the N_cy values against the N_cx values.


```
                        PLOT OF Y WITH X BY ID
       ++----+----+----+----+----+----+----+----+----+----+----+----+----++
  .58+                                                                    +
     |
     |                                              1
     |
     |
  .56+                                           2                         +
     |
     |            5    5                  1    1 1$  2        4
     |
     |
  .54+                                 221   1 11        44                +
     |
     |
     |         5 5 55 55          22$ 21          2 4  4 4
     |
  .52+            5      5    5    2  $  3              4   4 4             +
     |
     |            55    5          2 33$   2              4
     |
N_CY |
  .5+                              33                      4               +
     |
     |                              3    3                  4
     |
     |
  .48+                                                                     +
     |
     |                                                      4
     |
     |
  .46+                                                                     +
     |
     |
     |
     |
  .44+                                                                     +
     |
     |
     |
     |
  .42+                                                                     +
       ++----+----+----+----+----+----+----+----+----+----+----+----+----++
          .2        .3        .4        .5        .6        .7        .8

                                   N_CX
```
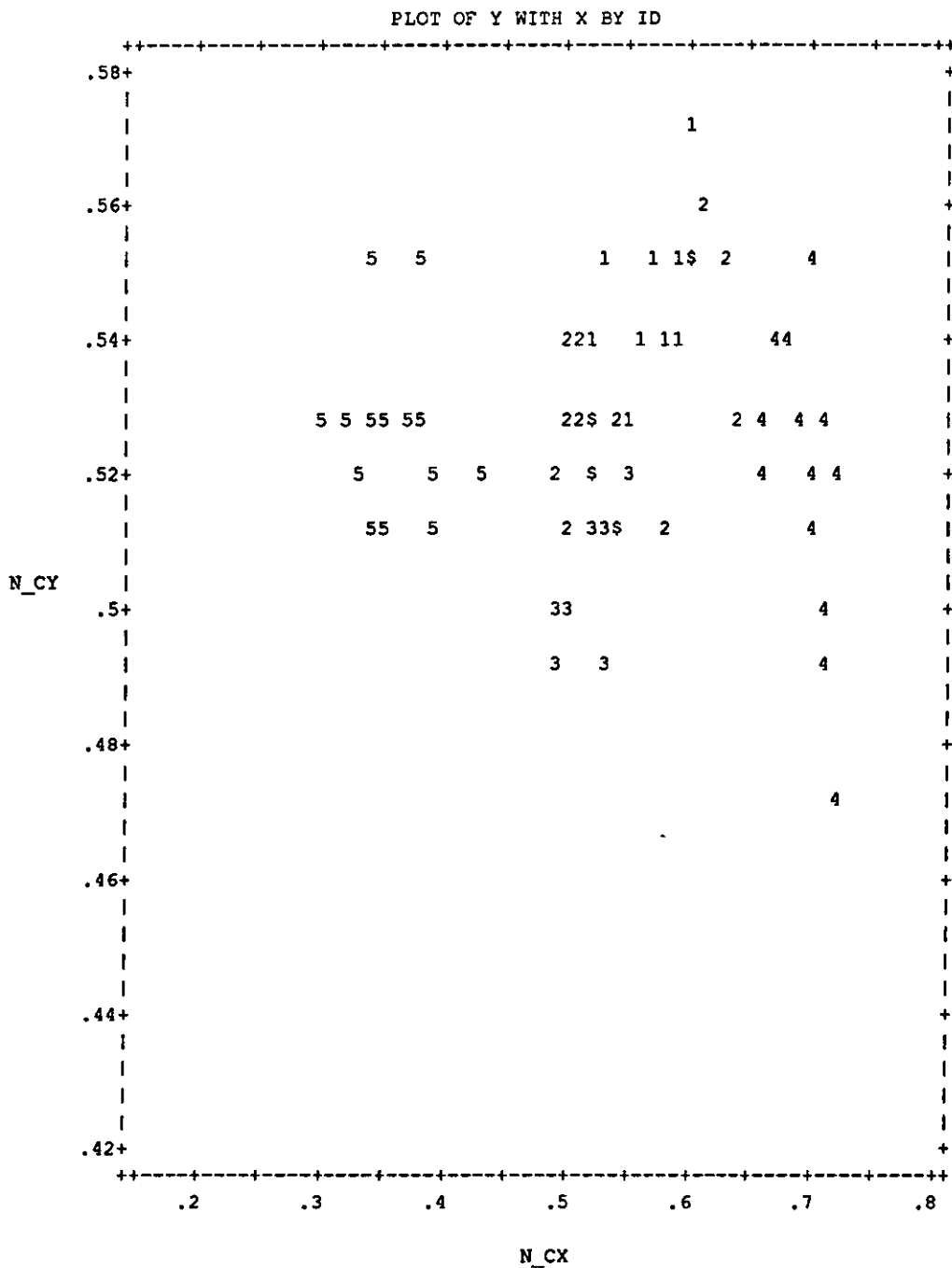
$ for multiple occurrence

```
Group 1: Pattern with Orange Colour in Plex
      2: Pattern with Dark-Brown in Plex
      3: Pattern with Dark-Brown in Cleo
      4: Pattern with Orange colour in Cleo
      5: Pattern with Yellow in Cleo
```

B-11

Figure B.5 A scatter diagram of the Q2 values against the Q1 values.
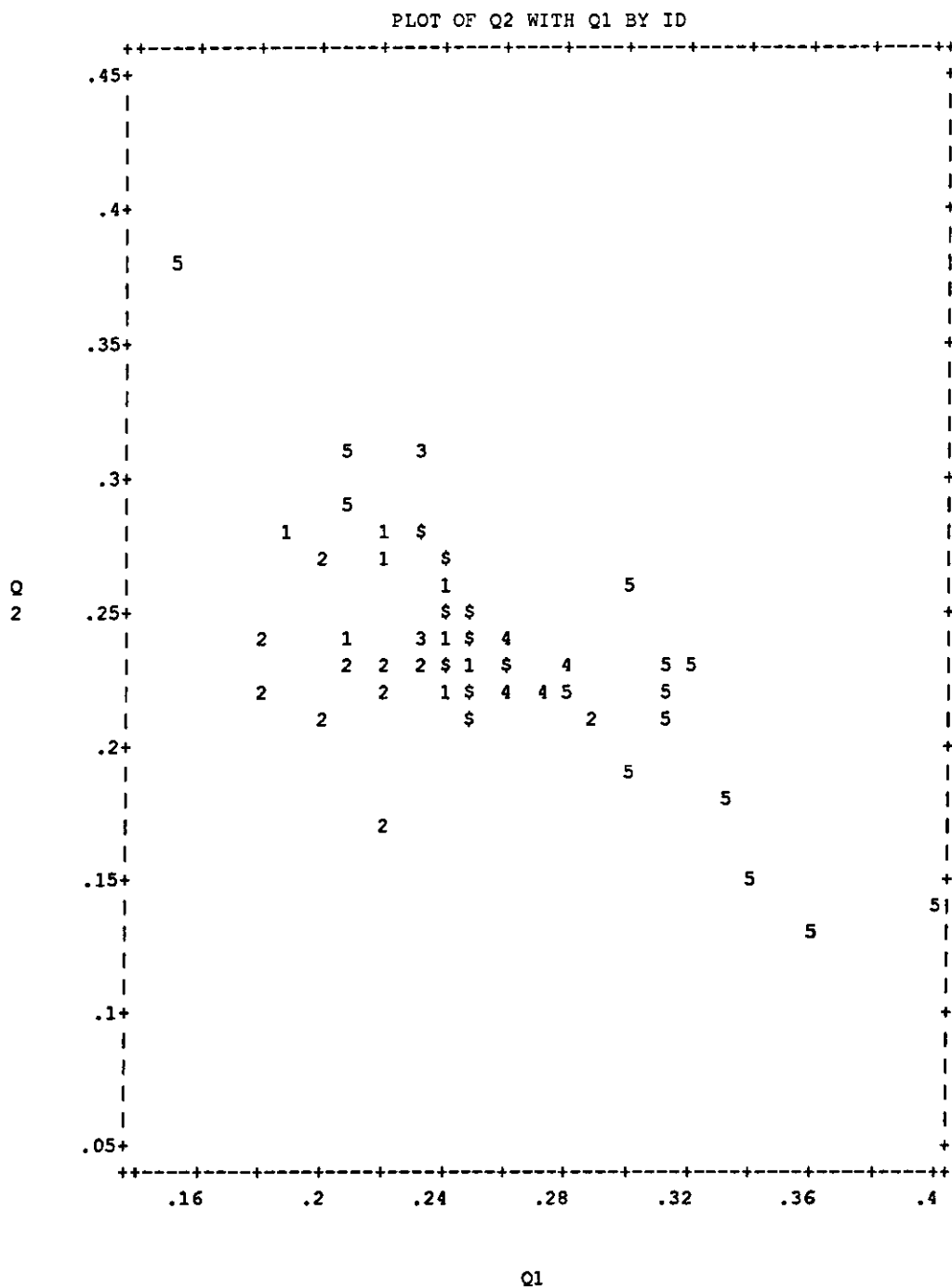
```
                          PLOT OF Q2 WITH Q1 BY ID
        ++----+----+----+----+----+----+----+----+----+----+----+----++
   .45+ +                                                             +
      |
      |
      |
      |
    .4+ +                                                             +
      |
      |    5
      |
      |
   .35+ +                                                             +
      |
      |
      |
      |                5        3
    .3+ +                                                             +
      |                5
      |          1        1  $
      |             2     1     $
 Q    |                      1              5
 2  .25+ +                   $ $                                      +
      |       2     1     3 1 $ 4
      |             2  2  2 $ 1   $      4        5 5
      |       2        2     1 $   4  4 5        5
      |          2           $           2       5
    .2+ +                                                             +
      |                               5
      |                                     5
      |          2
   .15+ +                               5                             +
      |                                                             5|
      |                                   5
      |
    .1+ +                                                             +
      |
      |
      |
      |
   .05+ +                                                             +
        ++----+----+----+----+----+----+----+----+----+----+----+----++
          .16      .2      .24      .28      .32      .36      .4

                                    Q1
```

        75 cases plotted.
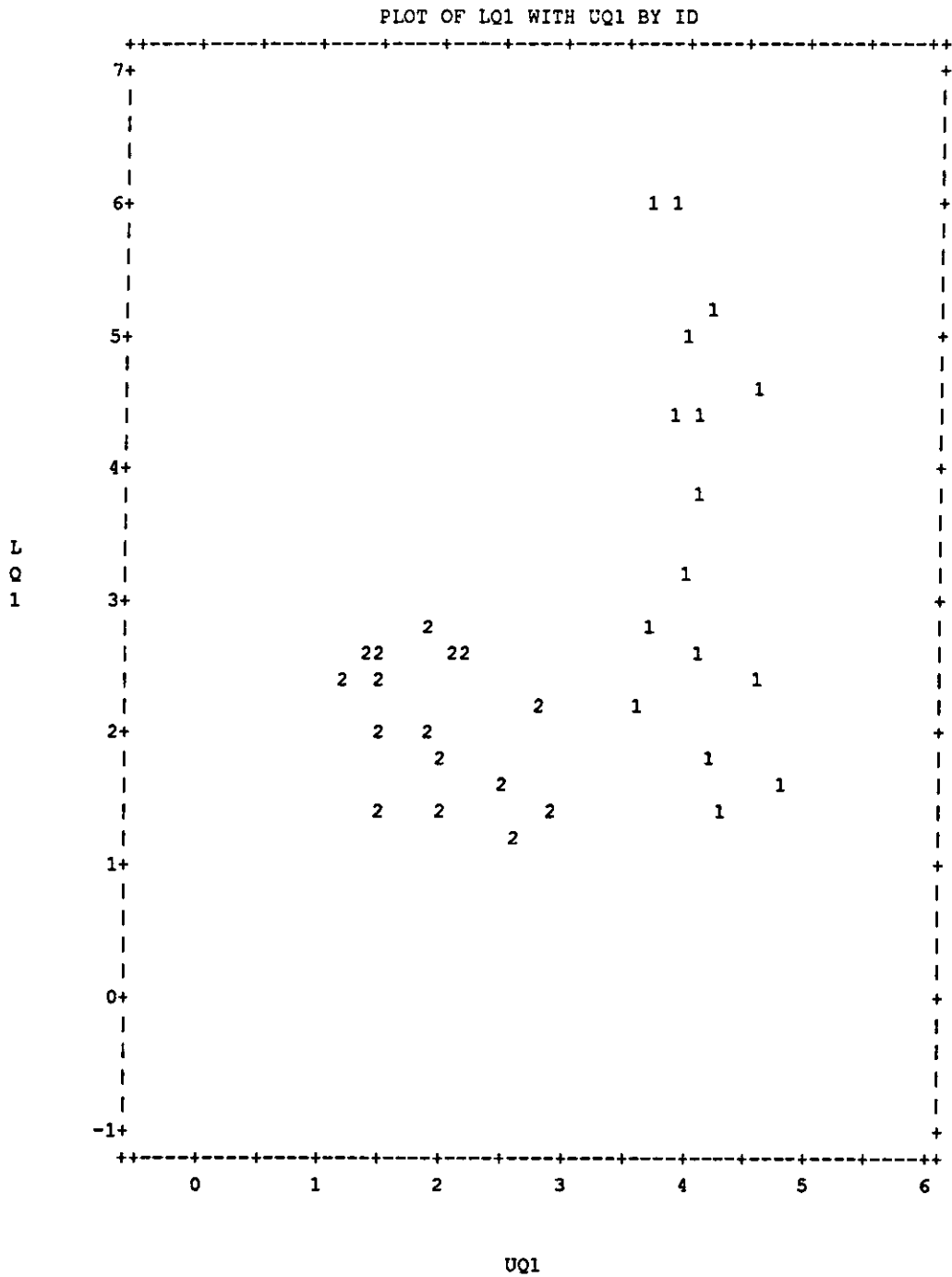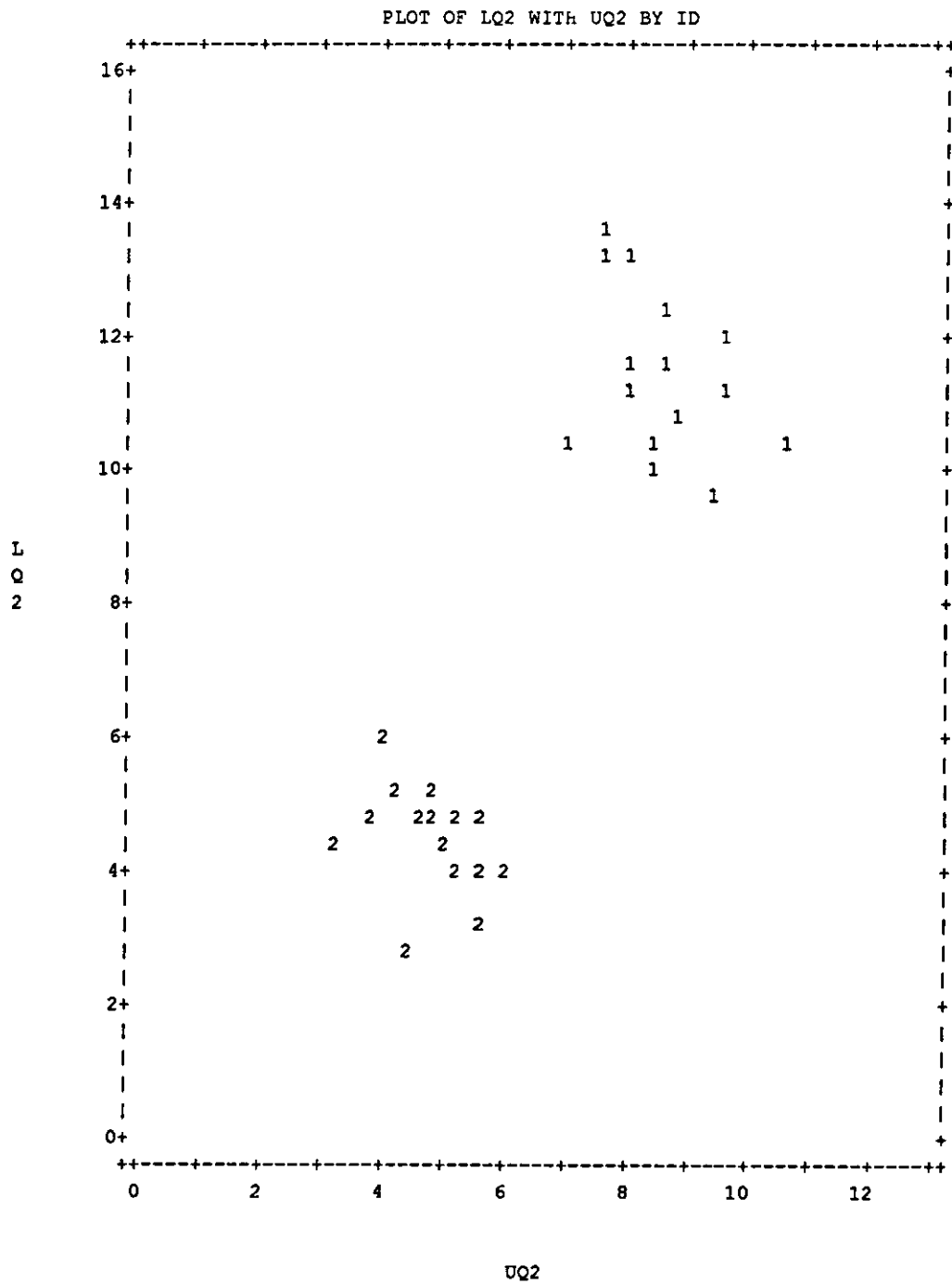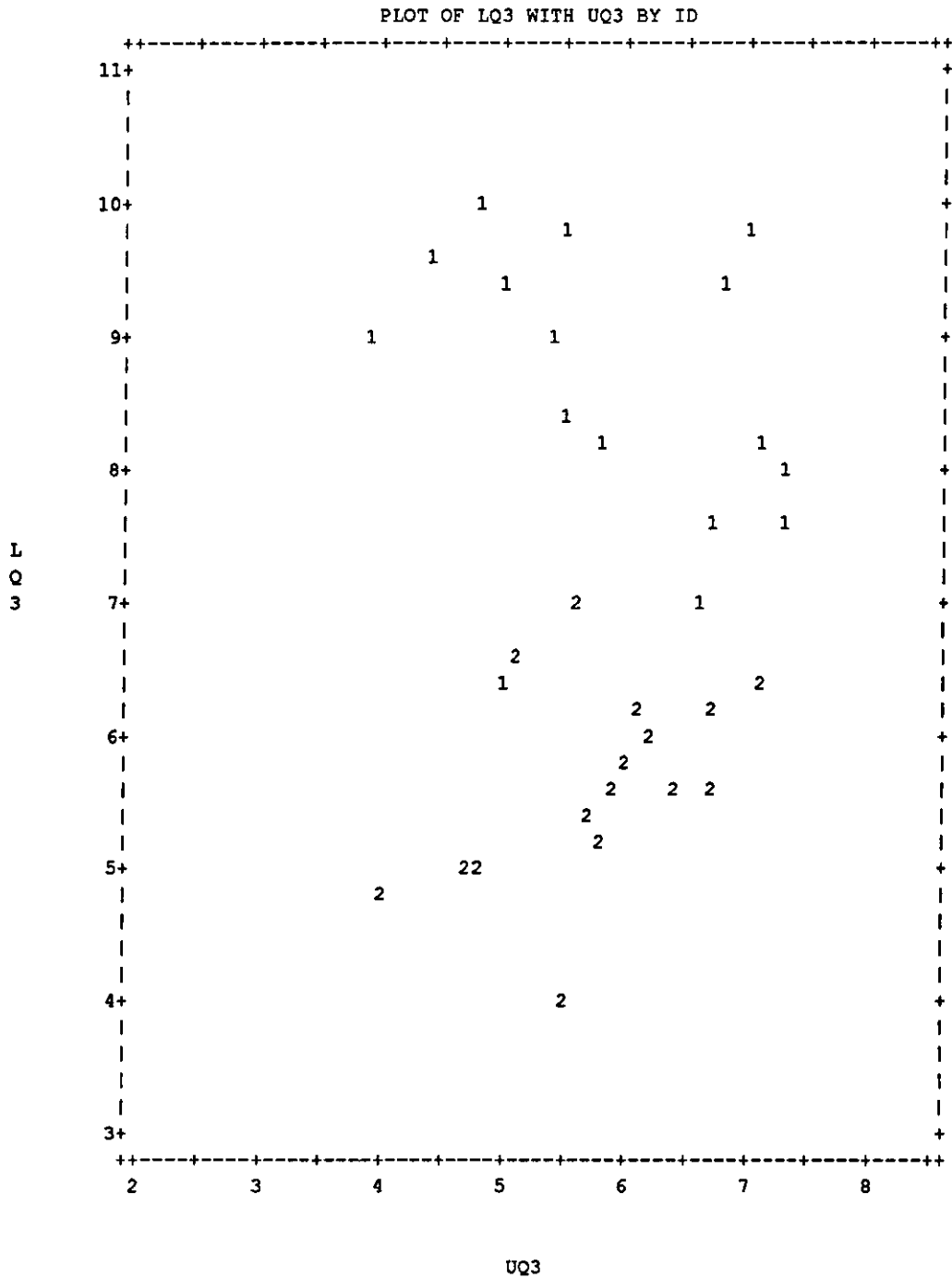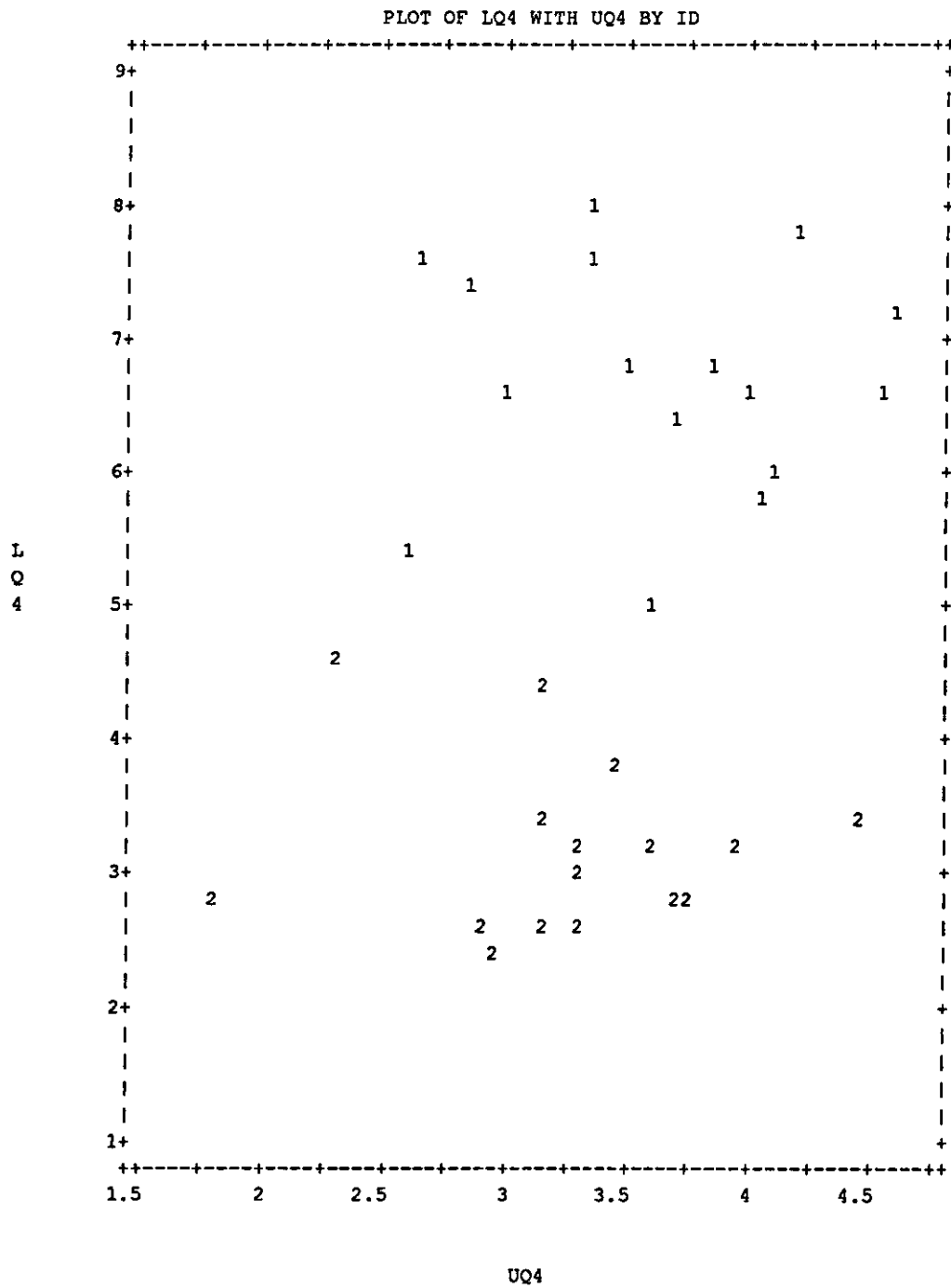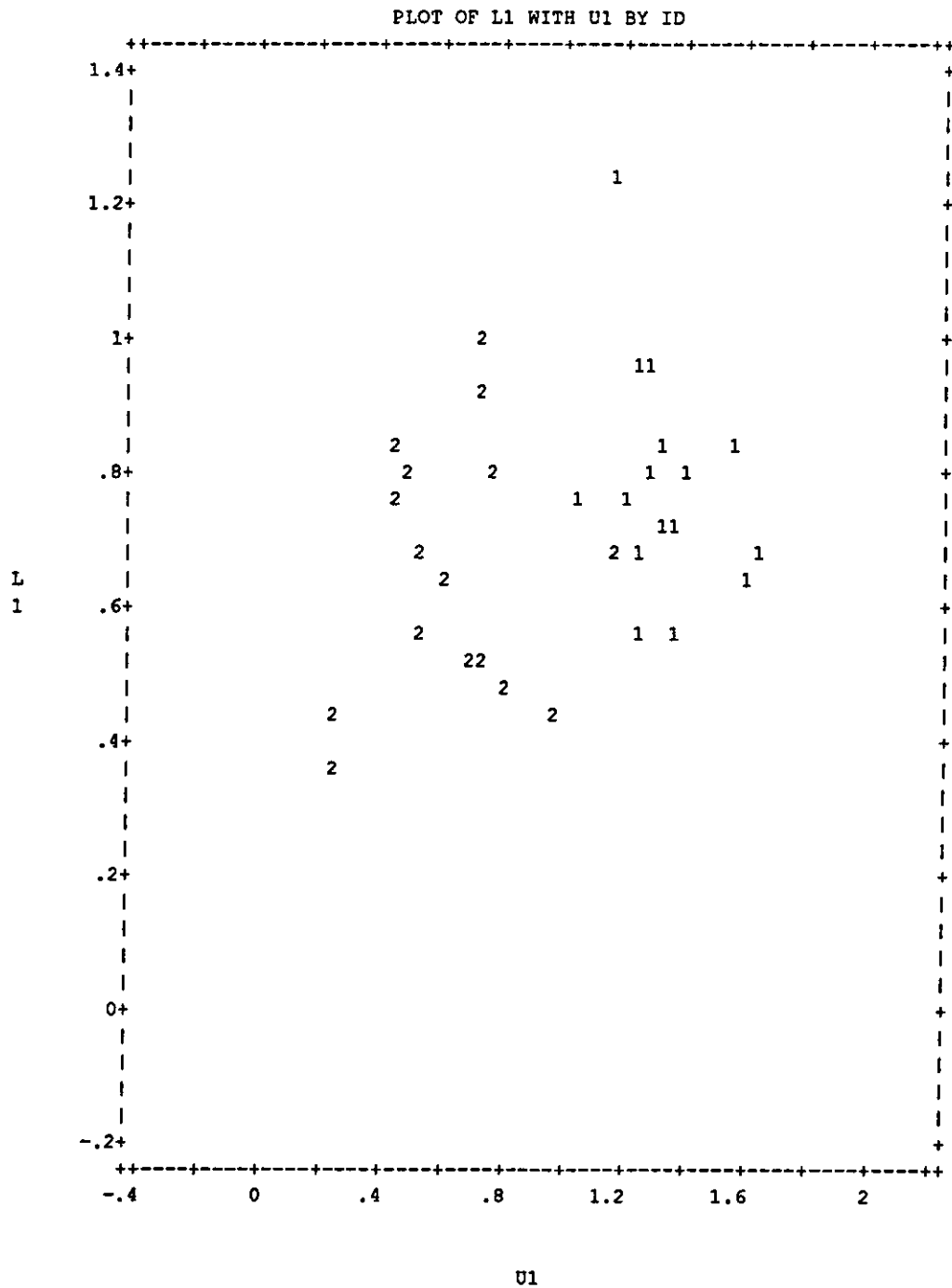Use first digit of ID as plotting symbol and $ for multiple occurrence.

B-12

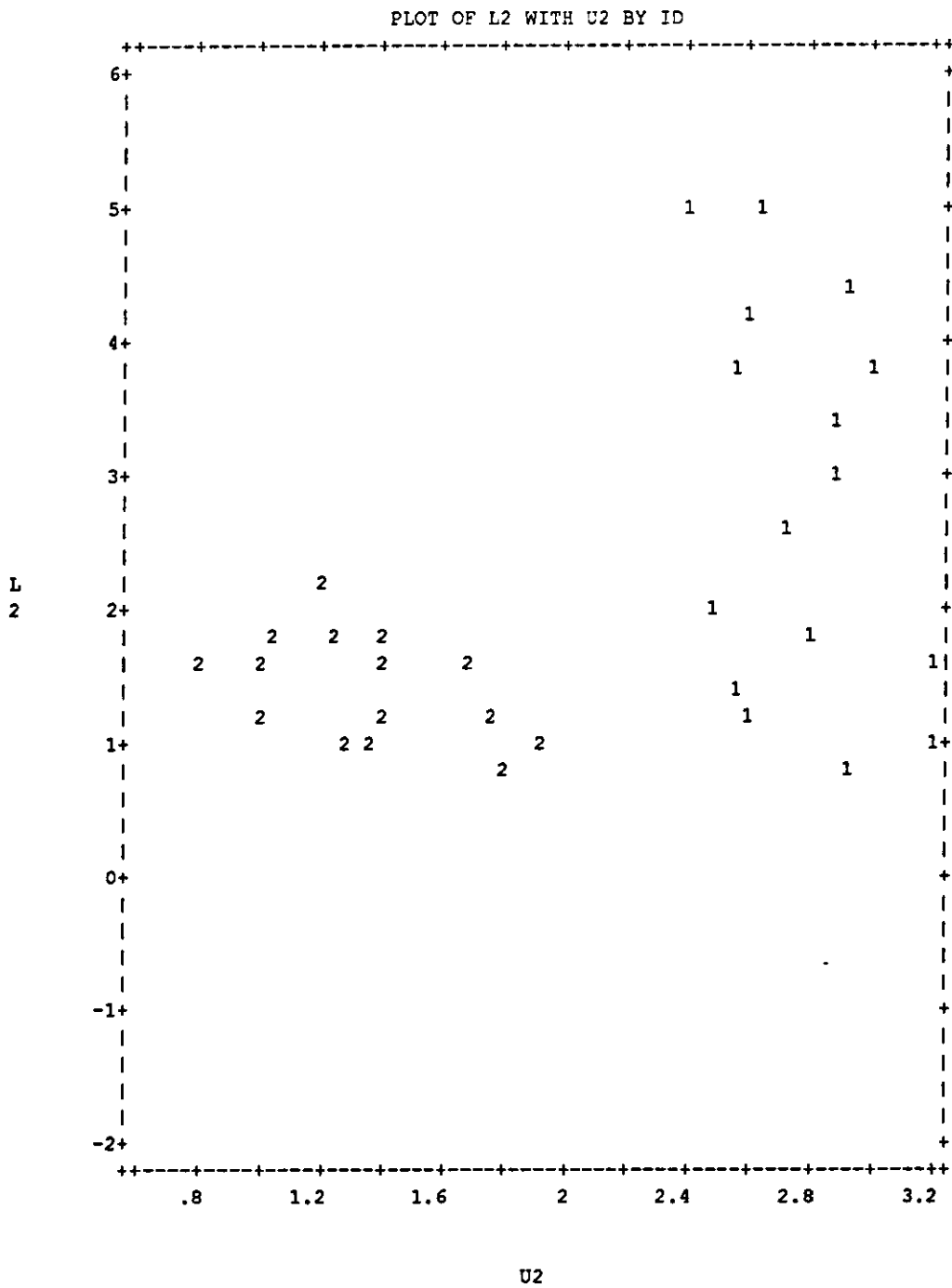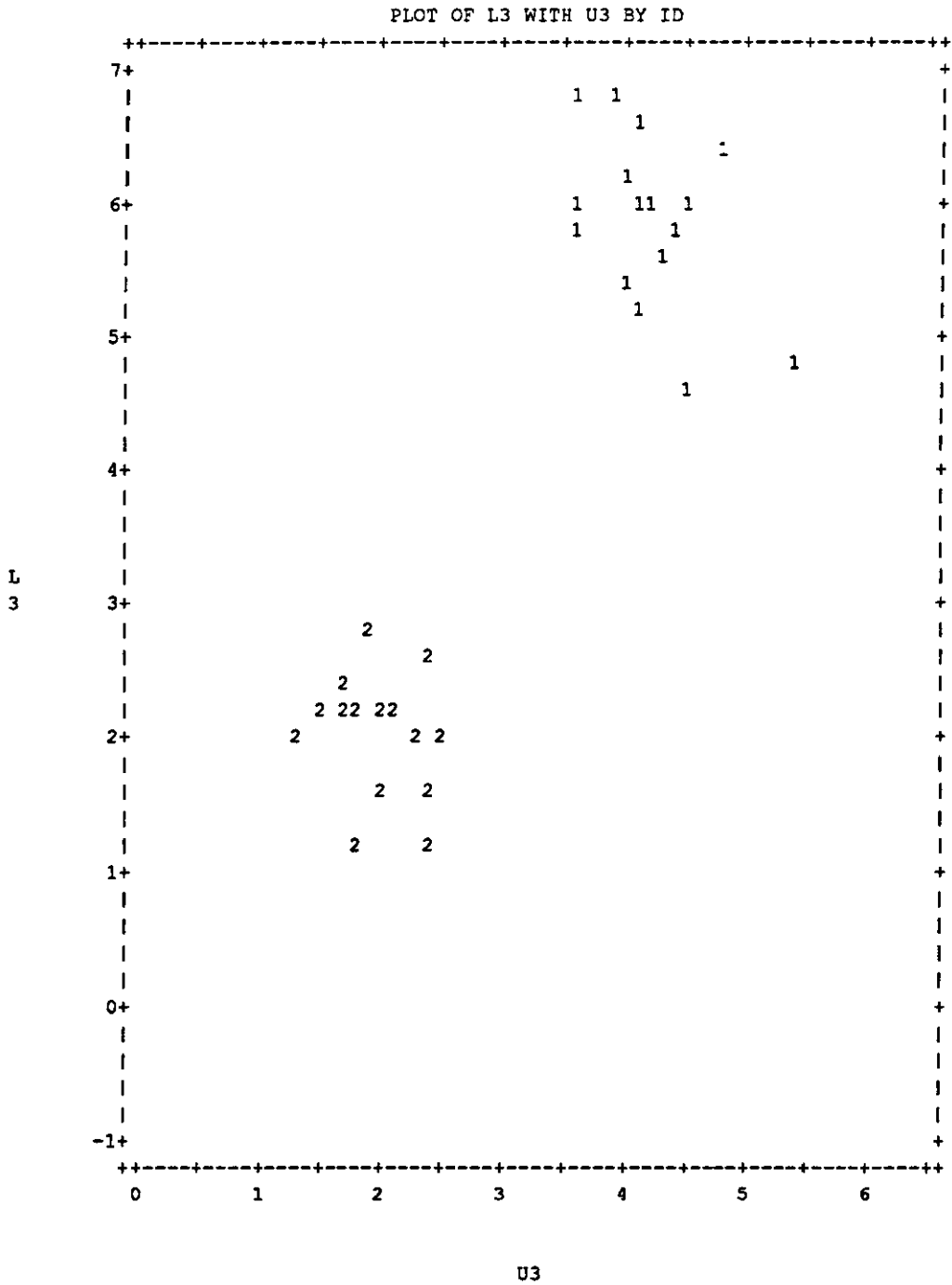# Figure B.6 A scatter diagram of the Q3 values against the Q4 values.

```
                              PLOT OF Q3 WITH Q4 BY ID
         ++----+----+----+----+----+----+----+----+----+----+----+----+----++
     .45+                                                                    +
        |
        |
        |
        |
     .4+                                                                     +
        |
        |           .
        |
        |   5
    .35+                                                                     +
        |
        |
        |
        |
     .3+                                                                     +
        |
        |          5 5    5         4
        |                 5       $ 4      4                      2
   Q    |                 5 4 4   4   3                           2
   3  .25+                5        4 4   5   3 3 $     2                  2   +
        |                         5 5    4   $ 1     $ 2   2
        |                                3   $     3   1 $
        |              5                         3   3 1
        |                                  3       $ 1       1     .
     .2+                                         1 1                        2+
        |                                        2 3         2
        |                                  3           1
        |                                              2
    .15+                                               2                     +
        |
        |
        |
        |
     .1+                                    -                               +
        |
        |
        |
        |
    .05+                                                                     +
         ++----+----+----+----+----+----+----+----+----+----+----+----+----++
         .12     .16      .2      .24      .28      .32      .36
```
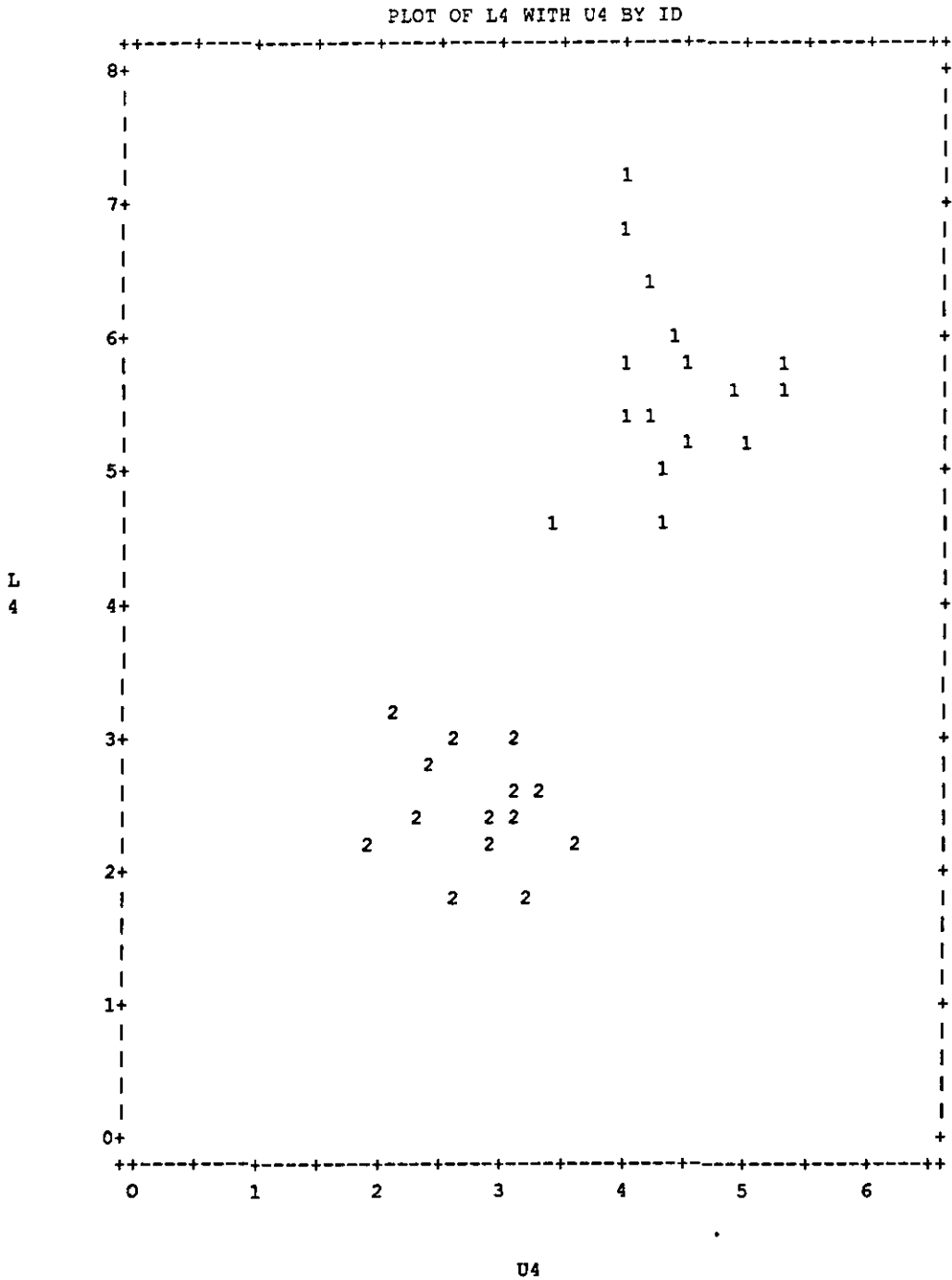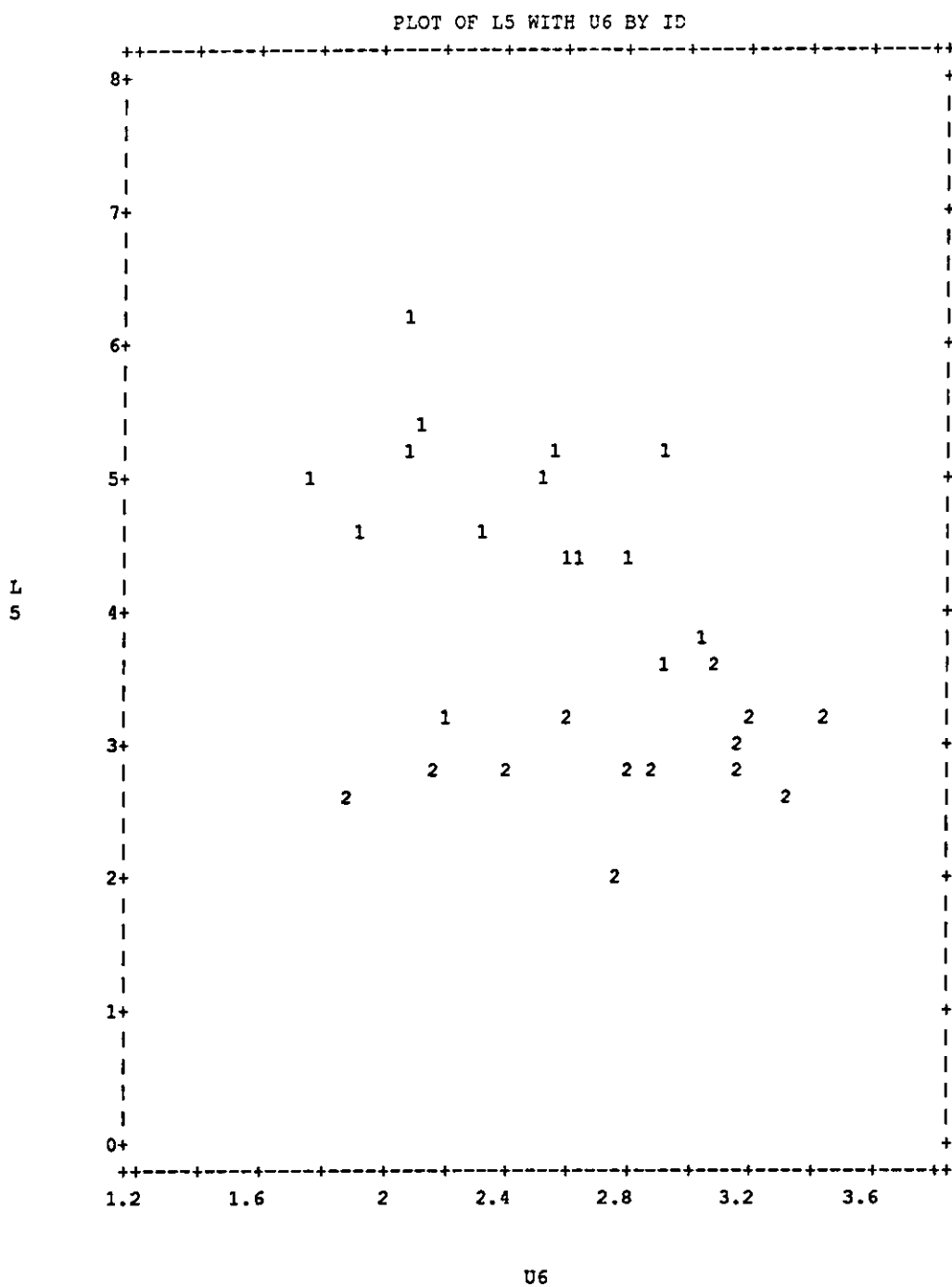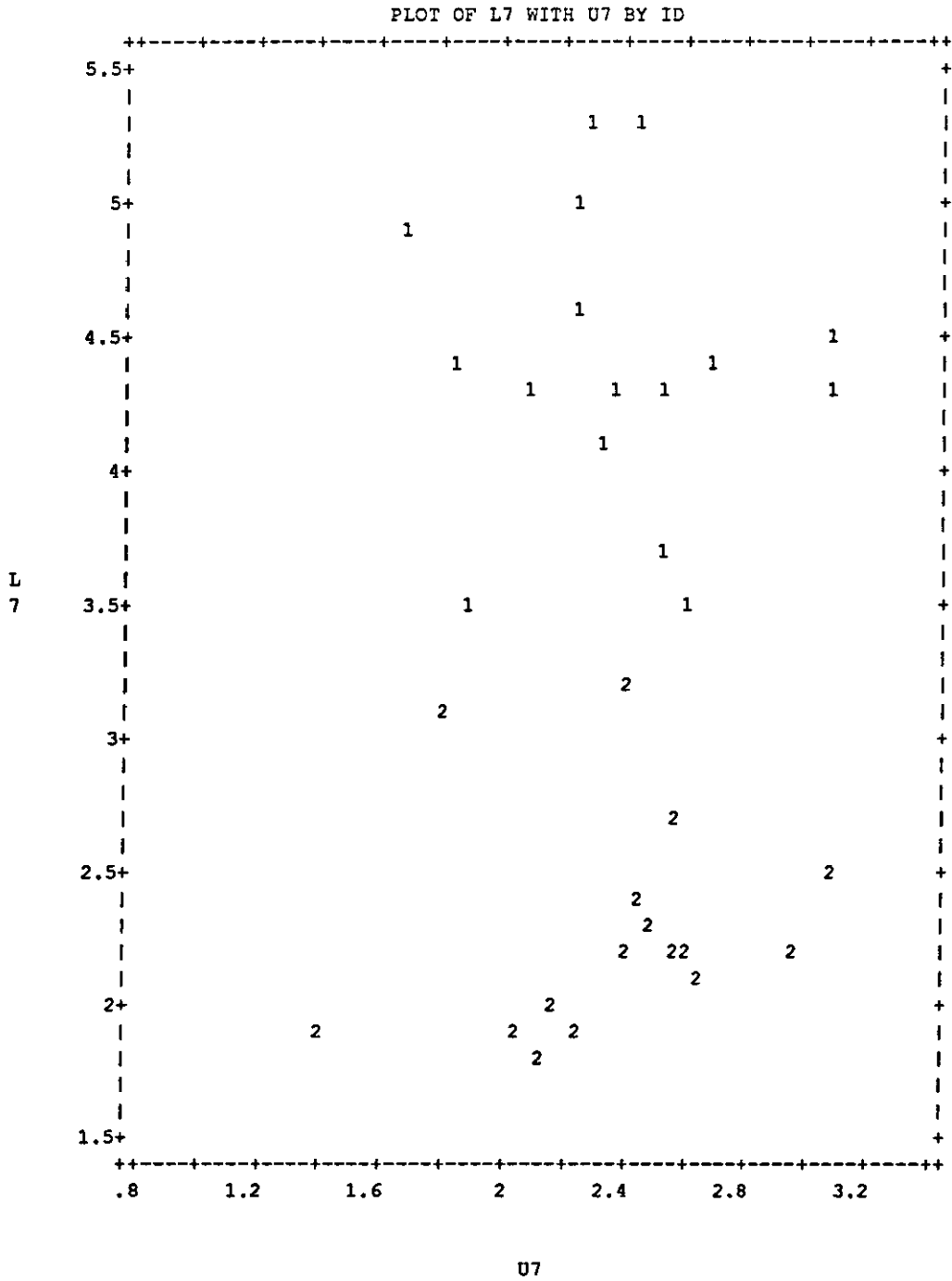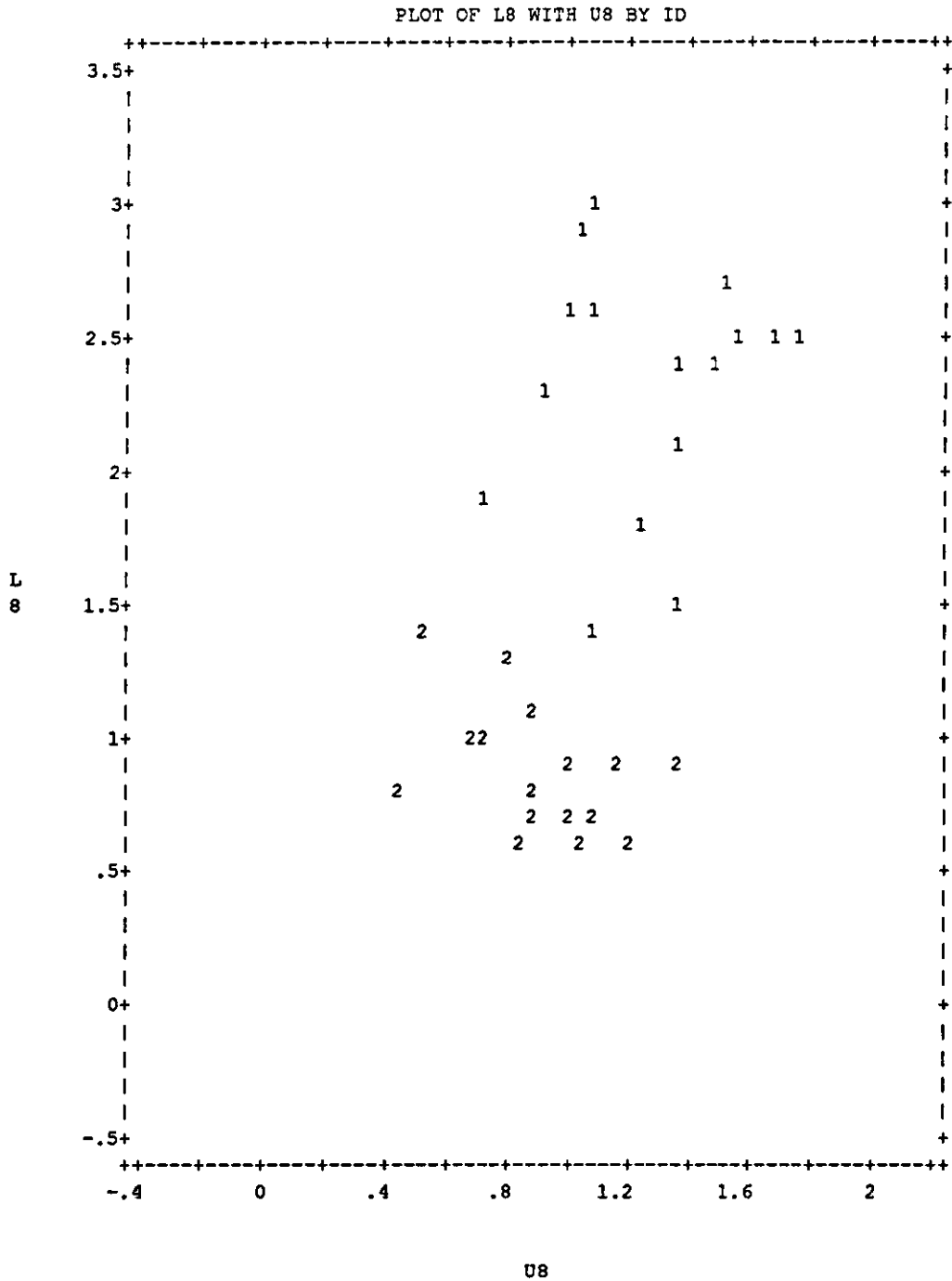
Q4

         75 cases plotted.
Use first digit of ID as plotting symbol and $ for multiple occurrence.

B-13

Figure B.7 A scatter diagram of the Q2 values against the Q3 values.

```
                        PLOT OF Q2 WITH Q3 BY ID

      ++----+----+----+----+----+----+----+----+----+----+----+----++
  .45+                                                              +
     |                                                              |
     |                                                              |
     |                                                              |
     |                                                              |
  .4+                                                               +
     |                                                              |
     |                              5                               |
     |                                                              |
     |                                                              |
  .35+                                                              +
     |                                                              |
     |                                                              |
     |                                                              |
     |             3                    5                           |
  .3+                                                               +
     |                                 5                            |
     |          2 1 3      3 1                                      |
     |       2    $ 1                                              |
  Q  |            1    5                5                           |
  2  .25+        1       3  3 3 4                                   +
     |              $ $  3  $ 4 $   4   4 4                         |
     |                      $ $  3   4 5                            |
     |              1  1 $ $  $  $                                  |
     |      2          2 $ 3  2                                     |
  .2+                                                               +
     |                  5                                           |
     |                                              5               |
     |                  2                                           |
  .15+                           5                                  +
     |                  5                                           |
     |                  5                                           |
     |                                                              |
  .1+                                                               +
     |                                                              |
     |                                                              |
     |                                                              |
  .05+                                                              +
      ++----+----+----+----+----+----+----+----+----+----+----+----++
     .12    .16     .2     .24     .28     .32     .36
```

Q3

75 cases plotted.
Use first digit of ID as plotting symbol and $ for multiple occurrence.

Figure B.8 A scatter diagram of the Q1 values against the Q4 values.

```
                          PLOT OF Q1 WITH Q4 BY ID
         ++---+----+----+----+----+----+----+----+----+----+----+----++
    .45+                                                              +
       |                                                              |
       |                                                              |
       |                                                              |
       |                      5                                       |
     .4+                                                              +
       |                                                              |
       |                                                              |
       |                                                              |
       |                            5                                 |
    .35+                                                              +
       |                         5                                    |
       |   5                                                          |
       |                      5                                       |
       |            5     5         5 5                               |
     .3+          5          5      5        5               2        +
       |                                                              |
       |                      5 4                                     |
       |                        4                                     |
 Q     |                      4 4 4   4   1                           |
 1   .25+                     4 4 4       $ $ 3   $ $   1             +
       |                          4     4 3     3   1 $   2           |
       |                          3   3 3 2   2                       |
       |                                          1 $           2     |
       |             5        5                     2 1               |
     .2+                                              2 2             +
       |                                1                             |
       |                                          2              2|
       |                                                              |
       |                                                              |
    .15+             5                                                +
       |                                                              |
       |                                                              |
       |                                                              |
       |                                                              |
     .1+                                                              +
       |                                                              |
       |                                                              |
       |                                                              |
       |                                                              |
    .05+                                                              +
         ++---+----+----+----+----+----+----+----+----+----+----+----++
        .12      .16      .2      .24      .28      .32      .36
```

Q4

```
        75 cases plotted.
Use first digit of ID as plotting symbol and $ for multiple occurrence.
```

Figure B.9 A scatter diagram of the L_m values against the A_m values.

```
                          PLOT OF L_m WITH A_m BY ID
        ++----+----+----+----+----+----+----+----+----+----+----+----++
     70+     5              5        5                                 +
      |                   5            5                               |
      |              5        5  5  5                                  |
      |                          5  5        5                         |
      |                                                                |
     60+                                                               +
      |                                                 2              |
      |                      5                                         |
      |                                                          4 44  |
      |                                         1 1    14    44    44  |
     50+                                            2    4    4    1   +
      |                                                           1  4 |
      |                                           1      1      4      |
      |                                                                |
      |                               1             1                  |
     40+                                                               +
      |                                                                |
      |                  1                                             |
      |                     1                                          |
 L_M  |                1                                               |
     30+            3 3      3                                         +
      |            $32$3 2   2 2 22                                    |
      |                                                                |
      |                                                                |
      |              2                                                 |
     20+                                                               +
      |              1                                                 |
      |                                                                |
      |                                                                |
      |                                                                |
     10+                                                               +
      |                                                                |
      |                                                                |
      |                                                                |
      |                                                                |
      0+                      2                                        +
      |                                                                |
      |                                                                |
      |                                                                |
      |                                                                |
    -10+                                                               +
        ++----+----+----+----+----+----+----+----+----+----+----+----++
       -12       -8       -4        0        4        8       12

                                   A_m

        75 cases plotted.
Use first digit of ID as plotting symbol and $ for multiple occurrence.
```

B-16

Figure B.10 A scatter diagram of the L_m values against the B_m values.

```
                        PLOT OF L_m WITH B_m BY ID
        ++----+----+----+----+----+----+----+----+----+----+----+----++
    70+               5 5           5                            +
     |           5                                              |
     |                5   55 5      5              5            |
     |                5    5          5                         |
     |                                                          |
    60+                                                         +
     |                                                        2|
     |                      5                                   |
     |                                                 444      |
     |                                  111 $444  4            |
    50+                               21    44               +
     |                                 41                       |
     |                               1 $                        |
     |                                                          |
     |                            1 1                           |
    40+                                                         +
     |                                                          |
     |              1                                           |
     |             1                                            |
L_m  |            1                                             |
    30+          3 3                                          +
     |          $$                                              |
     |                                                          |
     |                                                          |
     |        2                                                 |
    20+                                                         +
     |       1                                                  |
     |                                                          |
     |                                                          |
     |                                                          |
    10+                                                         +
     |                                                          |
     |                                                          |
     |                                                          |
     |                                                          |
     0+     2                                                 +
     |                                                          |
     |                                                          |
     |                                                          |
     |                                                          |
   -10+                                                         +
        ++----+----+----+----+----+----+----+----+----+----+----+----++
         0    20   40   60   80   100  120
```

B_m

75 cases plotted.
Use first digit of ID as plotting symbol and $ for multiple occurrence.

Figure B.11 A scatter diagram of the B_m values against the A_m values.

```
                        PLOT OF B WITH A BY ID
       ++----+----+----+----+----+----+----+----+----+----+----+----++
  140+                                                              +
     I
     I
     I
     I                                              2               I
  120+                                                              +
     I
     I
     I                                       4            44 I
     I                                          4            I
  100+                                             44     4 +
     I                                      1       4    44 I
     I                                     4   4       4 I
     I                               1 1                  I
     I                     5         1                    I
   80+                              2            11    +
     I                           1              4      4I
     I                           1                    I
     I                                            I
B_Mean I                    5                         I
   60+                 5           1                   +
     I             5                                   I
     I             5                          1        I
     I        5        5                               I
     I        5                    5                   I
   40+                      5                           +
     I                   5                             I
     I     5                  5                         I
     I               1                                 I
     I                 1                               I
   20+            51                                   +
     I         3 3        3                            I
     I         $32$3 2  2 2 22                         I
     I           $                                     I
     I                                                 I
    0+                 2                               +
     I
     I
     I
     I
  -20+                                                 +
       ++----+----+----+----+----+----+----+----+----+----+----+----++
      -12      -8       -4        0        4        8       12

                              A_Mean

        75 cases plotted.
Use first digit of ID as plotting symbol and $ for multiple occurrence.
```
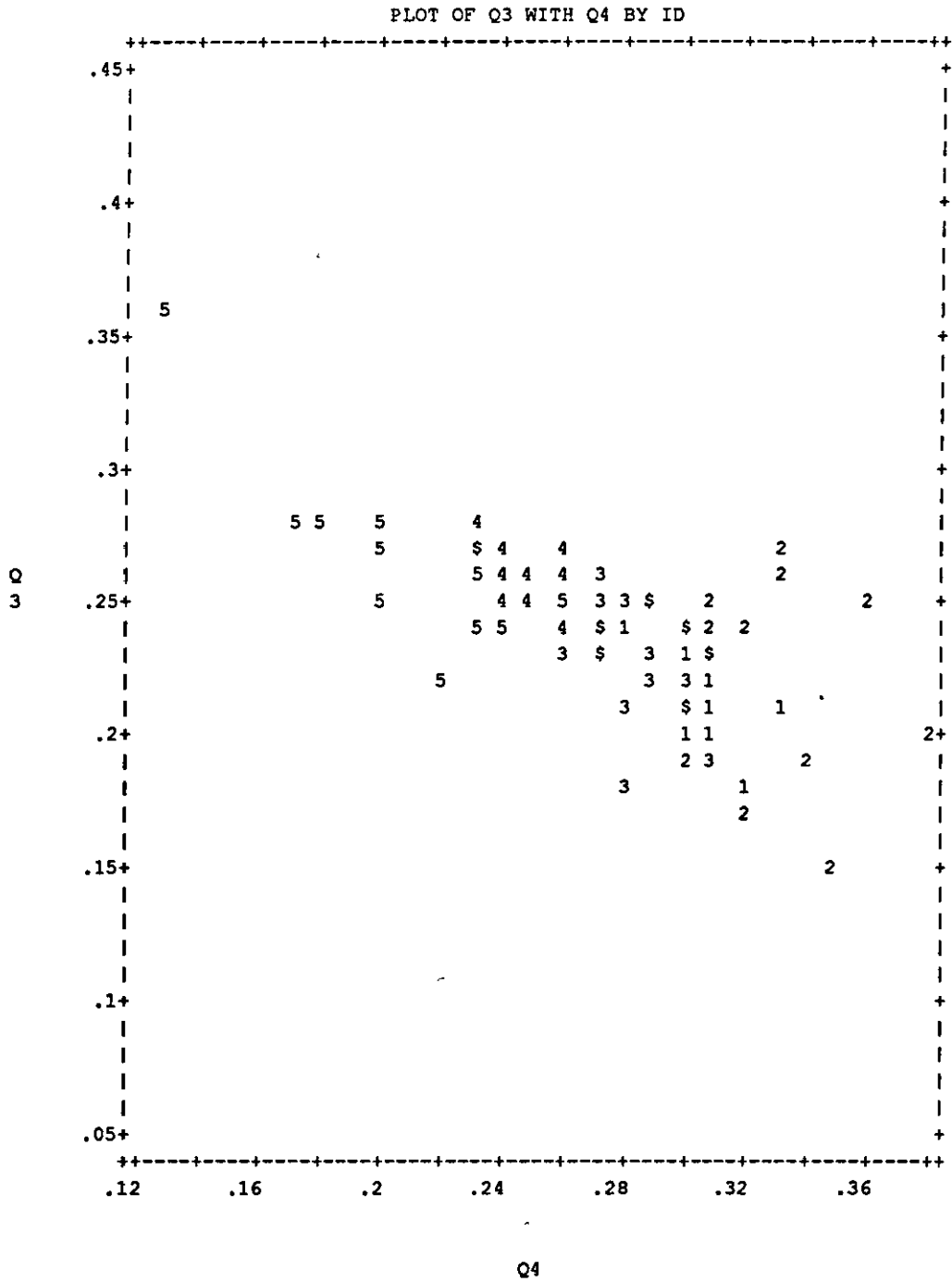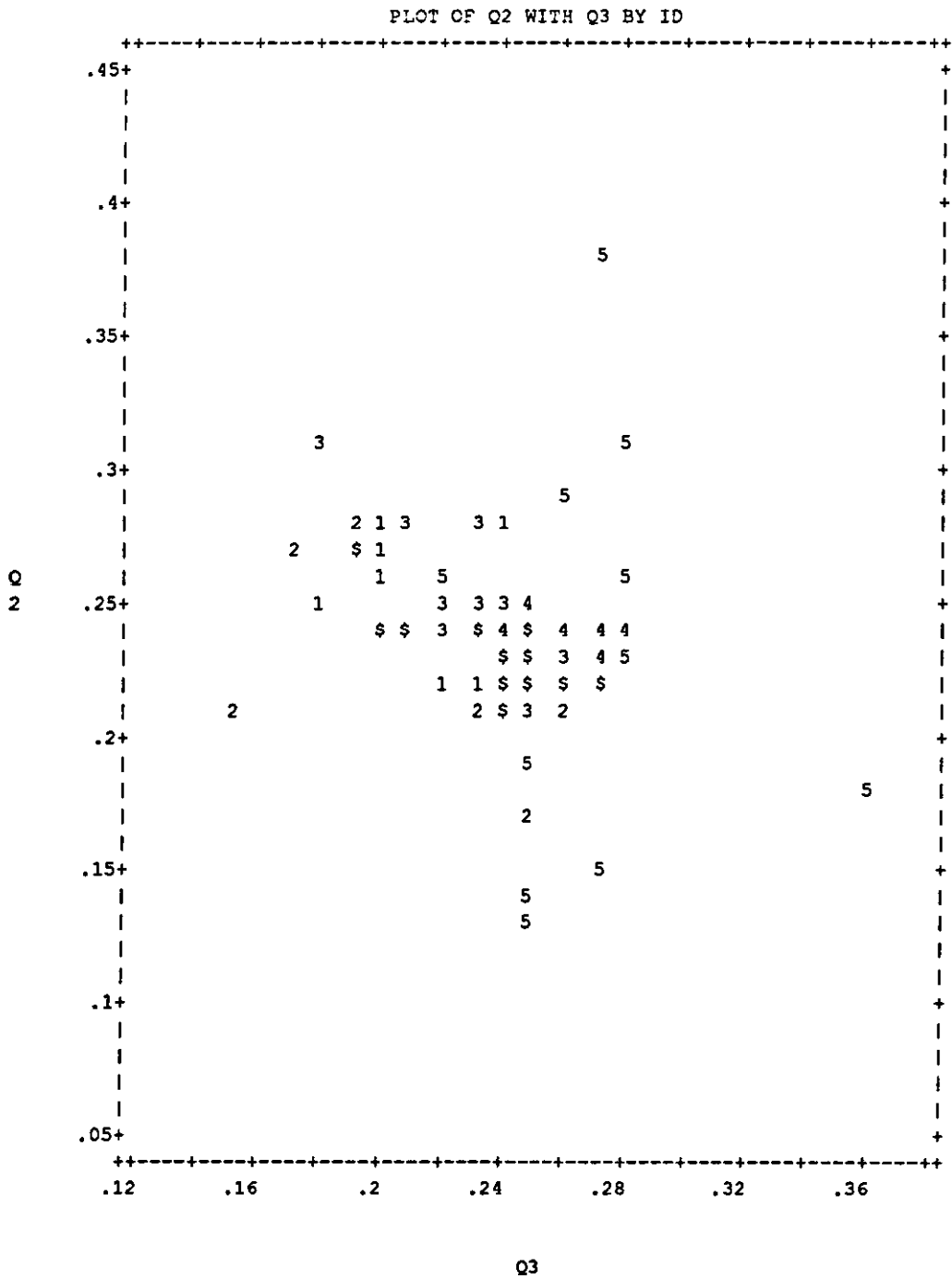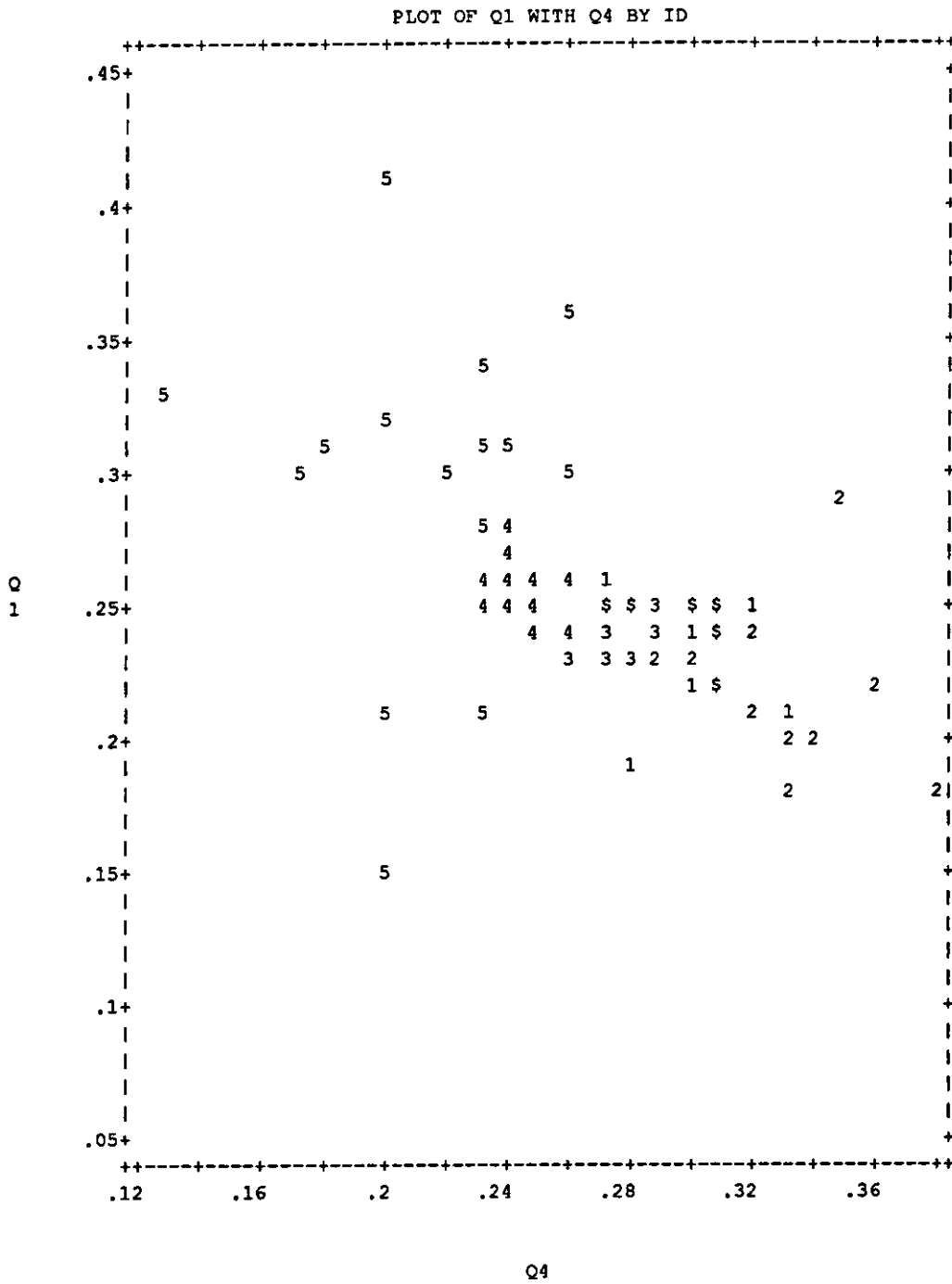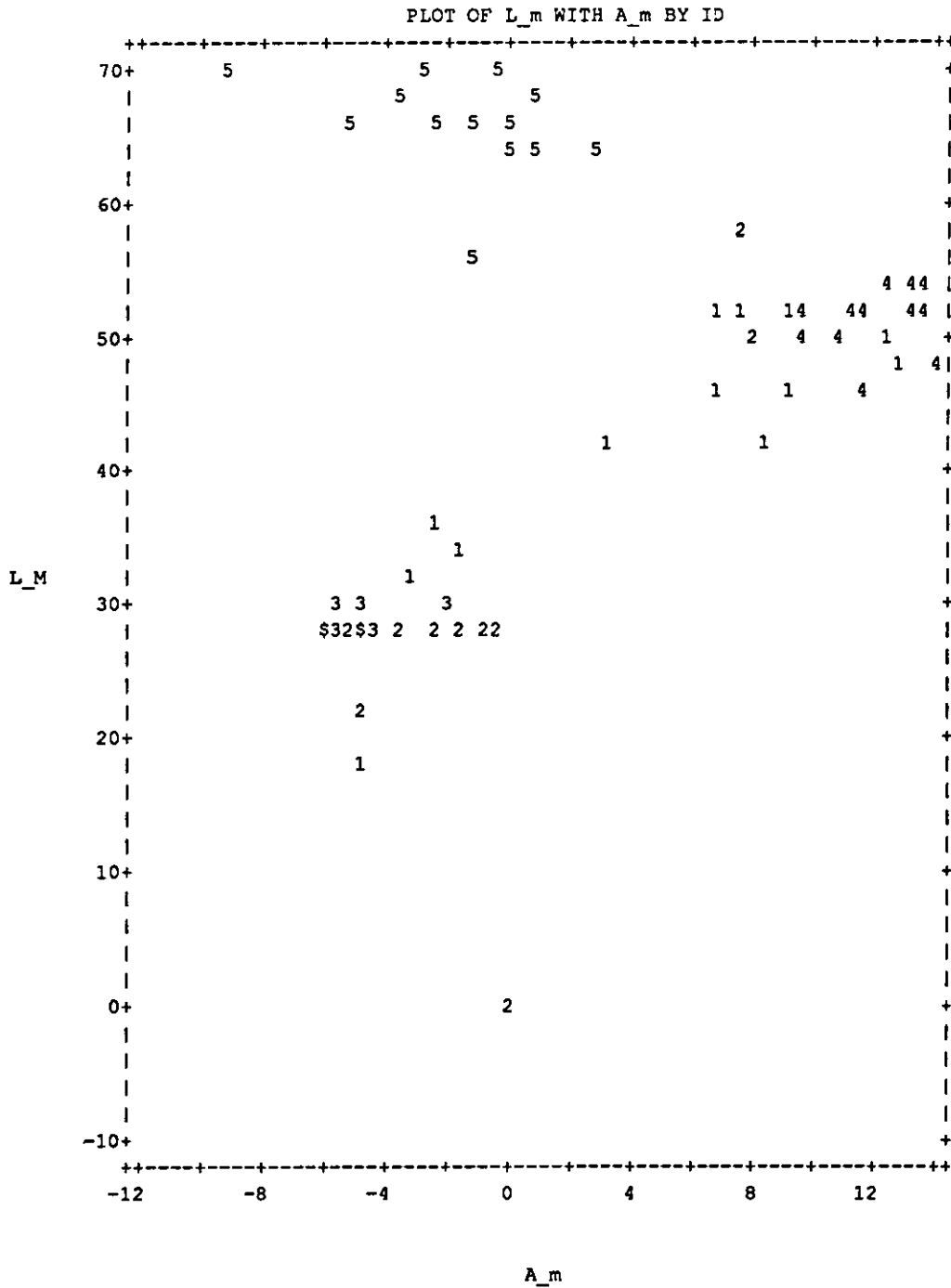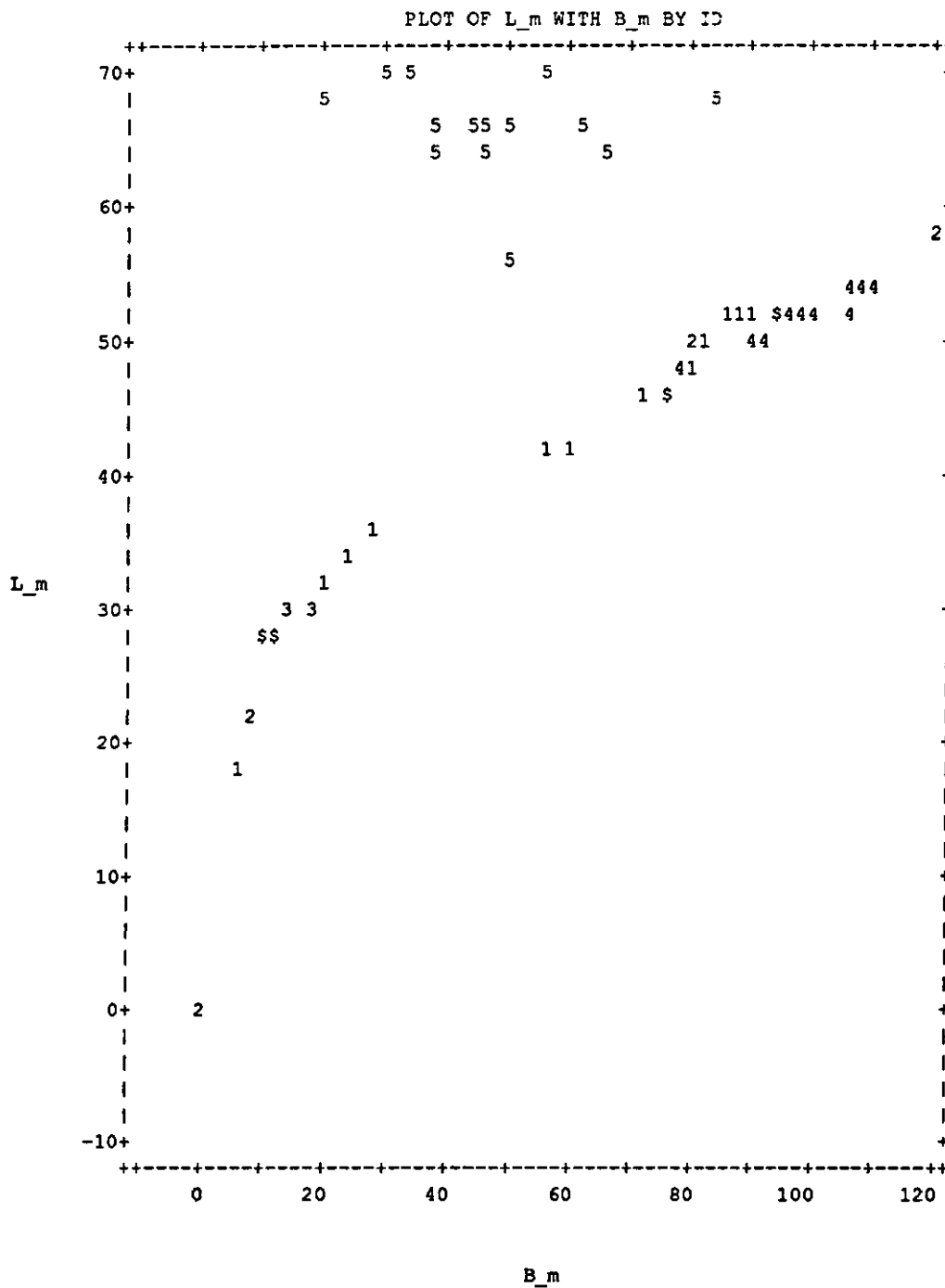
B-18